K/GDP/SAR/SUB-1

UE

URANIUM ENRICHMENT

MARTIN MARIETTA

SEISMIC HAZARD EVALUATION FOR THE PADUCAH GASEOUS DIFFUSION PLANT PADUCAH, KENTUCKY

Risk Engineering, Inc.
Golden, Colorado 80403

July 1991

SAFETY ANALYSIS REPORTS GDP

MANAGED BY
MARTIN MARIETTA ENERGY SYSTEMS, INC.
FOR THE UNITED STATES
DEPARTMENT OF ENERGY

K/GDP/SAR/SUB–1
(DE91015996)

Seismic hazard evaluation for the Paducah Gaseous Diffusion Plant, Paducah, Kentucky

Jul 1991

Oak Ridge K-25 Site, TN (United States); Risk Engineering, Inc., Golden, CO (United States)

Reproduced and Distributed by:

U.S. DEPARTMENT OF ENERGY
Office of Scientific and Technical Information
P.O. Box 62
Oak Ridge, TN 37831

May 9, 1991

K/GDP/SAR/SUB--1

DE91 015996

SEISMIC HAZARD EVALUATION FOR THE PADUCAH GASEOUS DIFFUSION PLANT PADUCAH, KENTUCKY

Report Prepared by
Risk Engineering, Inc.
5255 Pine Ridge Road
Golden, Colorado 80403
under
Subcontract No. 41K-VD559V

MARTIN MARIETTA ENERGY SYSTEMS, INC.
managing the
Oak Ridge K-25 Site
Oak Ridge National Laboratory
Oak Ridge Y-12 Plant
Paducah Gaseous Diffusion Plant
under Contract DE-AC05-84OR21400
and the
Portsmouth Gaseous Diffusion Plant
under contract DE-AC05-76OR00001
for the
U.S. DEPARTMENT OF ENERGY

EXECUTIVE SUMMARY

This study presents the results of an investigation of seismic hazard at the site of the Paducah Gaseous Diffusion Plant. Paducah is located near the northern end of the Reelfoot Rift—a large feature of the earth's crust that is believed to be associated with the New Madrid earthquakes of 1811 and 1812.

Results from three separate seismic hazard analyses are presented here. The EPRI/SOG analysis uses the input data and methodology developed by the Electric Power Research Institute, under the sponsorship of several electric utilities, for the evaluation of seismic hazard in the central and eastern United States. Section 2 of this report documents the application of the EPRI/SOG methodology to the Paducah site (for both rock and soil conditions). The LLNL analysis uses the input data and methodology developed by the Lawrence Livermore National Laboratory for the Nuclear Regulatory Commission. This analysis was performed by LLNL and results were transmitted to us. Section 3 of this report contains a summary of LLNL inputs and results (for both rock and soil conditions, and considering 4 and 5 LLNL ground motion experts).

Both the EPRI/SOG and LLNL studies characterize earth-science uncertainty on the causes and characteristics of earthquakes in the central and eastern United States. This is accomplished by considering multiple hypotheses on the locations and parameters of seismic source zones and by considering multiple attenuation functions for the prediction of ground shaking given earthquake size and location. These hypotheses were generated by multiple expert teams and experts. Furthermore, each team and expert was asked to generate multiple hypotheses in order to characterize his own internal uncertainty. The seismic-hazard calculations are performed for all hypotheses. Combining the results from each hypothesis with the weight associated to that hypothesis, one obtains an overall representation of the seismic hazard at Paducah and its uncertainty.

Combining the EPRI/SOG and LLNL results with equal weights — while considering their respective uncertainties — provides another set of seismic-hazard results. Section 4 explains the combination process and presents results (for both rock and soil conditions, and considering 4 and 5 LLNL ground motion experts).

Because both the EPRI/SOG and LLNL methodologies treat earthquakes as point sources, their results are not directly applicable to the Paducah site, due to the possibility of large

earthquakes in the New Madrid seismic zone. A third analysis, the extended-source seismic hazard analysis, was performed under this study. This analysis includes the earth-science uncertainties of the EPRI/SOG and LLNL inputs, and also models the effects of extended ruptures. Section 5 documents this analysis and presents results (for rock conditions only). Results from the extended-source analysis constitute the definitive seismic-hazard results for the Paducah site.

The following table summarizes results from all these analyses, for peak ground acceleration and spectral velocity at 1 Hz (5% damping).

Ground-Motion Amplitudes for Selected Values of
the Median Annual Exceedance Probability

Ground Motion Measure	Annual Exceedance Probability	EPRI	LLNL (4 GX†)	LLNL (5 GX†)	Combined EPRI+LLNL (4 GX†)	Combined EPRI+LLNL (5 GX†)	Extended Source
Peak Ground Acceleration on rock (g)	2×10^{-3} (500 yr)	0.15	0.18	0.23	0.16	0.16	0.22
	1×10^{-3} (1000 yr)	0.21	0.25	0.31	0.22	0.22	0.31
	2×10^{-4} (5000 yr)	0.40	0.47	0.57	0.42	0.43	0.62
Peak Ground Acceleration on soil (g)	2×10^{-3} (500 yr)	0.20	0.18	0.21	0.20	0.20	—
	1×10^{-3} (1000 yr)	0.25	0.25	0.29	0.25	0.26	—
	2×10^{-4} (5000 yr)	0.37	0.48	0.56	0.41	0.41	—
1-Hz Spectral Velocity on rock (cm/sec)	2×10^{-3} (500 yr)	4.1	9.2	14.0	5.2	5.6	15.0
	1×10^{-3} (1000 yr)	6.6	14.0	21.0	8.3	8.5	25.0
	2×10^{-4} (5000 yr)	18.0	32.0	47.0	20.0	23.0	57.0
1-Hz Spectral Velocity on soil (cm/sec)	2×10^{-3} (500 yr)	6.2	18.0	24.0	13.0	13.0	—
	1×10^{-3} (1000 yr)	10.0	27.0	36.0	21.0	21.0	—
	2×10^{-4} (5000 yr)	28.0	61.0	83.0	52.0	60.0	—

† 4GX and 5GX denote results obtained considering 4 and 5 LLNL ground-motion experts

In order to gain insight on the types of earthquakes that dominate the calculated hazard at the Paducah site, we evaluate the expected earthquake magnitude and distance to the site for various probabilities of exceedance and generate corresponding artificial ground motions. Section 6 documents these results.

CONTENTS

Section			Page
1	INTRODUCTION		1-1
	1.1	REFERENCES	1-2
2	EPRI/SOG METHODOLOGY AND RESULTS		2-1
	2.1	INTRODUCTION	2-1
	2.2	EPRI/SOG METHODOLOGY	2-1
		2.2.1 Basic Seismic Hazard Model	2-1
		2.2.2 Treatment of Uncertainty	2-5
		2.2.3 Development of Seismological Interpretations	2-7
		2.2.4 Computer Codes	2-10
	2.3	TECTONIC AND SEISMICITY INTERPRETATIONS	2-10
		2.3.1 Seismic Sources	2-12
		2.3.2 Maximum Magnitudes and Seismicity Options	2-14
		2.3.3 Seismic Sources near the Paducah Site	2-14
	2.4	GROUND-MOTION ATTENUATION	2-27
		2.4.1 Attenuation Functions for Rock	2-27
		2.4.2 Soil Amplification Factors	2-28
	2.5	CALCULATIONS	2-42
		2.5.1 Overview	2-42
		2.5.2 Screening of Seismic Sources	2-43
		2.5.3 Development of Source Combinations	2-43
		2.5.4 Results	2-44
	2.6	REFERENCES	2-44

3 LLNL METHODOLOGY AND RESULTS 3-1
3.1 METHODOLOGY 3-1
3.2 SEISMICITY INTERPRETATIONS 3-1
3.3 GROUND MOTION MODELS 3-2
3.3.1 Attenuation Functions for Rock 3-2
3.3.2 Site Amplification Factors 3-3
3.4 COMPUTATIONS 3-3
3.5 REFERENCES 3-4

4 COMBINATION OF EPRI/SOG AND LLNL RESULTS 4-1
4.1 OVERVIEW 4-1
4.2 COMBINATION OF EPRI/SOG AND LLNL RESULTS 4-1
4.2.1 Mechanics of the Combination Process 4-1
4.3 RESULTS 4-3

5 EXTENDED-SOURCE HAZARD ANALYSIS AND RESULTS 5-1
5.1 INTRODUCTION 5-1
5.2 TECTONIC AND SEISMICITY INTERPRETATIONS 5-2
5.2.1 Seismic Zonation 5-2
5.2.2 Seismicity Parameters 5-9
5.2.3 Other Parameters 5-16
5.3 ATTENUATION FUNCTIONS FOR EXTENDED RUPTURES 5-16
5.3.1 Motivation 5-16
5.3.2 Development 5-16
5.4 RESULTS 5-26
5.4.1 Uniform Hazard Spectra for Additional Damping Ratios 5-26
5.5 REFERENCES 5-27

6 CHARACTERISTICS OF CONTROLLING GROUND MOTIONS 6-1
6.1 INTRODUCTION 6-1
6.2 EXPECTED MAGNITUDE AND DISTANCE 6-1
6.3 ARTIFICIAL GROUND MOTIONS 6-2
6.4 DURATION CHARACTERISTICS 6-3
6.5 REFERENCES 6-4

7 CONCLUSIONS 7-1

A SIMULATION OF GROUND MOTIONS FROM EXTENDED RUPTURES A-1

A.1 INTRODUCTION A-1

A.2 MODEL FORMULATION A-1

A.2.1 Scaling of Whole Event and Sub-Events A-1

A.2.2 Generation of Ground Motions A-2

A.3 APPLICATION A-3

A.4 REFERENCES A-6

B TABULATED RESULTS B-1

B.1 RESULTS FROM THE EPRI/SOG ANALYSIS B-1

B.2 COMBINED RESULTS FROM EPRI/SOG AND LLNL ANALYSES B-9

B.3 RESULTS FROM THE EXTENDED-SOURCE ANALYSIS B-13

LIST OF FIGURES

Figure		Page
2-1	Seismic hazard computational model.	2–4
2-2	Logic tree representation of uncertain parameters in the EPRI/SOG methodology	2–7
2-3	EQHAZARD modules: their functions and data flow.	2–11
2-4	Map showing the seismic sources specified by the Bechtel team in the region around the Paducah site.	2–15
2-5	Map showing the seismic sources specified by the Dames and Moore team in the region around the Paducah Site.	2–16
2-6	Map showing the seismic sources specified by the Law team in the region around the Paducah Site.	2–17
2-7	Map showing the seismic sources specified by the Rondout team in the region around the Paducah Site.	2–18
2-8	Map showing the seismic sources specified by the Weston team in the region around the Paducah Site.	2–19
2-9	Map showing the seismic sources specified by the Woodward-Clyde team in the region around the Paducah Site.	2–20
2-10	Ground motions predicted by the EPRI/SOG attenuation equations for m_b 5 and 6.	2–31
2-11	Standard soil profile for sand-like Central and Eastern United States sites.	2–34
2-12	Shear-strain dependency of shear-wave damping and shear modulus.	2–35
2-13	Soil amplification factors for peak ground acceleration, for the 5 soil categories.	2–36
2-14	Soil amplification factors for 1-Hz spectral velocity (5% damping), for the 5 soil categories.	2–37
2-15	Soil amplification factors for 2.5-Hz spectral velocity (5% damping), for the 5 soil categories.	2–38

2-16 Soil amplification factors for 5-Hz spectral velocity (5% damping), for the 5 soil categories. 2–39

2-17 Soil amplification factors for 10-Hz spectral velocity (5% damping), for the 5 soil categories. 2–40

2-18 Soil amplification factors for 25-Hz spectral velocity (5% damping), for the 5 soil categories. 2–41

2-19 Peak ground acceleration hazard curves for Paducah (for rock site conditions) computed using the EPRI/SOG methodology. 2–54

2-20 0.5-Hz spectral velocity hazard curves for Paducah (for rock site conditions) computed using the EPRI/SOG methodology. 2–55

2-21 1-Hz spectral velocity hazard curves for Paducah (for rock site conditions) computed using the EPRI/SOG methodology. 2–56

2-22 2.5-Hz spectral velocity hazard curves for Paducah (for rock site conditions) computed using the EPRI/SOG methodology. 2–57

2-23 5-Hz spectral velocity hazard curves for Paducah (for rock site conditions) computed using the EPRI/SOG methodology. 2–58

2-24 10-Hz spectral velocity hazard curves for Paducah (for rock site conditions) computed using the EPRI/SOG methodology. 2–59

2-25 25-Hz spectral velocity hazard curves for Paducah (for rock site conditions) computed using the EPRI/SOG methodology. 2–60

2-26 Median uniform-hazard spectra for Paducah (rock site conditions) computed using the EPRI/SOG methodology. Results shown as uniform hazard spectra. 2–61

2-27 Peak ground acceleration hazard curves for Paducah (for soil site conditions) computed using the EPRI/SOG methodology. 2–62

2-28 Median uniform-hazard spectra for Paducah (for soil site conditions) computed using the EPRI/SOG methodology. 2–63

3-1 Map showing the seismic sources specified by LLNL seismicity expert 1 in the region around the Paducah site 3–5

3-2 Map showing the seismic sources specified by LLNL seismicity expert 2 in the region around the Paducah site 3–6

3-3 Map showing the seismic sources specified by LLNL seismicity expert 3 in the region around the Paducah site 3–7

3-4 Map showing the seismic sources specified by LLNL seismicity expert 4 in the region around the Paducah site 3–8

3-5 Map showing the seismic sources specified by LLNL seismicity expert 5 in the region around the Paducah site 3–9
3-6 Map showing the seismic sources specified by LLNL seismicity expert 6 in the region around the Paducah site 3–10
3-7 Map showing the seismic sources specified by LLNL seismicity expert 7 in the region around the Paducah site 3–11
3-8 Map showing the seismic sources specified by LLNL seismicity expert 10 in the region around the Paducah site 3–12
3-9 Map showing the seismic sources specified by LLNL seismicity expert 11 in the region around the Paducah site 3–13
3-10 Map showing the seismic sources specified by LLNL seismicity expert 12 in the region around the Paducah site 3–14
3-11 Map showing the seismic sources specified by LLNL seismicity expert 13 in the region around the Paducah site 3–15
3-12 Peak ground acceleration hazard curves for Paducah computed by LLNL for rock conditions using the LLNL methodology (all ground-motion Experts). 3–16
3-13 Median uniform-hazard spectra for Paducah computed by LLNL for rock conditions using the LLNL methodology (all ground-motion Experts). 3–17
3-14 Peak ground acceleration hazard curves for Paducah computed by LLNL for rock conditions using the LLNL methodology (excluding ground-motion Expert 5). 3–18
3-15 Median uniform-hazard spectra for Paducah computed by LLNL for rock conditions using the LLNL methodology (excluding ground-motion Expert 5). 3–19
3-16 Peak ground acceleration hazard curves for Paducah computed by LLNL for soil conditions using the LLNL methodology (all ground-motion experts). 3–20
3-17 Median uniform-hazard spectra for Paducah computed by LLNL for soil conditions using the LLNL methodology (all ground-motion experts). 3–21
3-18 Peak ground acceleration hazard curves for Paducah computed by LLNL for soil conditions using the LLNL methodology (excluding ground-motion Expert 5). 3–22

3-19 Median uniform-hazard spectra for Paducah computed by LLNL for soil conditions using the LLNL methodology (excluding ground-motion Expert 5). 3–23

4-1 Representation of the EPRI/SOG results as 30 equally weighted hazard curves. These results correspond to rock site conditions. 4–4

4-2 Discrete distribution representing uncertainty in the annual probability of exceeding 0.2 g PGA, as evaluated by the EPRI/SOG methodology 4–5

4-3 Discrete distribution representing uncertainty in the annual probability of exceeding 0.2 g PGA, as evaluated by the LLNL methodology 4–6

4-4 Discrete distribution representing uncertainty in the annual probability of exceeding 0.2 g PGA, as obtained by combining the EPRI/SOG and LLNL methodologies with equal weights 4–7

4-5 Peak-acceleration hazard curves for Paducah (for rock site conditions) obtained by combining results from the EPRI/SOG and LLNL (all ground-motion Experts) methodologies. 4–8

4-6 Median uniform-hazard spectra for Paducah (for rock site conditions) obtained by combining results from the EPRI/SOG and LLNL (all ground-motion Experts) methodologies. 4–9

4-7 Peak-acceleration hazard curves for Paducah (for rock site conditions) obtained by combining results from the EPRI/SOG and LLNL (excluding ground-motion Expert 5) methodologies. 4–10

4-8 Median uniform-hazard spectra for Paducah (for rock site conditions) obtained by combining results from the EPRI/SOG and LLNL (excluding ground-motion Expert 5) methodologies. 4–11

4-9 Peak-acceleration hazard curves for Paducah (for soil site conditions) obtained by combining results from the EPRI/SOG and LLNL (all ground-motion experts) methodologies. 4–12

4-10 Median uniform-hazard spectra for Paducah (for soil site conditions) obtained by combining results from the EPRI/SOG and LLNL (all ground-motion experts) methodologies. 4–13

4-11 Peak-acceleration hazard curves for Paducah (for soil site conditions) obtained by combining results from the EPRI/SOG and LLNL (excluding ground-motion Expert 5) methodologies. 4–14

4-12 Median uniform-hazard spectra for Paducah (for soil site conditions) obtained by combining results from the EPRI/SOG and LLNL (excluding ground-motion Expert 5) methodologies. 4–15

5-1 Type A faults in New Madrid region 5–4

5-2 Type B faults in New Madrid region 5–5

5-3 Type C faults in New Madrid region 5–6

5-4 Type D faults in New Madrid region 5–7

5-5 Type E faults in New Madrid region 5–8

5-6 Regions used for analysis of seismicity for Type A, B, C, and E faults. 5–10

5-7 Regions used for analysis of seismicity for Type D faults. 5–11

5-8 Observed and modeled seismicity for New Madrid fault types A, B, C, and E. 5–13

5-9 Observed and modeled seismicity for New Madrid fault type D. 5–14

5-10 Observed and modeled seismicity for Southern Illinois source. 5–15

5-11 Ground motions models used for the New Madrid source in the extended-source seismic-hazard calculations: predictions for 0.5-Hz spectral velocity 5–19

5-12 Ground motions models used for the New Madrid source in the extended-source seismic-hazard calculations: predictions for 1-Hz spectral velocity 5–20

5-13 Ground motions models used for the New Madrid source in the extended-source seismic-hazard calculations: predictions for 2.5-Hz spectral velocity 5–21

5-14 Ground motions models used for the New Madrid source in the extended-source seismic-hazard calculations: predictions for 5-Hz spectral velocity 5–22

5-15 Ground motions models used for the New Madrid source in the extended-source seismic-hazard calculations: predictions for 10-Hz spectral velocity 5–23

5-16 Ground motions models used for the New Madrid source in the extended-source seismic-hazard calculations: predictions for 25-Hz spectral velocity 5–24

5-17 Ground motions models used for the New Madrid source in the extended-source seismic-hazard calculations: predictions for peak ground acceleration 5–25

5-18 Peak ground acceleration hazard curves for Paducah (for rock site conditions) computed from the extended-source hazard analysis. 5–29

5-19 0.5-Hz spectral velocity hazard curves for Paducah (for rock site conditions) computed from the extended-source hazard analysis. 5–30

5-20 1-Hz spectral velocity hazard curves for Paducah (for rock site conditions) computed from the extended-source hazard analysis. 5–31

5-21 2.5-Hz spectral velocity hazard curves for Paducah (for rock site conditions) computed from the extended-source hazard analysis. 5–32

5-22 5-Hz spectral velocity hazard curves for Paducah (for rock site conditions) computed from the extended-source hazard analysis. 5–33

5-23 10-Hz spectral velocity hazard curves for Paducah (for rock site conditions) computed from the extended-source hazard analysis. 5–34

5-24 25-Hz spectral velocity hazard curves for Paducah (for rock site conditions) computed from the extended-source hazard analysis. 5–35

5-25 Median uniform-hazard spectra for Paducah (5 % damping; rock site conditions) computed from the extended-source hazard analysis. Results shown as uniform hazard spectra. 5–36

5-26 Median uniform-hazard spectra for Paducah (2 % damping; rock site conditions) computed from the extended-source hazard analysis. Results shown as uniform hazard spectra. 5–37

5-27 Median uniform-hazard spectra for Paducah (7 % damping; rock site conditions) computed from the extended-source hazard analysis. Results shown as uniform hazard spectra. 5–38

5-28 Median uniform-hazard spectra for Paducah (10 % damping; rock site conditions) computed from the extended-source hazard analysis. Results shown as uniform hazard spectra. 5–39

5-29 Median uniform-hazard spectra for Paducah (12 % damping; rock site conditions) computed from the extended-source hazard analysis. Results shown as uniform hazard spectra. 5–40

5-30 Median uniform-hazard spectra for Paducah (15 % damping; rock site conditions) computed from the extended-source hazard analysis. Results shown as uniform hazard spectra. 5–41

6-1 Magnitude of earthquakes that dominate the hazard for 1-Hz spectral velocity. Results shown as a function of amplitude. 6–5

6-2 Magnitude of earthquakes that dominate the hazard for 1-Hz spectral velocity. Results shown as a function of hazard. 6–5

6-3 Distance of earthquakes that dominate the hazard for 1-Hz spectral velocity. Results shown as a function of amplitude. 6–6

6-4 Distance of earthquakes that dominate the hazard for 1-Hz spectral velocity. Results shown as a function of hazard. 6–6

6-5 Magnitude of earthquakes that dominate the hazard for peak acceleration. Results shown as a function of amplitude. 6–7

6-6 Magnitude of earthquakes that dominate the hazard for peak acceleration. Results shown as a function of hazard. 6–7

6-7 Distance of earthquakes that dominate the hazard for peak acceleration. Results shown as a function of amplitude. 6–8

6-8 Distance of earthquakes that dominate the hazard for peak acceleration. Results shown as a function of hazard. 6–8

6-9 Artificial time history for a return period of 500 years; first horizontal component. 6–9

6-10 Response spectra from artificial time history for a return period of 500 years; first horizontal component 6–10

6-11 Artificial time history for a return period of 500 years; second horizontal component. 6–11

6-12 Response spectra from artificial time history for a return period of 500 years; second horizontal component 6–12

6-13 Artificial time history for a return period of 500 years; vertical component. 6–13

6-14 Response spectra from artificial time history for a return period of 500 years; vertical component 6–14

6-15 Artificial time history for a return period of 1000 years; first horizontal component. 6–15

6-16 Response spectra from artificial time history for a return period of 1000 years; first horizontal component 6–16

6-17 Artificial time history for a return period of 1000 years; second horizontal component. 6–17

6-18 Response spectra from artificial time history for a return period of 1000 years; second horizontal component 6–18

6-19 Artificial time history for a return period of 1000 years; vertical component. 6–19

6-20 Response spectra from artificial time history for a return period of 1000 years; vertical component 6–20

6-21 Artificial time history for a return period of 5000 years; first horizontal component. 6–21

6-22 Response spectra from artificial time history for a return period of 5000 years; first horizontal component 6–22

6-23 Artificial time history for a return period of 5000 years; second horizontal component. 6–23

6-24 Response spectra from artificial time history for a return period of 5000 years; second horizontal component 6–24

6-25 Artificial time history for a return period of 5000 years; vertical component. 6–25

6-26 Response spectra from artificial time history for a return period of 5000 years; vertical component 6–26

6-27 Cumulative energy plot for the 500-year artificial ground motions 6–27

6-28 Cumulative energy plot for the 1000-year artificial ground motions 6–28

6-29 Cumulative energy plot for the 5000-year artificial ground motions 6–29

A-1 Typical stochastic Brune displacement pulse A–3

A-2 Typical acceleration time history generated with the ground-motion simulation model A–4

A-3 Attenuation of peak acceleration with distance for m_{Lg} 7.6 and multiple combinations of event characteristics and azimuths. A–8

A-4 Attenuation of peak acceleration with distance for m_{Lg} 6.6 and multiple combinations of event characteristics and azimuths. A–9

A-5 Attenuation of peak acceleration with distance for California earthquakes with magnitudes comparable to m_{Lg} 7.6, according to the attenuation functions by Campbell and by Joyner and Boore. A–10

LIST OF TABLES

Table		Page
2-1	EPRI/SOG Earth-Science Teams	2–2
2-2	Summary of Bechtel Team Sources Near the Paducah Site	2–21
2-3	Summary of Dames and Moore Team Sources Near the Paducah Site	2–22
2-4	Summary of Law Engineering Team Sources Near the Paducah Site	2–23
2-5	Summary of Rondout Associates Team Sources Near the Paducah Site	2–24
2-6	Summary of Weston Geophysical Team Sources Near the Paducah Site	2–25
2-7	Summary of Woodward-Clyde Consultants Team Sources Near the Paducah Site	2–26
2-8	Attenuation Equations Used in the EPRI/SOG Calculations	2–29
2-9	Soil Categories and Depth Ranges	2–30
2-10	Screening of Seismic Sources: Bechtel Team	2–46
2-11	Screening of Seismic Sources: Dames and Moore Team	2–47
2-12	Screening of Seismic Sources: Law Engineering Team	2–48
2-13	Screening of Seismic Sources: Rondout Associates Team	2–49
2-14	Screening of Seismic Sources: Weston Geophysical Team	2–50
2-15	Screening of Seismic Sources: Woodward-Clyde Team	2–51
2-16	Sources used for Seismic Hazard Calculations	2–52
2-17	Source Combinations and Their Probabilities	2–53
2-18	Summary of Sources Contributing to the Seismic Hazard in the EPRI/SOG Calculations	2–64
5-1	Summary of EPRI and LLNL Seismic Zonations near Paducah	5–3
5-2	Estimates of Seismicity Parameters	5–12
5-3	Strong-Motion Durations used with Equation 5–3	5–27
6-1	Expected Magnitudes and Distances	6–2
6-2	Duration of Characteristic Ground Motions	6–4

7-1 Ground-Motion Amplitudes for Selected Values of the Median Annual Exceedance Probability 7–2

A-1 Characteristics of Whole Events and Sub-Events A–4
A-2 Event-Azimuth Codes used in Figures A–3 and A–4 A–6

B-1 Peak ground acceleration hazard curves (rock site conditions) B–1
B-2 0.5-Hz spectral velocity hazard curves (rock site conditions) B–1
B-3 1-Hz spectral velocity hazard curves (rock site conditions) B–2
B-4 2.5-Hz spectral velocity hazard curves (rock site conditions) B–2
B-5 5-Hz spectral velocity hazard curves (rock site conditions) B–3
B-6 10-Hz spectral velocity hazard curves (rock site conditions) B–3
B-7 25-Hz spectral velocity hazard curves (rock site conditions) B–4
B-8 Median uniform-hazard spectra (rock site conditions) B–4
B-9 Peak ground acceleration hazard curves (soil site conditions) B–5
B-10 0.5-Hz spectral velocity hazard curves (soil site conditions) B–5
B-11 1-Hz spectral velocity hazard curves (soil site conditions) B–6
B-12 2.5-Hz spectral velocity hazard curves (soil site conditions) B–6
B-13 5-Hz spectral velocity hazard curves (soil site conditions) B–7
B-14 10-Hz spectral velocity hazard curves (soil site conditions) B–7
B-15 25-Hz spectral velocity hazard curves (soil site conditions) B–8
B-16 Median uniform-hazard spectra (soil site conditions) B–8
B-17 Peak ground acceleration hazard curves (rock, all LLNL G-experts) B–9
B-18 Median uniform-hazard spectra (rock, all LLNL G-experts) B–9
B-19 Peak ground acceleration hazard curves (rock, 4 LLNL G-experts) B–10
B-20 Median uniform-hazard spectra (rock, 4 LLNL G-experts) B–10
B-21 Peak ground acceleration hazard curves (soil, all LLNL G-experts) B–11
B-22 Median uniform-hazard spectra (soil, all LLNL G-experts) B–11
B-23 Peak ground acceleration hazard curves (soil, 4 LLNL G-experts) B–12
B-24 Median uniform-hazard spectra (soil, 4 LLNL G-experts) B–12
B-25 Peak ground acceleration hazard curves B–13
B-26 0.5-Hz spectral velocity hazard curves B–13
B-27 1-Hz spectral velocity hazard curves B–14
B-28 2.5-Hz spectral velocity hazard curves B–14

B-29 5-Hz spectral velocity hazard curves B–15
B-30 10-Hz spectral velocity hazard curves B–15
B-31 25-Hz spectral velocity hazard curves B–16
B-32 Median uniform-hazard spectra (5% damping) B–16
B-33 Median uniform-hazard spectra (other damping ratios) B–17

Section 1
INTRODUCTION

This study investigates the probabilistic hazard of earthquake-induced ground shaking at the Paducah Gaseous Diffusion Plant, near Paducah, Kentucky. These results will be used to make decisions regarding seismic safety and levels of seismic design at the facility. An express purpose of this study is to use as a guideline the most recent studies of seismic hazard in the eastern US, which represent uncertainty in the seismic hazard caused by multiple, alternative hypotheses on the causes and characteristics of earthquakes.

Recent intensive studies of seismic hazard in the central and eastern United States (CEUS) have been completed by the Electric Power Research Institute (EPRI), funded by the Seismicity Owners Group (1), and by the Lawrence Livermore National Laboratory (LLNL), funded by the U.S. Nuclear Regulatory Commission (2). These studies represent major efforts to characterize the seismic hazard for nuclear power plants in the CEUS, and use the most recent, up-to-date understandings of seismicity and ground motion relations for the region.

These two studies are not directly applicable to the Paducah site because they treat earthquakes of all magnitudes as point sources. That is, these studies do not consider the rupture size associated with large earthquakes similar to the New Madrid, Missouri, earthquakes of 1811 and 1812. In this study a special seismic-hazard analysis is performed that considers the extent and orientation of ruptures from large earthquakes in the New Madrid region. Like the EPRI and LLNL studies, this finite–rupture analysis considers multiple alternative interpretations in order to characterize uncertainty in the seismic hazard.

Results from the EPRI and LLNL studies are used to quantify the relative contributions of the various seismic sources to the total seismic hazard. These studies also serve as a basis for the development of the geometry of faults in the Mississippi embayment and for seismicity parameters for all relevant sources in the region of the Paducah site.

The Paducah facility is located at latitude 37.12 north and longitude 88.82 west. Structures at the site are founded on deep soil, of approximately 360-foot thickness. Consistent with

other recent seismic hazard analyses, we report the distribution of peak horizontal ground acceleration (PGA) and spectral velocities (PSV) at multiple frequencies; we also show constant hazard spectra to demonstrate typical spectral amplitudes and shapes that might apply for earthquake ground motions of interest.

Section 2 of this report summarizes the application of the EPRI methodology for the Paducah site that was conducted under this study. The LLNL method was applied for the site by LLNL, who transmitted results to us for use in this analysis. Their results and our interpretation of them are described in Section 3. The synthesis of the results of the two studies is described in Section 4. Section 5 documents the application of the extended-source seismic-hazard analysis to the Paducah site, including the development of seismic sources, the selection of seismicity parameters and maximum magnitudes, and the selection of ground-motion attenuation functions. Section 6 investigates the characteristics of earthquakes that dominate the hazard at Paducah and generates the corresponding artificial ground motions. Finally, Section 7 presents conclusions of the study and some important qualifications to these results.

1.1 REFERENCES

1. *Seismic Hazard Methodology for the Central and Eastern United States.* Technical Report NP-4726-A, Electric Power Research Institute, July 1986. Revised, 1988. Vol. 1, Part 1: Methodology, Vol. 1, Part 2: Theory, Vol. 2: EQHAZARD Programmer's Manual, Vol. 3: EQHAZARD User's Manual, Vol. 4: Applications, Vols. 5 through 10: Tectonic Interpretations, Vol. 11: Nuclear Regulatory Commission Safety Review.

2. D. L. Bernreuter, J. B. Savy, R. W. Mensing, and J. C. Chen. *Seismic Hazard Characterization of 69 Plant Sites East of the Rocky Mountains.* Technical Report NUREG/CR5250, UCID-21517, U. S. Nuclear Regulatory Commission, 1988.

Section 2

EPRI/SOG METHODOLOGY AND RESULTS

2.1 INTRODUCTION

This Section describes the EPRI/SOG methodology and inputs for seismic-hazard analysis in the central and eastern United States (CEUS), documents the application of these for the Paducah site, and presents the results obtained from this application.

Two sets of results will be generated using the EPRI/SOG methodology; i.e, for rock and for generic deep-soil site conditions (EPRI soil category IV). These results will be combined in Section 4 with the corresponding results from the LLNL analysis, to generate aggregate seismic-hazard results for rock and soil site conditions.

The EPRI/SOG methodology calculates ground-motion exceedance probabilities using earth-science hypotheses about the causes and characteristics of earthquakes in the central and eastern United States. Scientific uncertainty about the causes of earthquakes and about the physical characteristics of potentially active tectonic features lead to uncertainties in the inputs to the seismic hazard calculations. These uncertainties are quantified by using the tectonic interpretations developed by six Earth Science Teams, who quantified the likelihood associated with alternative tectonic features and the likelihood associated with alternative characteristics of these potential sources.

These and other uncertainties are carried through the entire analysis. The result of the analysis is a suite of hazard curves and their associated weights; they quantify the seismic hazard at the site and its uncertainty.

Each team was comprised of at least four members with expertise in different earth-science disciplines. Table 2–1 lists the six teams and their members.

2.2 EPRI/SOG METHODOLOGY

2.2.1 Basic Seismic Hazard Model

The methodology to calculate seismic hazard at a site is well established in the literature (1,2,3,4,5). In the EPRI/SOG methodology, calculation of the hazard contributed by one source requires specification of three inputs:

Table 2-1

EPRI/SOG Earth-Science Teams

Team	Members
Bechtel Group, Inc.	Thomas Buschbach Robert D. Hatcher, Jr. Joseph Litehiser† Rolfe Stanley Isidore Zietz
Dames and Moore	Charles Fairhurst Robert Herrmann Lyle McGinnis James McWhorter† Rene Rodriguez
Law Engineering Testing Company	Robert Butler Martin Chapman John Dwyer Arch Johnston Timothy Long Malcolm Schaeffer William Seay Robert White†
Rondout Associates, Inc.	Noël Barstow† William Hinze Pradeep Talwani Barry Voight
Weston Geophysical Corporation	Richard Holt George Klimkiewicz† Gabriel LeBlanc Donald Wise
Woodward-Clyde Consultants	Terry Engelder John Kelleher Richard Quittmeyer Thomas Statton† Thomas Turcotte

†TeamLeader

1. Source geometry: the geographic description of the seismic source. A seismic source is a portion of the earth's crust, associated with a tectonic feature or with a concentration of historic seismicity, which may be capable of producing earthquakes. Source geometry determines the probability distribution of distance from the earthquake to the site: $f_R(r)$. In the EPRI/SOG methodology, each seismic source is divided into cells of 1 degree latitude by 1 degree longitude and $f_{R(i)}(r)$ is computed for each cell.

2. Seismicity: the rate of occurrence ν_i and magnitude distribution $f_{M(i)}(m)$ of earthquakes within each cell. Magnitude is characterized by the body-wave magnitude m_b.

3. Attenuation functions: a relationship that allows the estimation of ground motion at the site as a function of earthquake magnitude and distance.

These inputs are illustrated in Figure 2–1, parts a through c. Figure 2–1a shows the geometry of a seismic source and a cell within that source. From the cell's geometry, $f_{R(i)}(r)$, can be derived. The density function on magnitude $f_{M(i)}(m)$ is the doubly truncated exponential distribution as shown in figure 2-1b. Seismicity in a cell is completely specified by a minimum magnitude m_0, a maximum magnitude m_{max}, and parameters a and b. a is a measure of seismic activity per unit area, b is a measure of relative frequency of large versus small events, and $\log[\nu_i f_{M(i)}(m)]$ is proportional to $a + b\ m$ for $m_0 < m \leq m_{max}$. The ground motion is modeled by an attenuation function, as illustrated in figure 2-1c. Attenuation functions are usually of the form $\ln[Y] = f(M, R) + \epsilon$, where Y is ground-motion amplitude, M is magnitude, R is distance, and ϵ is a random variable that represents scatter. The attenuation function is used to calculate $G_{Y|m,r}(y) = P[Y > y|m, r]$: the probability that the ground-motion amplitude be larger than y, for given M and R. The seismic hazard contributed by a source is calculated as :

$$\frac{P[Y > y \text{ in time } t]}{t} \simeq \sum_i \nu_i \int\int P[Y > y|m, r]\ f_{M(i)}(m)\ f_{R(i)}(r)\ dm\ dr \qquad (2-1)$$

in which the summation is performed over all cells that comprise the source.

Equation 2–1 is formulated using the assumption that earthquakes (most particularly, successive earthquakes) are independent in size and location. In all seismic hazard applications, primary interest is focused on computing probabilities for high (rare) ground motions (as a result, the probability of two exceedances in time t is negligible). Thus, the quantity on the right side of Equation 2–1 — which is the rate of earthquakes with $Y > y$ — is a good approximation to the probability of exceeding amplitude y in time t. The same argument

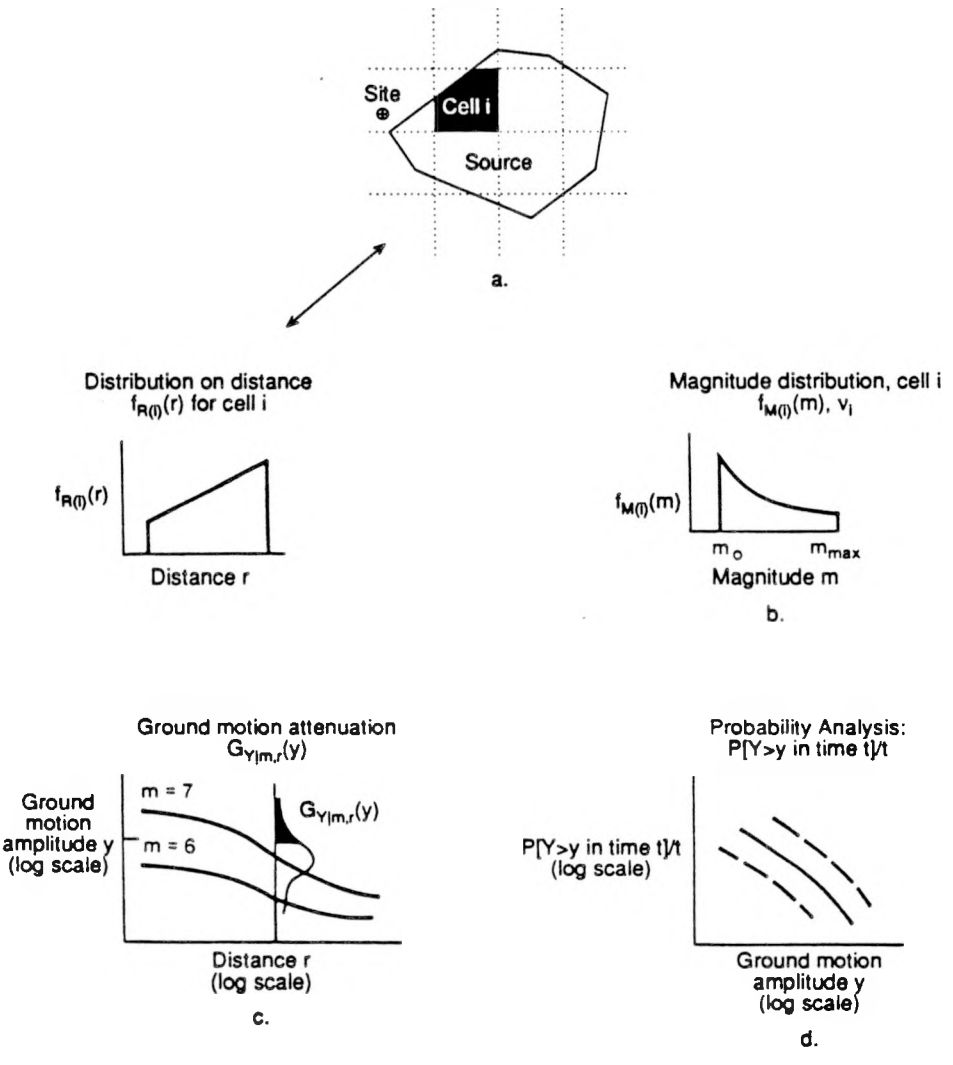

Figure 2-1. Seismic hazard computational model. Source: (6).

holds when considering hazard at a site from multiple sources. Terms similar to the right hand side of Equation 2–1 are summed to compute, to very good approximation, the total hazard at the site (see Figure 2–1d).

The calculation of hazard from all sources is performed for multiple values of y in order to generate the hazard curve, which gives the annual probability of exceedance as a function of y. This calculation is performed for 6 different measures of ground motion: peak ground acceleration and spectral velocities at 5 frequencies (1, 2.5, 5, 10, 25 Hz; 5% damping).

2.2.2 Treatment of Uncertainty

The most recent seismic-hazard studies distinguish between two types of variability: randomness and uncertainty. Randomness is probabilistic variability that results from natural physical processes. The size, location and time of the next earthquake on a fault and the details of the ground motion are examples of random events. In concept, these elements cannot be predicted even with collection of additional data, so the randomness component of variability is irreducible. The second category of variability is "uncertainty" which is the statistical or modeling variability that result from lack of knowledge about the true state of nature. In principle, this variability can be reduced with the collection of additional data.

These two types of variability are treated differently in advanced seismic hazard studies, as follows: integration is carried out over probabilistic variabilities to get a single hazard curve (see equation 2–1), whereas modeling uncertainties are expressed by multiple assumptions, hypotheses, or parameter values. These multiple interpretations result in a suite of hazard curves and their associated weights.

There are uncertainties associated with each of the three inputs to the seismic-hazard evaluation, as follows:

- Uncertainty about seismic sources (i.e., which tectonic features in a region are actually earthquake sources) arises because there are multiple hypotheses about the causes of earthquakes in EUS and because there is incomplete knowledge about the physical characteristics of tectonic features. Uncertainty may also arise about the geometry of a seismic source.
- Uncertainty in seismicity is generally divided into uncertainty in maximum magnitude and uncertainty in seismicity parameters a and b. Uncertainty about, m_{max}, the maximum magnitude that a given source can generate arises for the same reasons

described above. Estimates of m_{max} are obtained from physical characteristics of the source and from historic seismicity. Uncertainty in seismicity parameters a and b arises from statistical uncertainty and from uncertainty about the variability of a and b between cells in a given source.

- Uncertainty in the attenuation functions arises from alternative hypotheses about the dynamic characteristics of earthquakes in EUS. This uncertainty has been large because there have been few strong-motion recordings from earthquakes of engineering interest in EUS.

The EPRI/SOG methodology quantifies seismic hazard and its uncertainty by using as inputs the tectonic interpretations developed by six multidisciplinary Earth-Science Teams. In addition, each team quantified its uncertainty about seismic sources, maximum magnitudes, and seismicity parameters, as follows:

- Uncertainty about seismic sources was characterized by specifying an activity probability P^a to each seismic source and specifying activity dependencies among sources in the same region.

- Uncertainty about maximum magnitude is characterized by a discrete distribution of m_{max} for each source. That is, multiple values of m_{max} are specified and given weights.

- Uncertainty about seismicity parameters is characterized by considering multiple sets of parameter values of each source, and giving them weights. Each set of parameters is computed, for instance, using different assumptions about spatial continuity of a and b, or using different portions of the earthquake catalog.

Ground-motion attenuation in EUS, and its uncertainty, is quantified by considering three alternative attenuation functions for each ground-motion measure, and giving them weights (see Section 2.4). The development and selection of these attenuation equations is documented in (7) and in Appendix A of (6).

In order to organize and display the multiple hypotheses, assumptions, parameter values and their possible combinations, a logic tree approach is used. Logic trees are a convenient means to express alternative interpretations and their probabilities.

Each level of the logic tree represents one source of uncertainty. The branches emanating from one node represent possible values of a parameter. The probability assigned to a branch represents the likelihood of the parameter value associated with that branch, given certain values of the preceding parameters.

The logic tree in Figure 2–2 represents the treatment of parameter uncertainty in the EPRI/SOG methodology, for one team. Associated with each terminal node, there is one hazard curve, which corresponds to certain sources being active, each active source having a certain m_{max} and certain seismicity parameters, and a certain attenuation function being the true attenuation model. The probability associated with that end branch is the product of the probabilities of all branches traversed to reach that terminal node.

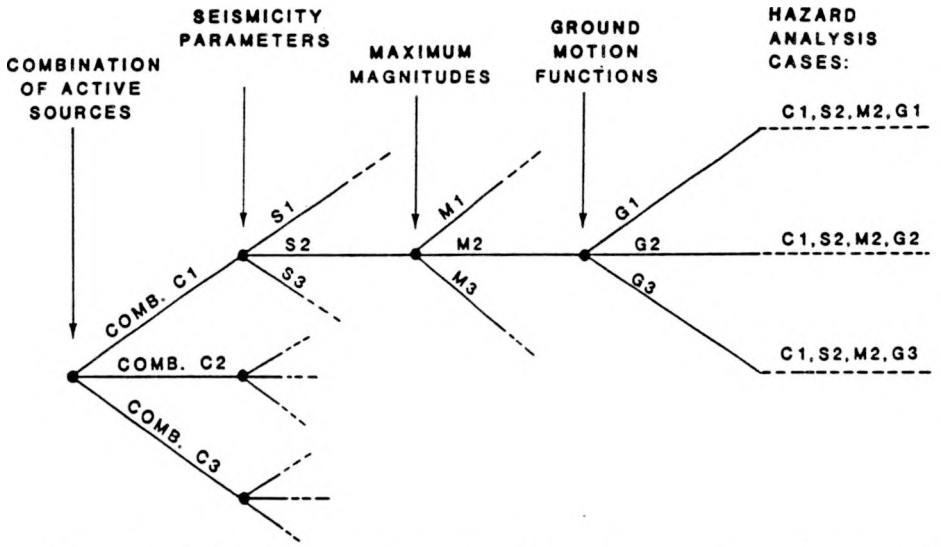

Figure 2-2. Logic tree representation of uncertain parameters in the EPRI/SOG methodology

The hazard curves obtained by the 6 teams are given equal weights and then combined. The resulting family of hazard curves and their associated probabilities, corresponding to all end branches of the six teams' logic trees, contains all the information about seismic hazard at the site, its uncertainty, and the different contributors to that uncertainty.

2.2.3 Development of Seismological Interpretations

This section briefly describes the development of the EPRI/SOG seismic sources and the estimation of their parameters; a complete description is found in Volume 1, Sections 3 and 4, of (8). Volumes 5 through 10 of (8) document the seismological interpretations by the six Earth-Science Teams. Section 2.3 describes the seismic sources that contribute to hazard at the Paducah site, and the characteristics of these sources.

Seismic Sources. In the EPRI/SOG methodology, seismic sources have the following characteristics:

- A seismic source is associated with potentially active tectonic features or with a cluster of seismicity.
- The entire source is either active or inactive.
- Every point within the source has the same maximum magnitude.
- The seismic source is composed of individual cells (1 degree latitude by 1 degree longitude). Seismicity parameters a and b may be specified separately for each cell within the source.

The EPRI/SOG seismic sources were developed using the tectonic framework: a structured approach to identify tectonic features that may be capable of generating earthquakes, interpret scientific knowledge concerning the causative mechanisms of earthquakes in EUS, delineate seismic sources, and assess probabilities of activity (P^a) for these sources.

In addition, the teams assessed joint activity probabilities for multiple sources in the same region. In most cases, the Teams specified joint activity probabilities through simple forms of dependence, such as perfect dependence or mutual exclusivity. Activity dependencies have no effect on the mean hazard (because the total hazard is a linear combination of source hazards), but they have an effect on uncertainty. Perfect dependence produces the highest uncertainty, mutual exclusivity produces the lowest uncertainty.

Seismicity Parameters. Seismicity parameters a and b are estimated using the maximum likelihood method. Parameters a and b (especially a) may be allowed to vary spatially within a seismic source. For computational convenience, they are assumed to be constant within each 1-degree cell within the source. The degree of spatial variability (or smoothing) of a and b between adjacent cells in each source is controlled by the seismicity option. Each team captured uncertainty on the appropriate degree of smoothing for each source (i.e., whether the source has homogeneous seismicity or if the activity rates follow the within-source pattern of historic activity) by specifying alternative seismicity options, with associated probabilities. In addition, the teams could specify a prior distribution (in the Bayesian sense) on b, and other parameters of the estimation algorithm, with each seismicity option.

Maximum Magnitudes. To calculate seismic hazard at a site, the largest possible earthquake magnitude that can occur in each seismic source must be estimated. This maximum magnitude m_{max} is generally uncertain. This uncertainty is represented by a probability distribution on the maximum magnitude that the source can generate.

Each team estimated a probability distribution of m_{max} for each active source that the team had identified. The following considerations were used to constrain the maximum-magnitude estimates:

- Physical Constraints. These approaches relate m_{max} to the size of the source or the thickness of the earth's crust.
- Historic Seismicity. These approaches involve the addition of an increment to the maximum historical magnitude, extrapolation of the magnitude-recurrence relation to some justified frequency of occurrence, and the statistical treatment of the earthquake catalog.
- Analogies With Other Sources or Regions. If one is able to identify a number of analogous sources, so that one can assume that they all have the same value of m_{max}, one can improve the precision of m_{max} estimates obtained from statistical analyses. The analyses of earthquakes in other intraplate regions of the world is another way to increase sample size. A study of this type was performed by EPRI (9,10); m_{max} values were obtained for various types of tectonic features.

The EPRI/SOG methodology uses discrete distributions to represent uncertainty in m_{max}. When a team specified continuous distributions or discrete distributions with excessive numbers of values, equivalent discrete distributions were developed.

Minimum Magnitude. The minimum magnitude m_0 introduced in Section 2.2.1 represents the smallest magnitude of interest in the hazard calculations. It is assumed that earthquakes with magnitudes lower than m_0 are incapable of causing damage. Therefore, the choice of m_0 is related to the type of facility being analyzed.

Based on the seismological characteristics of small earthquakes, analysis of structural response, and field studies of structural performance during low-intensity ground motions, it has been concluded that it is appropriate to use moment magnitude 5.0 (which corresponds to m_b approximately equal to 5.5) as the minimum magnitude for seismic-hazard calculations

(11,12). As an added measure of conservatism, the EPRI/SOG methodology uses m_b 5.0 as the minimum magnitude. This value is considered more than sufficiently conservative to compensate for the small probability that an earthquake with $m_b < 5.0$ could cause damage to an well-engineered structure.

2.2.4 Computer Codes

The computer package EQHAZARD performs seismic-hazard calculations using the EPRI/SOG methodology and seismological interpretations. This section provides a brief description of the various modules in EQHAZARD and their functions (see Figure 2–3). Volumes 2 and 3 of (8) contain a detailed description of these computer codes.

Modules for the Development of a Homogeneous Earthquake Catalog. The development of a homogeneous earthquake catalog is performed by five modules: CREINP, EQCONVERT, UNIMAG, EQCLUSTER, and CRECAT. These programs perform two main functions: (1) calculate a uniform value of m_b for each earthquake, using all size measures available (e.g., m_b, M_L, epicentral intensity, felt area); and (2) identify and eliminate secondary events (e.g., aftershocks). The result is a catalog of main events in which earthquake size is measured by the uniform m_b.

Module for the estimation of seismicity parameters—EQPARAM. EQPARAM estimates seismicity parameters for area seismic sources, using as basic inputs the earthquake catalog, the source geometries and seismicity parameters specified by one Earth Science team, and catalog incompleteness information.

Modules for the calculation of seismic hazard. EQHAZ calculates the seismic hazard at one site from each source specified by one Earth Science team. Hazard is simultaneously calculated for several measures of ground motion. EQPOST calculates the total hazard at the site and its uncertainty for one or more Earth Science Teams, and calculates the sensitivity of seismic hazard to attenuation function, maximum magnitudes, seismicity options, and earth-science teams. EQAG calculates the group-consensus mean log hazard as a weighted sum of the teams' results for that site.

2.3 TECTONIC AND SEISMICITY INTERPRETATIONS

The specification of potential sources of future earthquakes is the first step in the evaluation of earthquake hazards. Seismic sources indicate where earthquakes may occur; analysis of historical seismicity within those defined sources indicates the probabilities of occurrence

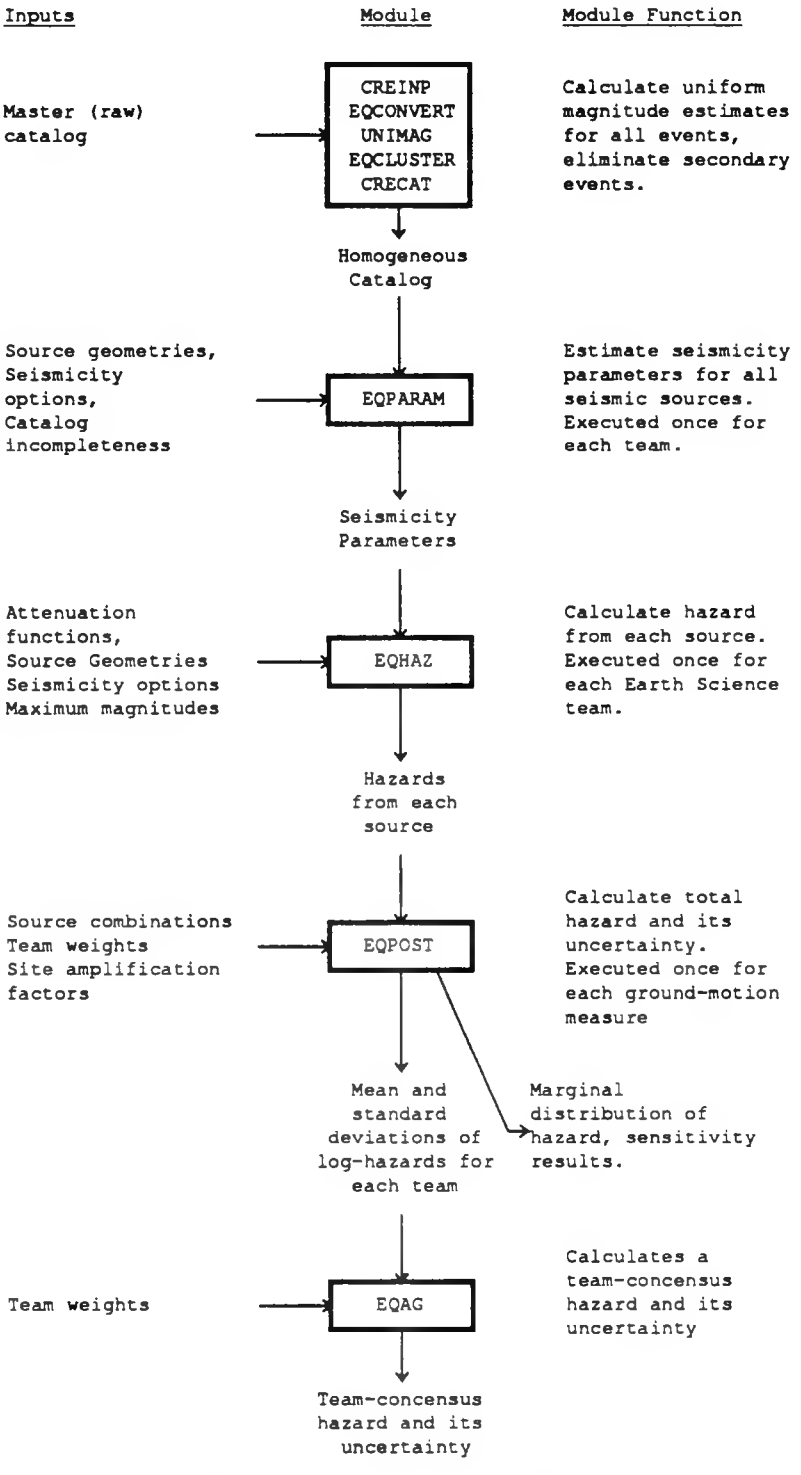

Figure 2-3. EQHAZARD modules: their functions and data flow. Source: (6).

and characteristics of future earthquakes (i.e. we fit a magnitude distribution to historical data within the source, once the source is defined).

In the EPRI/SOG methodology, a seismic source is defined as a region with a single probability of activity P^a and a single maximum magnitude (which may be uncertain). Within a seismic source the seismicity (quantified by parameters a and b) can vary in space.

In general, the sources derived by the six Teams are based on tectonic features and other evidence (including, in some cases, merely a spatial cluster of historical seismicity). Because of this derivation there is, conceptually, some causal association of earthquakes within a source: they are releasing crustal stresses of the same orientation and amplitude, and/or they are caused by slip on faults with the same general depth, orientation, and sense of slip. Because of these similarities the delineation conforms to the seismic source definition with regard to maximum magnitude and probability of activity.

This section reviews the characteristics of seismic sources in the EPRI/SOG methodology and briefly summarizes the interpretations by the 6 Teams. Volumes 5 through 10 of (8) describe and document these interpretations.

2.3.1 Seismic Sources

Sets of seismic sources were derived for the central and eastern US by the six Earth Science Teams, using the project data bases of geologic, geophysical, and seismological evidence (including historical seismicity). The bases for these derivations are given in detail in Volumes 5 through 10 of (8). During the project, multiple interpretations were encouraged, to express uncertainty on the causes of earthquakes and their physical expression in the form of seismic sources. In other words, if there were multiple theories on the physical causes of earthquakes, and these theories had different implications in terms of the regions within which future earthquakes were thought possible, the Teams were encouraged to express these uncertainties with multiple tectonic features and seismic sources. Each Team's uncertainty was quantified through its assessments of P^a for each source and a specification of the interdependency of activity (whether the state of activity of one source affects the activity of another). Five of the six Teams specified interdependencies among sources.

Joint activity probabilities were often specified through the following simple forms of dependence:

- Perfect Dependence (PD). Two sources A and B are perfectly dependent if the probability that A is active, given that B is active, is unity. This form of dependency

arises between tectonic features with the same physical characteristics (e.g., multiple faults with identical orientations).

- Independence. Two sources a and b are independent if the state of activity of source A does not affect the state of activity of source B. Mathematically, $P^a[A \text{ and } B] = P^a[A]P^a[B]$.

- Mutual Exclusivity (ME). Two sources A and B are mutually exclusive if the probability of A being active, given that B is active, is zero. Mutually exclusive sources are used to represent alternative hypotheses for the causes of seismicity in a region or uncertainty on the geographic extent of a seismic source.

- Default Sources. This is a special form of mutual exclusivity. It arises when an earthquake is known to have occurred in a region, but the candidate tectonic features (say, the features represented by sources A, B, and C) do not make a collectively exhaustive set (i.e., $P^a[A \text{ or } B \text{ or } C] < 1$). A default source D, with $P^a[D] = 1 - P^a[A \text{ or } B \text{ or } C]$ and $P[D|(A \text{ or } B \text{ or } C)] = 0$, must be added in order to have a model of seismicity that is consistent with historical seismicity.

The Weston and Woodward-Clyde teams characterized the probability of activity using P^*: the probability that the source is capable of generating earthquakes with magnitudes larger than 5. P^* and P^a are related through the distribution of maximum magnitude.

Background sources and their probabilities of activity P^a_{BG} require special description, as the interpretation is slightly different from that for primary sources. A background source represents a region where specific causes of earthquakes cannot be identified, but where a Team feels that earthquakes will occur. The regions of background sources are defined so that there is one maximum-magnitude (m_{max}) distribution for the entire source, but the interpretation of P^a_{BG} is not that the background is active with probability P^a_{BG} and inactive with probability $1 - P^a_{BG}$. Rather, P^a_{BG} represents the fraction of area of the background that is active. In the hazard calculations if the background contributes significantly the background hazard is weighted by P^a_{BG} to calculate the correct average contribution of hazard from the background.

All Teams except Dames and Moore and Rondout used background sources to some extent. P^a_{BG} was set to unity by all teams except Law Engineering. The Woodward-Clyde Consultants Team used local background sources of size 4 degrees by 4 degrees, centered at each EPRI/SOG site. For this study, we constructed a Woodward-Clyde background source centered at the Paducah site and calculated its seismicity parameters.

2.3.2 Maximum Magnitudes and Seismicity Options

Each team specified maximum magnitudes and seismicity options for each source it had identified.

Most teams specified maximum magnitudes in the form of discrete distributions with 2 to 4 values (i.e., they specified multiple alternative values of m_{max} with associated weights). The Law Engineering Team specified only one value of maximum magnitude for some sources. The Woodward-Clyde Team specified a larger number of values for all sources; these values were transformed into an equivalent discrete distribution with three values.

Each seismicity option specifies the assumptions used in the estimation of seismicity parameters a and b for that source. Each option specifies the cell-to-cell variability of a and b, the prior distribution of b, and the weight (or importance) given to small-magnitude earthquakes in the estimation process. Alternatively, a seismicity option may directly specify the values of a and b. All teams except Law and Rondout specified 2 to 4 alternative seismicity options (with associated weights) for most sources.

2.3.3 Seismic Sources near the Paducah Site

Figures 2–4 through 2–9 show the seismic sources near the Paducah site, as identified by the six Earth-Science Teams[1].

Tables 2–2 through 2–7 list those seismic sources near Paducah that contribute to seismic hazard at the site. These tables also include the sources' maximum magnitudes, seismicity options, and activity probabilities.

[1] For the sake of clarity, only the dominant sources (typically, those that contribute 10% or more to the total hazard) are included in these maps.

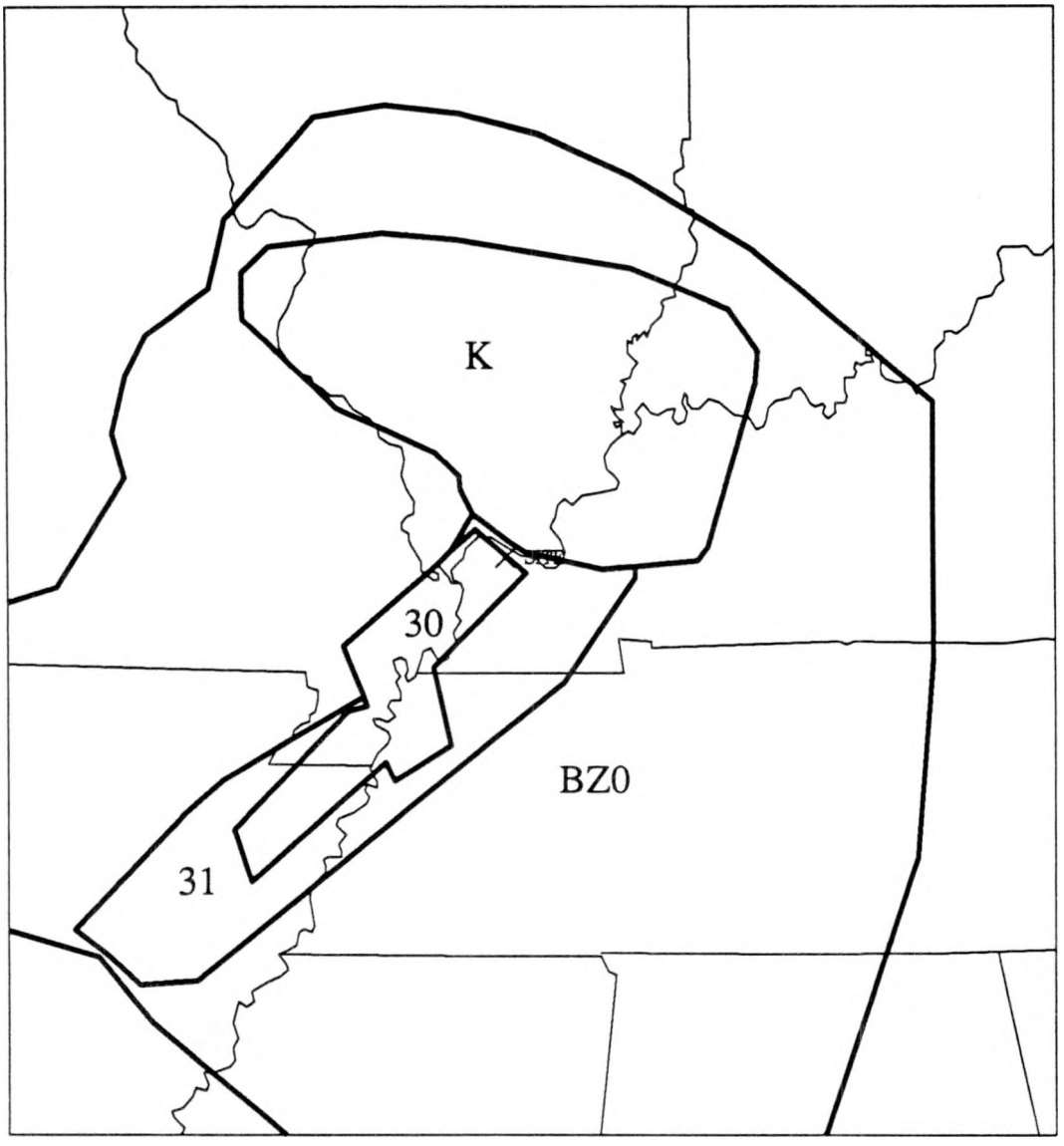

Figure 2-4. Map showing the seismic sources specified by the Bechtel team in the region around the Paducah site.

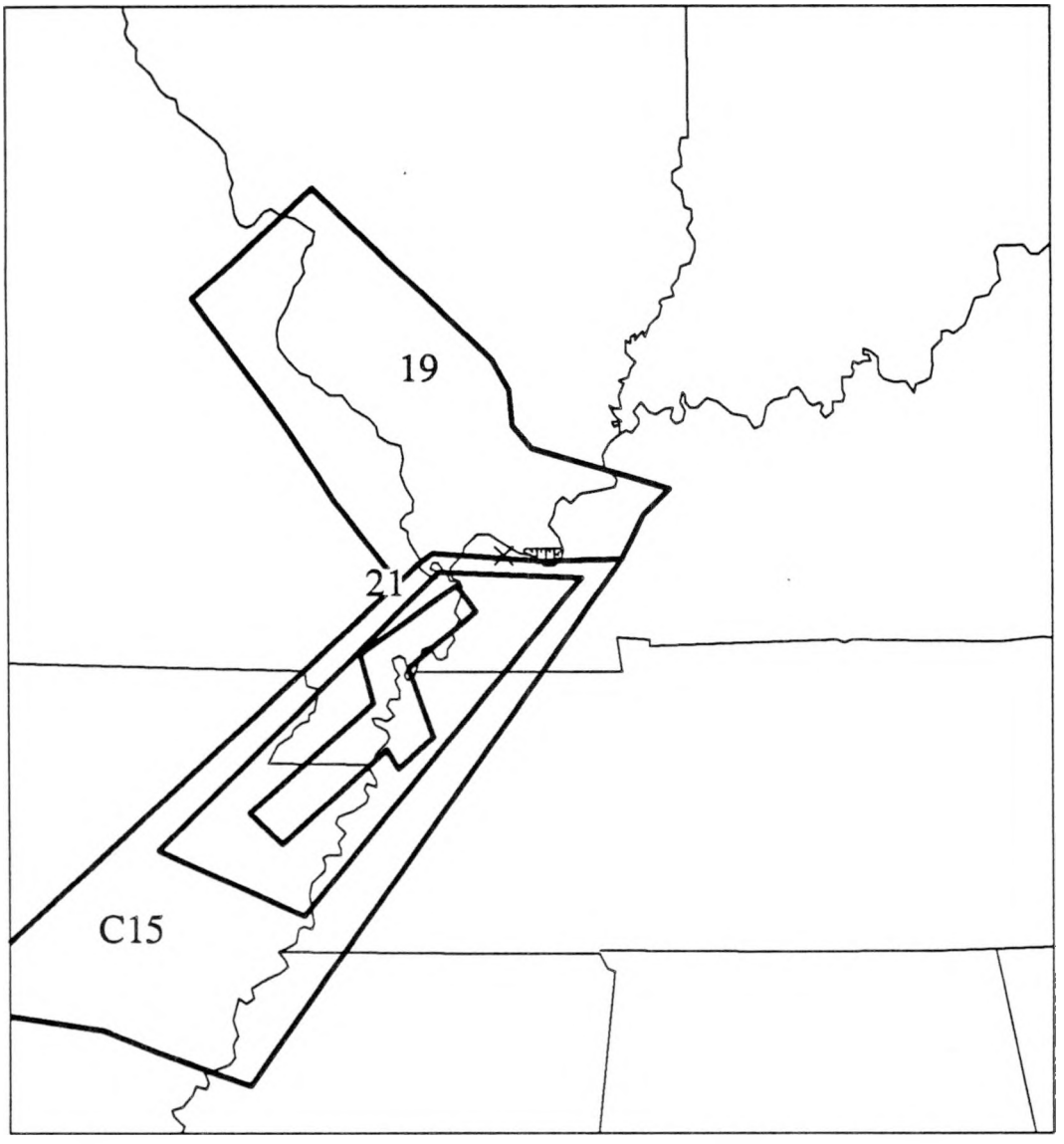

Figure 2-5. Map showing the seismic sources specified by the Dames and Moore team in the region around the Paducah Site.

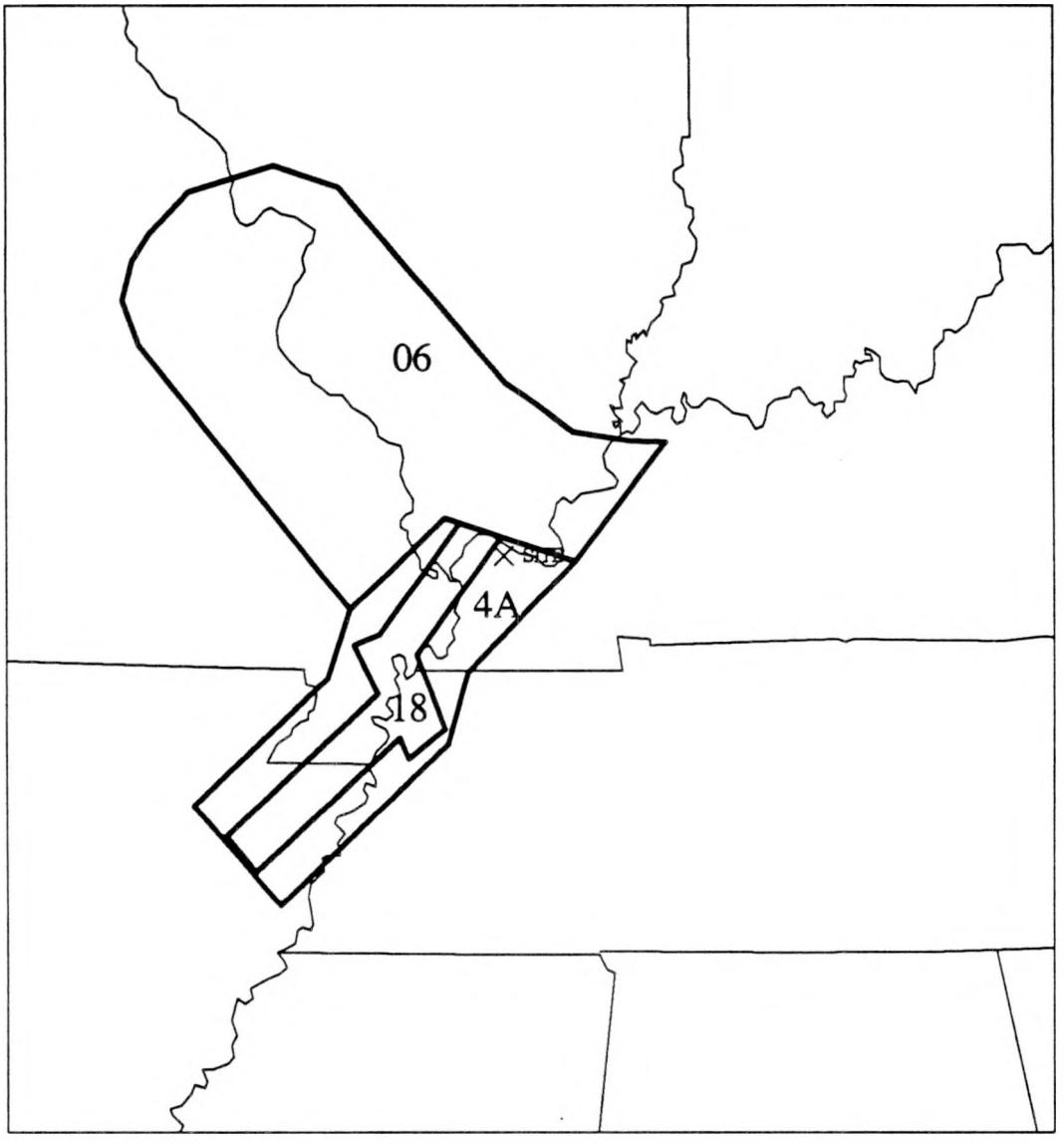

Figure 2-6. Map showing the seismic sources specified by the Law team in the region around the Paducah Site. Note: source 4B is omitted for clarity; this source is similar to source 4A, except that it extends further to the southwest.

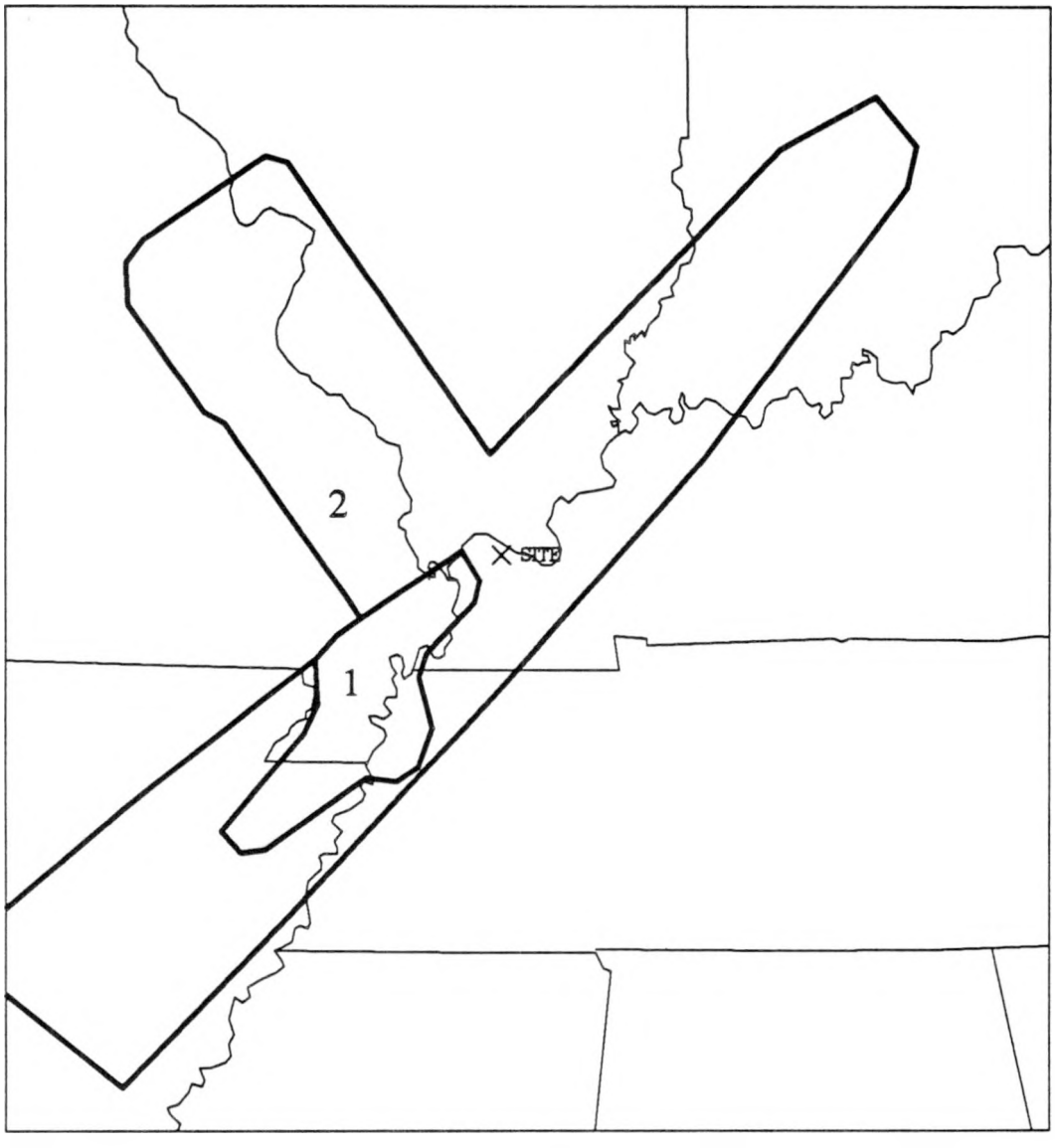

Figure 2-7. Map showing the seismic sources specified by the Rondout team in the region around the Paducah Site.

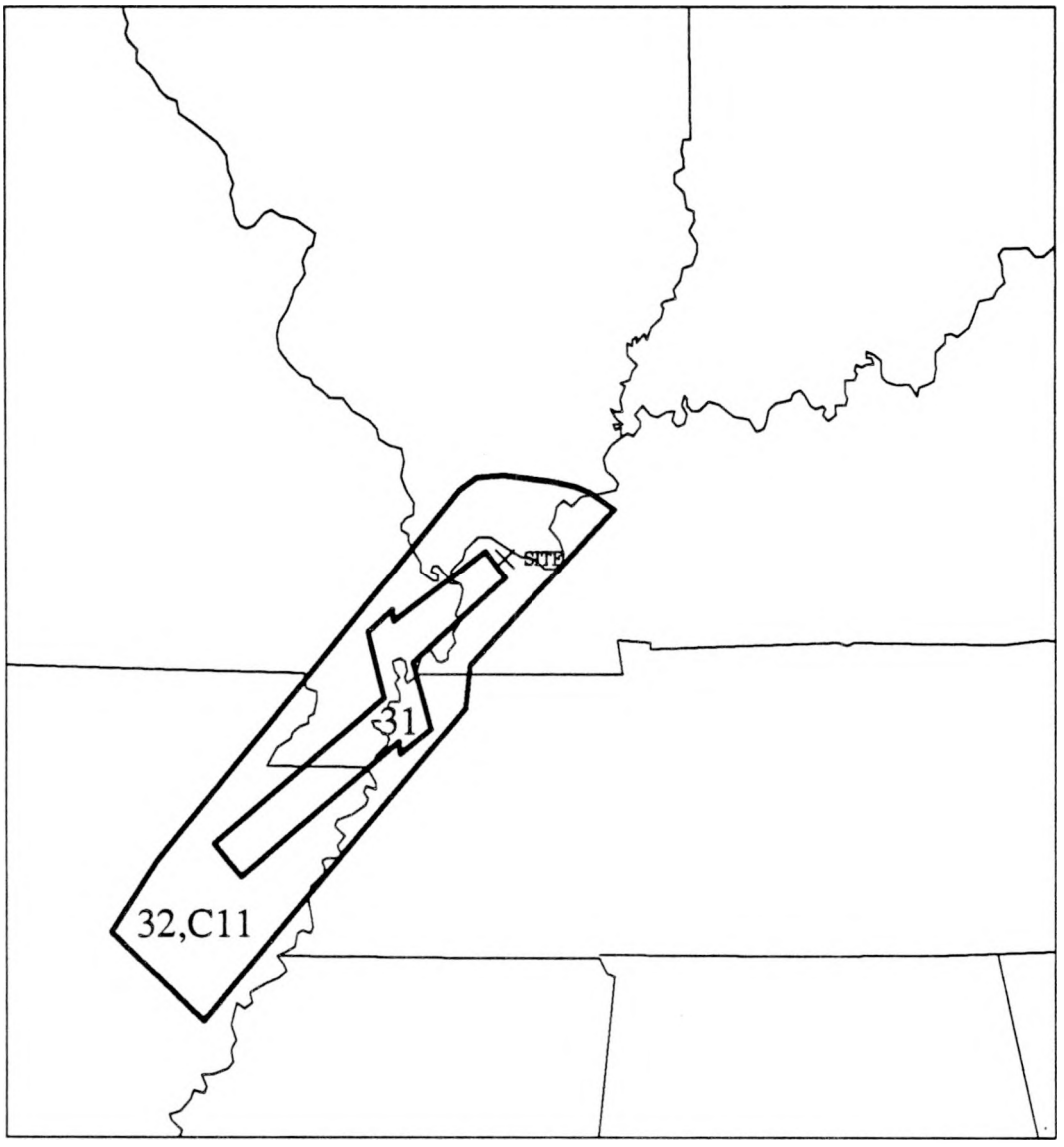

Figure 2-8. Map showing the seismic sources specified by the Weston team in the region around the Paducah Site.

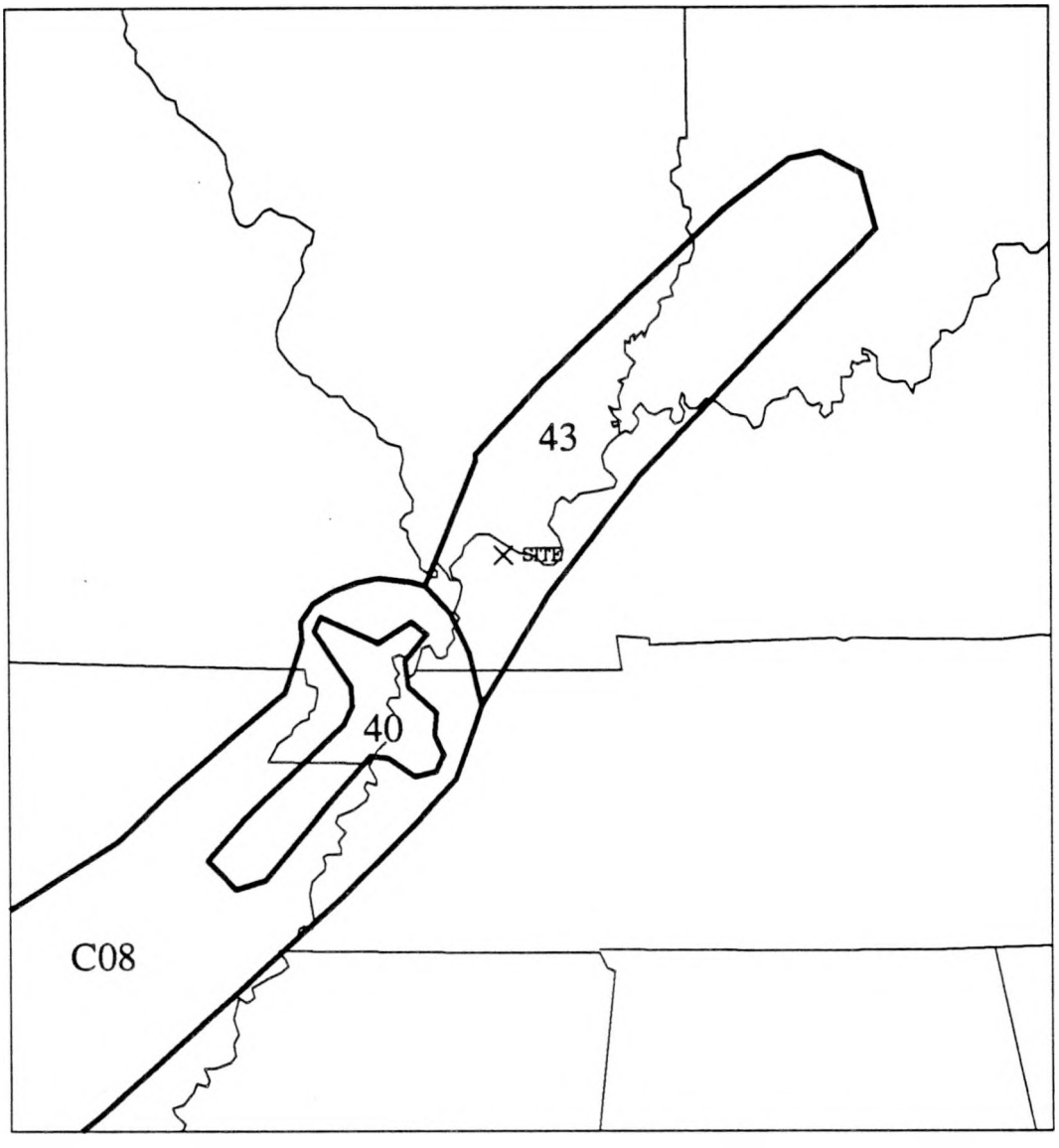

Figure 2-9. Map showing the seismic sources specified by the Woodward-Clyde team in the region around the Paducah Site.

Table 2-2

Summary of Bechtel Team Sources Near the Paducah Site

Source	Description	Seis. Opts.[1] and Probs.	Max. Mags. and Probs.	P^a	Inter-dependencies
BZ0	New Madrid Region	1[0.33] 2[0.34] 3[0.33]	5.7[0.10] 6.0[0.40] 6.3[0.40] 6.6[0.10]	1.00	Background; $P_B = 1.00$; does not contain 30
31	Reelfoot Rift	1[0.33] 2[0.34] 4[0.33]	5.7[0.10] 6.0[0.40] 6.3[0.40] 6.6[0.10]	0.60	
34	Wabash Valley Fault	1[0.33] 2[0.34] 4[0.33]	5.5[0.10] 5.8[0.40] 6.0[0.40] 6.6[0.10]	0.35	ME with K
J(=53)	Ozarks	1[0.33] 2[0.34] 4[0.33]	6.0[0.10] 6.3[0.40] 6.6[0.50]	0.15	
K(=54)	S. Illinois	1[0.33] 2[0.34] 4[0.33]	6.0[0.10] 6.3[0.40] 6.6[0.50]	0.35	ME with 33, 34, 35
30	New Madrid	1[0.33] 2[0.34] 4[0.33]	7.4[0.10] 7.5[0.90]	1.00	Not contained in BZ0

[1] Seismicity options are defined as follows:
1 = constant a, constant b (no prior b);
2 = low smoothing on a, high smoothing on b (no prior b);
3 = low smoothing on a, low smoothing on b (no prior b);
4 = low smoothing on a, low smoothing on b (weak prior of 1.05).

Weights on magnitude intervals are [1.0,1.0,1.0,1.0,1.0,1.0,1.0]

Table 2-3

Summary of Dames and Moore Team Sources Near the Paducah Site

Source	Description	Seis. Opts.[1] and Probs.	Max. Mags. and Probs.	P^a	Inter-dependencies
18	So. Illinois	1[0.29] 2[0.10] 3[0.46] 4[0.15]	6.0[0.75] 7.2[0.25]	1.00†	
19	St. Louis Arm	1[0.38] 2[0.13] 3[0.37] 4[0.12]	6.5[0.75] 7.2[0.25]	1.00†	
21	New Madrid	(Use seism. params. from 21B‡ 3[0.75] 4[0.25]	7.2[0.25] 7.5[0.75]	1.0	
22	Reelfoot Rift (Use C15=22−21B in calculations)	1[0.26] 2[0.09] 3[0.49] 4[0.16]	6.9[0.75] 7.2[0.25]	1.0†	
23B	Default	1[0.75] 2[0.25]	6.4[0.80] 7.2[0.20]	0.47	Default for 23

[1] Seismicity options are defined as follows:
1 = no smoothing on a, no smoothing on b (strong prior of 1.04);
2 = no smoothing on a, no smoothing on b (weak prior of 1.04);
3 = constant a, constant b (strong prior of 1.04);
4 = constant a, constant b (weak prior of 1.04).
Weights on magnitude intervals are [0.1,0.2,0.4,1.0,1.0,1.0,1.0]

† P^a of source and its default, which have the same geometry.

‡ To account for differences in areas, the value of a or source 21 is equal to the value of a for source 21B plus the quantity $\log_{10}(\text{Area}_{21B}/\text{Area}_{21}) = 0.560$.

Table 2-4

Summary of Law Engineering Team Sources Near the Paducah Site

Source	Description	Seis. Opts.[1] and Probs.	Max. Mags. and Probs.	P^a	Inter-dependencies
4A	Reelfoot Rift	1d[1.00]	6.2[0.50] 6.8[0.50]	0.90	ME with 4B
4B	Alternate Config. of 4A	1d[1.00]	6.2[0.50] 6.8[0.50]	0.10	ME with 4A
6	St. Louis Arm	1d[1.00]	5.3[0.20] 5.9[0.50] 6.8[0.30]	0.86	
7	Wabash Valley Arm	1d[1.00]	5.5[0.20] 6.0[0.50] 6.8[0.30]	0.85	
18	Postulated Faults in Reelfoot Rift	2d[1.00]	7.4[1.00]	1.00	

[1] Seismicity options are defined as follows:
1d = high smoothing on a, constant b (strong prior of 0.90);
2d = constant a, constant b (strong prior of 0.90);

Weights on magnitude intervals are all 1.0 for the above options

Table 2-5

Summary of Rondout Associates Team Sources Near the Paducah Site

Source	Description	Seis. Opts.[1] and Probs.	Max. Mags. and Probs.	P^a	Inter-dependencies
1	New Madrid, MO	5[1.00] (A=3.851), b=1.001)	7.1[0.10] 7.3[0.80] 7.4[0.10]	1.00	
2	New Madrid Rift	1[1.00] (a=−0.920, b=0.820)	6.6[0.30] 6.8[0.60] 7.0[0.15]	1.00	
4	S. Illinois-Indiana	1[1.00] (a=−1.160, b=0.850)	6.6[0.30] 6.8[0.60] 7.0[0.10]	1.00	

[1] Seismicity options are defined as follows:
1 = a and b as listed above;
5 = A, b values as listed above with weights shown;

Weights on magnitude intervals are [1.0,1.0,1.0,1.0,1.0,1.0,1.0]

Table 2-6

Summary of Weston Geophysical Team Sources Near the Paducah Site

Source	Description	Seis. Opts.[1] and Probs.	Max. Mags. and Probs.	P^*	Inter-dependencies
31	New Madrid	1b[1.00]	7.2[1.00]	0.95	
32	Reelfoot Rift	1b[0.80] 2b[0.20]	7.2[1.00]	1.00	
33	Indiana Arm NMRC source	1b[0.70] 2b[0.30]	6.0[0.68] 6.6[0.27] 7.2[0.05]	1.00	
34	St. Louis Arm NRMC source	1b[0.70] 2b[0.30]	5.4[0.23] 6.0[0.52] 6.6[0.21] 7.2[0.04]	1.00	
C11	32–31	1b[1.00]	6.0[0.13] 6.6[0.77] 7.2[0.10]	NA	NA

[1] Seismicity options are defined as follows:
1b = constant a, constant b (medium prior of 0.90);
2b = medium smoothing on a, medium smoothing on b (medium prior of 0.90);

Weights on magnitude intervals are all 1.0 for the above options

Table 2-7

Summary of Woodward-Clyde Consultants Team Sources Near the Paducah Site

Source	Description	Seis. Opts.[1] and Probs.	Max. Mags. and Probs.	P^*	Inter-dependencies
40	Disturbed Zone of Reelfoot Rift and NOTA†	2[0.33] 3[0.34] 4[0.33]	7.2[0.33] 7.5[0.34] 7.9[0.33]	1.00	NA
41	Reelfoot Rift and NOTA† (Use C08=41−49 in calculations)	2[0.25] 3[0.25] 4[0.25] 5[0.25]	5.4[0.33] 6.8[0.34] 7.2[0.33]	1.00	
42	St. Louis Arm and NOTA†	2[0.25] 3[0.25] 4[0.25] 5[0.25]	5.4[0.33] 6.8[0.34] 7.2[0.33]	1.00	NA
43	Southern Indiana Arm and NOTA†	2[0.25] 3[0.25] 4[0.25] 5[0.25]	5.8[0.33] 6.3[0.34] 7.4[0.33]	1.00	NA
44	New Madrid Loading volume and NOTA†	2[0.25] 3[0.25] 4[0.25] 5[0.25]	5.6[0.33] 6.3[0.34] 7.6[0.33]	1.00	No geographical overlap with 40 thru 43

[1] Seismicity options are defined as follows:
2 = high smoothing on *a*, high smoothing on *b* (no prior);
3 = high smoothing on *a*, high smoothing on *b* (medium prior of 1.00);
4 = high smoothing on *a*, high smoothing on *b* (medium prior of 0.90);
5 = high smoothing on *a*, high smoothing on *b* (medium prior of 0.80);

Weights on magnitude intervals are all 1.0.

† NOTA: None Of The Above

2.4 GROUND-MOTION ATTENUATION

2.4.1 Attenuation Functions for Rock

This section presents the ground-motion attenuation functions used in the EPRI/SOG calculations. The attenuation functions predict six measures of rock-site ground motions: peak acceleration and spectral velocities at six frequencies. Three sets of attenuation functions, with associated weights, characterize uncertainty in ground-motion predictions. The NRC has stated that these attenuation functions are acceptable for computations of seismic hazard (13).

The attenuation functions used in the EPRI/SOG seismic-hazard calculations are based on simplified physical models of energy release at the seismic source and of wave propagation. The model of energy release describes the Fourier spectrum and duration of shaking at a hypothetical site close to the earthquake, and how these vary with seismic moment (seismic moment is a measure of earthquake size). The model of wave propagation describes how the spectrum and duration of shaking vary as the waves travel through the crust. This model contains the effects of geometric spreading (including *Lg* waves at longer distances), anelastic attenuation, and dispersion. The combined predictions of these models are consistent with seismograph and accelerograph data from the region.

Uncertainty on attenuation functions arises from uncertainty on the parameters of these models and on the derivation of peak time-domain amplitudes from Fourier spectra. The most important of these are uncertainty on source scaling, on the magnitude-moment relation, and on the spectra to time-domain derivation. These uncertainties are captured by considering three alternative formulations of these models, as follows:

1. The attenuation functions obtained by McGuire et al. (7) using an ω-square model with stress drop of 100 bars. This set of attenuation functions is assigned a weight of 0.5.

2. The attenuation functions obtained by Boore and Atkinson (14) using an ω-square model. This set of attenuation functions is assigned a weight of 0.25.

3. The attenuation function obtained from the velocity and acceleration attenuation equations obtained by Nuttli (15) using the "increasing stress-drop" assumption coupled with the dynamic amplification factors by Newmark and Hall (16). The attenuation functions in (15) were derived using a procedure analogous to that of Herrmann and Nuttli (17). This set of attenuation functions is given a weight of 0.25.

Table 2–8 contains the coefficients of these models. Figure 2–10 shows their predictions for magnitudes 5 and 6. The attenuation functions for 0.5-Hz spectral velocity from the models by McGuire et al. (7) and Nuttli (15) were calculated for this study, by using these models' assumptions.

2.4.2 Soil Amplification Factors

The EPRI/SOG soil amplification factors were developed using an approach analogous to that implemented in the program SHAKE. The rock-motion input to the analysis was specified as a random process with frequency content typical of ground motions in the central and eastern United States [see (7)].

The standard soil profile was chosen to be consistent with the generally stiff soils typical of the central and eastern United States (see Figure 2–11). The profile is based upon the sand-like and till-like profiles established by Bernreuter et al. (5). Amplification factors were calculated for five depth categories, as defined in Table 2–9. The modulus reduction and damping curves are shown in Figure 2–12.

Soil amplification factors are computed as the ratio of 5% damping response spectral acceleration (Sa) computed at the surface of each site to 5% damping response spectral acceleration (Sa) computed for the surface bedrock motion. In addition, both peak acceleration (Ap) and peak ground velocity (Vp) are computed for the site and surface bedrock as well. Levels of input motion (rock outcrop) of 0.1, 0.3, 0.5, 0.75, and 1.0 g are used to accommodate effects of material nonlinearity upon soil response. Figures 2–13 through 2-18 show the calculated amplification factors for peak acceleration and spectral velocities. Additional details on the development of these amplification factors are provided in Section 6 of (7).

The seismic hazard calculations for a soil site are performed as follows:

1. Calculation of the hazard curves as if the site was a rock site, using the attenuation functions in Table 2–8.

2. Introduction of the amplitude-dependent soil amplification factors, which is done by multiplying each ground-motion amplitude in the hazard curves obtained in step 1 by the corresponding soil-amplification factor. Uncertainty in the amplification factors is introduced by shifting the mean hazard curve and the 0.15 and 0.85 fractile hazard curves (assuming that uncertainty in the hazard and uncertainty in the amplification factor are both lognormal, and that the latter has a coefficient of variation of 30%).

Table 2-8

Attenuation Equations Used in the EPRI/SOG Calculations

$$(\ln[Y] = a + bm_b + c\ln[R] + dR)$$

MODEL	WEIGHT	Y†	a	b	c	d
McGuire et al. (7)	0.5	PSV(0.5 Hz)	-12.36	2.81	-1.00	-0.0015
		PSV(1 Hz)	-7.95	2.14	-1.00	-0.0018
		PSV(2.5 Hz)	-3.82	1.49	-1.00	-0.0024
		PSV(5 Hz)	-2.11	1.20	-1.00	-0.0031
		PSV(10 Hz)	-1.55	1.05	-1.00	-0.0039
		PSV(25 Hz)	-1.63	0.98	-1.00	-0.0053
		Accel.	2.55	1.00	-1.00	-0.0046
Boore and Atkinson (14)	0.25	All Frequencies and Acceleration	More complicated functional form; see Equations 12 and 13 and Table 3 of (14).			
Nuttli (15), Newmark-Hall Amplification Factors	0.25	PSV(0.5 Hz) ‡	0.99	1.15	-0.83	-0.0028
		PSV(1 Hz) ‡	0.29	1.15	-0.83	-0.0028
		PSV(2.5 Hz) ‡	-0.62	1.15	-0.83	-0.0028
		PSV(5 Hz) ‡	-1.32	1.15	-0.83	-0.0028
		PSV(10 Hz) ‡	-2.13	1.15	-0.83	-0.0028
		PSV(25 Hz) ‡	-3.53	1.15	-0.83	-0.0028
		Accel.	1.38	1.15	-0.83	-0.0028

† Spectral velocities have units of cm/sec; acceleration has units of cm/sec^2; R has units of km. Variability of $\ln[Y]$ around the predicted value is characterized by a normal distribution with $\sigma = 0.5$.

‡ For given m_b and R, $\ln[Y]$ is the smaller of $a + bm_b + c\ln[R] + dR$ and $-8.3 + 2.3m_b - 0.83\ln[R] - 0.0012R$.

Table 2-9

Soil Categories and Depth Ranges

Category	Depth (ft)	Range (ft)
I	20	10–30
II	50	30–80
III	120	80–180
IV	250	180–400
V	500	>400

The Paducah site was classified as Category IV (180 to 400 feet of soil), based on a depth of 350 feet (18). The amplification factor for 0.5-Hz spectral velocity was assumed equal to that for 1 Hz.

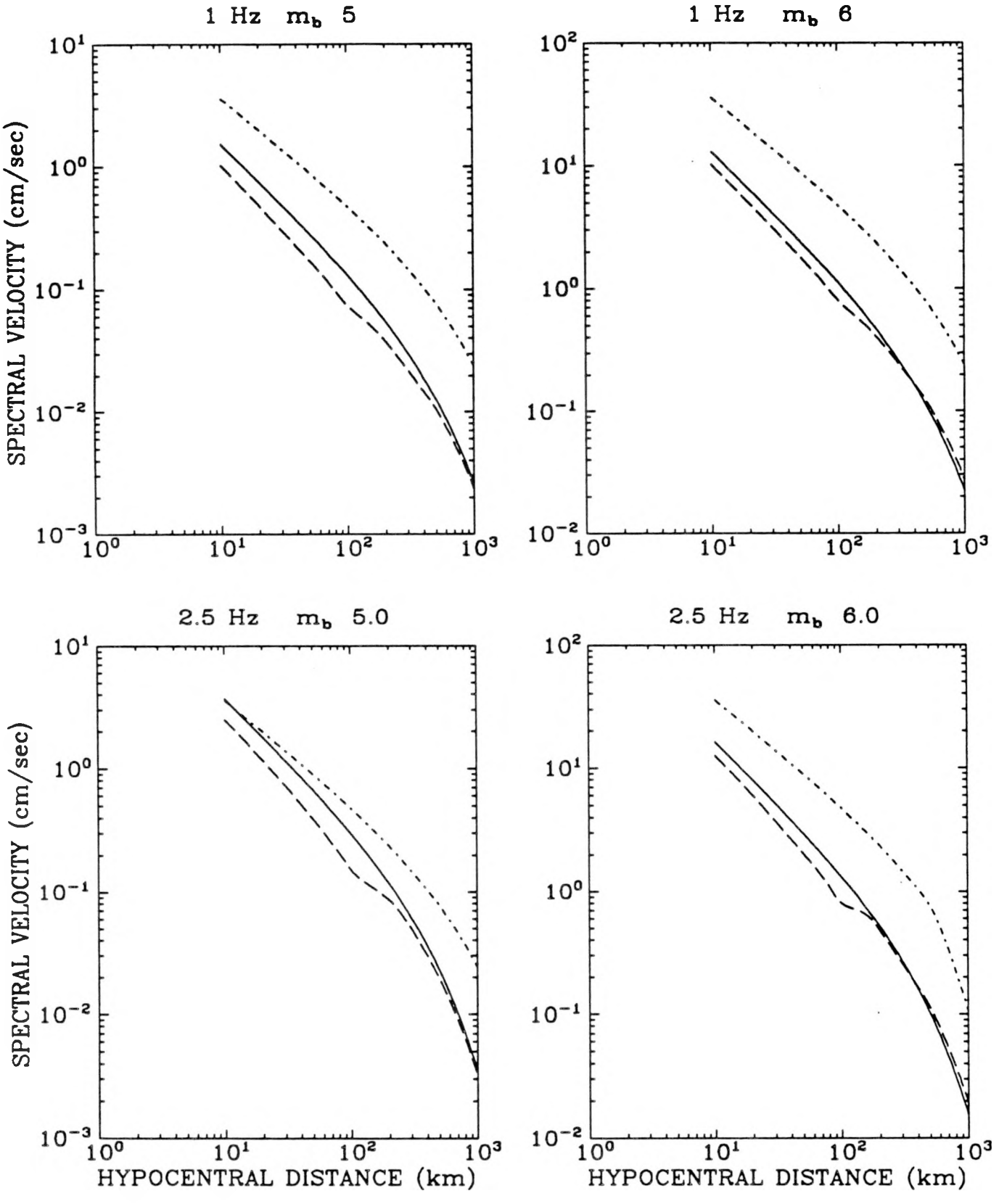

Figure 2-10. Ground motions predicted by the EPRI/SOG attenuation equations for m_b 5 and 6. Key: McGuire et al. (7) (solid), Boore and Atkinson (14) (– – –), and Nuttli (15) (– · –).

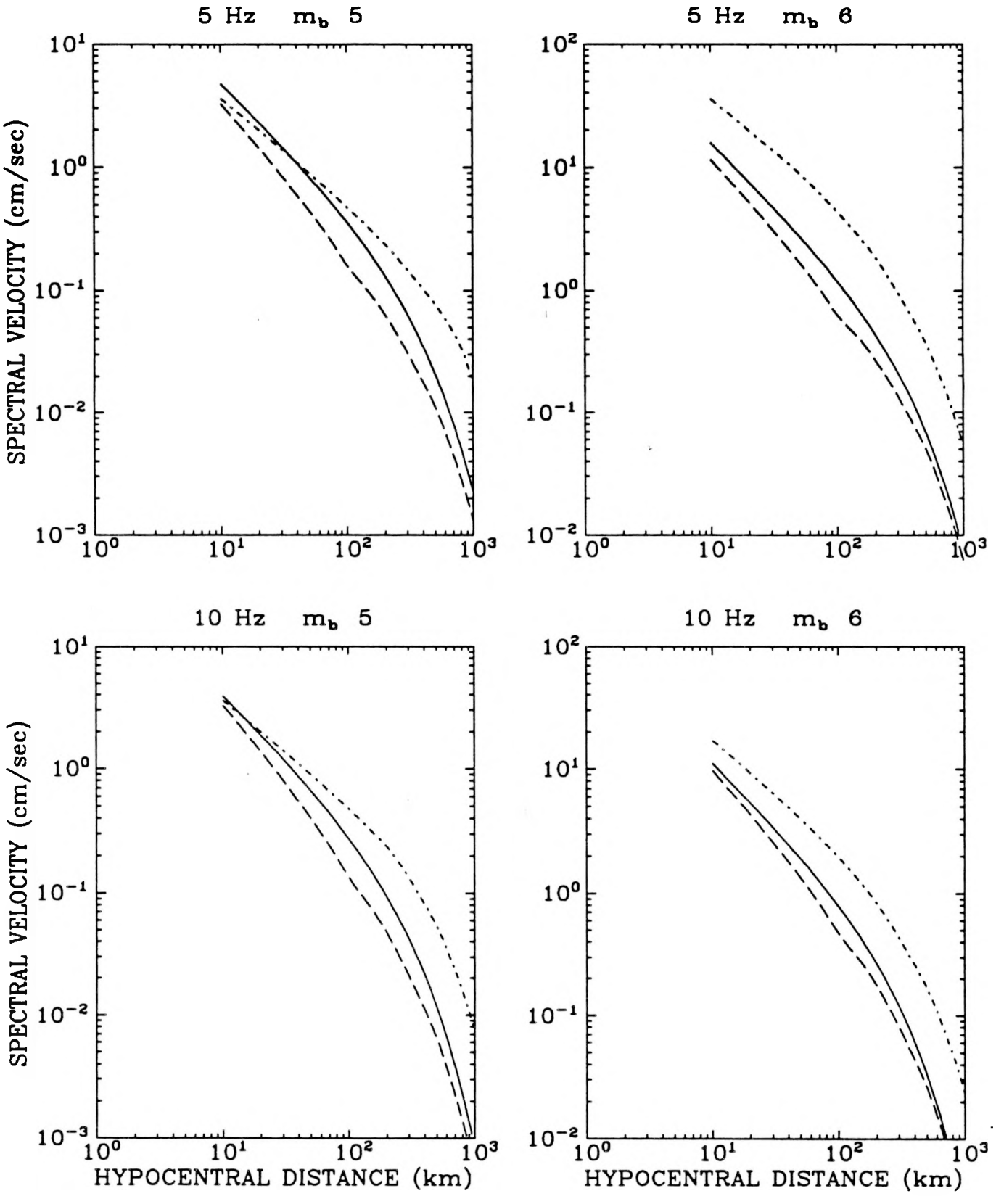

Figure 2–10 (continued). Ground motions predicted by the EPRI/SOG attenuation equations for m_b 5 and 6. Key: McGuire et al. (7) (solid), Boore and Atkinson (14) (– – –), and Nuttli (15) (– · –).

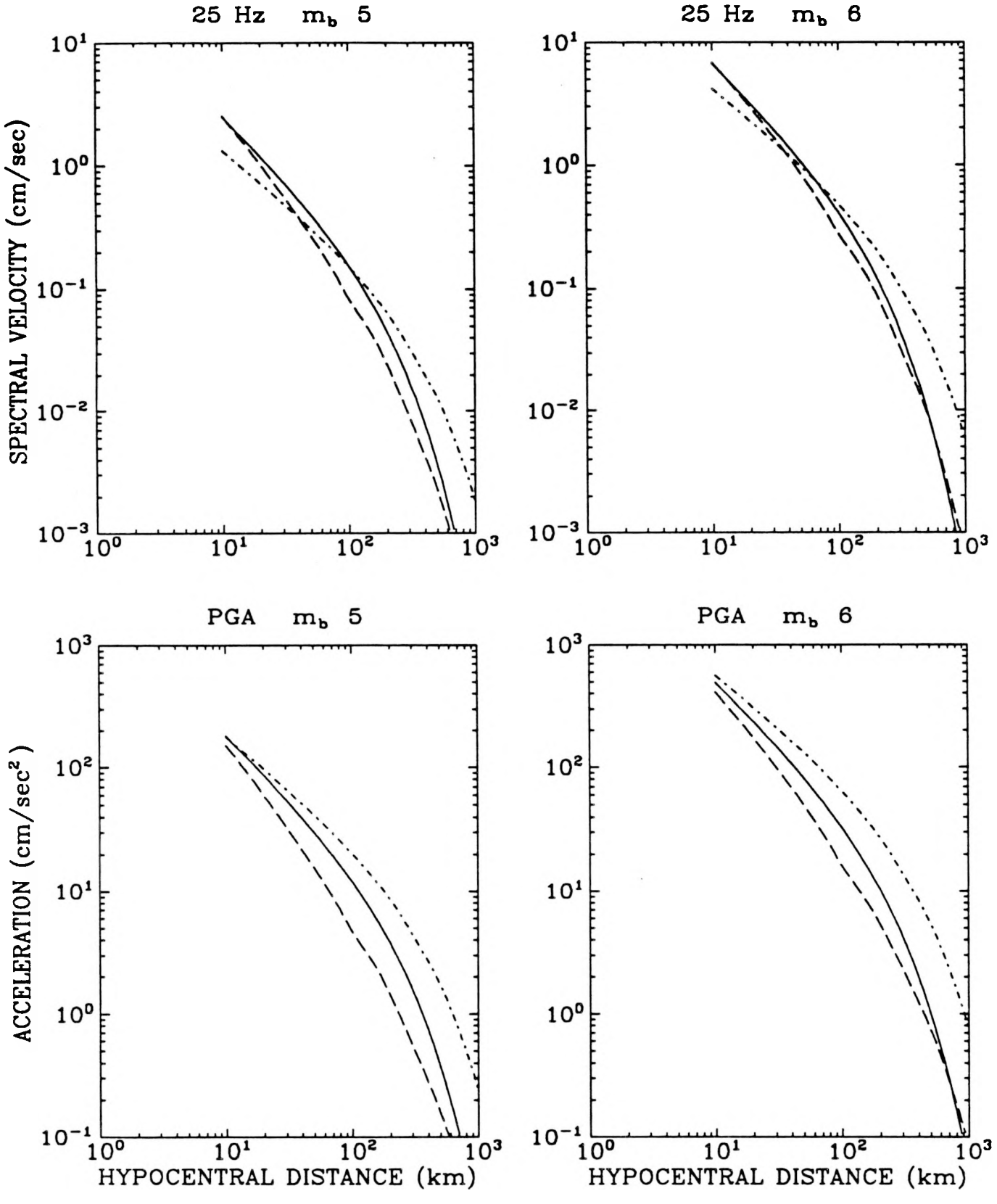

Figure 2-10 (continued). Ground motions predicted by the EPRI/SOG attenuation equations for m_b 5 and 6. Key: McGuire et al. (7) (solid), Boore and Atkinson (14) (– – –), and Nuttli (15) (– · –).

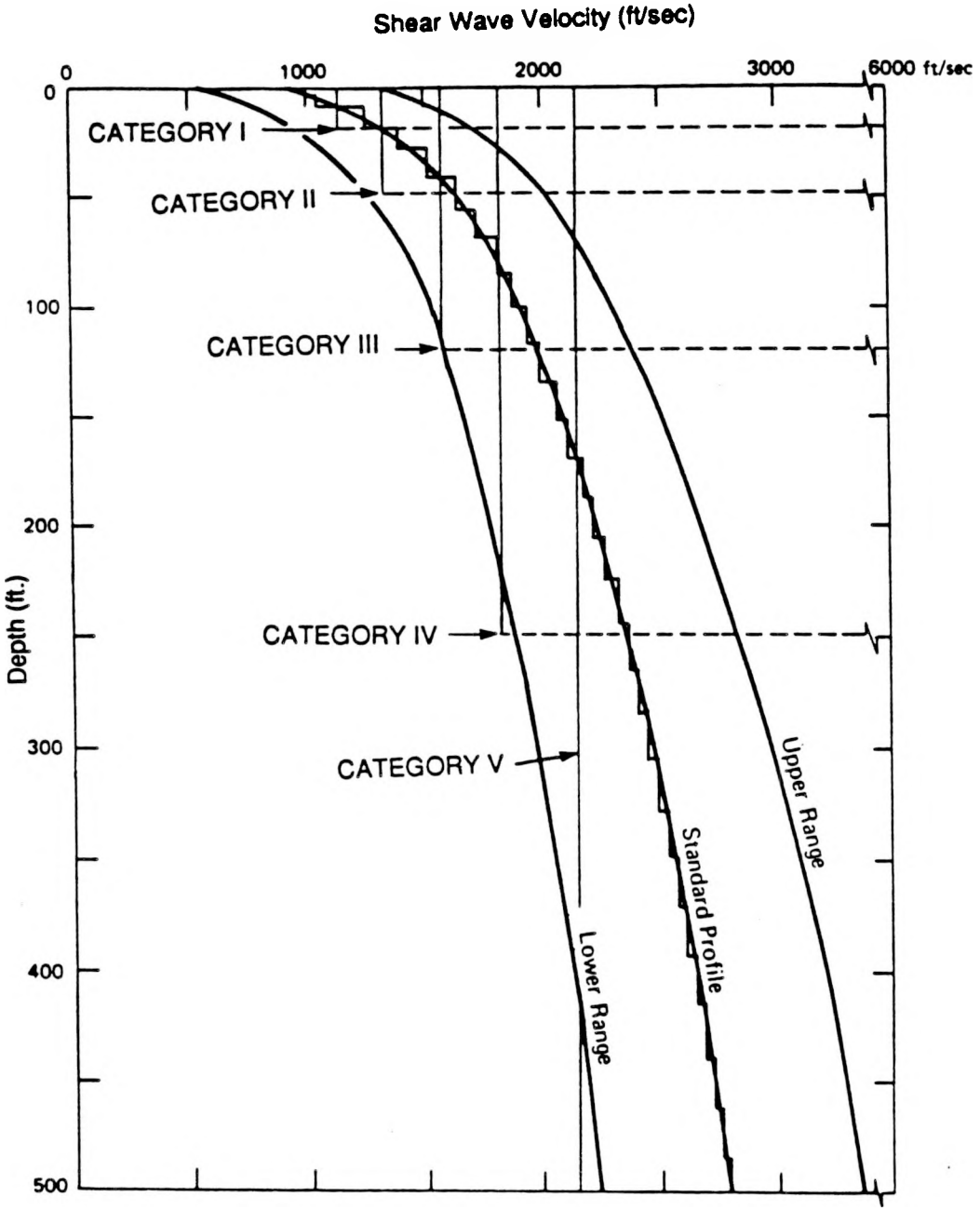

Figure 2-11. Standard soil profile for sand-like Central and Eastern United States sites (gradient). Soil categories I–V are indicated by their respective soil column depths. See Table 2–10 for definition of the soil categories.

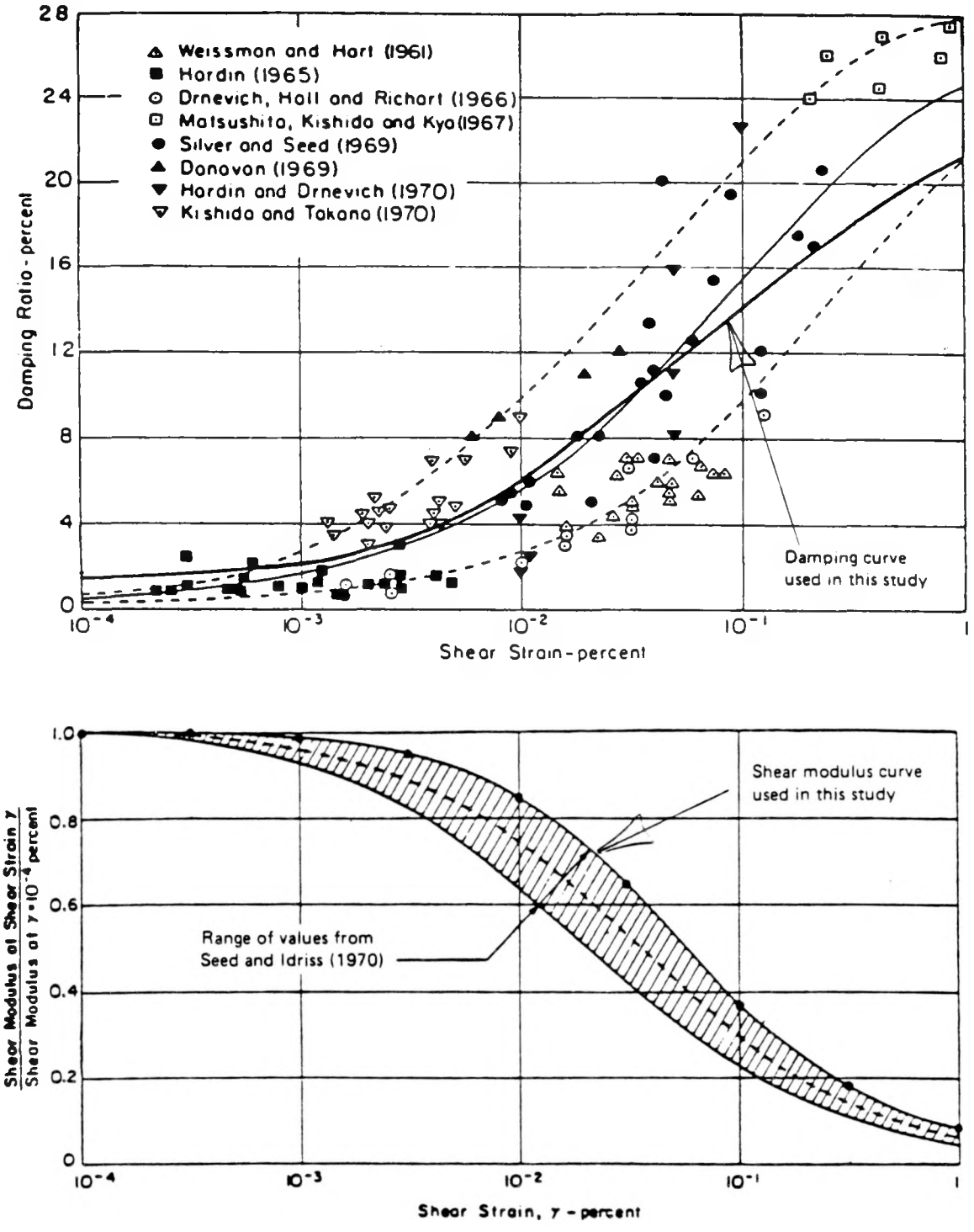

Figure 2-12. Shear-strain dependency of shear-wave damping and shear modulus.

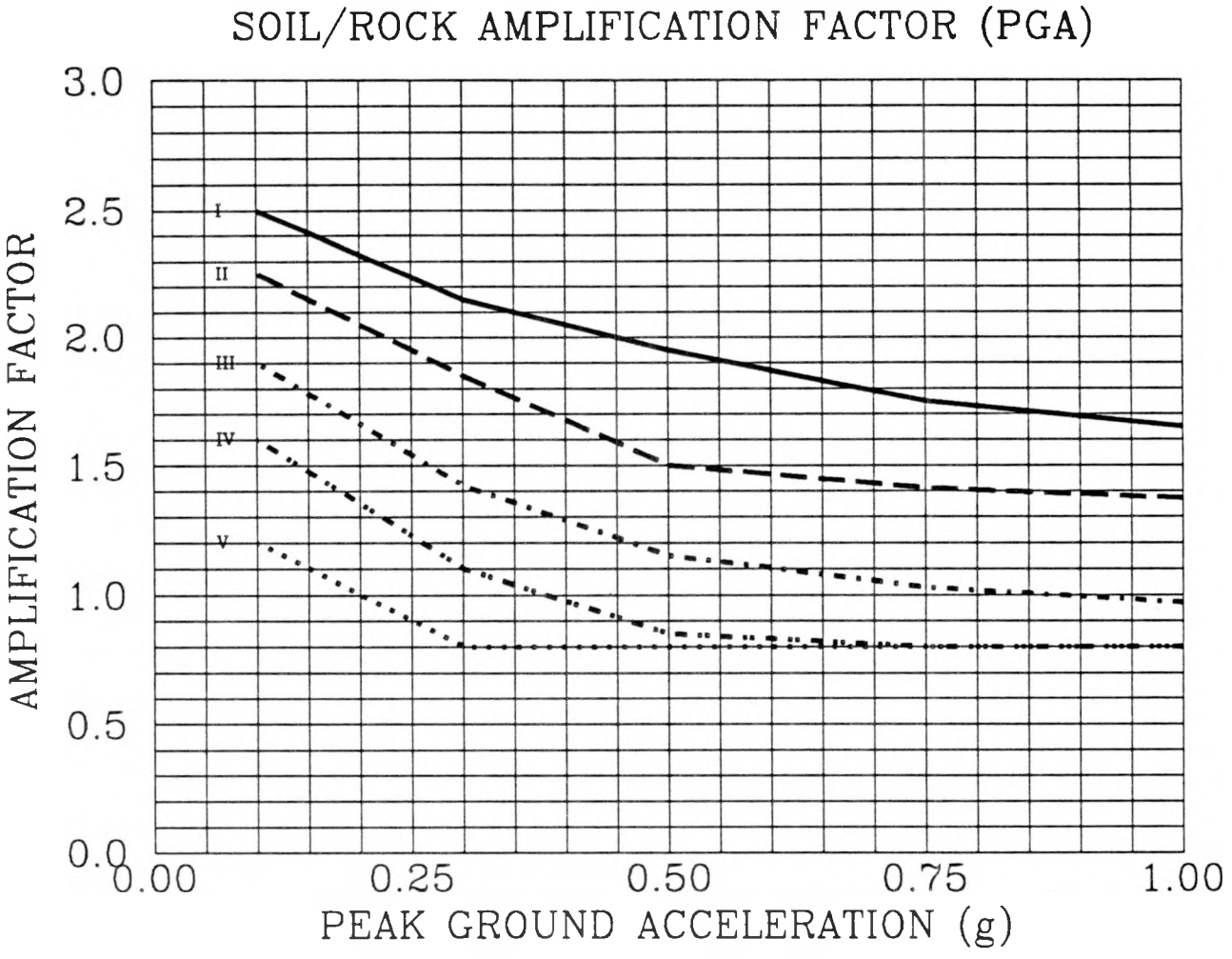

Figure 2-13. Soil amplification factors for peak ground acceleration, for the 5 soil categories. See Table 2–9 for the definition of soil categories.

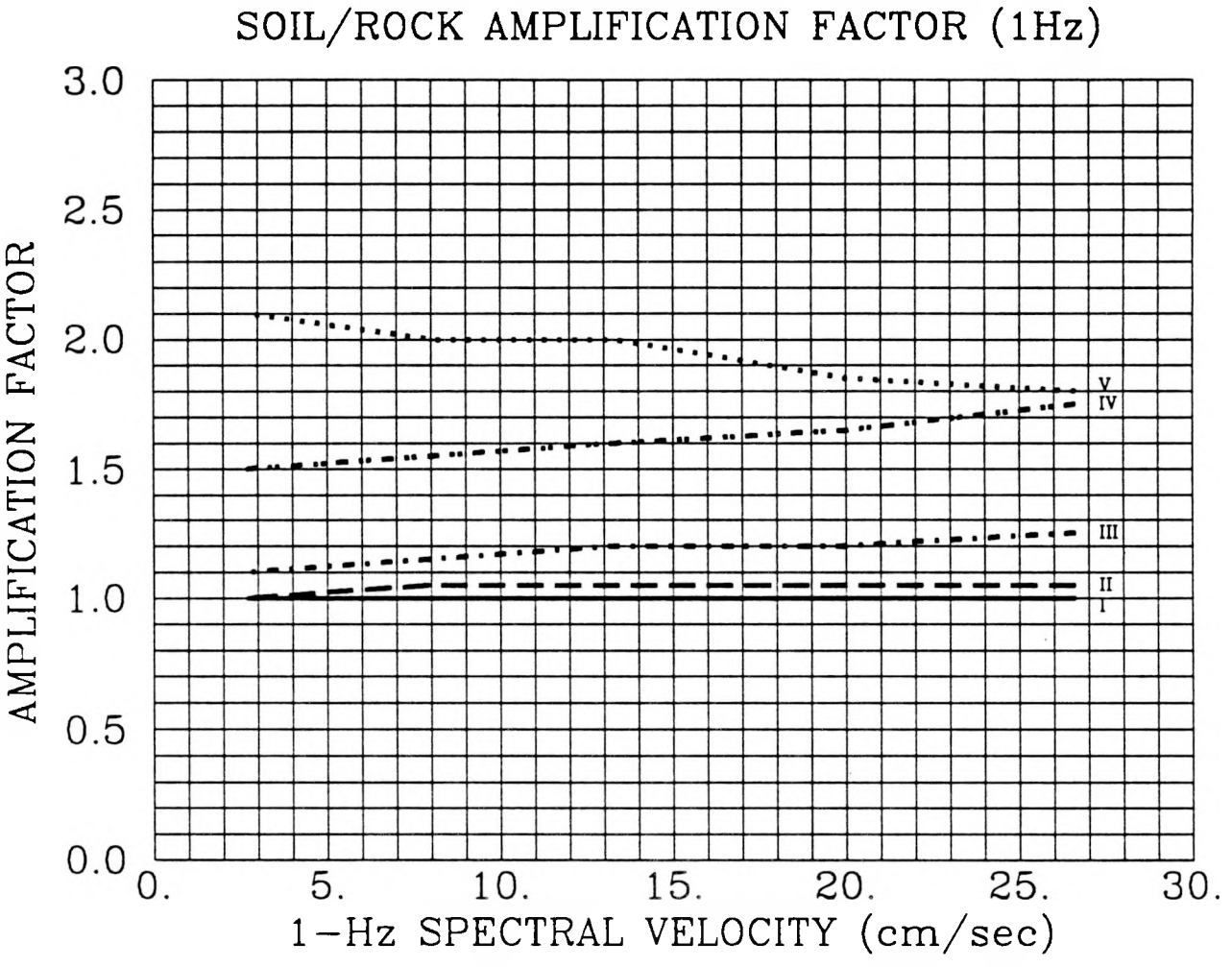

Figure 2-14. Soil amplification factors for 1-Hz spectral velocity (5% damping), for the 5 soil categories. See Table 2–9 for the definition of soil categories.

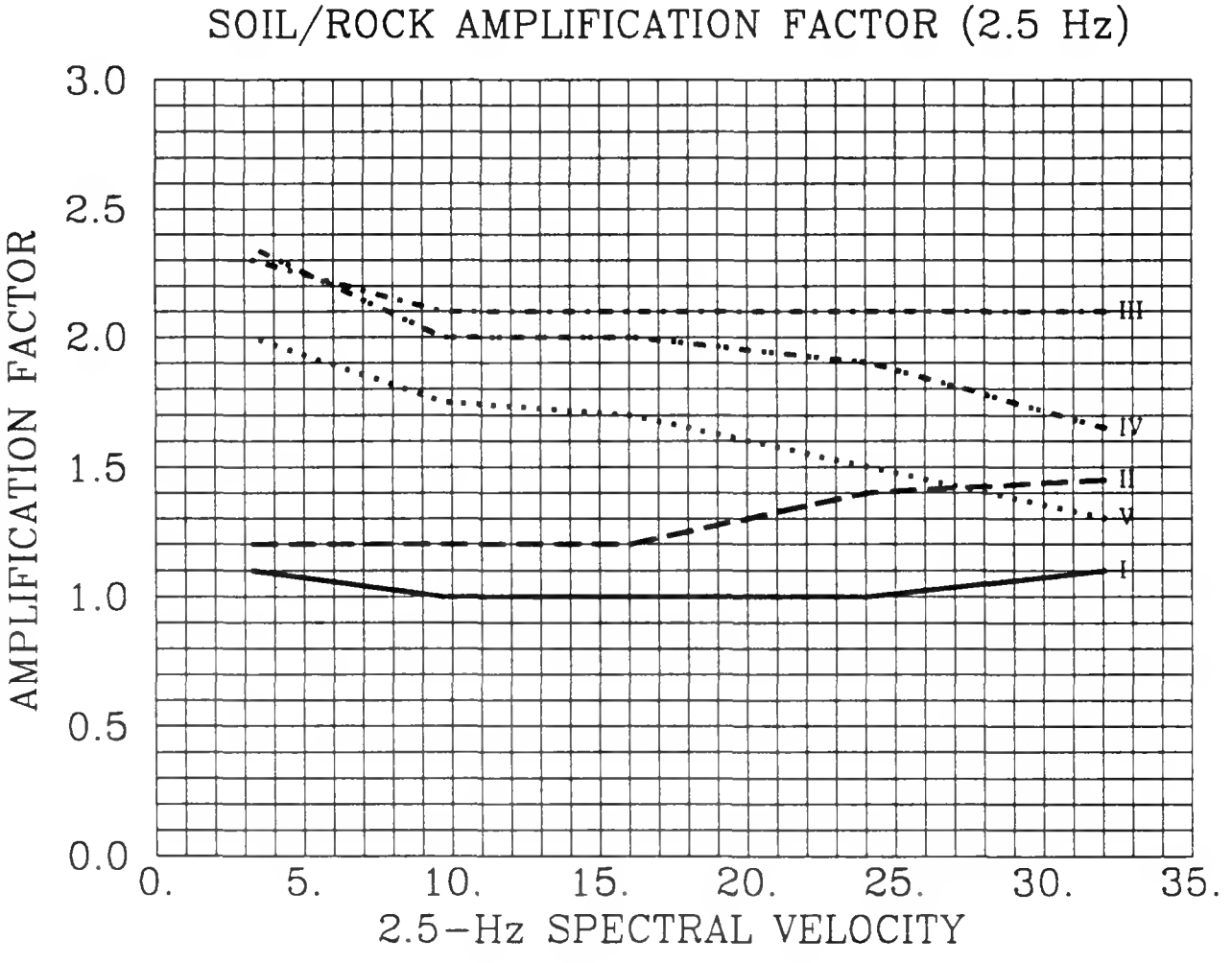

Figure 2-15. Soil amplification factors for 2.5-Hz spectral velocity (5% damping), for the 5 soil categories. See Table 2–9 for the definition of soil categories.

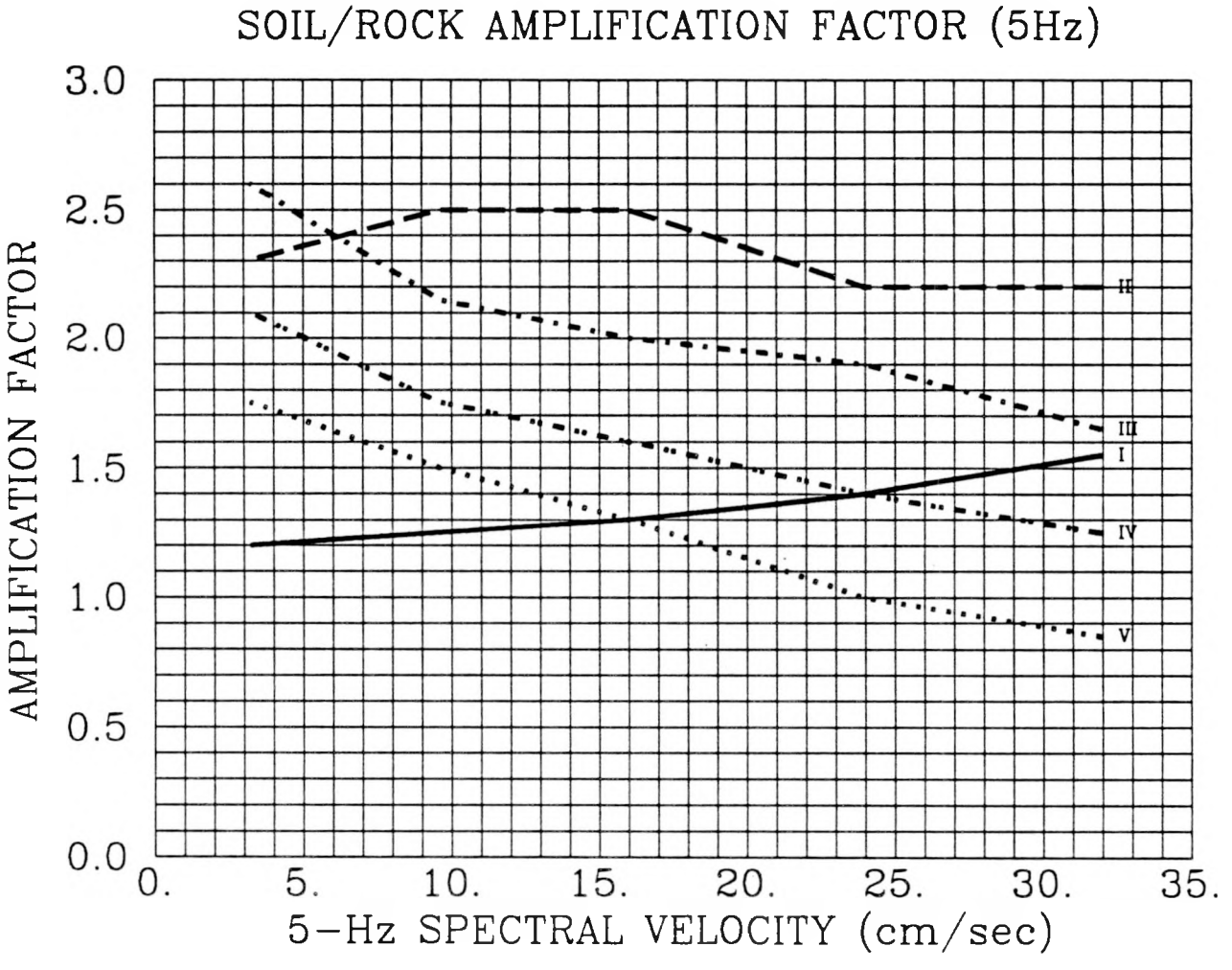

Figure 2-16. Soil amplification factors for 5-Hz spectral velocity (5% damping), for the 5 soil categories. See Table 2-9 for the definition of soil categories.

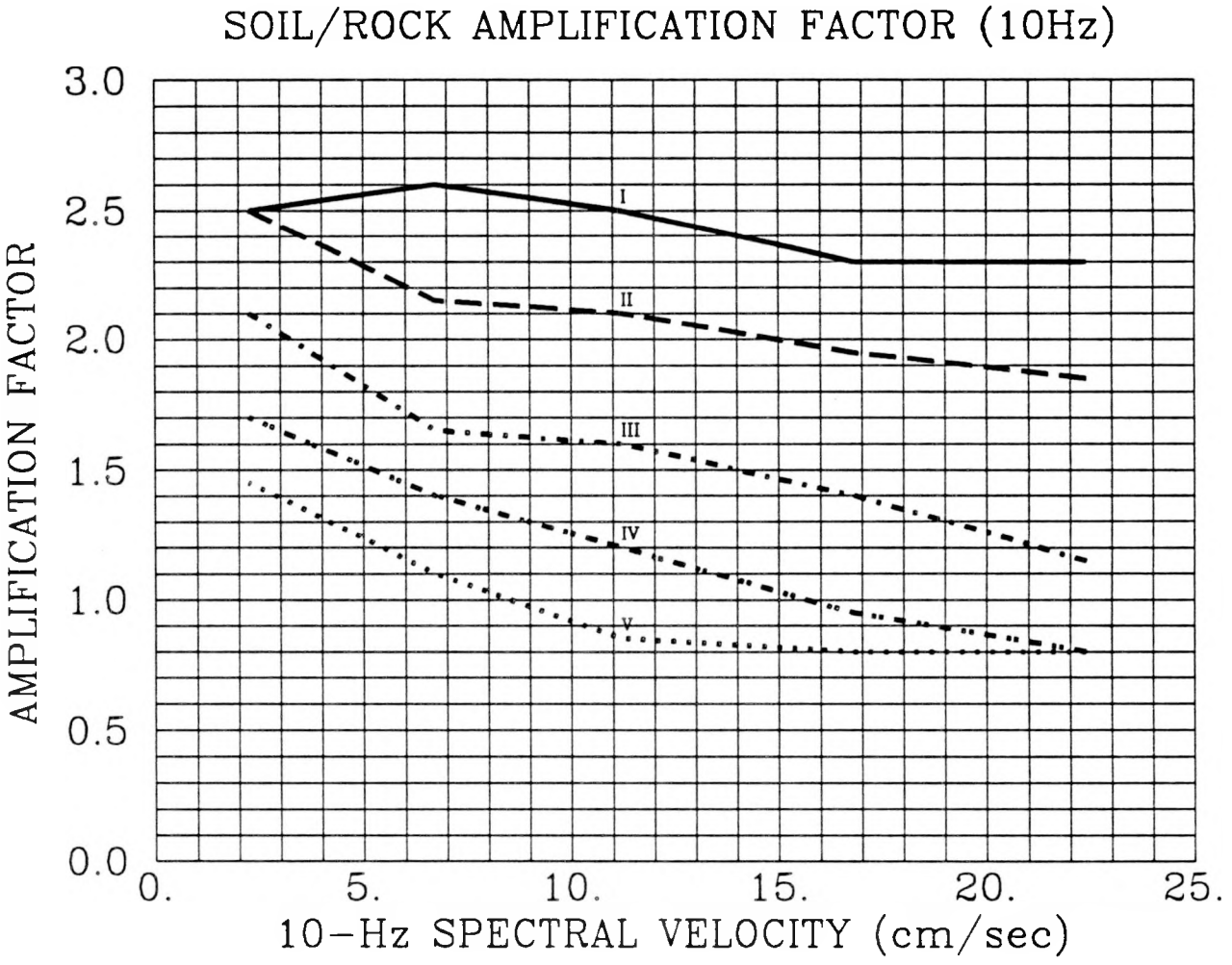

Figure 2-17. Soil amplification factors for 10-Hz spectral velocity (5% damping), for the 5 soil categories. See Table 2-9 for the definition of soil categories.

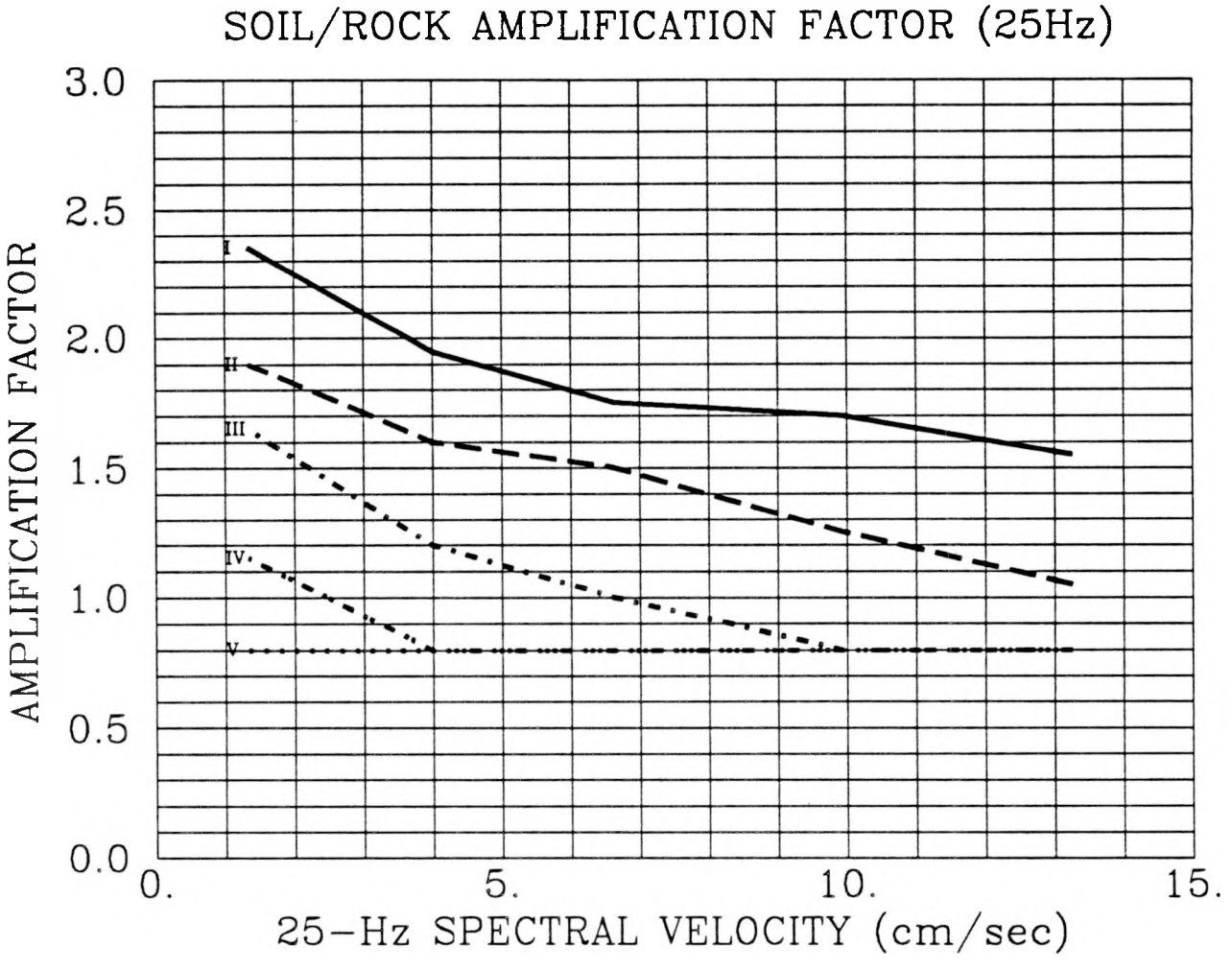

Figure 2-18. Soil amplification factors for 25-Hz spectral velocity (5% damping), for the 5 soil categories. See Table 2-9 for the definition of soil categories.

2.5 CALCULATIONS

2.5.1 Overview

The seismic-hazard calculations for the Paducah site used the EPRI/SOG methodology and inputs, and followed the same steps as the EPRI/SOG calculations documented in(6). These steps are as follows:

1. Identify all sources within 200 km of the site and include them in the screening calculations (step 2). Include also the New Madrid and Charleston sources if they are within 500 km of the site.

2. Use EQHAZ to perform screening calculations for each team considering one PGA amplitude (0.25g) and one 1-Hz amplitude (10 cm/sec) and using the three sets of attenuation functions (see Section 2.4.1). Evaluate the mean hazard from each source, and its percent contribution to the total hazard considering the source's P^a. Eliminate those sources that make negligible contributions to the hazard for both ground-motion measures, so that the combined hazards from all excluded sources is less than 1% of the total hazard.

3. Perform EQHAZ calculations for all amplitudes and 6 measures of ground motion (i.e., peak acceleration and 5% damped spectral velocity at 0.5, 1, 2.5, 5, 10, and 25 Hz) using all attenuation functions. These calculations are performed separately for each team.

4. Develop source combinations for each team, considering all sources included in step 2, their activity probabilities and dependencies. These source combinations are sometimes simplified as described in Volume 3 of (8), while maintaining the conservative criteria of step 2.

5. Simplify the logic trees for some sites and teams, by considering only 1 seismicity option for each source. (The hazard associated with that one seismicity option is the weighted average of hazards from the original seismicity options.) This simplification was performed for the Bechtel team only, because the number of sources selected in step 2 was too large and EQPOST runs with the full logic trees would require excessive computer time. Test runs indicate that the effect of this simplification is insignificant.

6. Perform EQPOST calculations using the source-hazard results from step 3 and the source combinations from step 4. These calculations are performed separately for each ground-motion measure. For soil sites, introduce site-amplification factors and their uncertainty.

This study used the source geometries and seismicity parameters that were generated during the EPRI/SOG project. These data were used to develop the geometry and seismicity input files for the EQHAZ calculations in steps 2 and 3.

2.5.2 Screening of Seismic Sources

The screening of seismic sources is performed in order to reduce the number of sources considered in the analysis, thereby simplifying the development of source combinations and reducing the computer time required for the final calculations. The screening for the Paducah site is performed using the Nuttli attenuation functions, thus ensuring that the mean hazard is computed accurately.

The screening is based on the contribution of each source to the mean value of total hazard. Tables 2–10 through 2–15 show the results of the screening calculations. Results for each team contain one table for peak ground acceleration and one table for 1-Hz spectral velocity. Each table shows the contribution to the total hazard from each source within 200 km of the site. A source's contribution to the total hazard depends on the mean hazard when the source is active (column 2) and on the activity probability P^a or P^* of the source (column 3)[2]. Donut sources do not have activity probabilities and cannot be included in the computation of total hazard. The decision to include or exclude these sources must be made by considering which sources form the donut and considering the hazard in column 2. Table 2–16 lists the sources selected for final calculations.

2.5.3 Development of Source Combinations

The source combinations represent all possible states of activity of the seismic sources that contribute to hazard at the site (i.e., all the sources selected in the screening process above). The source combinations are developed considering the following three types of information: (1) the activity probabilities P^a or P^* of the various sources, (2) the interdependencies of source activities, and (3) the geographic relationships among sources.

The most common geographic relationship occurs with background sources. If the site is within a background source and within a standard source, the background is included only in source combinations where the standard source is not active. In some instances, "donut" sources of the type *BACKGROUND − STANDARD SOURCE* have also been digitized and analyzed. In those instances, the appropriate donut should be included in each source combination, depending on which standard sources are active.

Table 2–17 shows the source combinations and their probabilities, for the six Earth Science Teams.

[2]In the headings of Tables 2–10 through 2–15 we do not distinguish between P^a and P^*.

2.5.4 Results

Seismic hazard calculations were performed for peak acceleration and 6 spectral velocities, using the ERPI/SOG software modules EQHAZ and EQPOST, and considering the seismic sources and source combinations in Tables 2–16 and 2–17. Two sets of results are presented, corresponding to rock and to Category-IV soil conditions.

Results for rock are presented in Figures 2–19 through 2–26 in the form of hazard curves and uniform-hazard spectra.

Results for soil—obtained using the EPRI/SOG amplification factors for soil category IV (soil depths of 180 to 400 feet)—are presented in Figures 2-27 and 2–28.

The highest frequency shown in the response spectra in Figures 2–26 and 2–28 is 25 Hz. Studies of the frequency content of ground motions in the central and eastern United States (18, for example) indicate that the maximum spectral acceleration occurs at approximately 30 Hz and that the spectral acceleration approaches the peak ground acceleration at frequencies near 80 Hz.

Table 2-18 lists the seismic sources that contribute significantly to the calculated hazard at the Paducah site, according to each team's interpretations of seismic sources and their parameters. This table also summarizes the most important parameters of these sources; namely, distance to the site, activity rate, rate per unit area, and distribution of maximum magnitude. The information in this table will be used in the specification of seismic sources and their parameters for the extended-source seismic-hazard calculations.

2.6 REFERENCES

1. C. A. Cornell. "Engineering Seismic Risk Analysis". *Bulletin of the Seismological Society of America*, 58(5):1583–1606, October 1968.

2. C. A. Cornell. *Dynamic Waves in Civil Engineering*, chapter 27: "Probabilistic Analysis of Damage to Structures under Seismic Loads". Wiley Interscience, 1971.

3. A. Der Kiureghian and A. H. S. Ang. *A Line Source Model for Seismic Risk Analysis.* Technical Report UILU-ENG-75-2023, Univ. of Illinois, October 1975. pp. 134.

4. R. K. McGuire. *FORTRAN Computer Program for Seismic Risk Analysis.* Open File Report 76-67, U. S. Geological Survey, 1976. pp. 1-90.

5. D. L. Bernreuter, J. B. Savy, R. W. Mensing, J. C. Chen, and B. C. Davis. *Seismic Hazard Characterization of the Eastern United States.* Technical Report LLNL UCID-20421, Volumes 1 and 2, Lawrence Livermore National Laboratory, Livermore, Ca., 1985.

6. R. K. McGuire, G. R. Toro, J. P. Jacobson, T. F. O'Hara, and W. J. Silva. *Probabilistic Seismic Hazard Evaluations in the Central and Eastern United States: Resolution of the Charleston Earthquake Issue.* Special Report NP-6395-D, Electric Power Research Institute, April 1989.

7. R. K. McGuire, G. R. Toro, and W. J. Silva. *Engineering Model of Earthquake Ground Motion for Eastern North America.* Technical Report NP-6074, Electric Power Research Institute, 1988.

8. *Seismic Hazard Methodology for the Central and Eastern United States.* Technical Report NP-4726-A, Electric Power Research Institute, July 1986. Revised, 1988. Vol. 1, Part 1: Methodology, Vol. 1, Part 2: Theory, Vol. 2: EQHAZARD Programmer's Manual, Vol. 3: EQHAZARD User's Manual, Vol. 4: Applications, Vols. 5 through 10: Tectonic Interpretations, Vol. 11: Nuclear Regulatory Commission Safety Review.

9. K. J. Coppersmith, A. C. Johnston, and W. J. Arabasz. "Assessment of Maximum Earthquake Magnitudes in the Eastern United States". *Earthquake Notes*, 57–1:12, 1986.

10. A. C. Johnston, A. G. Metzger, K. J. Coppersmith, and W. J. Arabasz. "A Systematic Global Overview of Large Intraplate Earthquakes". *Earthquake Notes*, 57–1:12, 1986.

11. M. W. McCann and J. W. Reed. *Selection of a Lower Bound Magnitude for Seismic Hazard Assessment.* Technical Report, Electric Power Research Institute, Palo Alto, California, 1988.

12. M. W. McCann and J. W. Reed, editors. *Engineering Characterization of Small-Magnitude Earthquakes*, Electric Power Research Institute, Palo Alto, California, 1988.

13. L. Reiter. EPRI Ground Motion Models for Eastern North America. NRC Letter to R.A. Thomas, August 3, 1988.

14. D. M. Boore and G. M. Atkinson. "Stochastic Prediction of Ground Motion and Spectral Response Parameters at Hard-Rock Sites in Eastern North America". *Bulletin of the Seismological Society of America*, 77(2):440–467, 1987.

15. O. W. Nuttli. Letter dated September 19, 1986 to J. B. Savy. Reproduced in: D. Bernreuter, J. Savy, R. Mensing, J. Chen, and B. Davis. *Seismic Hazard Characterization of 69 Nuclear Plant Sites East of the Rocky Muntains: Questionnaires.* U. S. Nuclear Regulatory Commission, Technical Report NUREG/CR-5250, UCID-21517, Volume 7, 1989. Prepared by the Lawrence Livermore National Laboratory.

16. N. M. Newmark and W. J. Hall. *Earthquake Spectra and Design.* Earthquake Engineering Research Institute, Berkeley, CA, 1982.

17. R. B. Herrmann and O. W. Nuttli. "Strong Motion Investigations in the Central United States". In *Proceedings: 7th World Conference on Earthquake Engineering, Istanbul*, pp. 533–536, 1980.

18. K. E. Shaffer. Paducah and Portsmouth Soil Depth References. Written Communication to Robin K. McGuire. Martin Marietta Energy Systems, May 2, 1991.

19. W. J. Silva and R. K. Green. "Magnitude and Distance Scaling of Response Spectral Shapes for Rock sites with Application to North American Tectonic Environments". *Earthquake Spectra*, 5(4):591–624, 1989.

Table 2-10

Screening of Seismic Sources: Bechtel Team

SCREENING OF SEISMIC SOURCES

site: Paducah team: BEC peak accel.

Source	Hazard	P*	Haz.P*	%	Acum. %	Include
30	5.33E-04	1.000	5.33E-04	61.4	61.4	Y
BZ0	1.75E-04	1.000	1.75E-04	20.2	81.6	Y
31	1.69E-04	0.600	1.01E-04	11.6	93.2	Y
K	1.52E-04	0.350	5.31E-05	6.1	99.3	Y
33	2.23E-05	0.200	4.47E-06	0.5	99.8	N
J	7.44E-06	0.150	1.12E-06	0.1	100.0	N
34	7.02E-07	0.350	2.46E-07	0.0	100.0	N
35	4.97E-07	0.150	7.45E-08	0.0	100.0	N
36	6.83E-08	0.400	2.73E-08	0.0	100.0	N

site: Paducah team: BEC 1-Hz PSV

Source	Hazard	P*	Haz.P*	%	Acum. %	Include
30	7.66E-04	1.000	7.66E-04	59.2	59.2	Y
BZ0	2.71E-04	1.000	2.71E-04	21.0	80.1	Y
K	3.95E-04	0.350	1.38E-04	10.7	90.8	Y
31	1.57E-04	0.600	9.42E-05	7.3	98.1	Y
J	7.68E-05	0.150	1.15E-05	0.9	99.0	Y
34	1.89E-05	0.350	6.60E-06	0.5	99.5	Y
33	2.76E-05	0.200	5.52E-06	0.4	99.9	N
35	5.63E-06	0.150	8.44E-07	0.1	100.0	N
36	5.41E-07	0.400	2.17E-07	0.0	100.0	N

Table 2-11

Screening of Seismic Sources: Dames and Moore Team

SCREENING OF SEISMIC SOURCES

site: Paducah team: DAM peak accel.

Source	Hazard	P*	Haz.P*	%	Acum. %	Include
21	9.93E-05	1.000	9.93E-05	37.1	37.1	Y
19	9.79E-05	1.000	9.79E-05	36.6	73.7	Y
C15	6.27E-05	1.000	6.27E-05	23.4	97.2	Y
18	6.74E-06	1.000	6.74E-06	2.5	99.7	Y
23B	9.31E-07	0.470	4.37E-07	0.2	99.8	N
71	3.08E-07	1.000	3.08E-07	0.1	100.0	N
23	1.30E-07	0.530	6.90E-08	0.0	100.0	N
18A	4.76E-08	1.000	4.76E-08	0.0	100.0	N
69	8.59E-10	1.000	8.59E-10	0.0	100.0	N
10B	1.21E-09	0.390	4.72E-10	0.0	100.0	N
donut sources, etc.						
21B	2.67E-04					
C03	5.71E-10					
C06	5.79E-07					
22	2.35E-04					

site: Paducah team: DAM 1-Hz PSV

Source	Hazard	P*	Haz.P*	%	Acum. %	Include
21	4.47E-04	1.000	4.47E-04	56.8	56.8	Y
19	1.35E-04	1.000	1.35E-04	17.1	73.9	Y
C15	9.99E-05	1.000	9.99E-05	12.7	86.6	Y
18	8.27E-05	1.000	8.27E-05	10.5	97.1	Y
23B	1.89E-05	0.470	8.87E-06	1.1	98.2	Y
71	4.79E-06	1.000	4.79E-06	0.6	98.8	Y
18A	4.42E-06	1.000	4.42E-06	0.6	99.4	Y
23	7.91E-06	0.530	4.19E-06	0.5	99.9	N
69	6.69E-07	1.000	6.69E-07	0.1	100.0	N
10B	3.32E-07	0.390	1.30E-07	0.0	100.0	N
donut sources, etc.						
21B	5.06E-04					
C03	1.19E-07					
C06	8.53E-06					
22	4.36E-04					

Table 2-12

Screening of Seismic Sources: Law Engineering Team

SCREENING OF SEISMIC SOURCES

site: Paducah team: LAW peak accel.

Source	Hazard	P*	Haz.P*	%	Acum. %	Include
18	4.52E-04	1.000	4.52E-04	47.2	47.2	Y
04A	4.64E-04	0.900	4.18E-04	43.7	90.9	Y
04B	4.69E-04	0.100	4.69E-05	4.9	95.8	Y
06	3.16E-05	0.860	2.72E-05	2.8	98.6	Y
117	6.39E-06	1.000	6.39E-06	0.7	99.3	Y
C07	6.36E-06	1.000	6.36E-06	0.7	100.0	N
07	5.17E-07	0.850	4.40E-07	0.0	100.0	N
118	1.39E-10	1.000	1.39E-10	0.0	100.0	N
15	2.80E-10	0.380	1.06E-10	0.0	100.0	N
116	1.00E-10	1.000	1.00E-10	0.0	100.0	N
donut sources, etc.						
117A	6.37E-06					

site: Paducah team: LAW 1-Hz PSV

Source	Hazard	P*	Haz.P*	%	Acum. %	Include
18	8.25E-04	1.000	8.25E-04	63.9	63.9	Y
04A	3.88E-04	0.900	3.49E-04	27.1	91.0	Y
06	7.07E-05	0.860	6.08E-05	4.7	95.7	Y
04B	3.75E-04	0.100	3.75E-05	2.9	98.6	Y
07	1.54E-05	0.850	1.31E-05	1.0	99.6	Y
117	2.50E-06	1.000	2.50E-06	0.2	99.8	N
C07	2.48E-06	1.000	2.48E-06	0.2	100.0	N
15	8.91E-10	0.380	3.39E-10	0.0	100.0	N
118	1.23E-10	1.000	1.23E-10	0.0	100.0	N
116	1.00E-10	1.000	1.00E-10	0.0	100.0	N
donut sources, etc.						
117A	2.49E-06					

Table 2-13

Screening of Seismic Sources: Rondout Associates Team

SCREENING OF SEISMIC SOURCES

site: Paducah team: RND peak accel.

Source	Hazard	P*	Haz.P*	%	Acum. %	Include
1	3.80E-04	1.000	3.80E-04	50.8	50.8	Y
2	3.67E-04	1.000	3.67E-04	49.0	99.8	Y
4	1.24E-06	1.000	1.24E-06	0.2	100.0	N
3	3.61E-08	1.000	3.61E-08	0.0	100.0	N
52	2.16E-08	1.000	2.16E-08	0.0	100.0	N
48	1.23E-10	0.870	1.07E-10	0.0	100.0	N
6	1.07E-10	0.830	8.86E-11	0.0	100.0	N
14	1.08E-10	0.670	7.22E-11	0.0	100.0	N

site: Paducah team: RND 1-Hz PSV

Source	Hazard	P*	Haz.P*	%	Acum. %	Include
1	1.14E-03	1.000	1.14E-03	62.6	62.6	Y
2	6.32E-04	1.000	6.32E-04	34.9	97.5	Y
4	4.24E-05	1.000	4.24E-05	2.3	99.9	Y
3	2.45E-06	1.000	2.45E-06	0.1	100.0	N
48	4.17E-08	0.870	3.63E-08	0.0	100.0	N
52	3.35E-08	1.000	3.35E-08	0.0	100.0	N
14	4.81E-08	0.670	3.23E-08	0.0	100.0	N
6	2.66E-08	0.830	2.21E-08	0.0	100.0	N

Table 2-14

Screening of Seismic Sources: Weston Geophysical Team

SCREENING OF SEISMIC SOURCES

site: Paducah team: WGC peak accel.

Source	Hazard	P*	Haz.P*	%	Acum. %	Include
31	4.55E-04	0.950	4.33E-04	47.3	47.3	Y
C11	4.38E-04	0.950	4.16E-04	45.5	92.8	Y
32	1.14E-03	0.050	5.70E-05	6.2	99.0	Y
33	4.55E-06	1.000	4.55E-06	0.5	99.5	N
34	2.97E-06	1.000	2.97E-06	0.3	99.8	N
106	1.48E-06	1.000	1.48E-06	0.2	100.0	N
101	4.79E-09	1.000	4.79E-09	0.0	100.0	N
donut sources, etc.						
C16	2.73E-09					
C15	3.39E-09					
C12	3.67E-09					
C14	4.10E-09					
C13	4.27E-09					

site: Paducah team: WGC 1-Hz PSV

Source	Hazard	P*	Haz.P*	%	Acum. %	Include
31	6.83E-04	0.950	6.49E-04	52.3	52.3	Y
C11	4.47E-04	0.950	4.25E-04	34.3	86.6	Y
32	1.60E-03	0.050	8.00E-05	6.5	93.1	Y
33	4.61E-05	1.000	4.61E-05	3.7	96.8	Y
34	3.47E-05	1.000	3.47E-05	2.8	99.6	Y
106	4.50E-06	1.000	4.50E-06	0.4	100.0	N
101	3.18E-07	1.000	3.18E-07	0.0	100.0	N
donut sources, etc.						
C16	2.16E-07					
C15	2.57E-07					
C12	2.70E-07					
C14	3.02E-07					
C13	3.17E-07					

Table 2-15

Screening of Seismic Sources: Woodward-Clyde Team

SCREENING OF SEISMIC SOURCES

site: Paducah team: WCC peak accel.

Source	Hazard	P*	Haz.P*	%	Acum. %	Include
43	8.03E-04	1.000	8.03E-04	87.9	87.9	Y
40	3.52E-05	1.000	3.52E-05	3.9	91.8	Y
C08	3.06E-05	1.000	3.06E-05	3.4	95.1	Y
42	3.03E-05	1.000	3.03E-05	3.3	98.4	Y
44	1.43E-05	1.000	1.43E-05	1.6	100.0	Y
donut sources, etc.						
41	4.33E-05					

site: Paducah team: WCC 1-Hz PSV

Source	Hazard	P*	Haz.P*	%	Acum. %	Include
43	8.62E-04	1.000	8.62E-04	50.4	50.4	Y
40	3.46E-04	1.000	3.46E-04	20.2	70.6	Y
C08	2.08E-04	1.000	2.08E-04	12.2	82.8	Y
42	1.95E-04	1.000	1.95E-04	11.4	94.2	Y
44	9.95E-05	1.000	9.95E-05	5.8	100.0	Y
donut sources, etc.						
41	3.57E-04					

Table 2-16

Sources used for Seismic Hazard Calculations

Team	Sources
Bechtel	30, BZ0, J, K, 31, 34
Dames and Moore	18, 19, 21, 23B, 71, C15(=22−21B)
Law Engineering	04A, 04B, 06, 07, 18
Rondout	1, 2, 4
Weston Geophysical	31, 32, 33, 34, C11
Woodward-Clyde	40, C08(=41−40), 42, 43, 44

Table 2-17

Source Combinations and Their Probabilities

Team	Prob.	Active Sources					
Bechtel	0.03150	30	BZ0	K	31	J	
	0.17850	30	BZ0	K	31		
	0.02100	30	BZ0	K	J		
	0.11900	30	BZ0	K			
	0.03150	30	BZ0	34	31	J	
	0.17850	30	BZ0	34	31		
	0.02100	30	BZ0	34	J		
	0.11900	30	BZ0	34			
	0.02700	30	BZ0	31	J		
	0.15300	30	BZ0	31			
	0.01800	30	BZ0	J			
	0.10200	30	BZ0				
Dames & Moore	0.47000	18	19	21	71	C15	23B
	0.53000	18	19	21	71	C15	
Law Engineering	0.65790	18	04A	06	07		
	0.11610	18	04A	06			
	0.10710	18	04A	07			
	0.01890	18	04A				
	0.07310	18	04B	06	07		
	0.01290	18	04B	06			
	0.01190	18	04B	07			
	0.00210	18	04B				
Rondout Associates	1.00000	1	2	4			
Weston Geophysical	0.95000	33	34	31	C11		
	0.05000	33	34	32			
Woodward-Clyde	1.00000	40	C08	42	43	44	

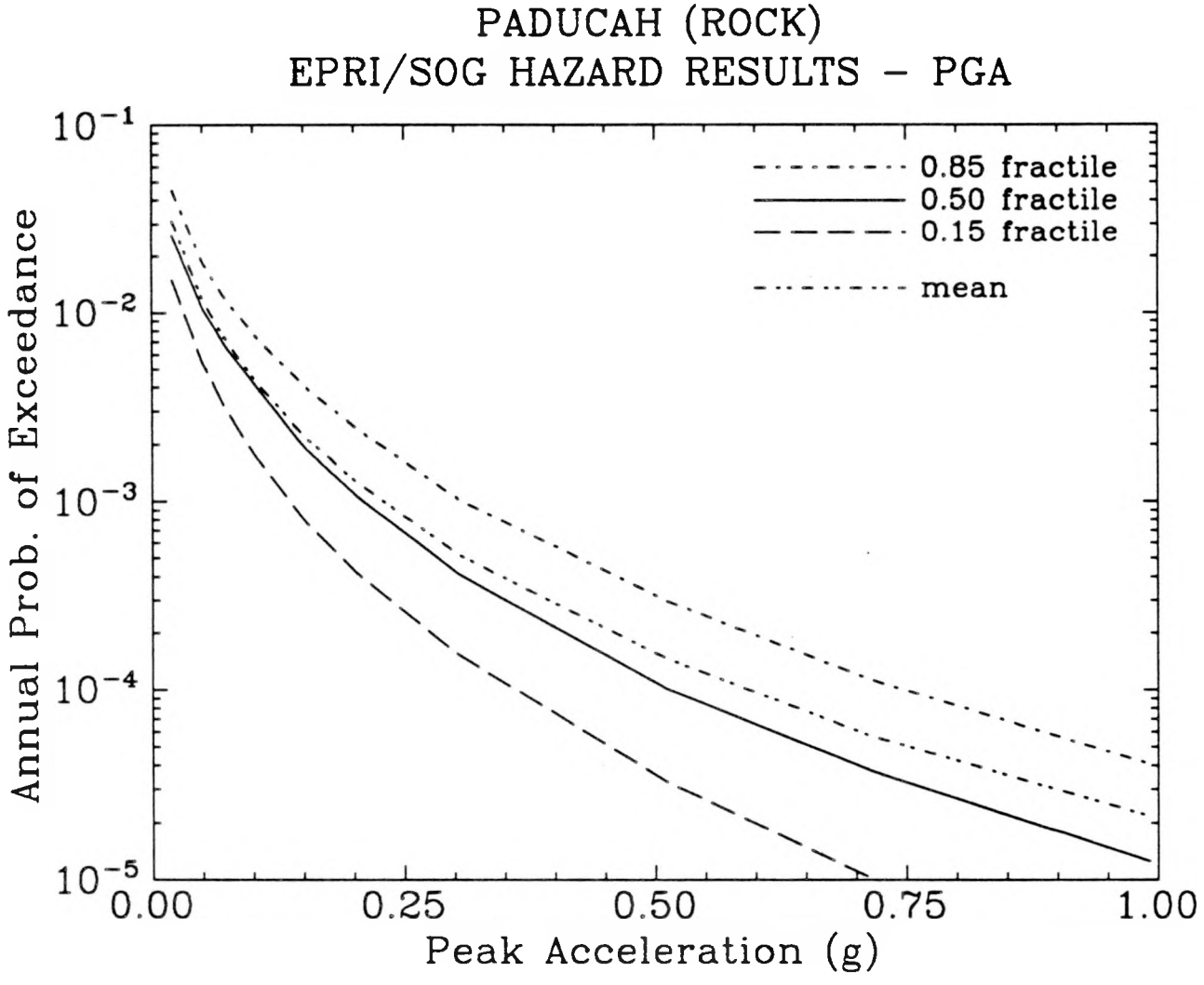

Figure 2-19. Peak ground acceleration hazard curves for Paducah (for rock site conditions) computed using the EPRI/SOG methodology.

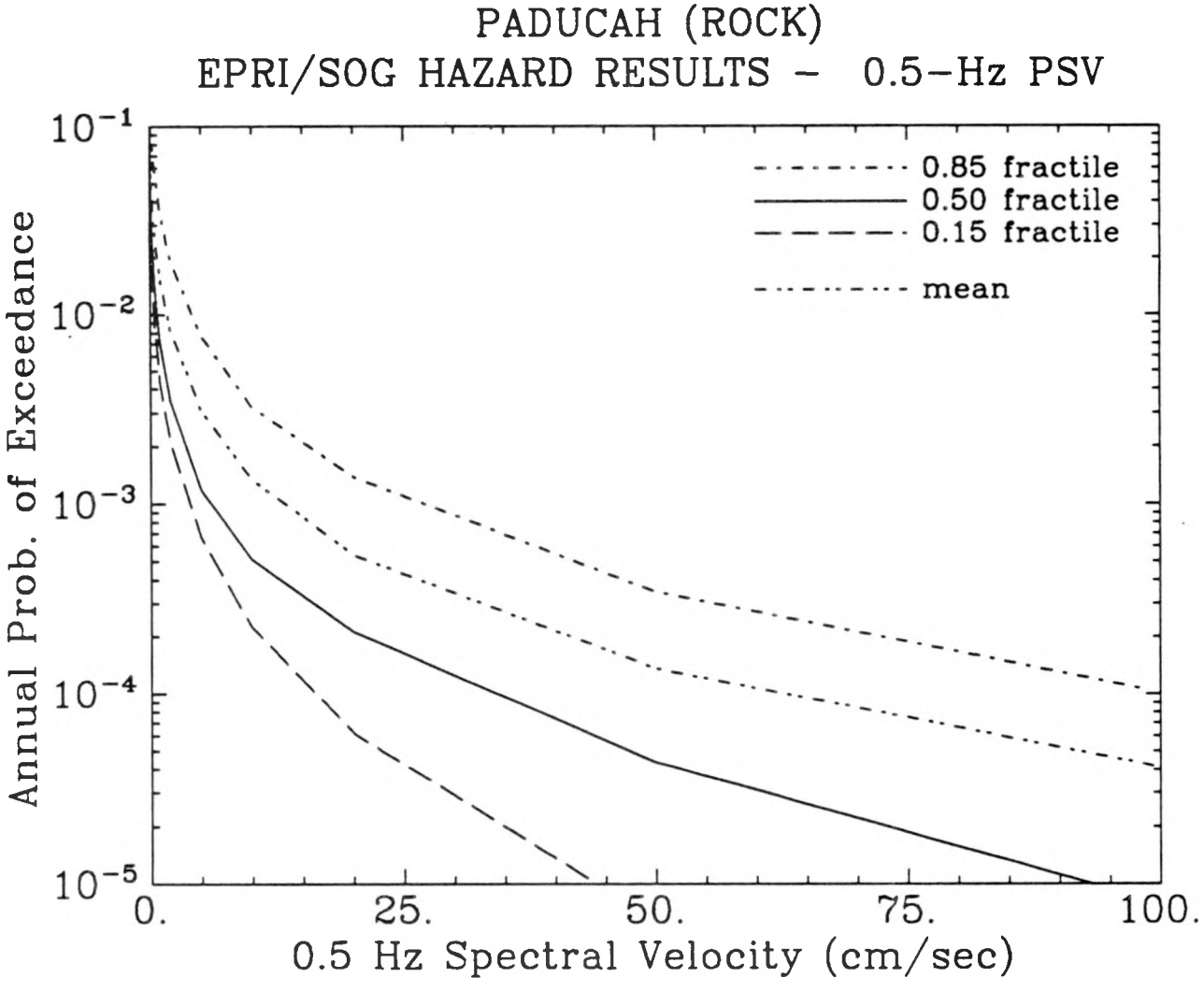

Figure 2-20. 0.5-Hz spectral velocity hazard curves for Paducah (for rock site conditions) computed using the EPRI/SOG methodology.

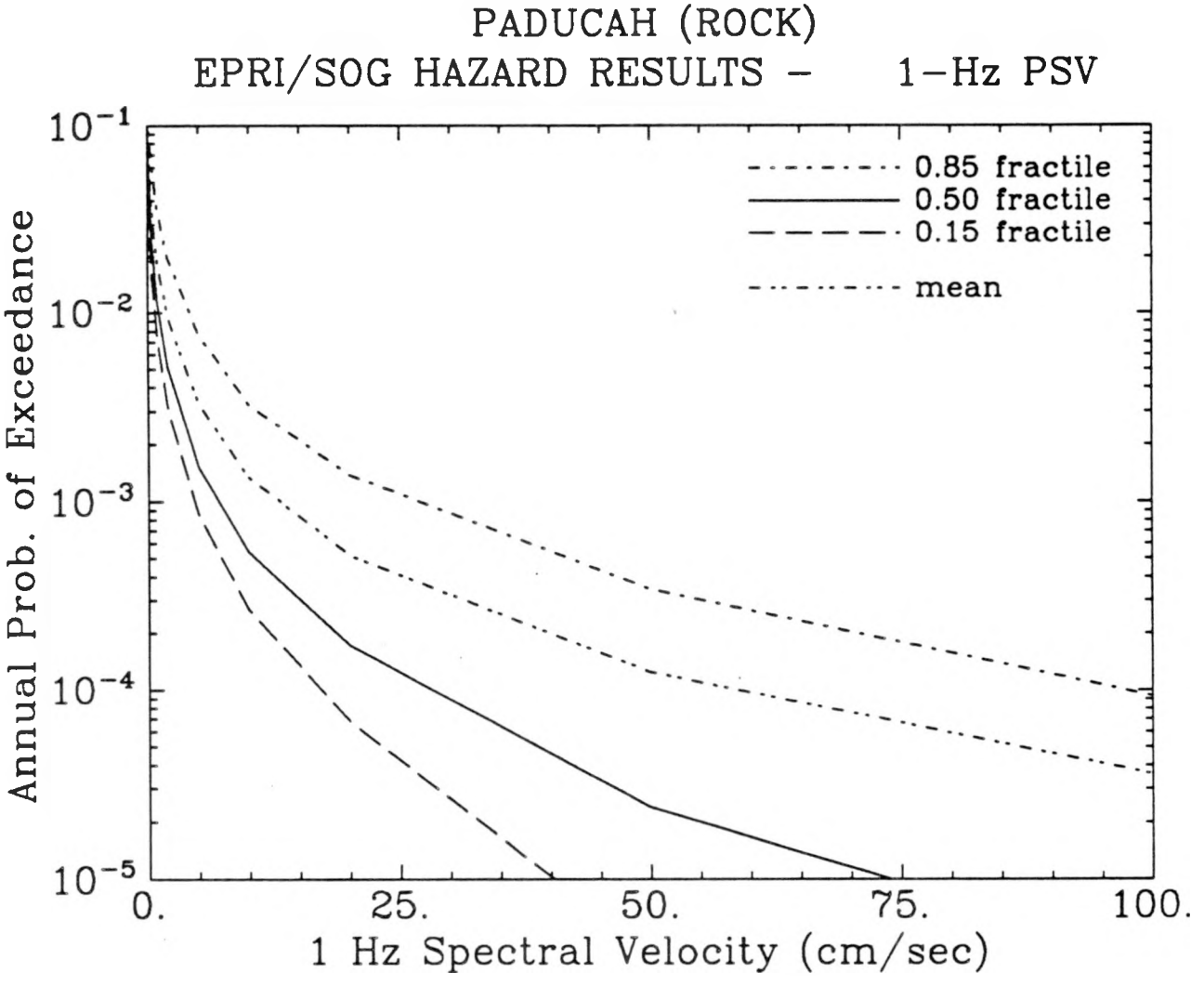

Figure 2-21. 1-Hz spectral velocity hazard curves for Paducah (for rock site conditions) computed using the EPRI/SOG methodology.

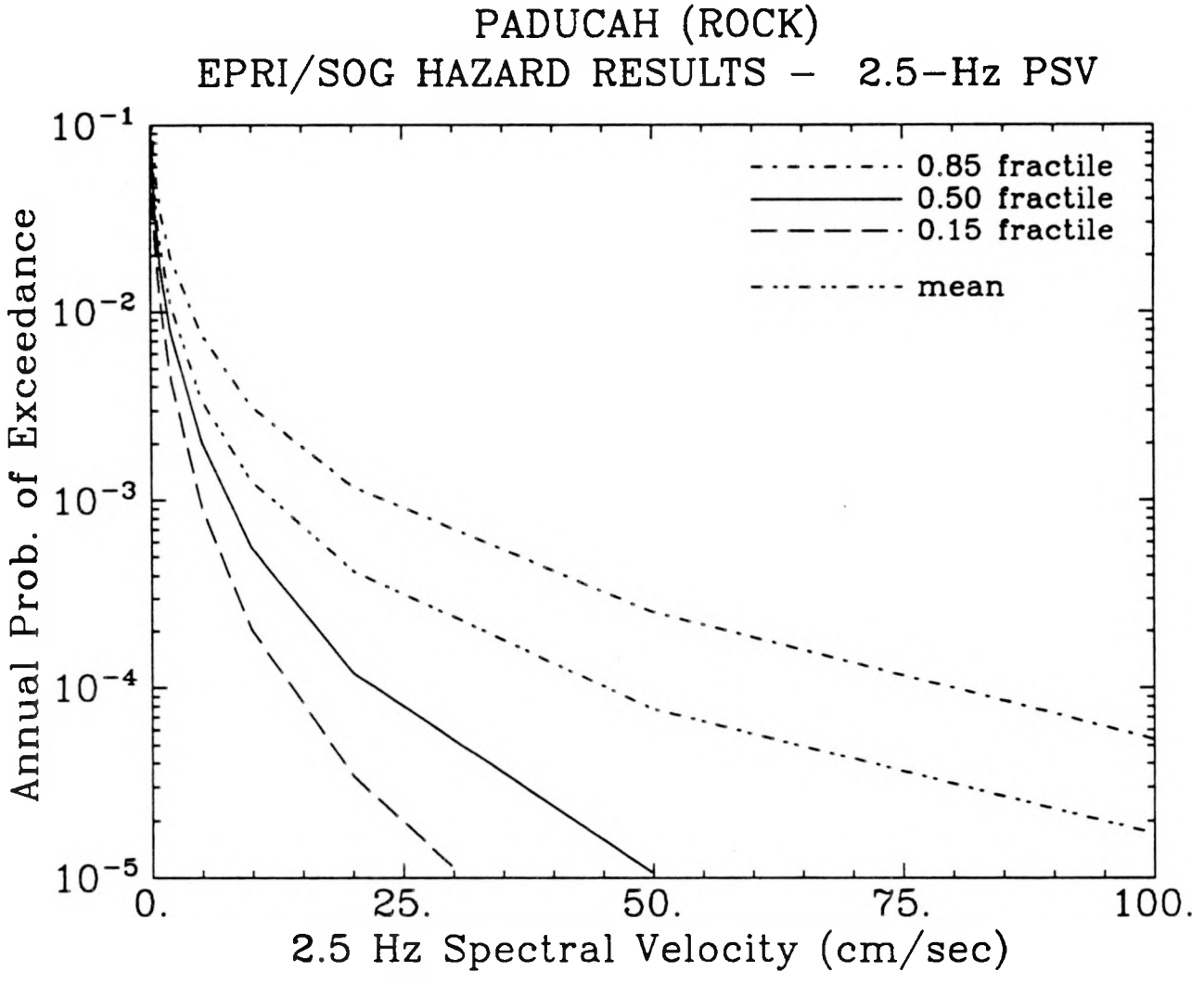

Figure 2-22. 2.5-Hz spectral velocity hazard curves for Paducah (for rock site conditions) computed using the EPRI/SOG methodology.

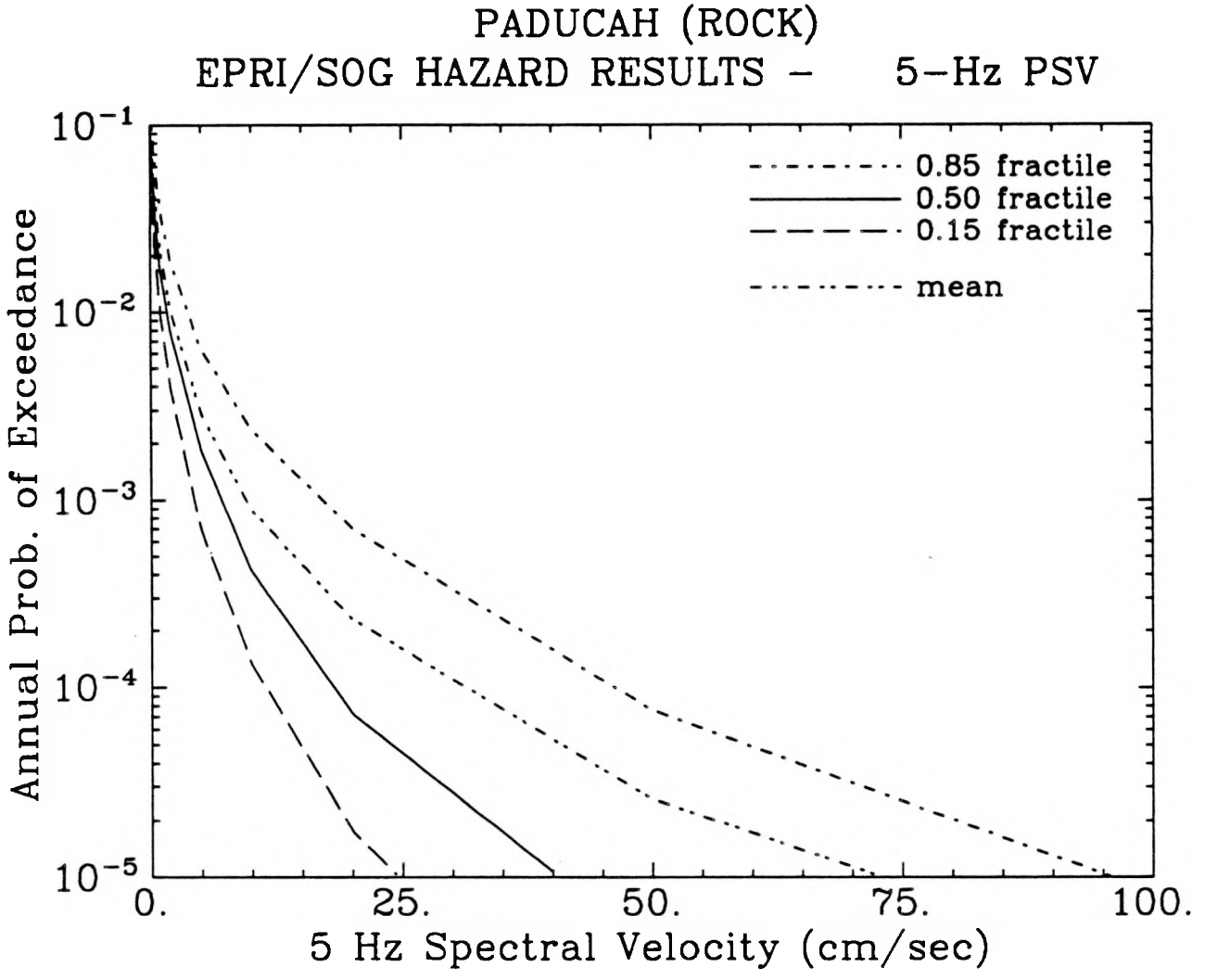

Figure 2-23. 5-Hz spectral velocity hazard curves for Paducah (for rock site conditions) computed using the EPRI/SOG methodology.

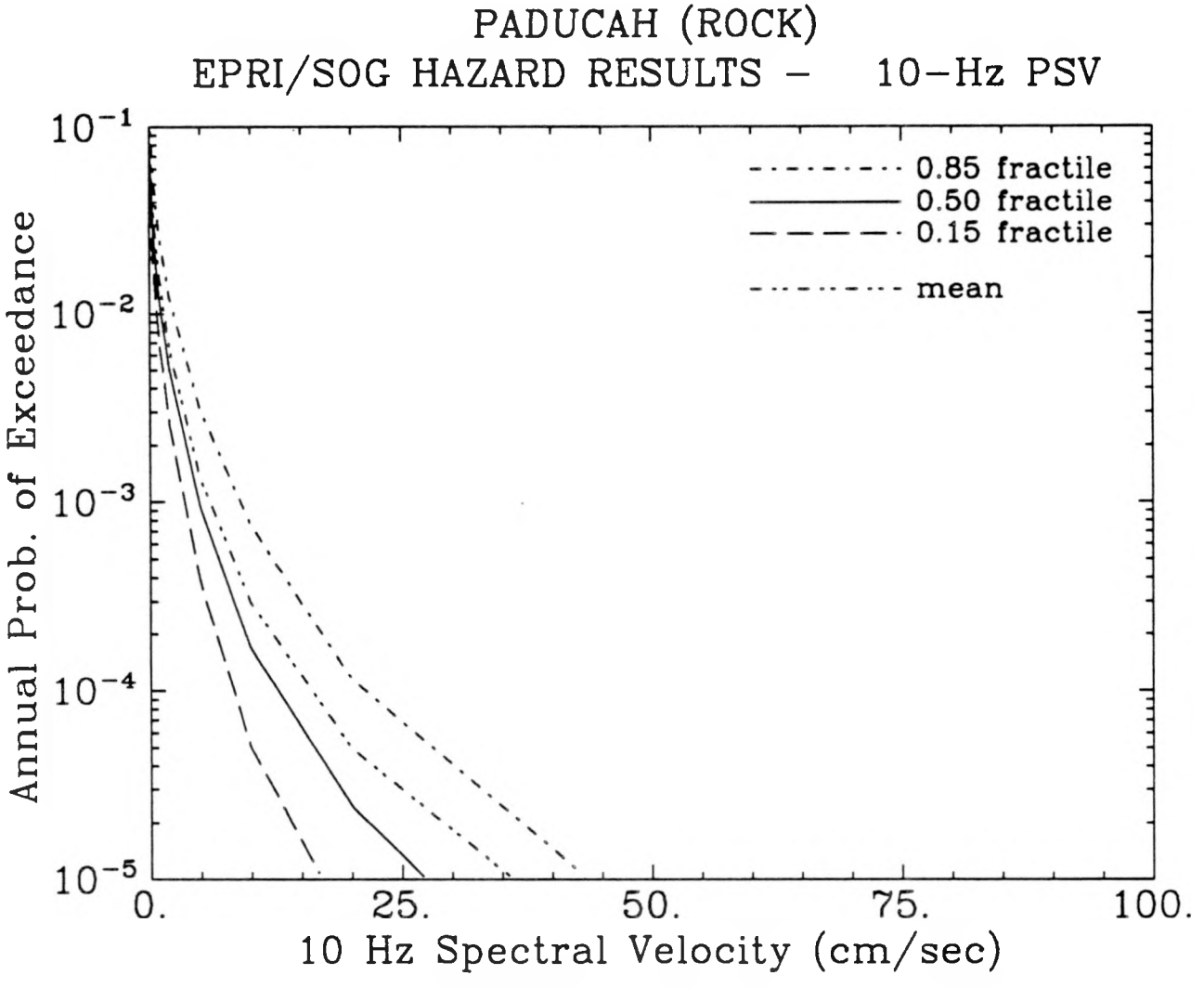

Figure 2-24. 10-Hz spectral velocity hazard curves for Paducah (for rock site conditions) computed using the EPRI/SOG methodology.

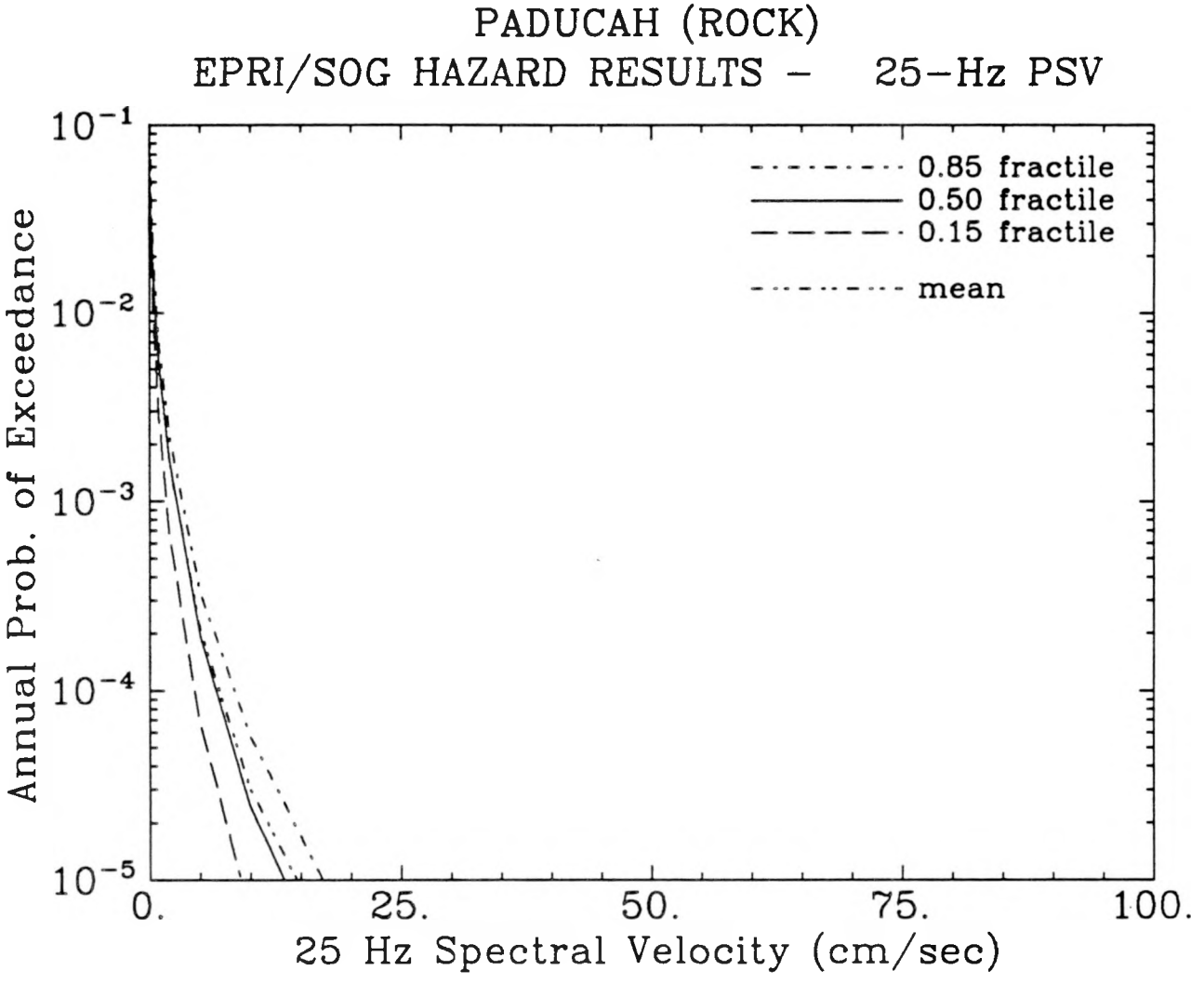

Figure 2-25. 25-Hz spectral velocity hazard curves for Paducah (for rock site conditions) computed using the EPRI/SOG methodology.

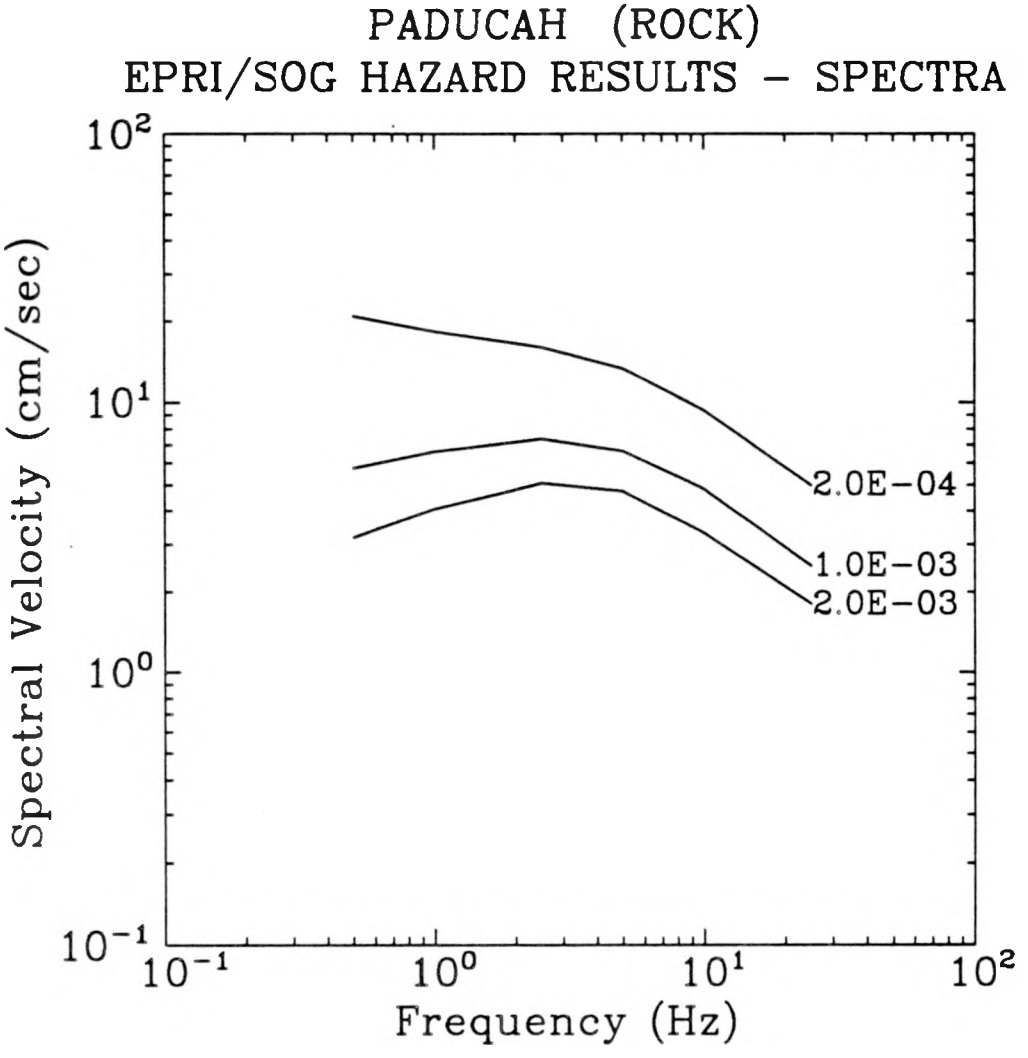

Figure 2-26. Seismic hazard at Paducah (for rock site conditions) computed using the EPRI/SOG methodology. Results shown as uniform hazard spectra for four values of the annual probability of exceedance.

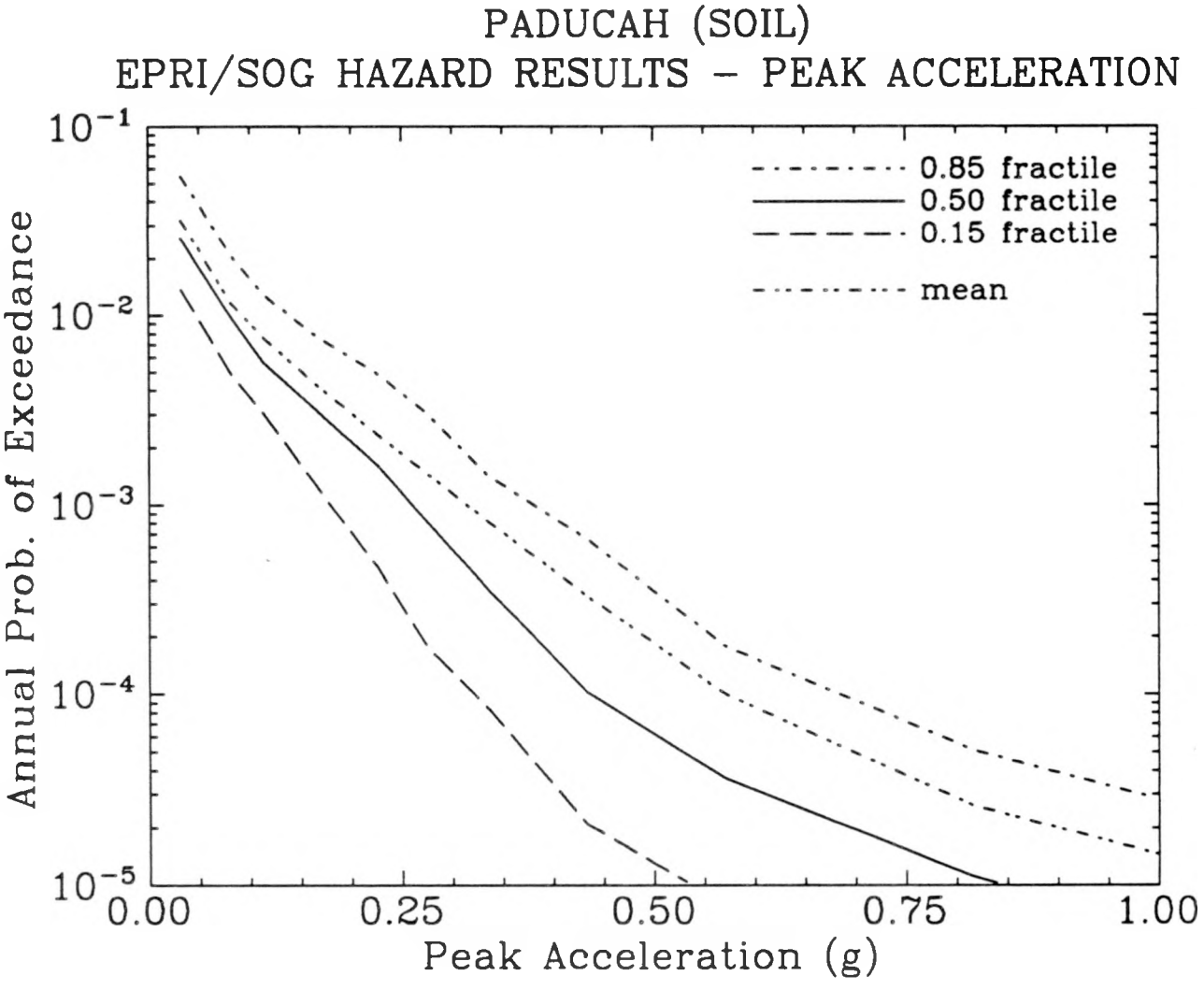

Figure 2-27. Peak ground acceleration hazard curves for Paducah (for soil site conditions) computed using the EPRI/SOG methodology.

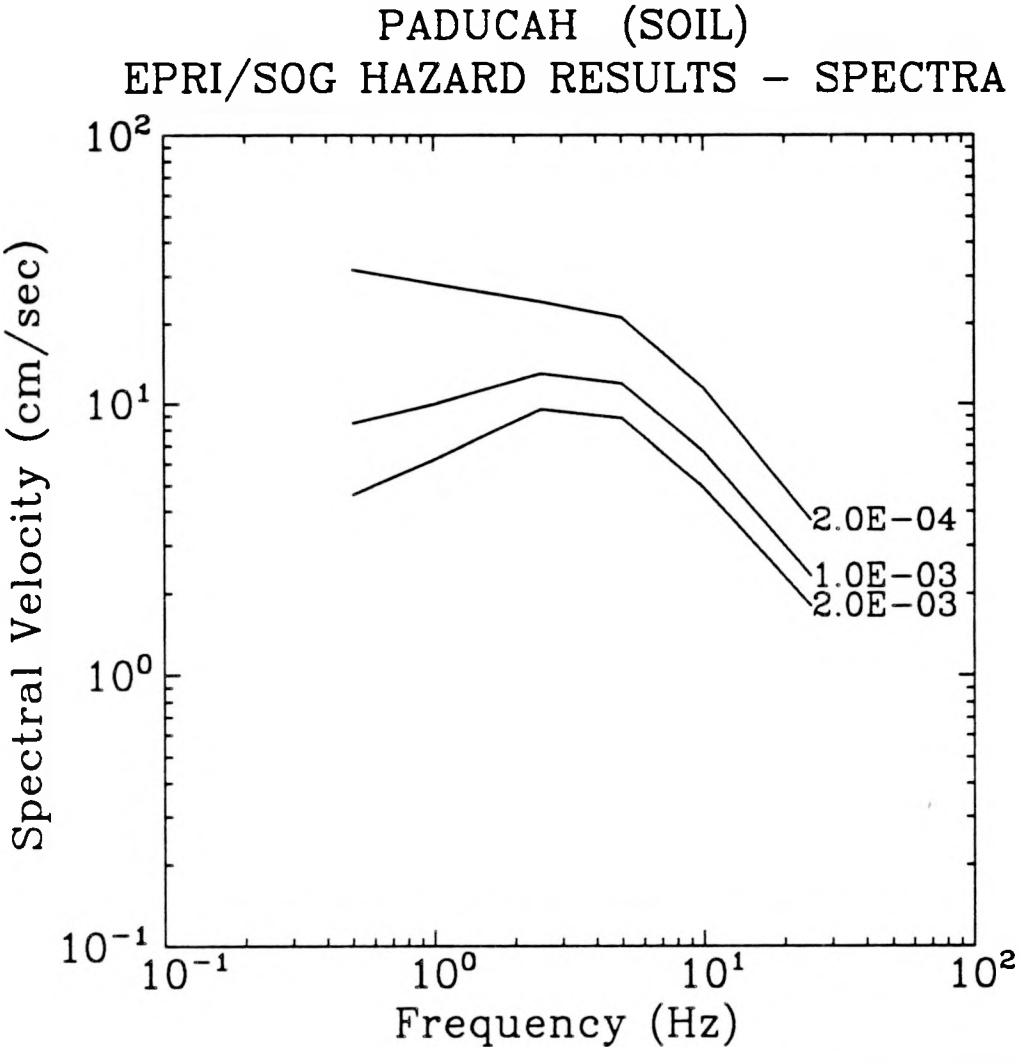

Figure 2-28. Median uniform-hazard spectra for Paducah (for soil site conditions) computed using the EPRI/SOG methodology.

Table 2-18

Summary of Sources Contributing to the
Seismic Hazard in the EPRI/SOG Calculations

Team	Source	%Contrib (0.25g)	R(km)	b	Rate ($M > 5$)	Rate/Area ($M > 5$)	$m_{b,max}$
Bechtel	30 (NM)	61	0	0.96	2.9E-02	3.3E-02	7.4(0.1) 7.5(0.9)
	BZ0	20	1.8	0.77	1.0E-01	4.3E-03	6.2
	31	12	1.8	0.98	1.8E-02	1.1E-02	6.1
Dames & Moore	21 (NM)	37	33	1.02	3.0E-02	6.8E-02	7.2(0.25) 7.5(0.75)
	19	37	0.3	0.99	1.1E-02	4.8E-03	6.5
	C15	23	0	0.98	1.8E-02	7.4E-03	6.9
Law	4A, 4B	49	0	0.85	1.9E-02	1.9E-02	6.5
	18 (NM)	47	11	0.9	2.9E-02	4.8E-02	7.4(1.0)
Rondout	1 (NM)	51	20		7.0E-02	8.5E-02	7.1(0.1) 7.3(0.8) 7.4(0.1)
	2	49	0	0.92	4.2E-02	5.6E-03	6.8
Weston	C11	47	0	0.815	2.3E-02	1.2E-02	6.6
	31(NM)	46	7	0.914	2.8E-02	5.3E-02	7.2(1.0)
Woodward-Clyde	43	88	0	0.778	3.0E-02	1.4E-02	5.8(0.33) 6.3(0.34) 7.4(0.43)
	40 (NM)	4	66	0.9	2.5E-02	4.2E-02	7.2(0.33) 7.5(0.34) 7.9(0.43)
	C08	3	47	0.8	1.8E-02	4.4E-03	6.8

Section 3

LLNL METHODOLOGY AND RESULTS

3.1 METHODOLOGY

The second source of interpretations for this study consists of the study of seismic hazard in the EUS conducted by LLNL (1). This study culminates a decade of effort funded by the U.S. Nuclear Regulatory Commission to characterize earthquake sources, seismicity parameters, and ground motion estimates for the region, for the purpose of evaluating seismic hazard at nuclear plant sites. Two panels of experts were formed. Eleven seismicity experts familiar with the region were polled for interpretations of seismic sources and ground motion parameter values, and five ground motion experts were polled for opinions on appropriate attenuation equations to estimate PGA and response spectrum amplitudes. Uncertainties in the interpretations were represented by discrete and continuous distributions, and uncertainty in the seismic hazard was derived by Monte Carlo sampling of the input distributions, producing a seismic hazard curve for each set of simulated variables and thus representing the uncertainty in the seismic hazard as a function of uncertainty in expert interpretation.

LLNL performed its methodology for the Paducah site under a separate agreement, and provided results for use in this study (2,3). We summarize herein some of the important inputs to the LLNL analysis and our interpretations of them for this study.

3.2 SEISMICITY INTERPRETATIONS

The eleven seismicity experts provided sets of seismic sources for the CEUS; the basic set of sources for the region are reproduced in Figures 3–1 through 3–11, for comparison to the EPRI sources. Some LLNL experts also specified alternative geometries of sources; these are not reproduced here but are available in the LLNL documentation (1). By contrast to the EPRI study, which specified uncertainty on the seismic activity of each source separately, the LLNL experts specified global alternatives for sets of sources that might be active simultaneously.

Seismicity parameters (rates of activity and Richter b-values) for the sources were provided by the seismicity experts, although the LLNL team made available the results of calculations of these parameters using a standard method and an earthquake catalog specified by the

expert. Distributions and correlations were also specified to represent the uncertainty of these parameters. In addition, the distribution of maximum possible earthquake size was specified for each source by each expert. (Most of them used magnitude to characterize earthquake size; one used MM intensity, and a second used a combination of the two.)

3.3 GROUND MOTION MODELS

3.3.1 Attenuation Functions for Rock

Five earth scientists and engineers were asked to derive ground motion estimation equations for the EUS for the LLNL study. These equations were to estimate PGA and response spectrum amplitude as a function of earthquake magnitude and distance. Estimating such equations for the EUS is problematic because of the lack of recorded strong earthquake motions in the area with which to calibrate empirical techniques or validate theoretical models. Any method thought to be adequate by the five experts was acceptable. The five participants were asked to specify uncertainty in their choice of ground motion equations by designating multiple models with subjective weights.

One set of models—the models selected by ground-motion Expert 5—gives substantially higher ground motion estimates than the others for PGA and response spectrum amplitudes. For PGA this model is designated "G16-A3" in the LLNL report (1); it is a combination of two equations, a correlation between PGA and MM intensity published by Trifunac from California data, and an MM intensity attenuation equation published by Gupta and Nuttli. This selection, and the corresponding models for spectral velocity, received 100% weight from Expert 5, and zero weight from the other panelists. Comparing the predictions from this equation to data available from EUS seismographs and accelerographs indicates that equation G16-A3 severely over-estimates ground motions in the EUS, particularly at distances greater than 20 km from the earthquake source. [See Figures 5–123 through 5–125 of (4) for these comparisons.]

There are good reasons why equation G16-A3 might lead to poor estimates of ground motion in the EUS. This function was obtained by substitution of a stochastic relationship between instrumental ground-motion and intensity into a stochastic intensity-attenuation relation. This type of substitution of one regression into another is mathematically incorrect and has been demonstrated to produce significant biases when applied to intensity-attenuation data (5). In particular, after such a substitution the dependent variable does not appear to be as strongly correlated to the independent variable as it should be, which is the behavior evident in comparisons of data with estimates from G16-A3. For example, the data in Figures 5-123 through 5-125 of (4) show a much stronger dependence on distance than do the estimates.

Further, this model was given zero weight by four of the LLNL panelists (and 100% weight by the fifth), an indication that the model has a small following in the scientific community [see Tables 3.5 and 3.6 in Volume 1 of (1)].

At the request of MMES, LLNL has calculated seismic-hazard at Paducah with and without the attenuation equations selected by Expert 5.

3.3.2 Site Amplification Factors

LLNL developed generic site amplification factors using a modeling approach similar to that used by EPRI/SOG. The two main differences between the LLNL and EPRI/SOG computations are as follows: (1) LLNL did not consider soil nonlinearity, and (2) LLNL used input ground motions typical of the western United States. Additional details on the LLNL site-amplification factors are contained in (1); comparisons of the LLNL and EPRI/SOG amplification factors are contained in (4). In the LLNL methodology, a site is assigned to one of the ten soil categories based on its depth to bedrock and shear-wave velocity.

Four of the five LLNL ground-motion experts adopted the above site-amplification factors. Ground-motion Expert 5 selected a different set of amplification factors, which are used in connection with this expert's attenuation functions.

LLNL has calculated seismic-hazard at Paducah for for rock conditions and for deep-soil site conditions (>300 ft.). This depth range is consistent with the actual depth of 350 feet obtained in recent site investigations (6).

3.4 COMPUTATIONS

The Monte Carlo simulation procedure used by LLNL to express uncertainty in seismic hazard as a function of uncertain input was conducted as follows. There were 55 possible combinations of the eleven seismicity experts and the five (or four) ground motion experts, and each combination was considered separately. For each, 50 simulations of uncertain parameters were made, drawing from the distributions on seismicity parameters, ground motion equations, and attenuation randomness terms specified by each expert. This resulted in 2750 combinations of parameters from which a family of 2750 seismic hazard curves could be calculated. Each of these seismic hazard curves was then assigned a weight based on a self-weighting provided by the experts. This led to an uncertainty distribution on the frequency of exceedance for any PGA or PSV level, from which fractiles of seismic hazard can be computed and plotted as fractile seismic hazard curves.

LLNL calculated four sets of seismic hazard results, corresponding to rock and soil conditions, and to calculations with and without ground-motion Expert 5. These results are presented in Figures 3-12 through 3-19, in the form of PGA hazard curves and median uniform-hazard spectra.

3.5 REFERENCES

1. D. L. Bernreuter, J. B. Savy, R. W. Mensing, and J. C. Chen. *Seismic Hazard Characterization of 69 Plant Sites East of the Rocky Mountains.* Technical Report NUREG/CR5250, UCID-21517, U. S. Nuclear Regulatory Commission, 1988.

2. B.C. Davis. "Paducah and Portsmouth Seismic Hazard Results"; Material handed out at meeting and computer files sent to G.R. Toro. Lawrence Livermore National Laboratory, July 9, 1990, and August 30, 1990.

3. B. C. Davis and J. B. Savy. *Paducah and Portsmouth Seismic Hazard Analysis.* Technical Report, Lawrence Livermore National Laboratory, November 1990. Report to Martin Marietta Energy Systems.

4. R. K. McGuire, G. R. Toro, and W. J. Silva. *Probabilistic Seismic Hazard Evaluations in the Central and Eastern United States — Appendix A: Model of Earthquake Ground Motion for the Central and Eastern United States.* Technical Report, Electric Power Research Institute, 1989. EPRI Project RP101-53, prepared by Risk Engineering, Inc.

5. C. A. Cornell, H. Banon, and A. F. Shakal. "Seismic Motion and Response Prediction Alternatives". *Earthquake Engineering and Structural Dynamics*, 7:295–315, 1979.

6. K. E. Shaffer. Paducah and Portsmouth Soil Depth References. Written Communication to Robin K. McGuire. Martin Marietta Energy Systems, May 2, 1991.

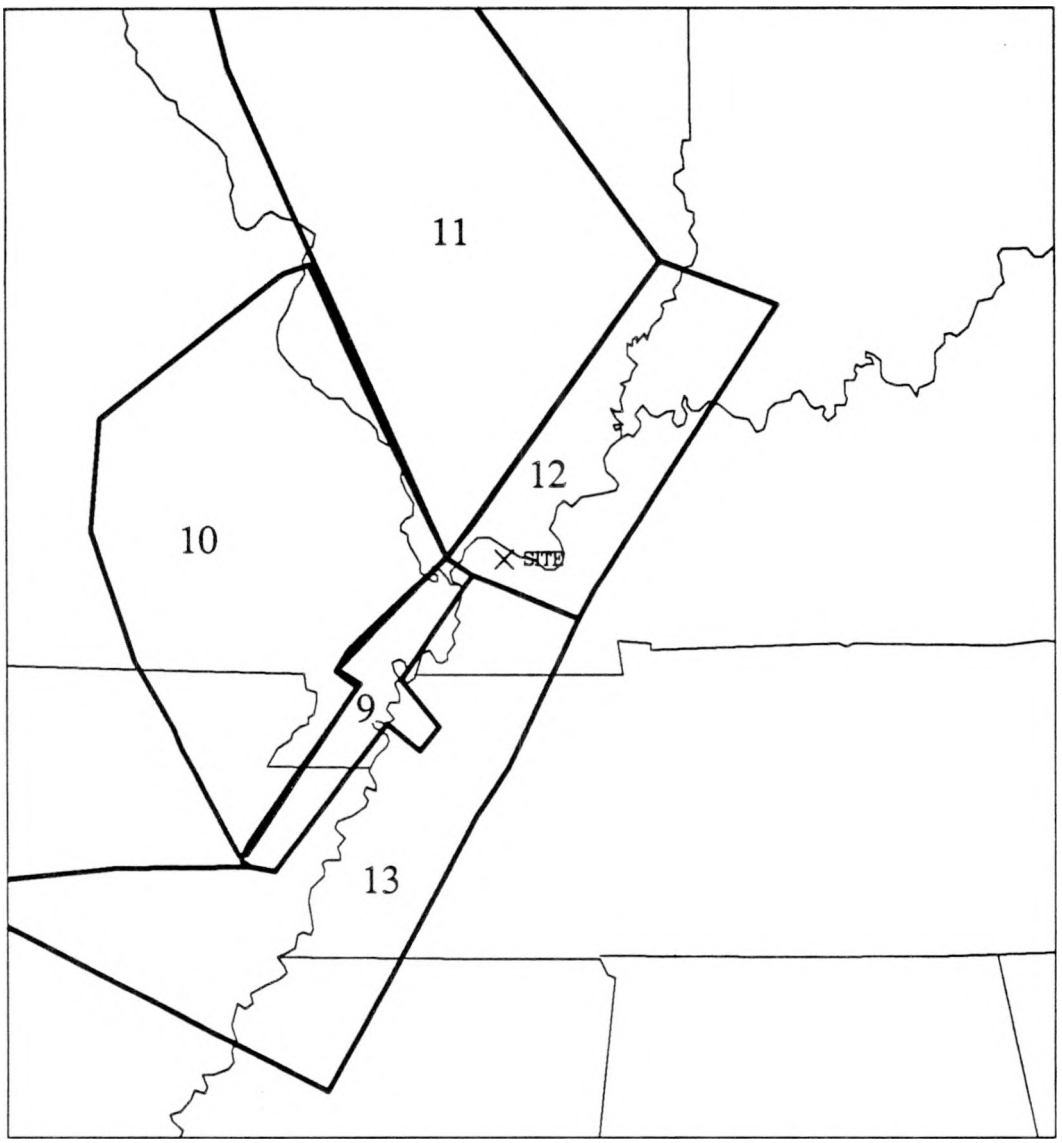

Figure 3-1. Map showing the seismic sources specified by LLNL seismicity expert 1 in the region around the Paducah site. Source: Volume 1 of (1).

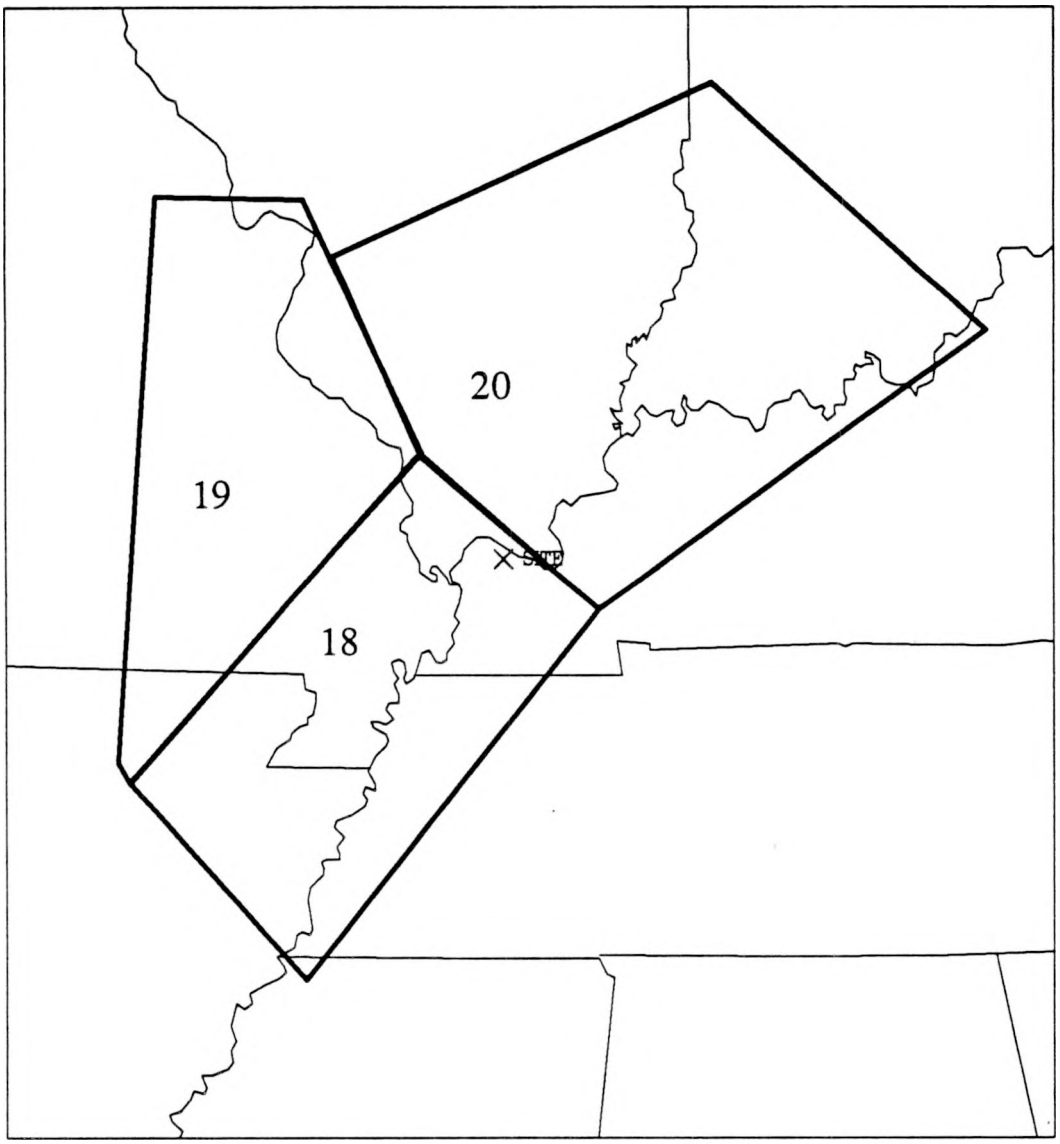

Figure 3-2. Map showing the seismic sources specified by LLNL seismicity expert 2 in the region around the Paducah site. Source: Volume 1 of (1).

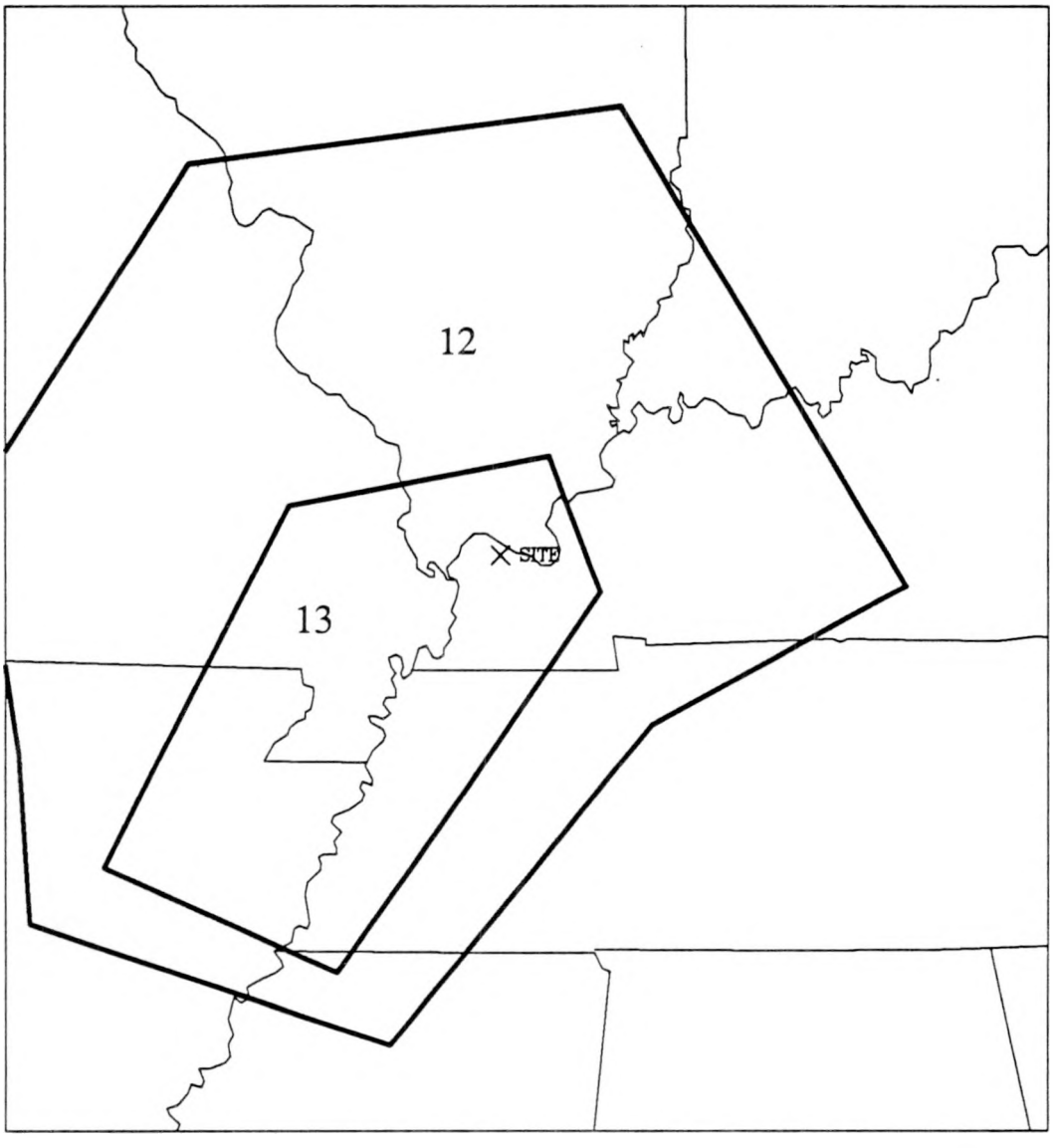

Figure 3-3. Map showing the seismic sources specified by LLNL seismicity expert 3 in the region around the Paducah site. Source: Volume 1 of (1).

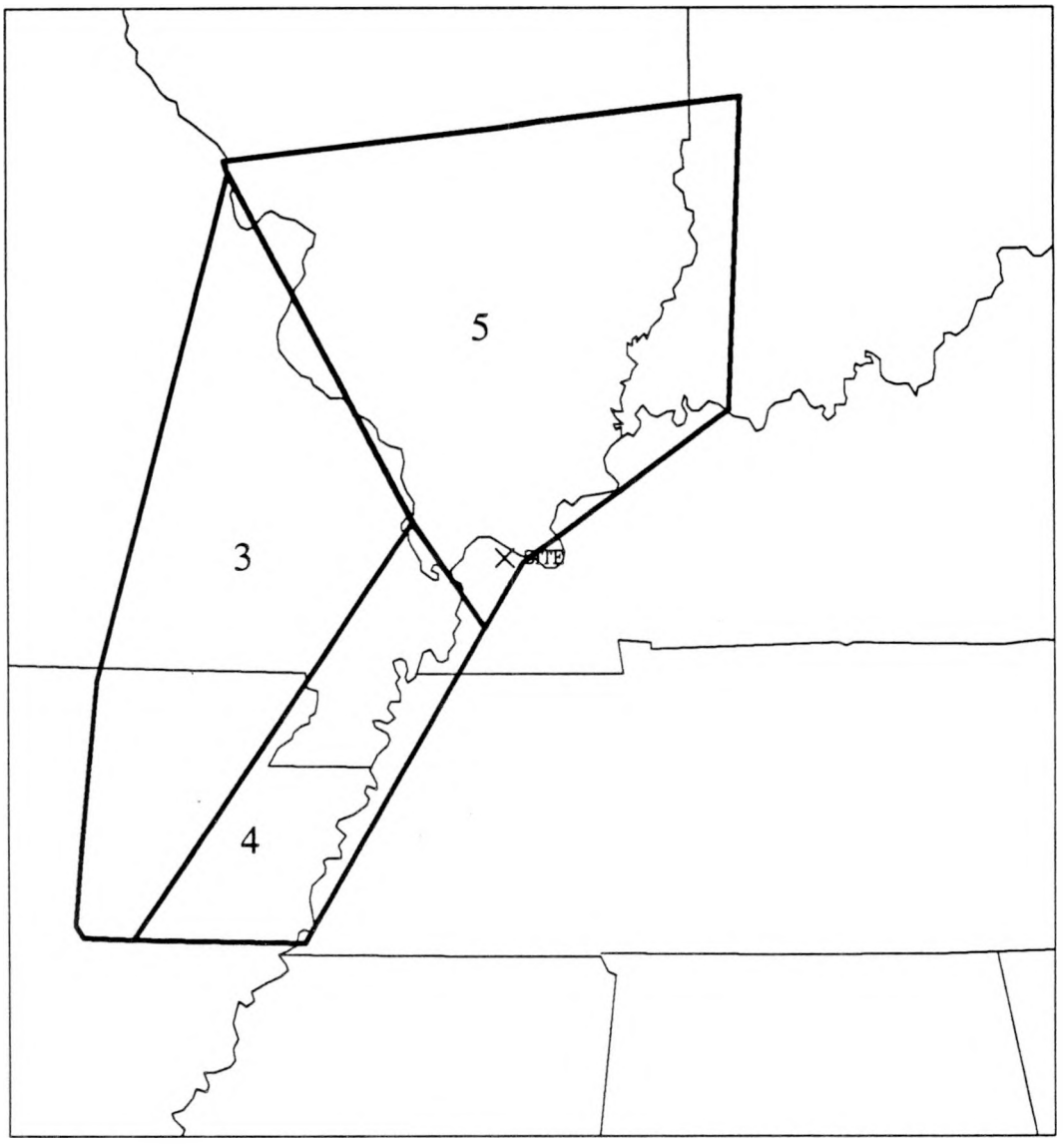

Figure 3-4. Map showing the seismic sources specified by LLNL seismicity expert 4 in the region around the Paducah site. Source: Volume 1 of (1).

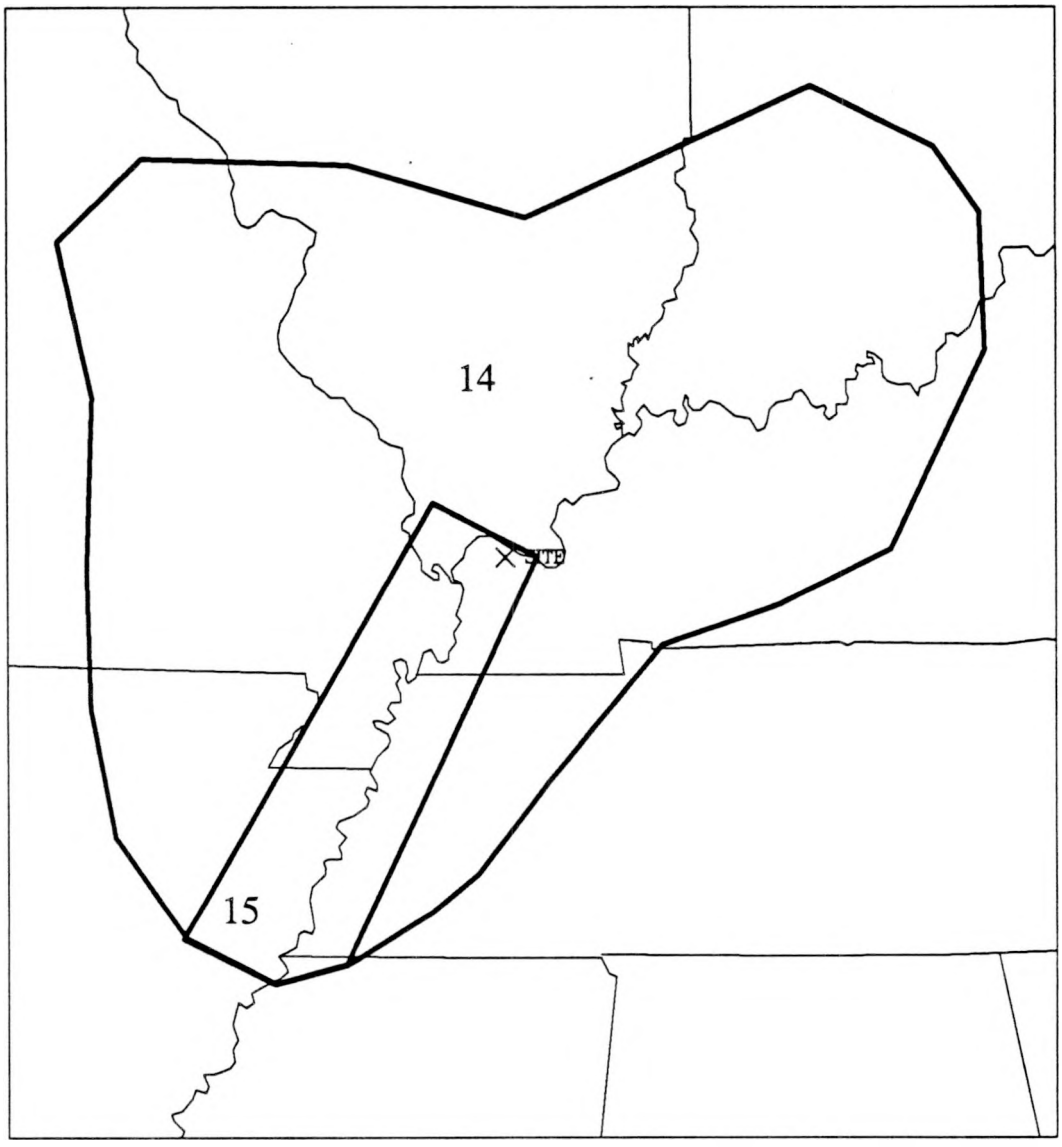

Figure 3-5. Map showing the seismic sources specified by LLNL seismicity expert 5 in the region around the Paducah site. Source: Volume 1 of (1).

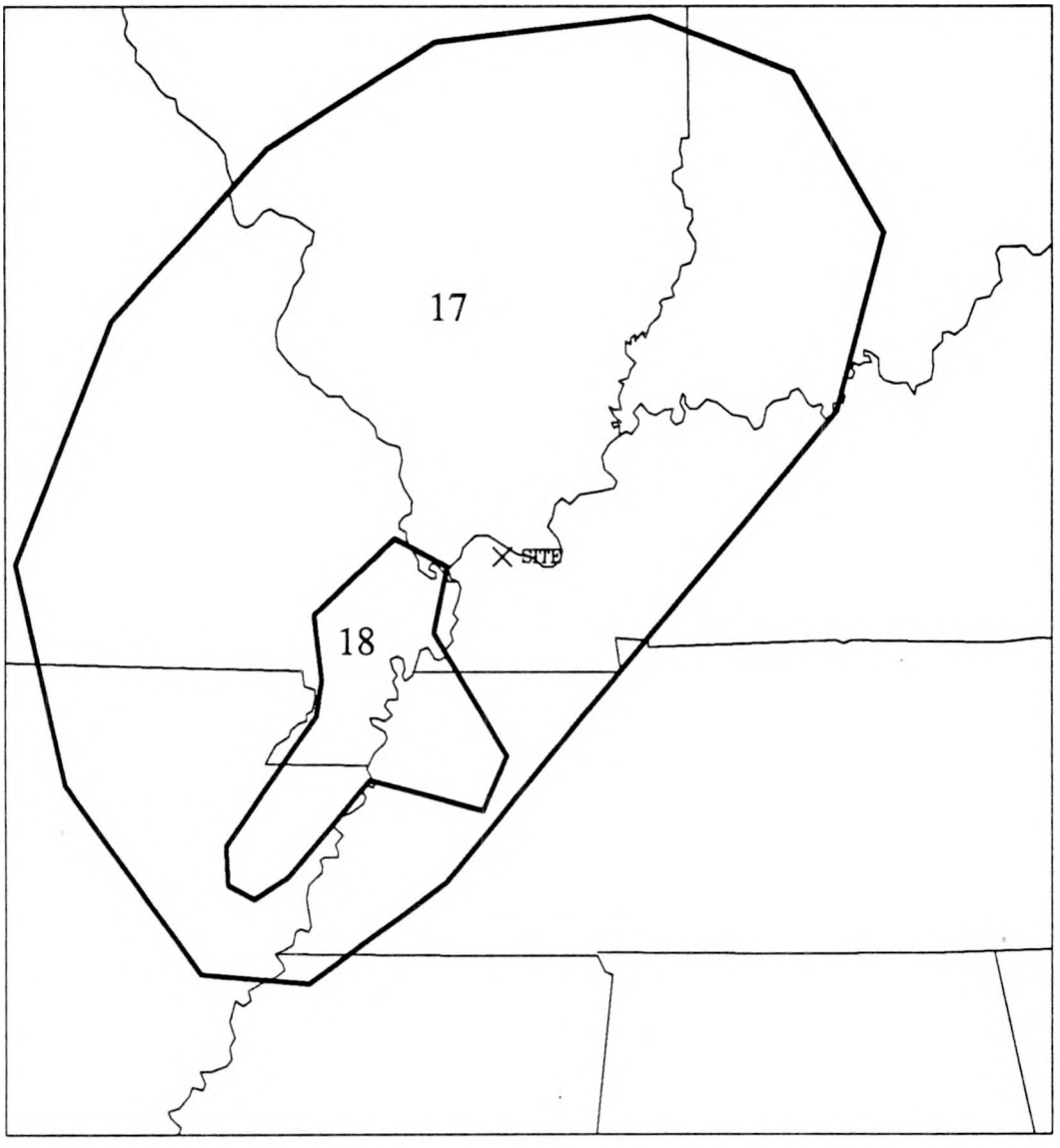

Figure 3-6. Map showing the seismic sources specified by LLNL seismicity expert 6 in the region around the Paducah site. Source: Volume 1 of (1).

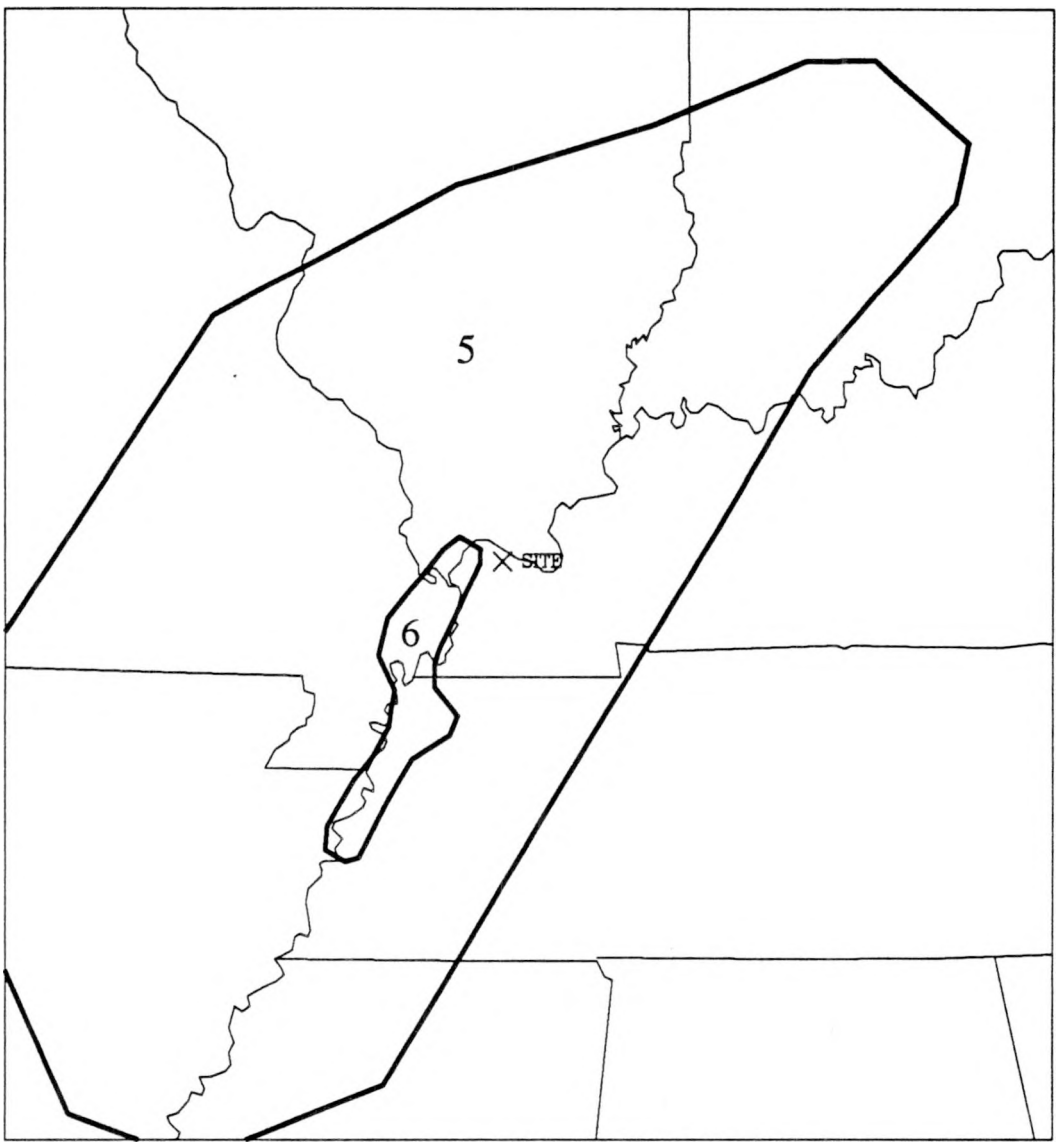

Figure 3-7. Map showing the seismic sources specified by LLNL seismicity expert 7 in the region around the Paducah site. Source: Volume 1 of (1).

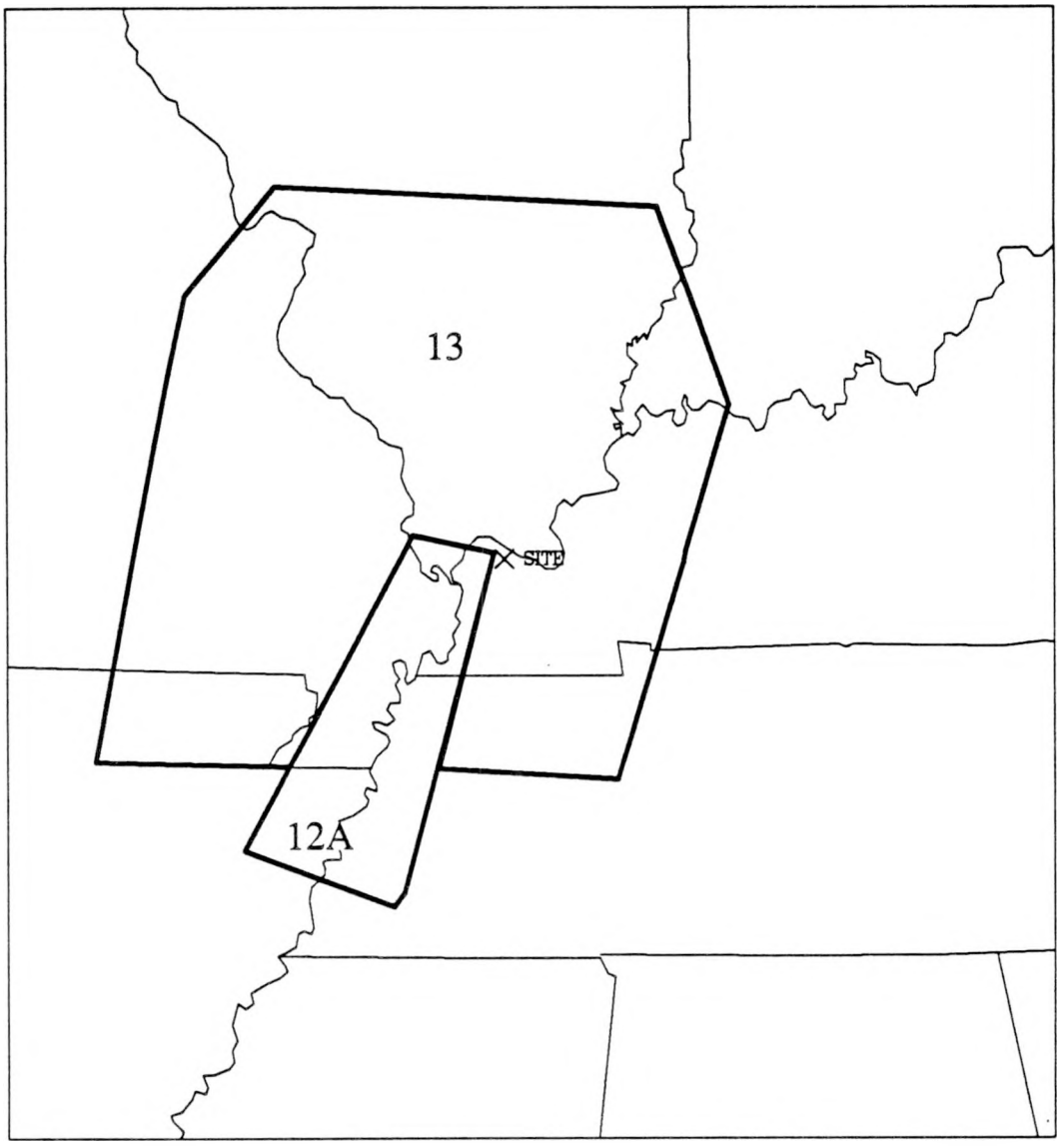

Figure 3-8. Map showing the seismic sources specified by LLNL seismicity expert 10 in the region around the Paducah site. Source: Volume 1 of (1).

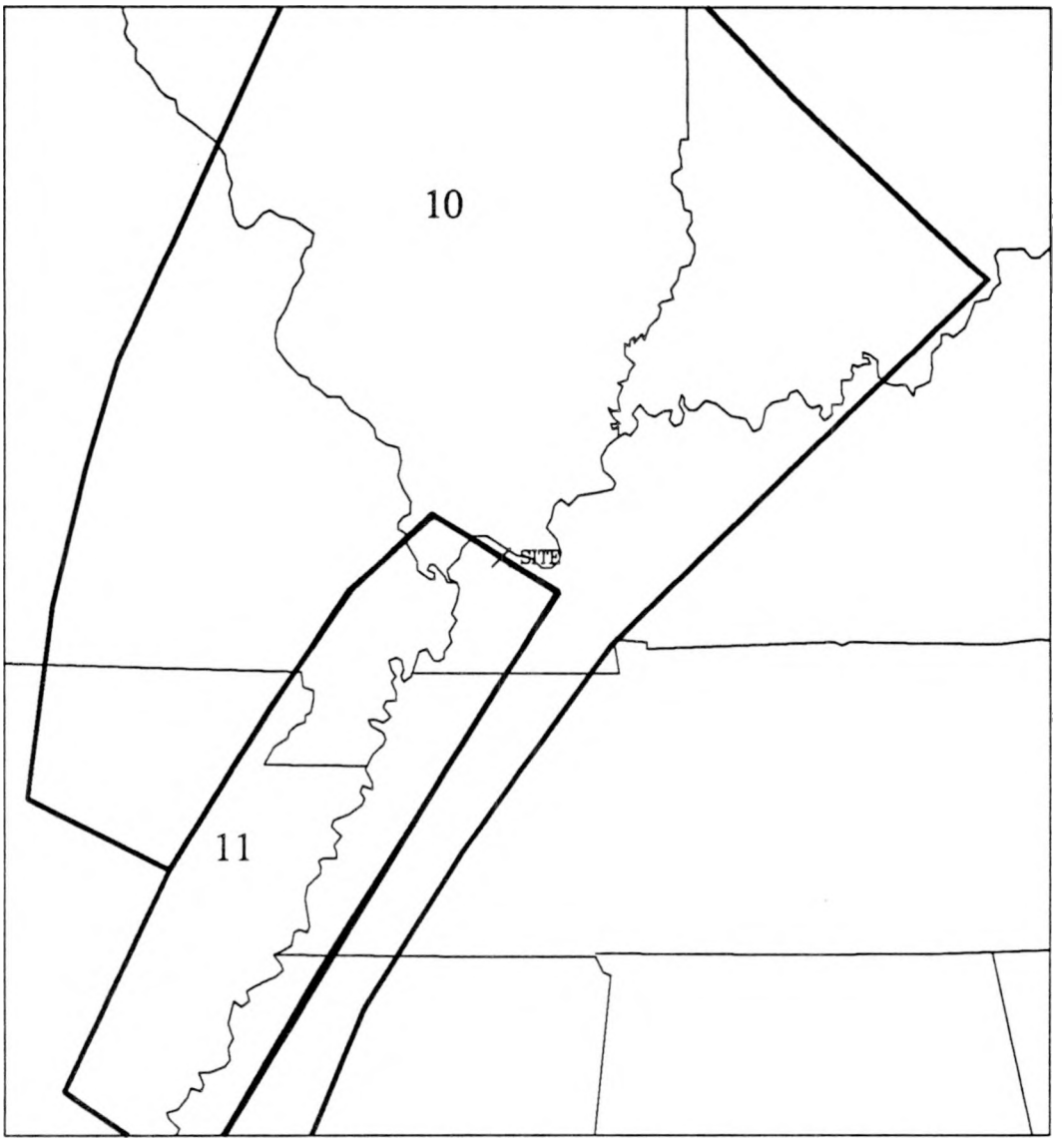

Figure 3-9. Map showing the seismic sources specified by LLNL seismicity expert 11 in the region around the Paducah site. Source: Volume 1 of (1).

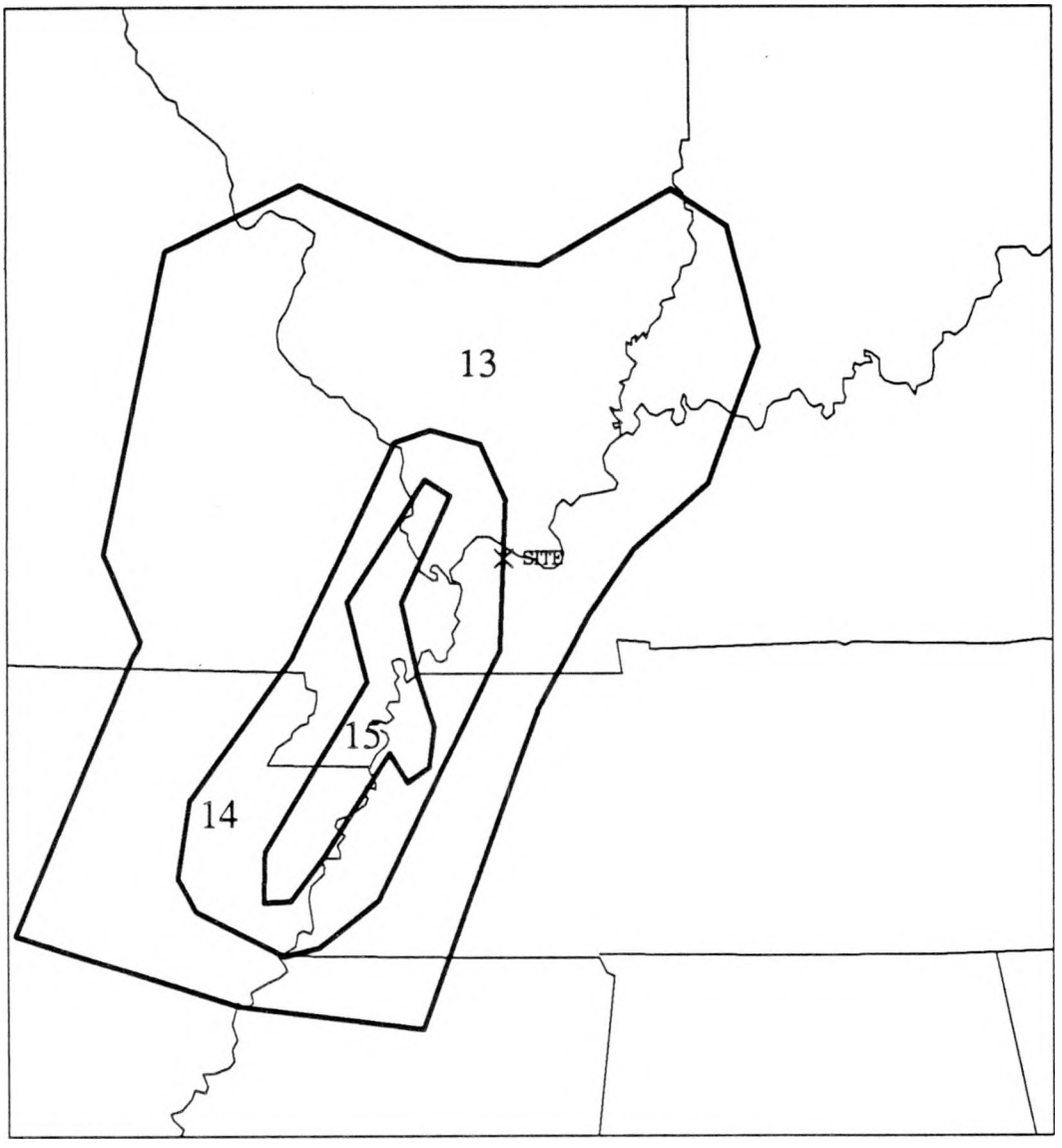

Figure 3-10. Map showing the seismic sources specified by LLNL seismicity expert 12 in the region around the Paducah site. Source: Volume 1 of (1).

Figure 3-11. Map showing the seismic sources specified by LLNL seismicity expert 13 in the region around the Paducah site. Source: Volume 1 of (1).

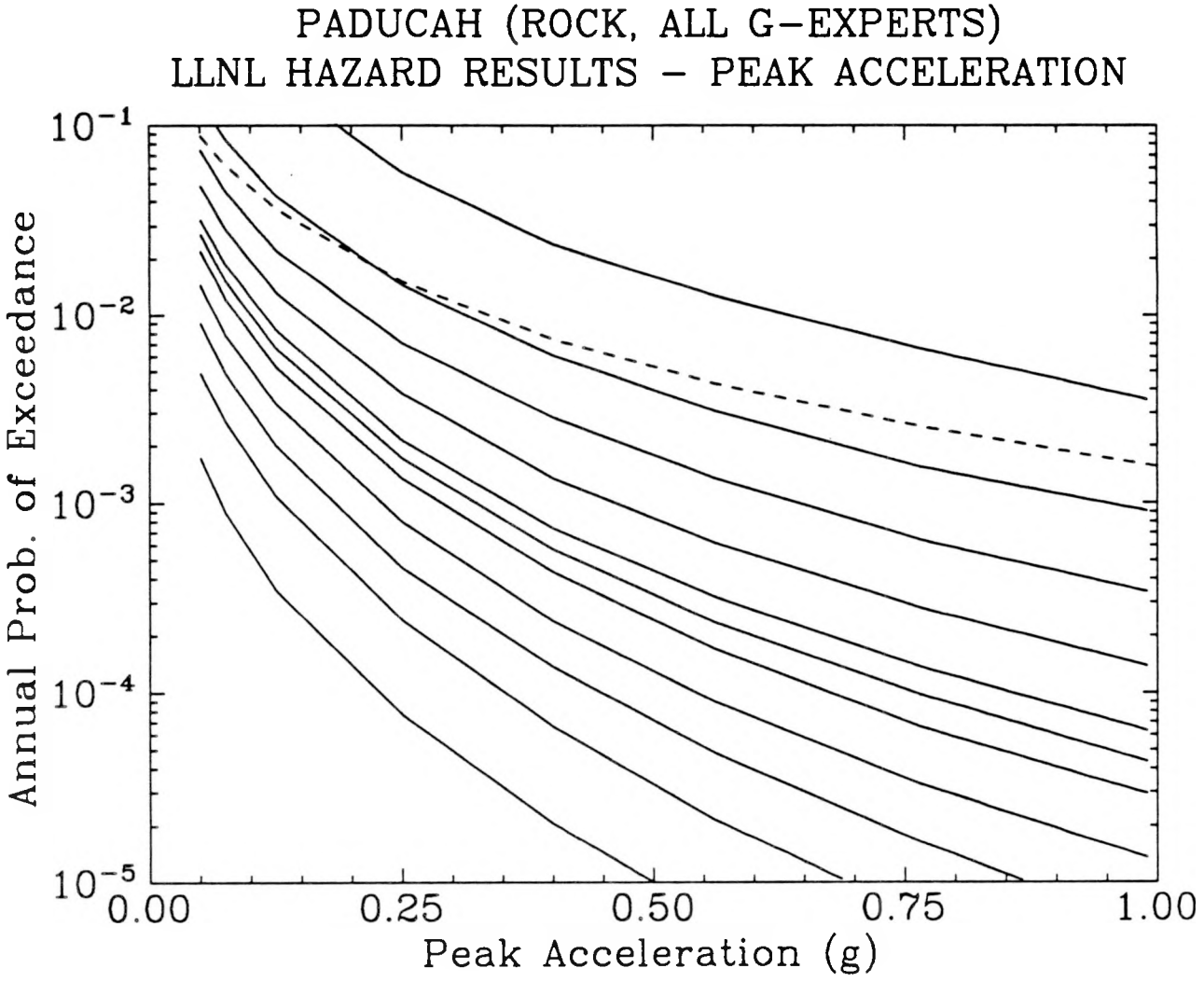

Figure 3-12. Peak-acceleration hazard curves for Paducah computed by LLNL for rock conditions using the LLNL methodology (all ground-motion Experts). The solid curves correspond to the following fractile hazard curves: 0.05 (bottom), 0.15, 0.25, 0.35, 0.45, 0.50, 0.55, 0.65, 0.75, 0.85, 0.95 (top); the dashed curve represents the mean hazard curve.

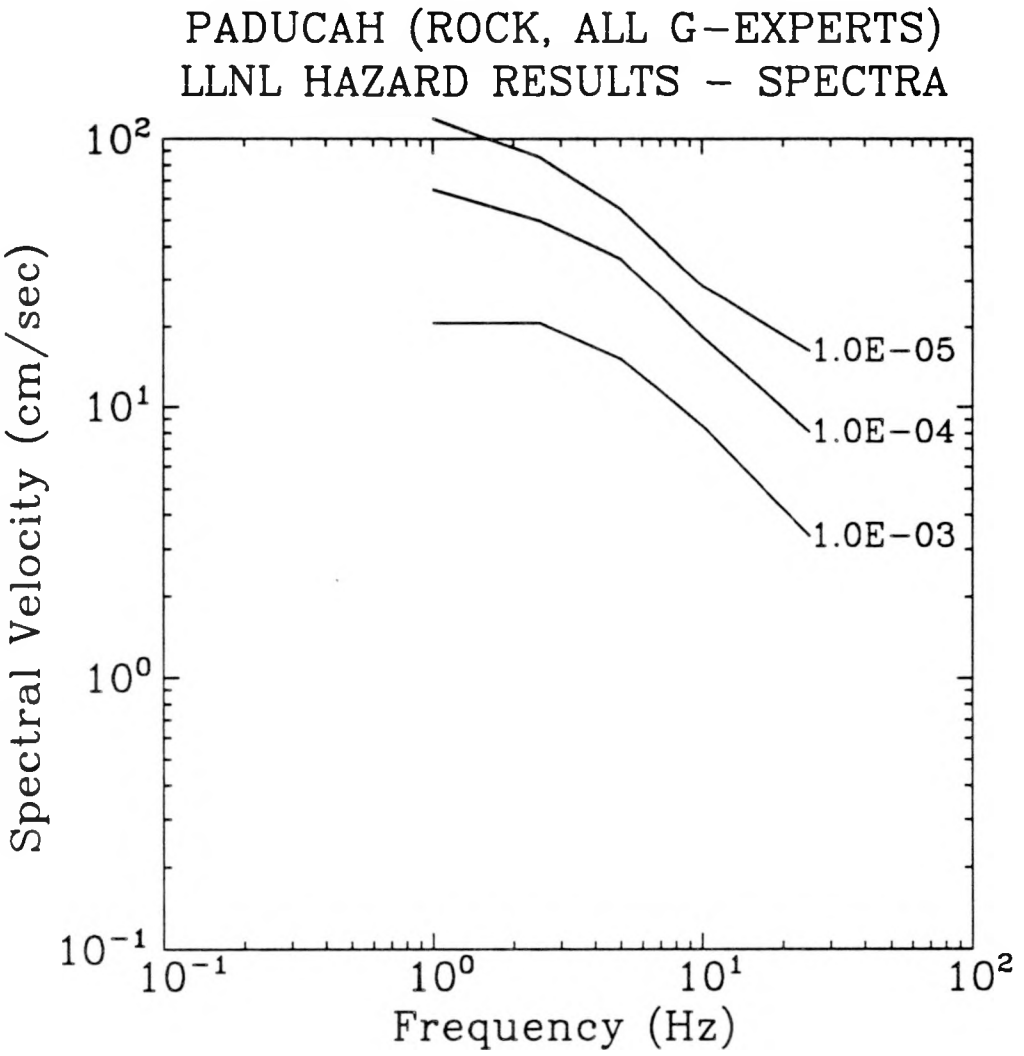

Figure 3-13. Median uniform-hazard spectra for Paducah computed by LLNL for rock conditions using the LLNL methodology (all ground-motion Experts).

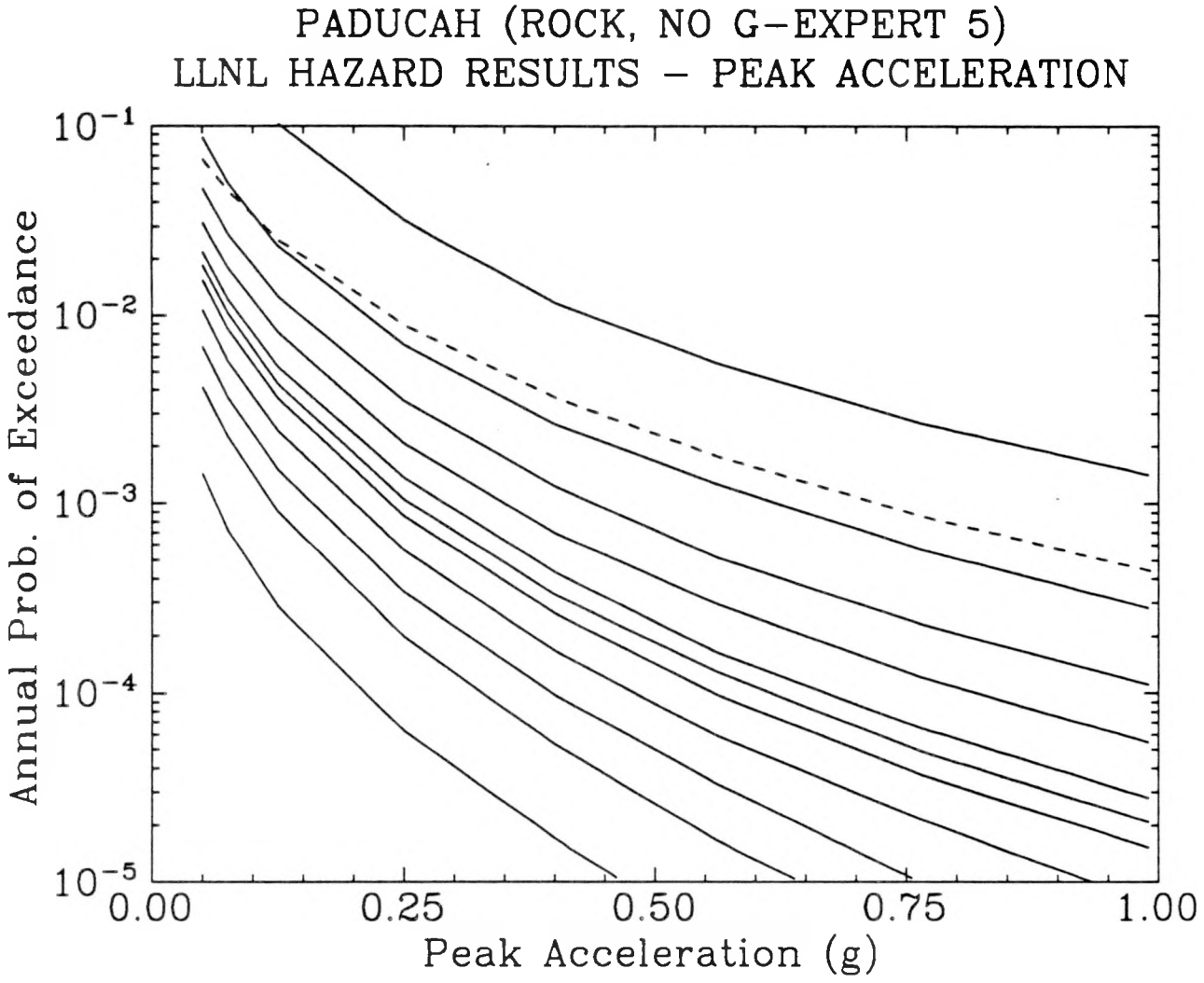

Figure 3-14. Peak-acceleration hazard curves for Paducah computed by LLNL for rock conditions using the LLNL methodology (excluding ground-motion Expert 5). The solid curves correspond to the following fractile hazard curves: 0.05 (bottom), 0.15, 0.25, 0.35, 0.45, 0.50, 0.55, 0.65, 0.75, 0.85, 0.95 (top); the dashed curve represents the mean hazard curve.

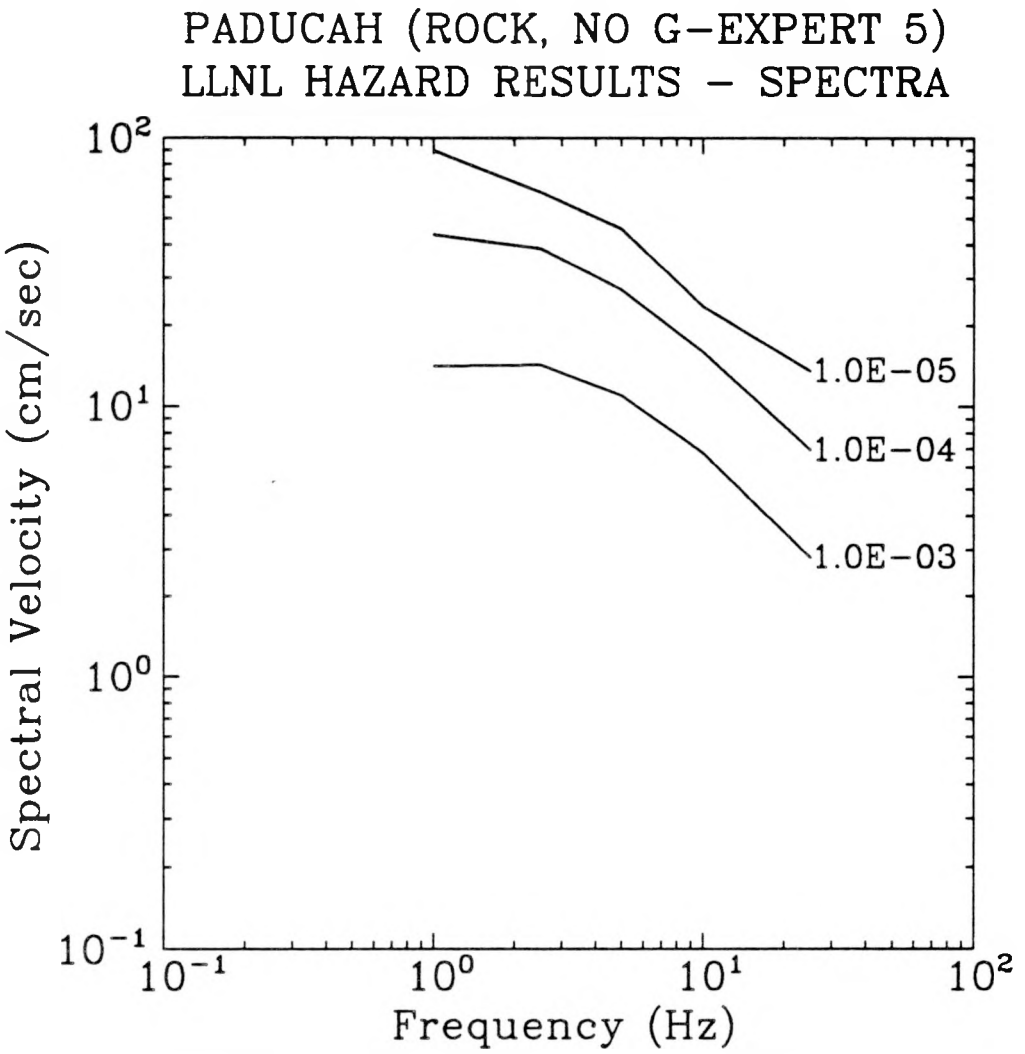

Figure 3-15. Median uniform-hazard spectra for Paducah computed by LLNL for rock conditions using the LLNL methodology (excluding ground-motion Expert 5).

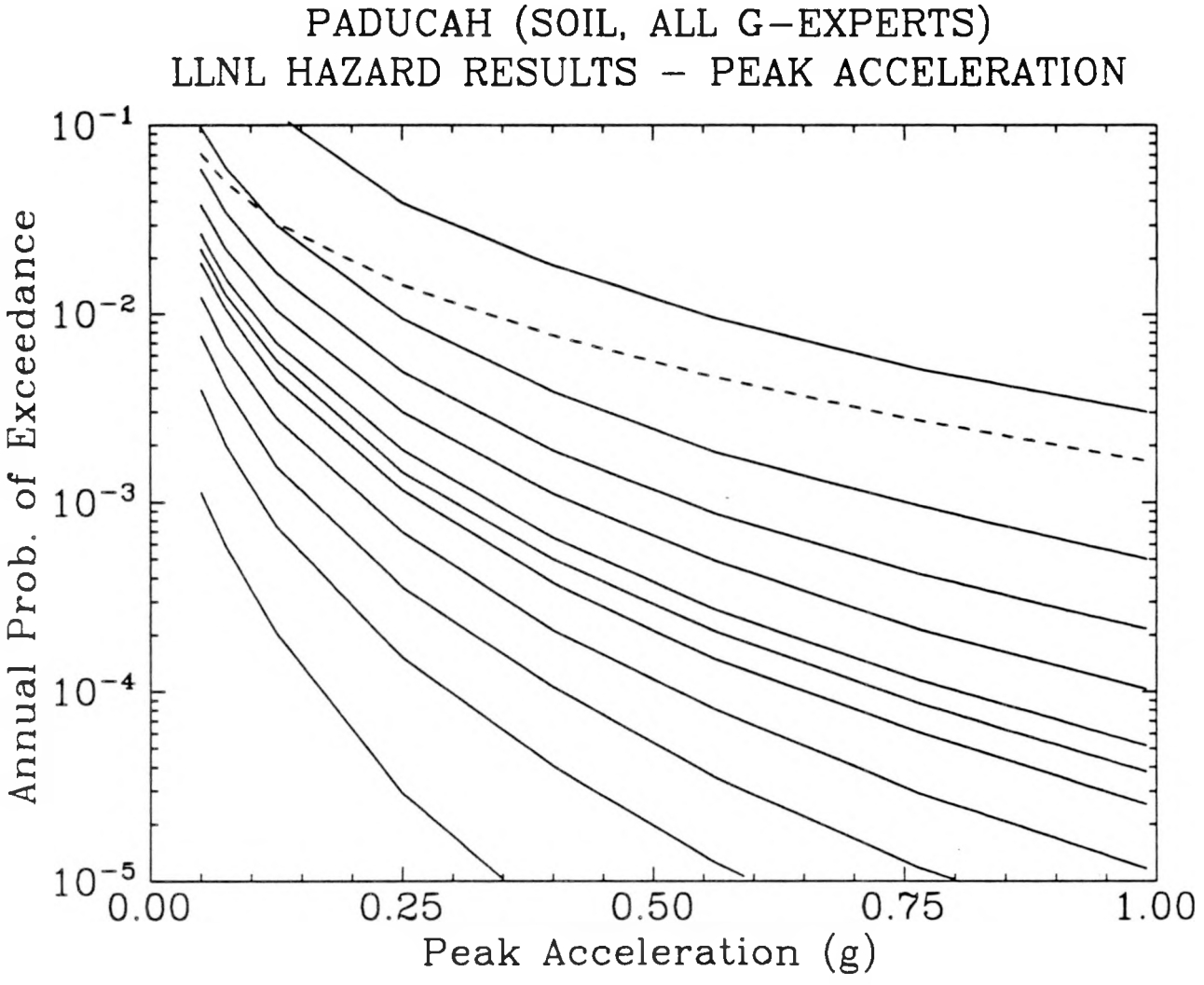

Figure 3-16. Peak-acceleration hazard curves for Paducah computed by LLNL for soil conditions using the LLNL methodology (all ground-motion experts). The solid curves correspond to the following fractile hazard curves: 0.05 (bottom), 0.15, 0.25, 0.35, 0.45, 0.50, 0.55, 0.65, 0.75, 0.85, 0.95 (top); the dashed curve represents the mean hazard curve.

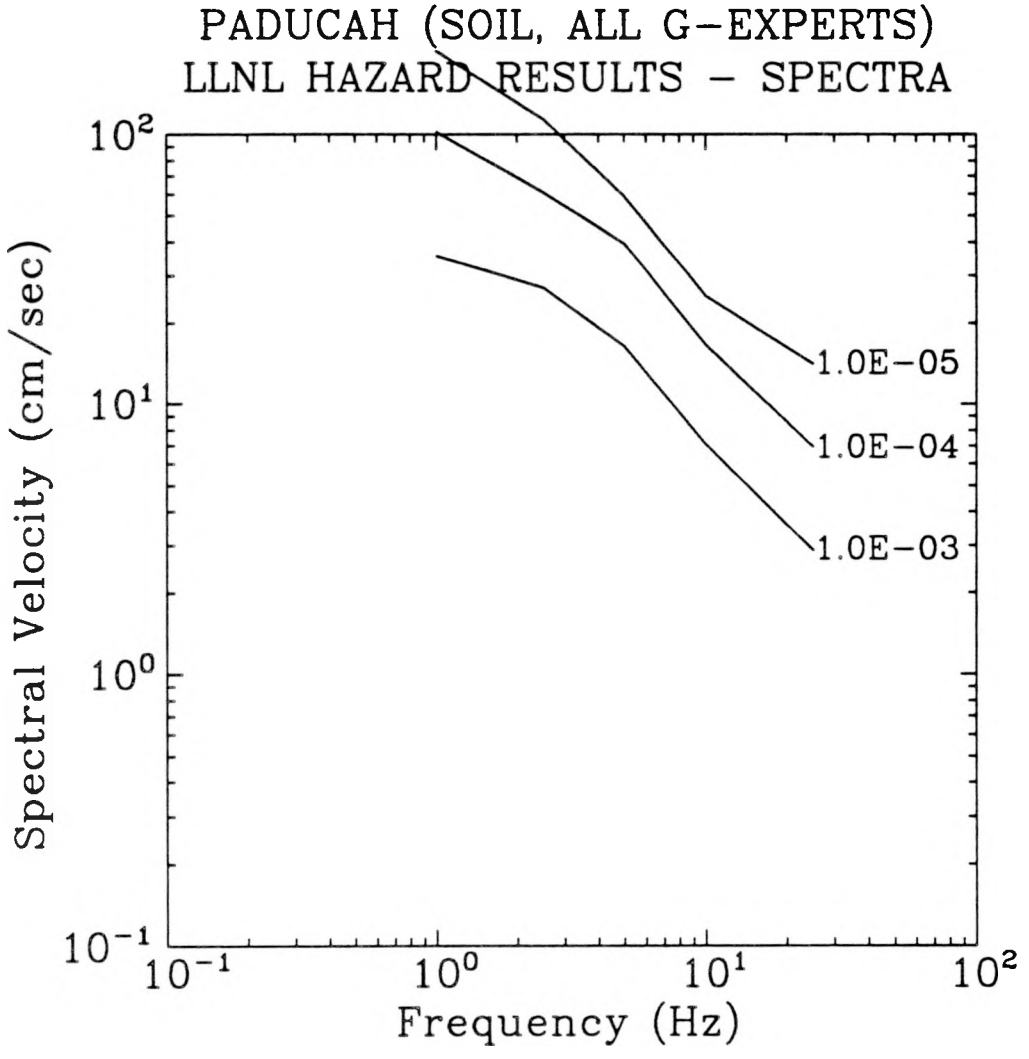

Figure 3-17. Median uniform-hazard spectra for Paducah computed by LLNL for soil conditions using the LLNL methodology (all ground-motion experts).

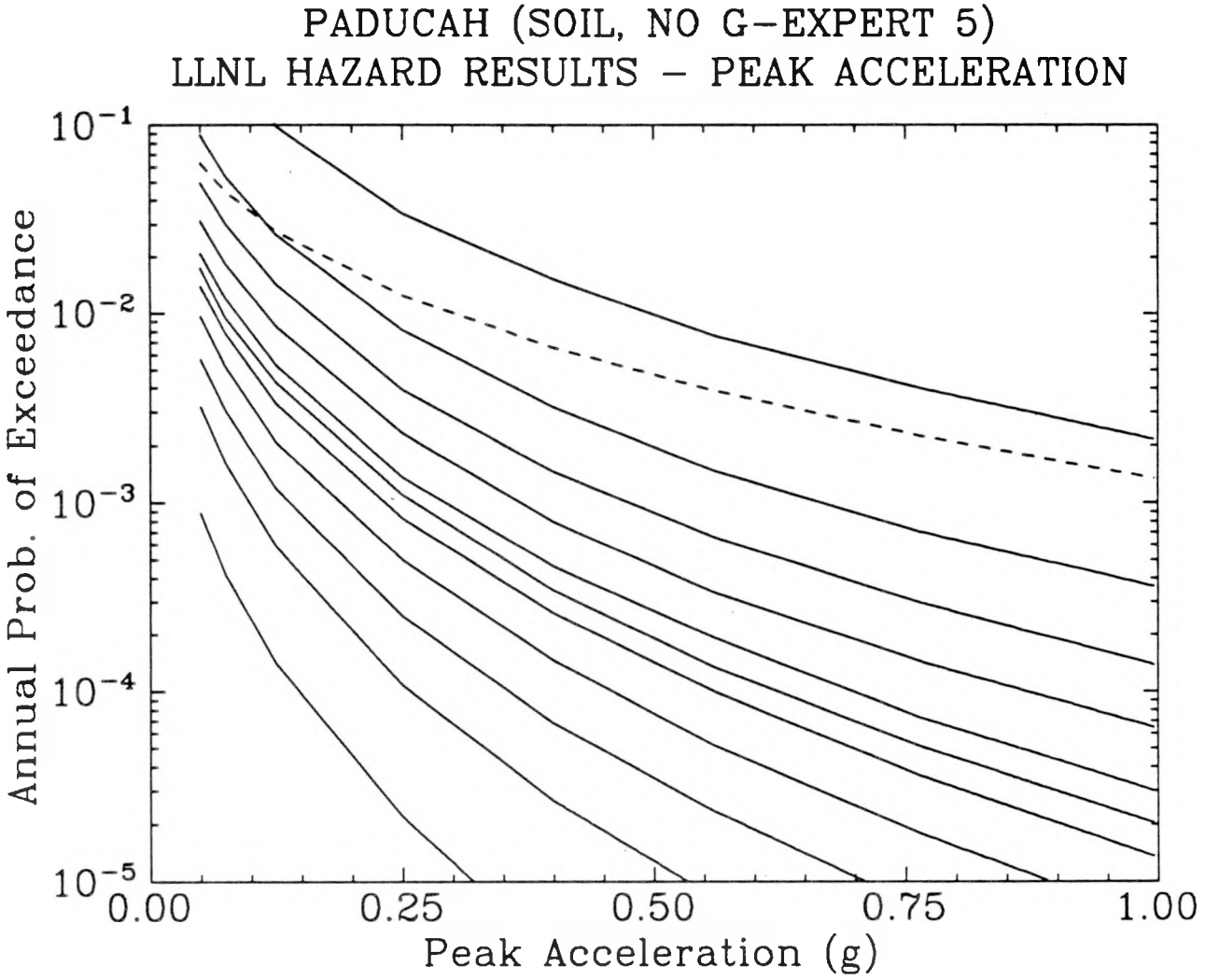

Figure 3-18. Peak-acceleration hazard curves for Paducah computed by LLNL for soil conditions using the LLNL methodology (excluding ground-motion Expert 5). The solid curves correspond to the following fractile hazard curves: 0.05 (bottom), 0.15, 0.25, 0.35, 0.45, 0.50, 0.55, 0.65, 0.75, 0.85, 0.95 (top); the dashed curve represents the mean hazard curve.

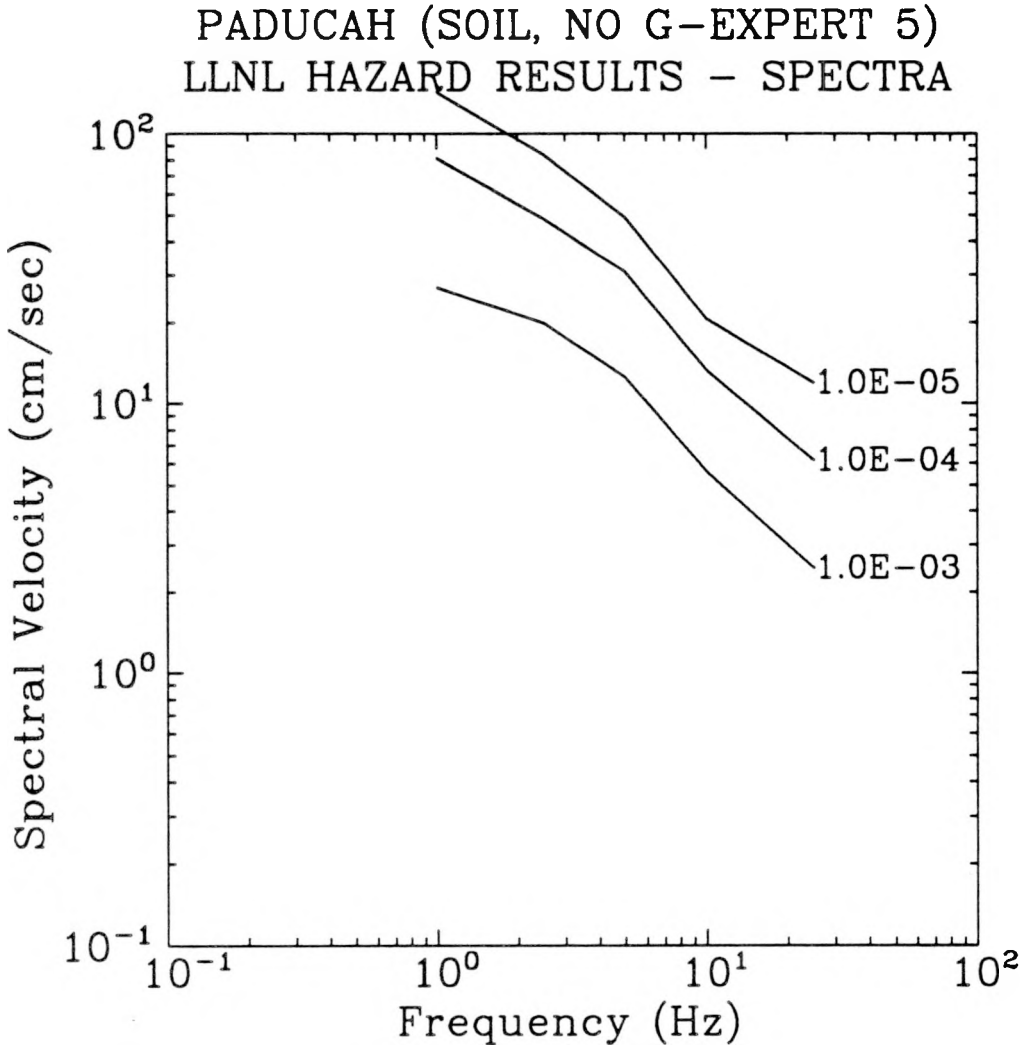

Figure 3-19. Median uniform-hazard spectra for Paducah computed by LLNL for soil conditions using the LLNL methodology (excluding ground-motion Expert 5).

Section 4

COMBINATION OF EPRI/SOG AND LLNL RESULTS

4.1 OVERVIEW

This Section describes the procedure used to combine the EPRI/SOG and LLNL seismic hazard results presented in Sections 2 and 3, in order to obtain a synthesized representation of seismic hazard and its uncertainty at the Paducah site. Results are then presented as fractile hazard curves, mean hazard curve, and median uniform-hazard spectra.

4.2 COMBINATION OF EPRI/SOG AND LLNL RESULTS

The EPRI/SOG and LLNL results are given equal weights to obtain an overall representation of the seismic hazard and its uncertainty. The choice of equal weights is justified given the comparable caliber of the two studies. Both studies elicited interpretations by multiple experts—in order to capture all hypotheses with scientific validity—and both studies underwent extensive peer reviews.

For the development of combined hazard results, the EPRI/SOG results are represented by the 30 equally weighted hazard curves. The LLNL results are represented by 10 equally weighted hazard curves, which correspond to the 0.05, 0.15, ... 0.95 fractile curves shown in Section 3.

We combine these 40 hazard curves, giving a weight of 1/60 to each EPRI/SOG curve and 1/20 to each LLNL curve. We then compute fractile and mean curves[1] from these combined curves.

4.2.1 Mechanics of the Combination Process

We combine the EPRI/SOG and LLNL seismic hazard results by operating with their uncertainty distributions on the hazard at each calculated ground-motion amplitude. This section contains a detailed description of this process and gives some insights about its results. To illustrate this process, we will consider the evaluation of combined hazard estimates for a peak acceleration of 0.2 g (for rock conditions and considering all LLNL ground-motion experts).

[1] We deliberately use the mean curve computed from these 40 hazard curves—instead of combining the original mean hazard curves shown in Sections 2 and 3—in order to avoid the well-known instabilities in the mean LLNL hazard curves.

For the purposes of the combination process, the EPRI/SOG results are represented by 30 equally weighted hazard curves. These curves are constructed from each team's 0.10, 0.30, 0.50, 0.70, and 0.90 fractile curves. Figure 4–1 shows the 30 curves obtained for rock conditions.

For each ground-motion amplitude (e.g., each value of PGA), a discrete probability distribution of hazard is constructed by reading the hazard curves at this amplitude. Figure 4–2 shows the distribution of hazard at 0.2 g (PGA), as obtained from the EPRI/SOG analysis. Each spike in the probability mass function in Figure 4–2 (top) represents one hazard curve; all spikes have heights of 0.0333=1/30 because all hazard curves carry equal weights. The bottom portion of Figure 4–2 shows the corresponding cumulative distribution, and illustrates the process of evaluating the median (or 0.50 fractile).

We follow a similar process for the LLNL results, which are represented by 10 equally weighted fractile hazard curves (corresponding to 0.05, 0.15, 0.25, 0.35, 0.45, 0.55, 0.65, 0.75, 0.85, and 0.95 fractiles). Figure 4–3 shows the distribution of hazard at 0.2 g, as obtained from the fractile hazard curves in Figure 3–12.

We combine the EPRI/SOG and LLNL results by combining their corresponding probability mass functions, with equal weights, as shown in Figure 4–4. Each of 30 spikes from the EPRI/SOG results gets a weight of 1/60, while each of 10 spikes from the LLNL results gets a weight of 1/20. We then construct the combined cumulative distribution and use it to evaluate the median and other fractiles (see bottom of Figure 4–4). We also use this combined distribution to evaluate the mean hazard.

Figure 4–4 shows that, unlike the mean, the median of the combined results depends on the distributions of the EPRI/SOG and LLNL results (i.e., it is impossible to calculate the median of the combined results from the EPRI/SOG and LLNL medians). Because the EPRI/SOG results have a tighter distribution of uncertainty, the median of the combined results tends to fall closer to the EPRI/SOG median.

We follow a similar procedure for spectral velocities; the only difference being that LLNL reported only the 0.05, 0.15, 0.50, 0.85, and 0.95 fractile hazard curves. Other LLNL fractile hazard curves were generated from the above fractile hazard curves assuming that each half of the body of the uncertainty distribution is approximately lognormal. The combined PSV hazard curves are then used to generate uniform-hazard spectra. Because LLNL did not generate results for 0.5-Hz spectral velocities, it was assumed that the ratio of 0.5 Hz to 1-Hz ordinates is the same for LLNL and for EPRI/SOG.

4.3 RESULTS

Four sets of combined EPRI/SOG–LLNL hazard results are generated, as follows: rock site conditions using all LLNL ground-motion Experts (Figs. 4–5 and 4–6), rock site conditions using 4 LLNL ground-motion Experts (Figs. 4–7 and 4–8), soil site conditions using all LLNL ground-motion Experts (Figs. 4–9 and 4–10), and soil site conditions using 4 LLNL ground-motion Experts (Figs. 4–11 and 4–12).

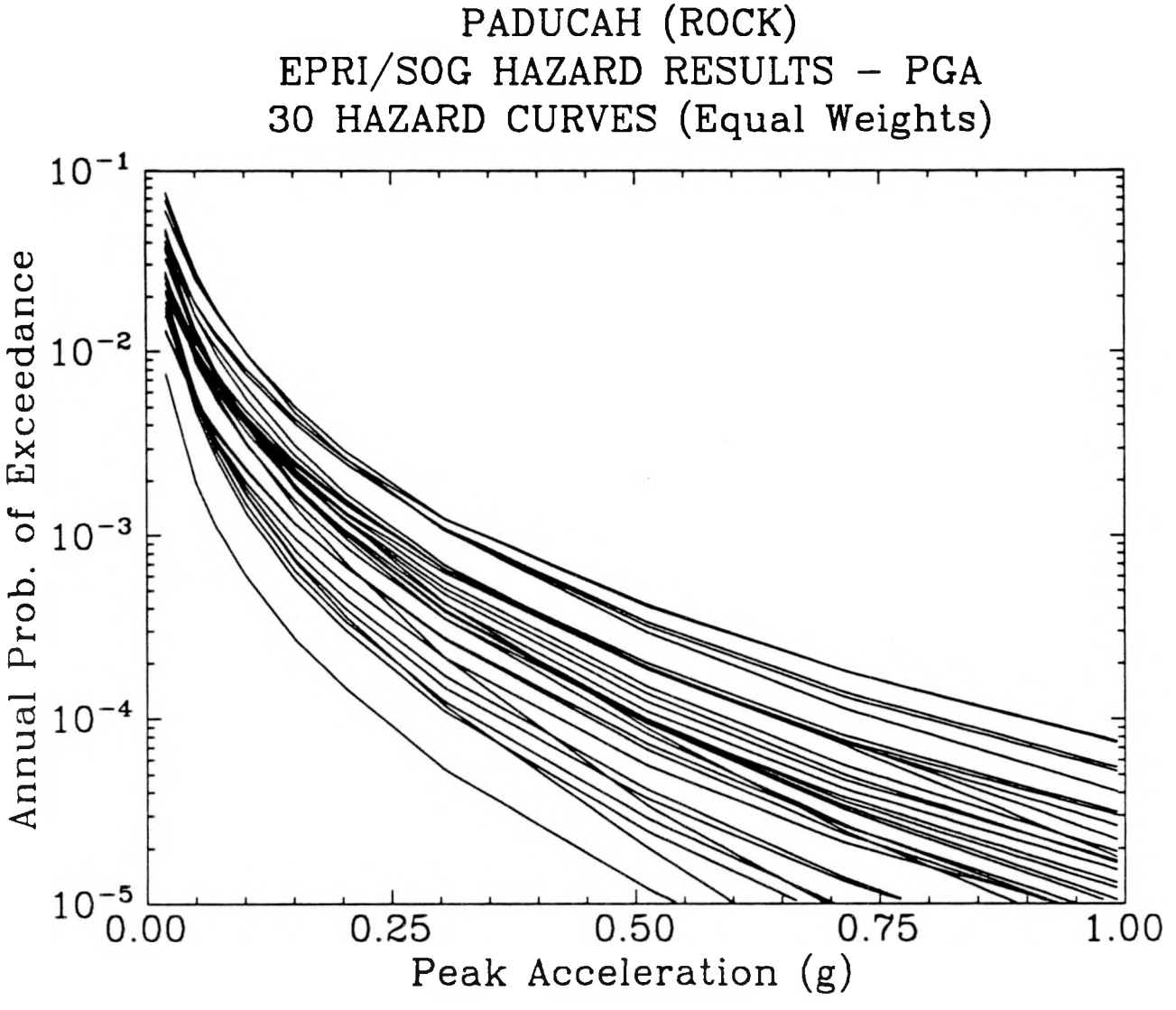

Figure 4-1. Representation of the EPRI/SOG results as 30 equally weighted hazard curves. These results correspond to rock site conditions.

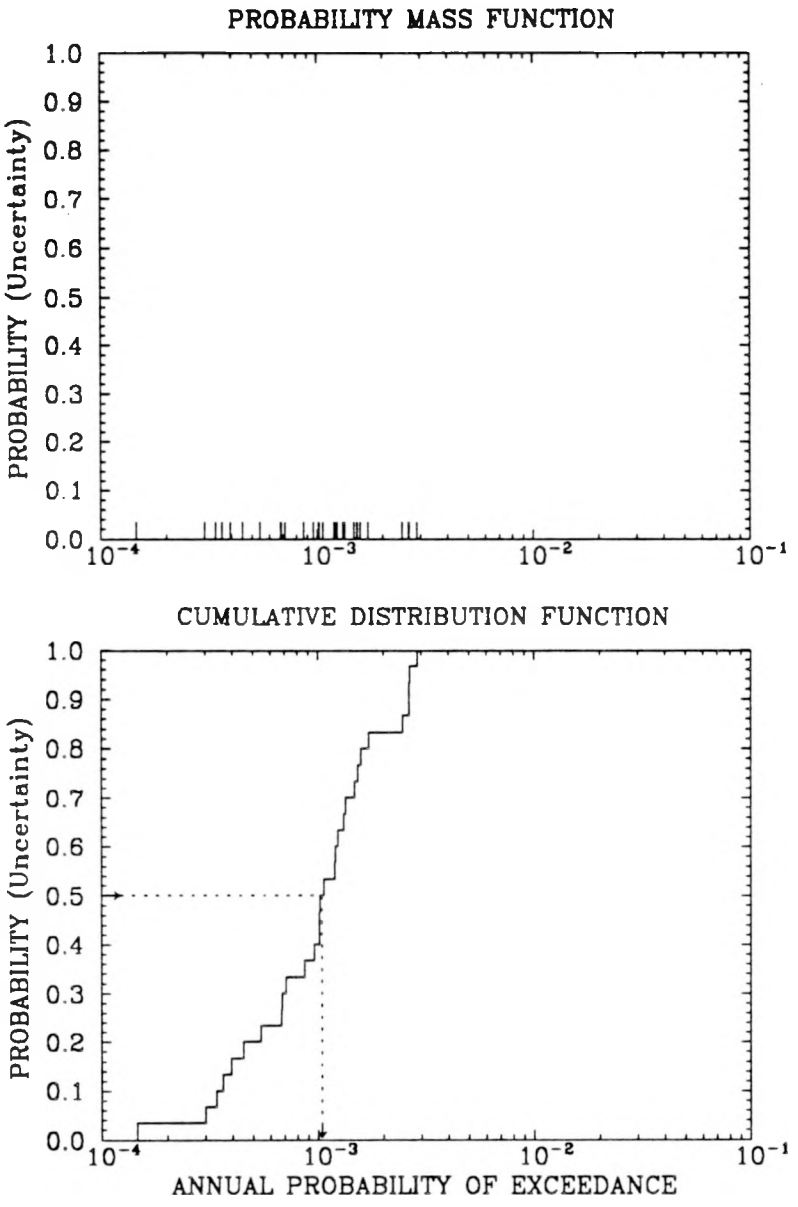

Figure 4-2. Discrete distribution representing uncertainty in the annual probability of exceeding 0.2 g PGA, as evaluated by the EPRI/SOG methodology. Top: probability mass function; bottom: cumulative distribution function. The dashed lines illustrate the evaluation of the median.

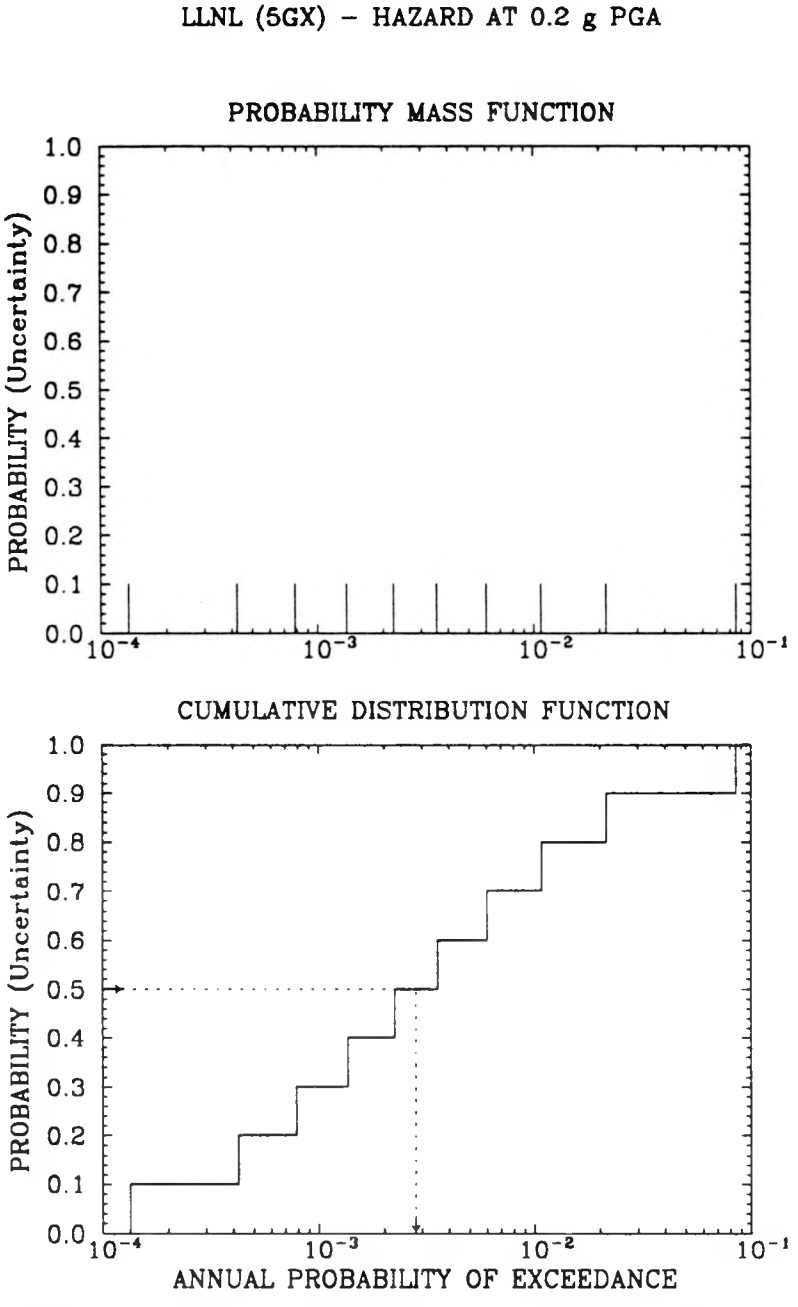

Figure 4-3. Discrete distribution representing uncertainty in the annual probability of exceeding 0.2 g PGA, as evaluated by the LLNL methodology. Top: probability mass function; bottom: cumulative distribution function. The dashed lines illustrate the evaluation of the median.

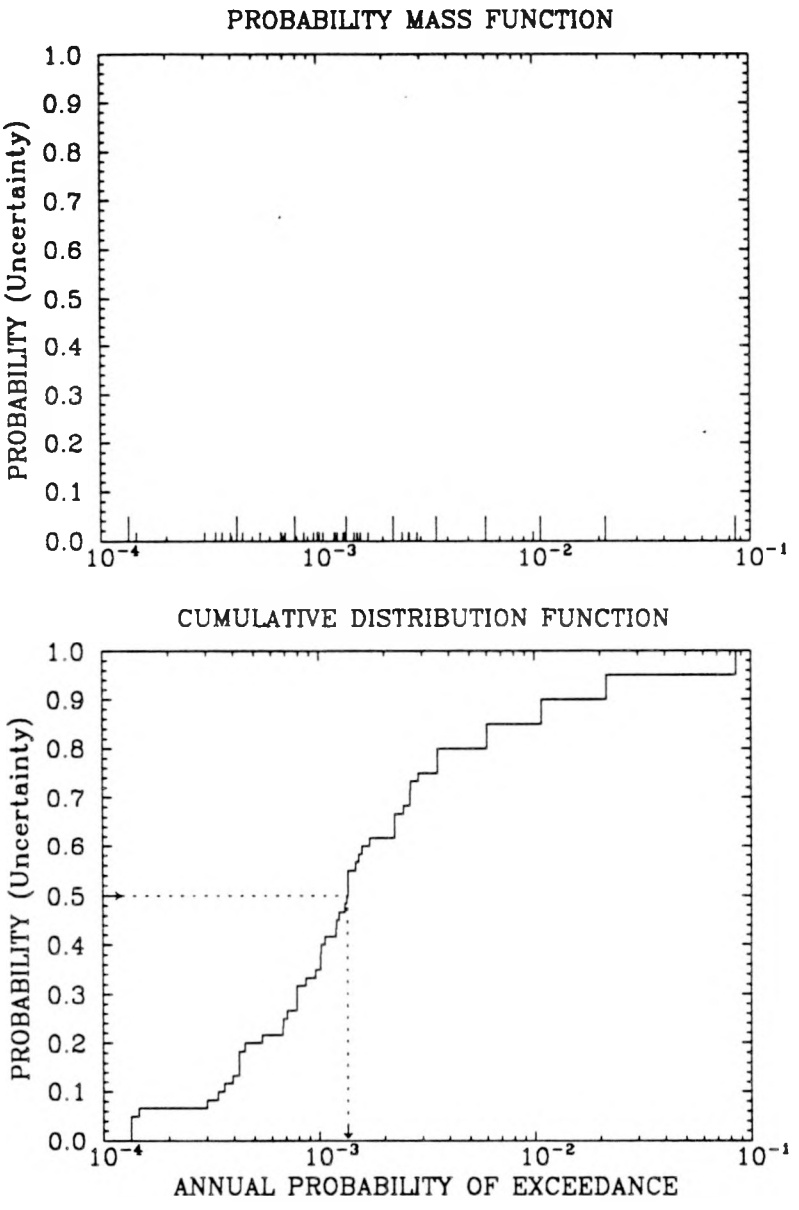

Figure 4-4. Discrete distribution representing uncertainty in the annual probability of exceeding 0.2 g PGA, as obtained by combining the EPRI/SOG and LLNL methodologies with equal weights. Top: probability mass function; bottom: cumulative distribution function. The dashed lines illustrate the evaluation of the median.

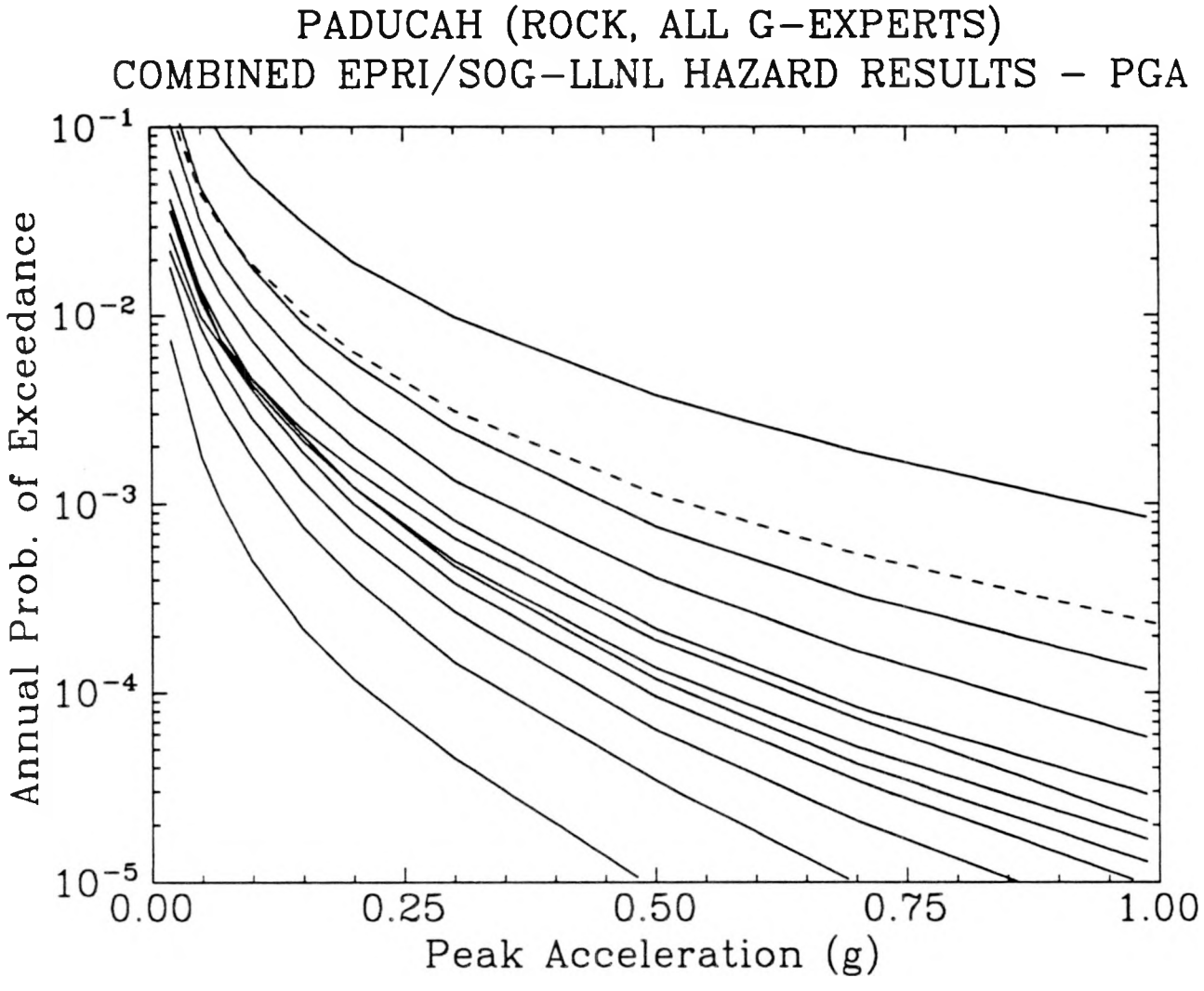

Figure 4-5. Peak-acceleration hazard curves for Paducah (for rock site conditions) obtained by combining results from the EPRI/SOG and LLNL (all ground-motion Experts) methodologies. The solid curves correspond to the following fractile hazard curves: 0.05 (bottom), 0.15, 0.25, 0.35, 0.45, 0.50, 0.55, 0.65, 0.75, 0.85, 0.95 (top); the dashed curve represents the mean hazard curve.

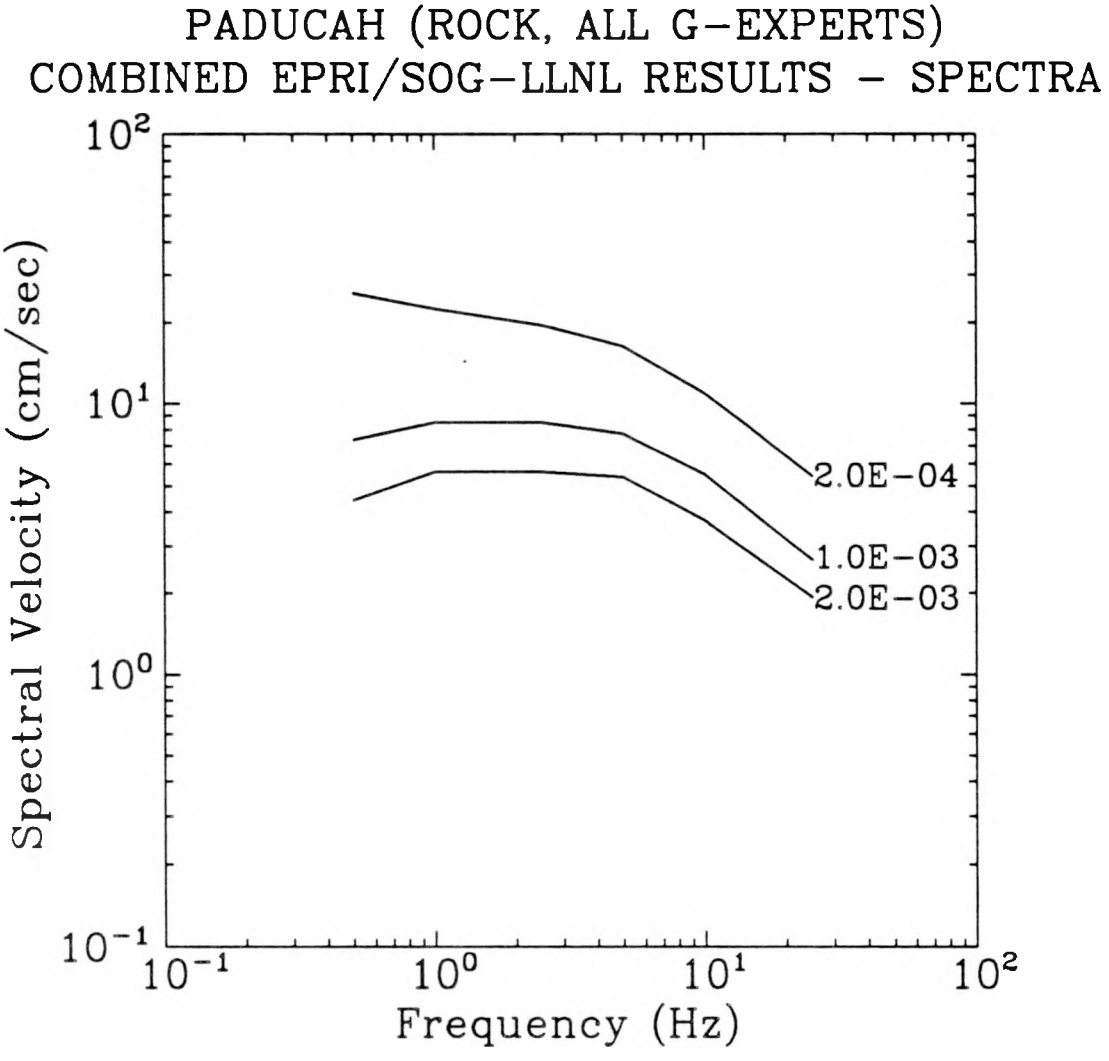

Figure 4-6. Median uniform-hazard spectra for Paducah (for rock site conditions) obtained by combining results from the EPRI/SOG and LLNL (all ground-motion Experts) methodologies.

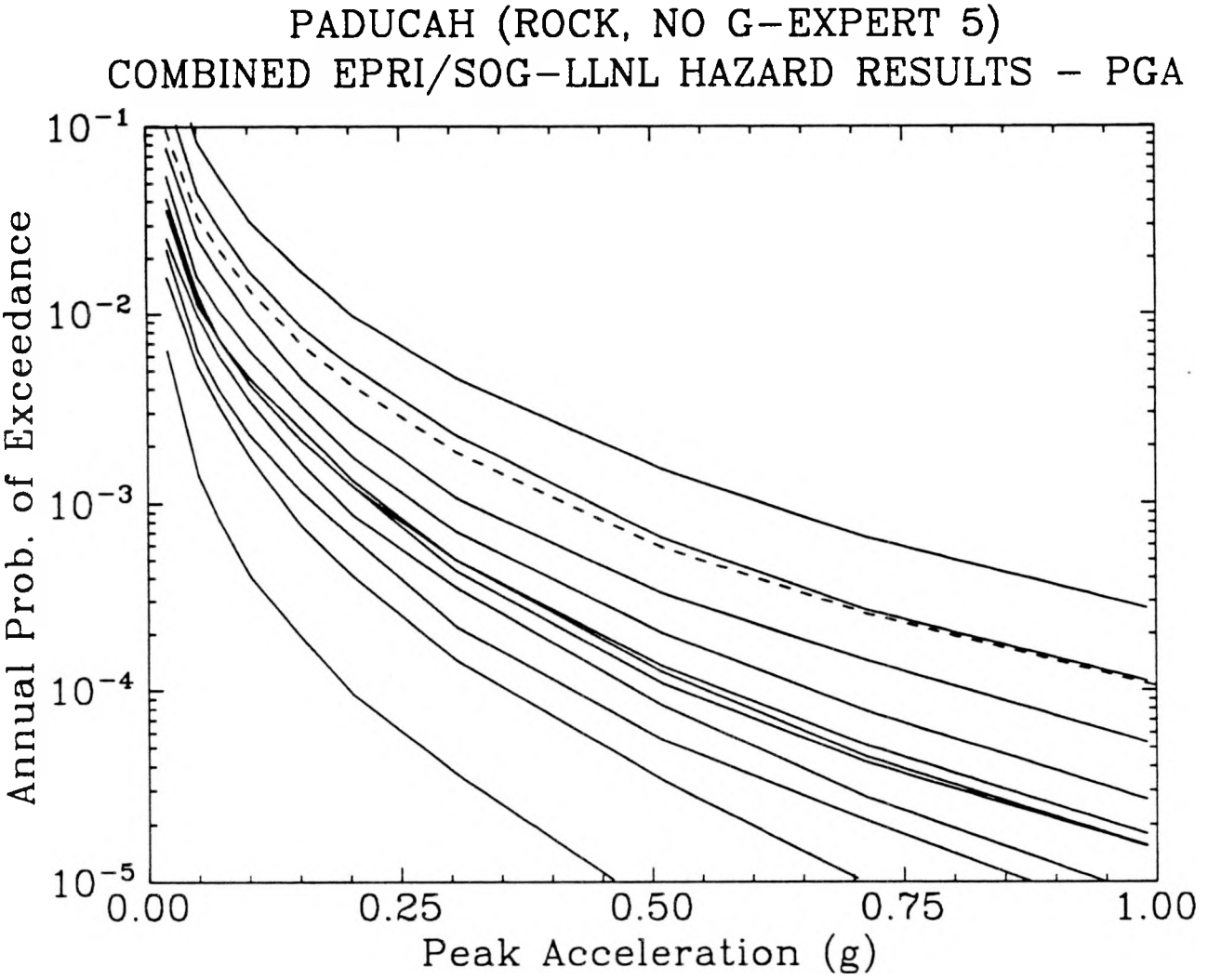

Figure 4-7. Peak-acceleration hazard curves for Paducah (for rock site conditions) obtained by combining results from the EPRI/SOG and LLNL (excluding ground-motion Expert 5) methodologies. The solid curves correspond to the following fractile hazard curves: 0.05 (bottom), 0.15, 0.25, 0.35, 0.45, 0.50, 0.55, 0.65, 0.75, 0.85, 0.95 (top); the dashed curve represents the mean hazard curve.

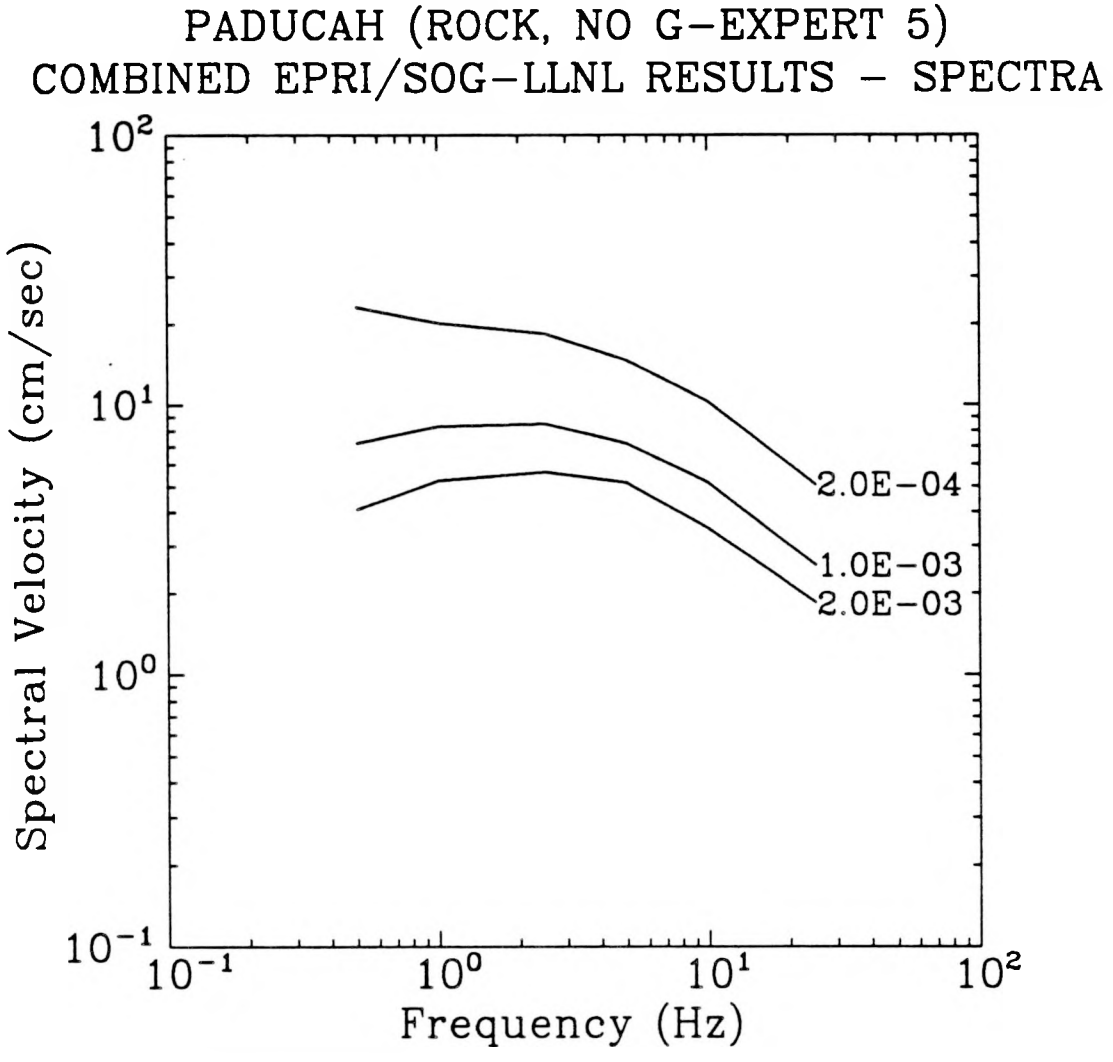

Figure 4-8. Median uniform-hazard spectra for Paducah (for rock site conditions) obtained by combining results from the EPRI/SOG and LLNL (excluding ground-motion Expert 5) methodologies.

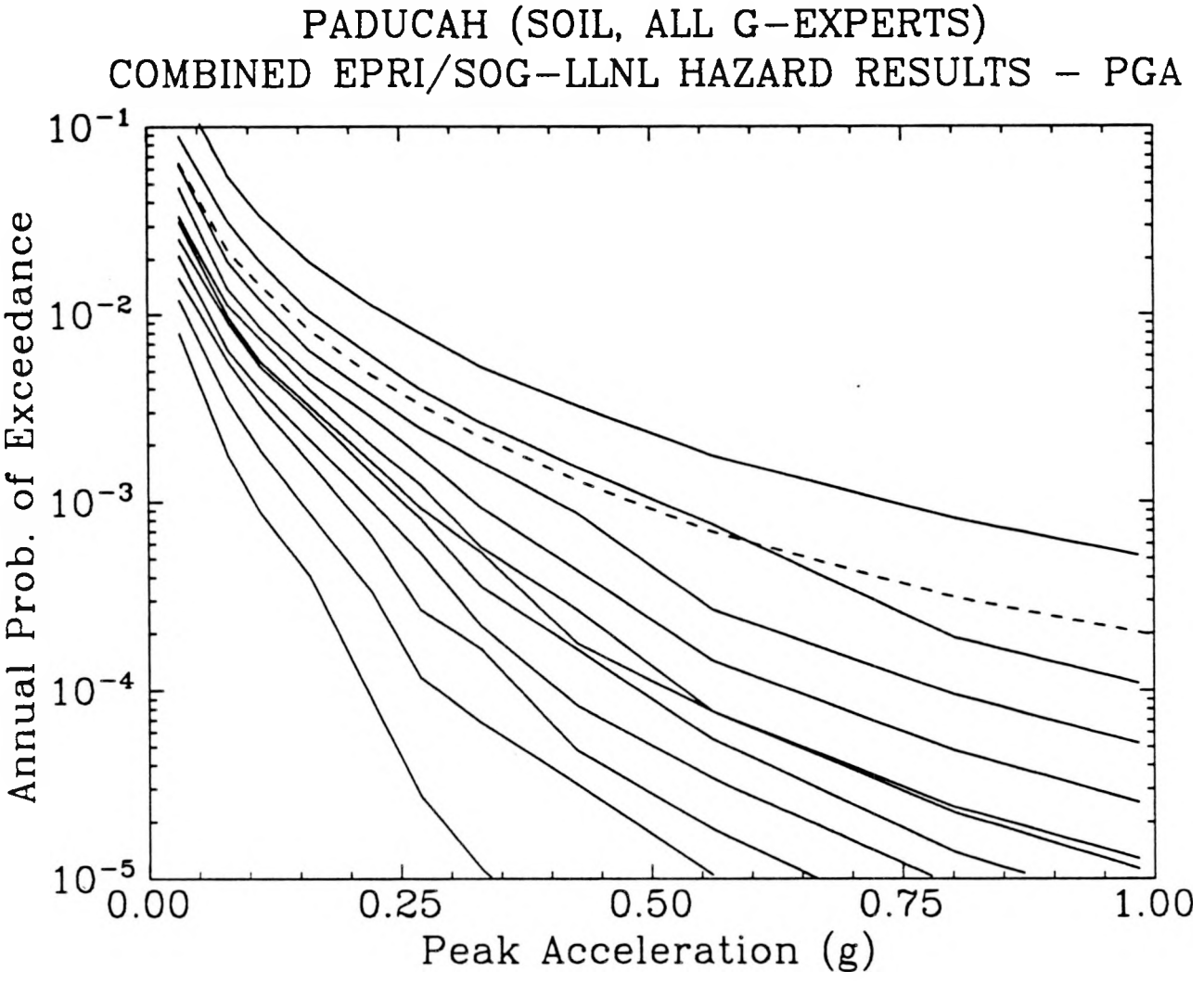

Figure 4-9. Peak-acceleration hazard curves for Paducah (for soil site conditions) obtained by combining results from the EPRI/SOG and LLNL (all ground-motion experts) methodologies. The solid curves correspond to the following fractile hazard curves: 0.05 (bottom), 0.15, 0.25, 0.35, 0.45, 0.50, 0.55, 0.65, 0.75, 0.85, 0.95 (top); the dashed curve represents the mean hazard curve.

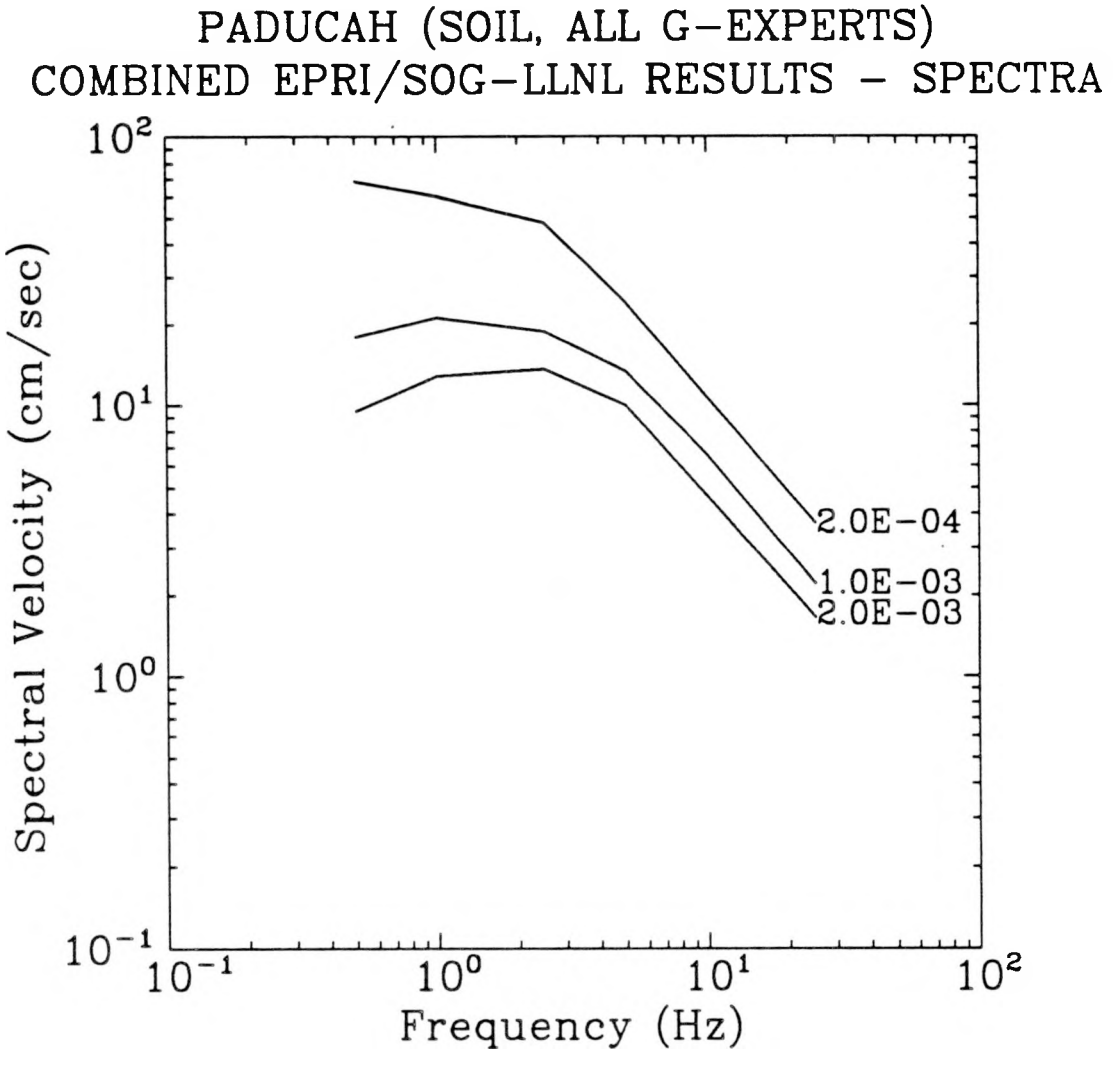

Figure 4-10. Median uniform-hazard spectra for Paducah (for soil site conditions) obtained by combining results from the EPRI/SOG and LLNL (all ground-motion experts) methodologies.

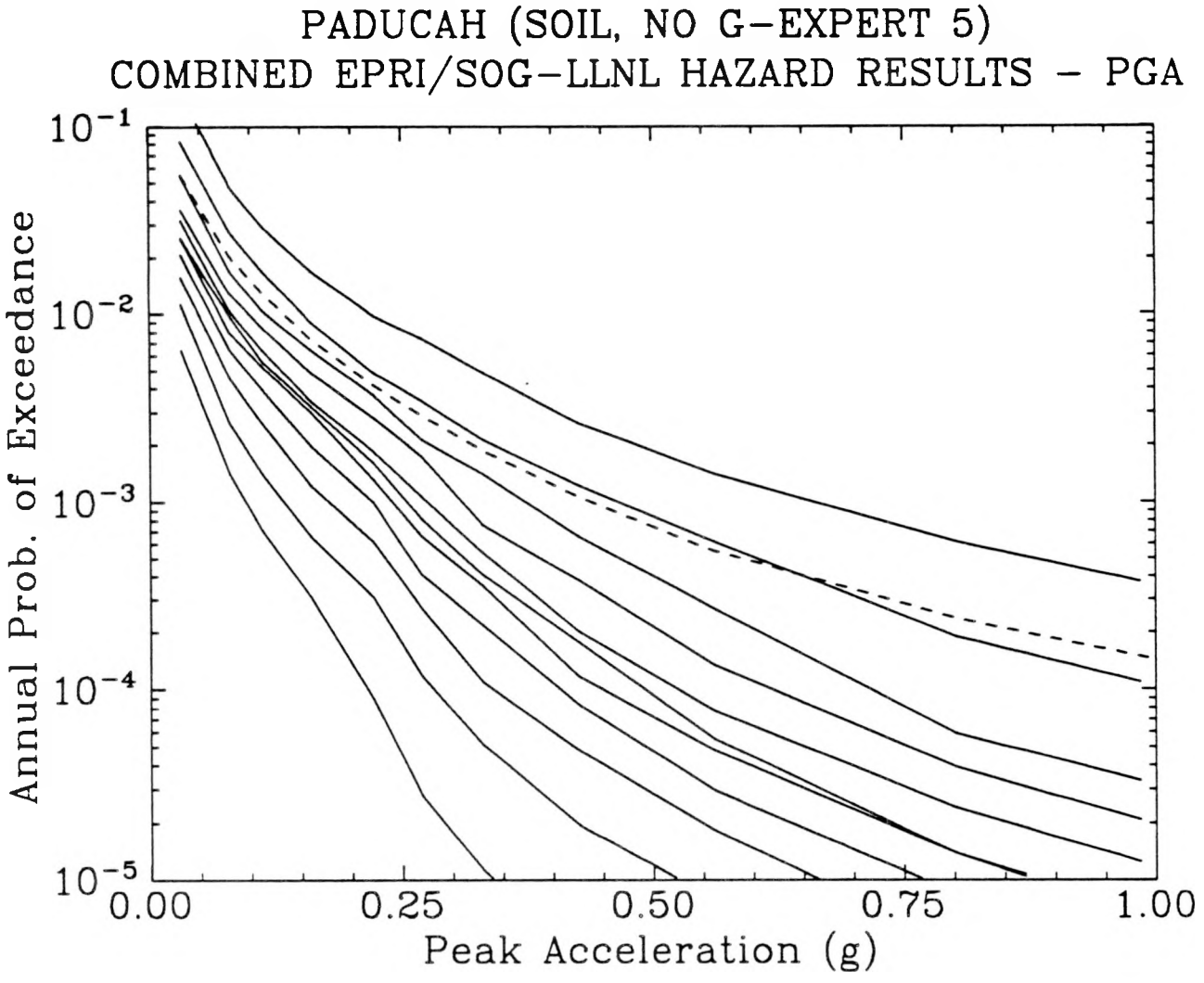

Figure 4-11. Peak-acceleration hazard curves for Paducah (for soil site conditions) obtained by combining results from the EPRI/SOG and LLNL (excluding ground-motion Expert 5) methodologies. The solid curves correspond to the following fractile hazard curves: 0.05 (bottom), 0.15, 0.25, 0.35, 0.45, 0.50, 0.55, 0.65, 0.75, 0.85, 0.95 (top); the dashed curve represents the mean hazard curve.

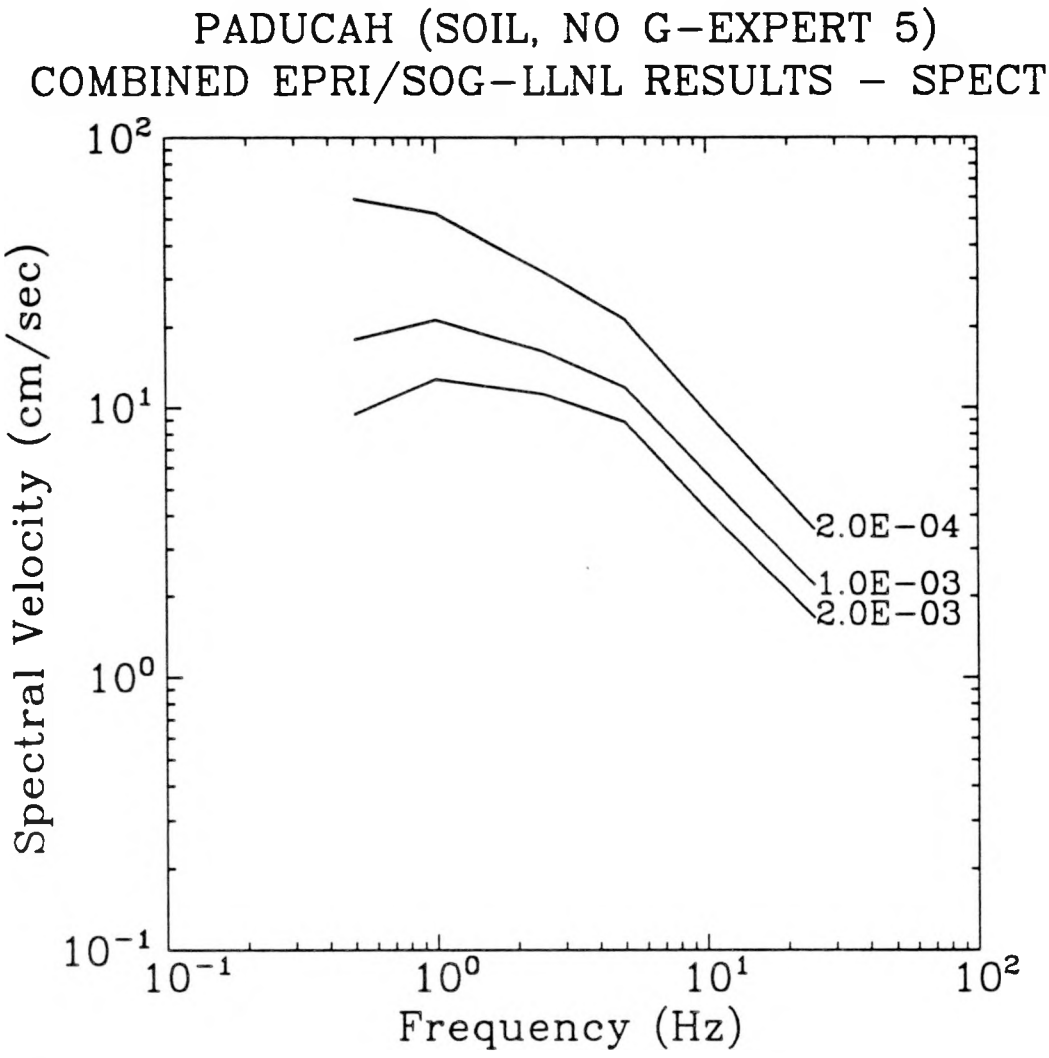

Figure 4-12. Median uniform-hazard spectra for Paducah (for soil site conditions) obtained by combining results from the EPRI/SOG and LLNL (excluding ground-motion Expert 5) methodologies.

Section 5

EXTENDED-SOURCE HAZARD ANALYSIS AND RESULTS

5.1 INTRODUCTION

As a result of the proximity of the Paducah site to potential earthquakes in the Mississippi embayment, a model for seismic hazard was derived that incorporates the important aspects of earthquakes in the near-source region. The specific features of seismicity that are modeled are as follows:

1. Earthquakes in the Mississippi embayment are treated with finite lengths of fault rupture. This means that, even if an earthquake epicenter is some distance from the site of interest, there is some chance that the fault rupture will be very close to the site, generating large ground motions.

2. The depth distribution of earthquakes is modeled for large intra-plate earthquakes. Specifically it is recognized that large earthquakes may occur at relatively deep depths (greater than 15 km), as compared to the shallow moderate seismicity that often occurs at depths less than 15 km.

3. A characteristic magnitude model is used to describe seismicity in the Mississippi embayment. This recognizes that the rate of occurrence of large events is greater than what is predicted from extrapolation of smaller events, and allows consistency between the seismic hazard model and rates of occurrence of large events estimated from paleoseismic events.

4. The prediction of seismic ground motions accounts for the large source size and for the distribution of energy along that source. As a result there is an important saturation effect of ground motion amplitudes with closer distance to the causative rupture, as compared with a simple point-source model in which all energy is released from one location.

These aspects are an important part of the accurate estimation of seismic hazard for any site that is potentially close to the source of large earthquakes. Modeling these features gives a more accurate representation of the hazard, making the seismic hazard model consistent with known characteristics of large earthquakes and the associated ground motions.

5.2 TECTONIC AND SEISMICITY INTERPRETATIONS

5.2.1 Seismic Zonation

To represent earthquake occurrences in the central Mississippi valley region, the seismic zonations developed during the EPRI and LLNL studies were used to derive a set of zones that span the range of current interpretations in the region. These interpretations have been described in detailed in Sections 2 and 3 .

Table 5–1 summarizes interpretations made by the five EPRI teams and the eleven LLNL seismicity experts, as described in Sections 2 and 3. With respect to the Paducah site the important feature of zonation is the proximity of potential seismogenic faults in the Mississippi embayment. Therefore Table 5–1 categorizes the interpretations by the distance between zones representing potential large earthquakes in the New Madrid, Missouri area, and the Paducah site.

The summary presented in Table 5–1 categorizes the interpretations by the distance from the Paducah site to the source representing New Madrid seismicity. These are Type A (sources that are very close or include the site), Type B (sources that are about 10 km away), Type C (sources that are about 20 km away), and Type D (sources that are about 40 km away). Overall there are about equal numbers of interpretations of each type. We have also considered a fifth interpretation (Type E), in which the New Madrid source contains the site and extends 50 km past the site. This interpretation represents the unlikely hypothesis that the Reelfoot Ridge extends further to the north, as hinted by the geophysical observations by Hildebrand et al. (1). Consequently five fault geometries are used, corresponding to the five source types, to develop a fault representation of the New Madrid region that reflects the distance distribution as expressed by interpretations in the EPRI and LLNL studies and the reference cited above. Interpretations A through D are each given a weight of 23.75 %; interpretation E is give a weight of 5%.

These fault representations are shown in Figures 5–1 through 5–5 for the four types. As part of the detail of the Type A representation, the faults actually extend past the site by 10 km. The faults are represented with a spacing of 2.5 km near the site and 20 km at the western boundary of the Mississippi embayment to obtain better precision on the distances of earthquakes close to the site, and activity rates are assigned in proportion to the spacing between fault representations. In other words earthquakes are modeled as equally–likely in space anywhere within the New Madrid source region, but a closer spacing of faults is used near the site to obtain better precision in the calculations.

Table 5-1

Summary of EPRI and LLNL Seismic Zonations near Paducah

	Distance to New Madrid Source	Distance Type†	New Madrid Source $m_{b,max}$‡	Host Source $m_{b,max}$‡
EPRI Teams:				
Bechtel	0 km	A	7.5	—
Dames & Moore	32 km	D	7.5	6.5
Law Engin.	8 km	B	7.4	6.5
Rondout	18 km	C	7.3	6.8
Weston	8 km	B	7.2	6.6
WCC	63 km	D	7.5	6.3
LLNL experts:				
No. 1	21 km	C	7.4	6.0
No. 2	0 km	A	7.8	—
No. 3	0 km	A	7.5	—
No. 4	34 km	D	7.5	6.5
No. 5	0 km	A	7.75	—
No. 6	33 km	D	7.3	7.3
No. 7	14 km	B	7.8	6.5
No. 10	7 km	B	7.3	6.3
No. 11	0 km	A	7.0	—
No. 12	40 km	D	7.5	6.2/6.8
No. 13	40 km	D	7.4	6.2/6.2

†Interpretations are categorized by distance: A $\simeq$ 0 km, B $\simeq$ 10 km, C $\simeq$ 20 km, D $\simeq$ 40 km.
‡Central maximum magnitude designated by the team or expert.

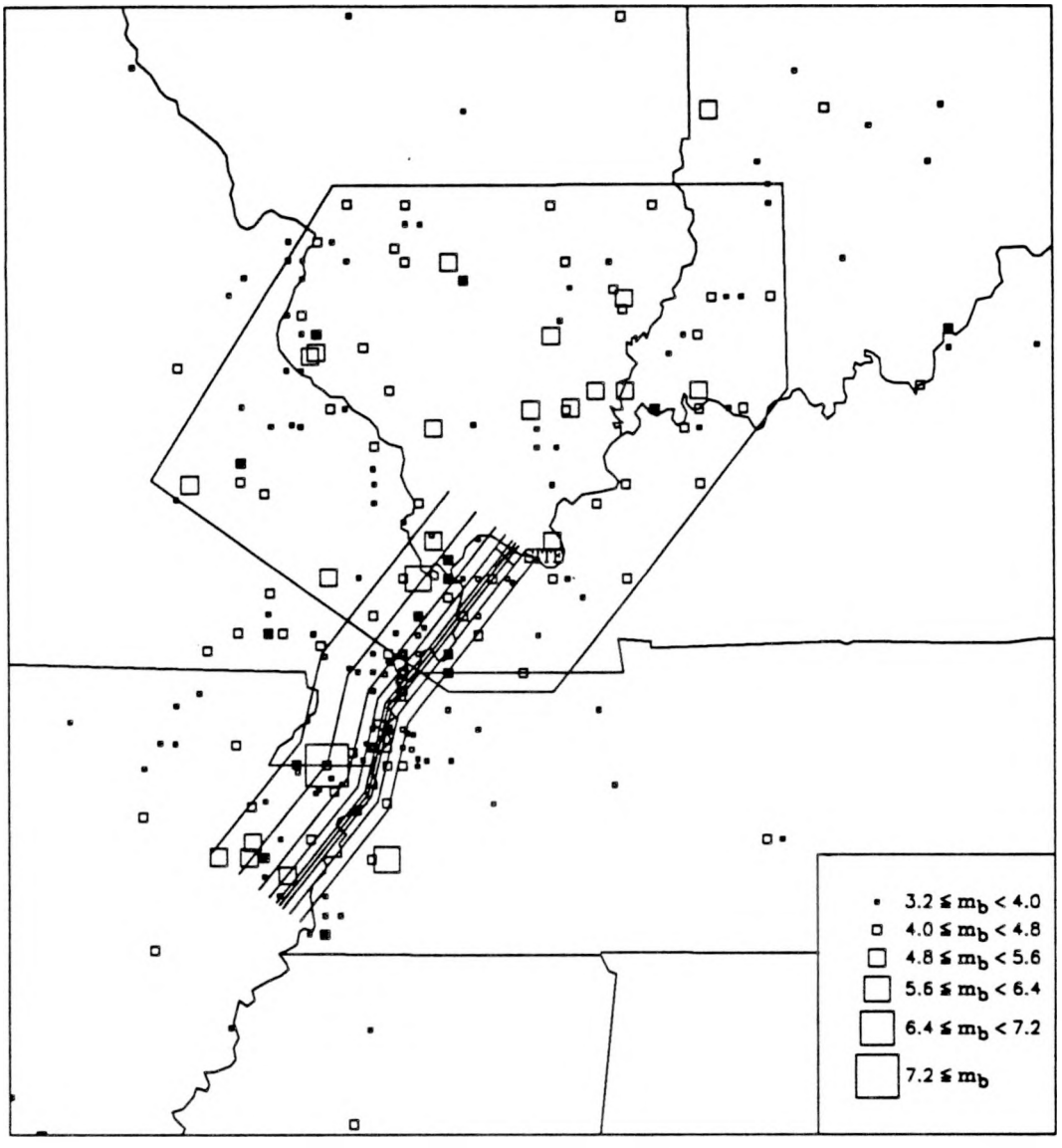

Figure 5-1. Type A faults in New Madrid region. Also shown is the southern Illinois seismic source. The historical seismicity is based on the EPRI catalog.

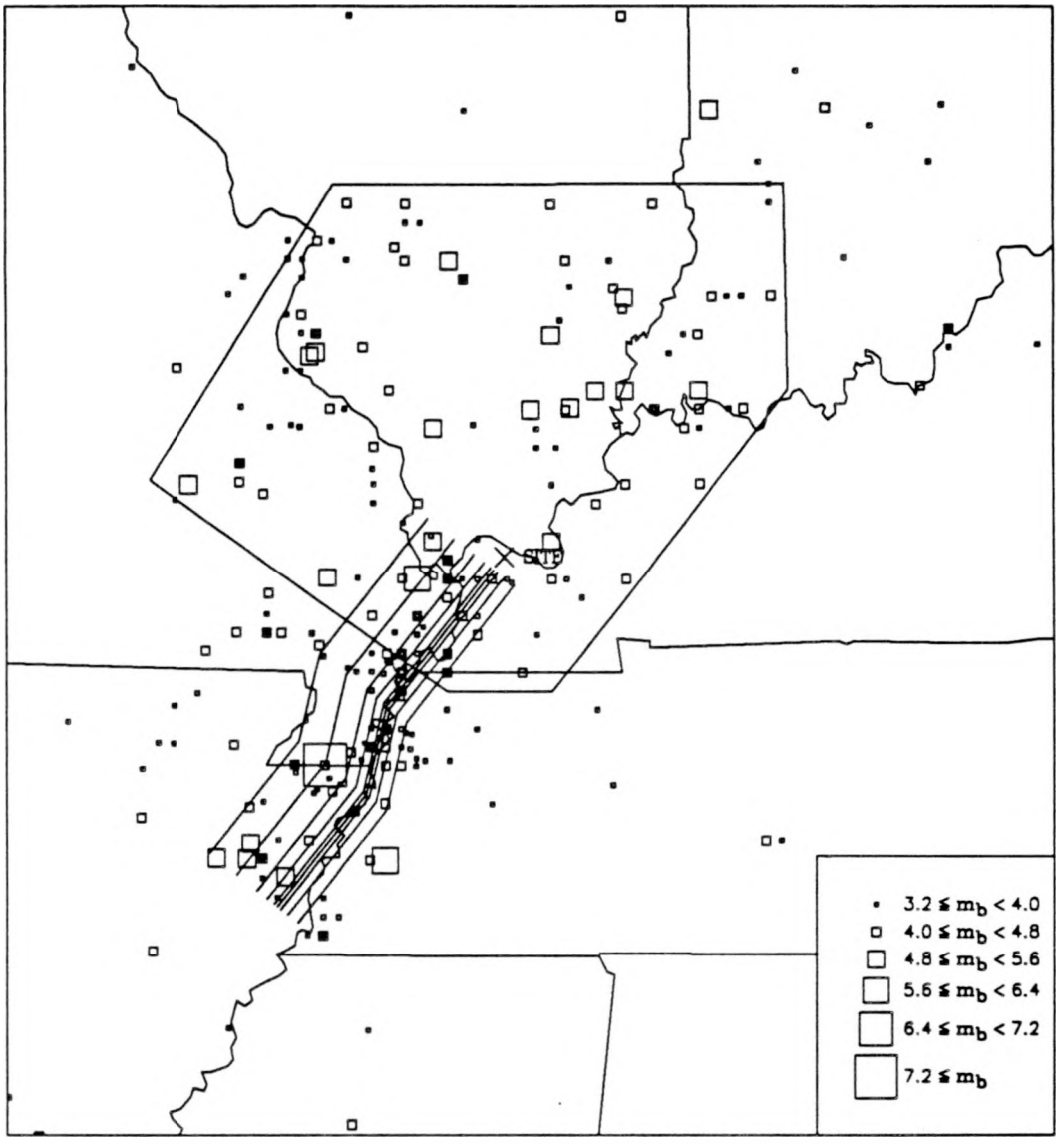

Figure 5-2. Type B faults in New Madrid region. Also shown is the southern Illinois seismic source. The historical seismicity is based on the EPRI catalog.

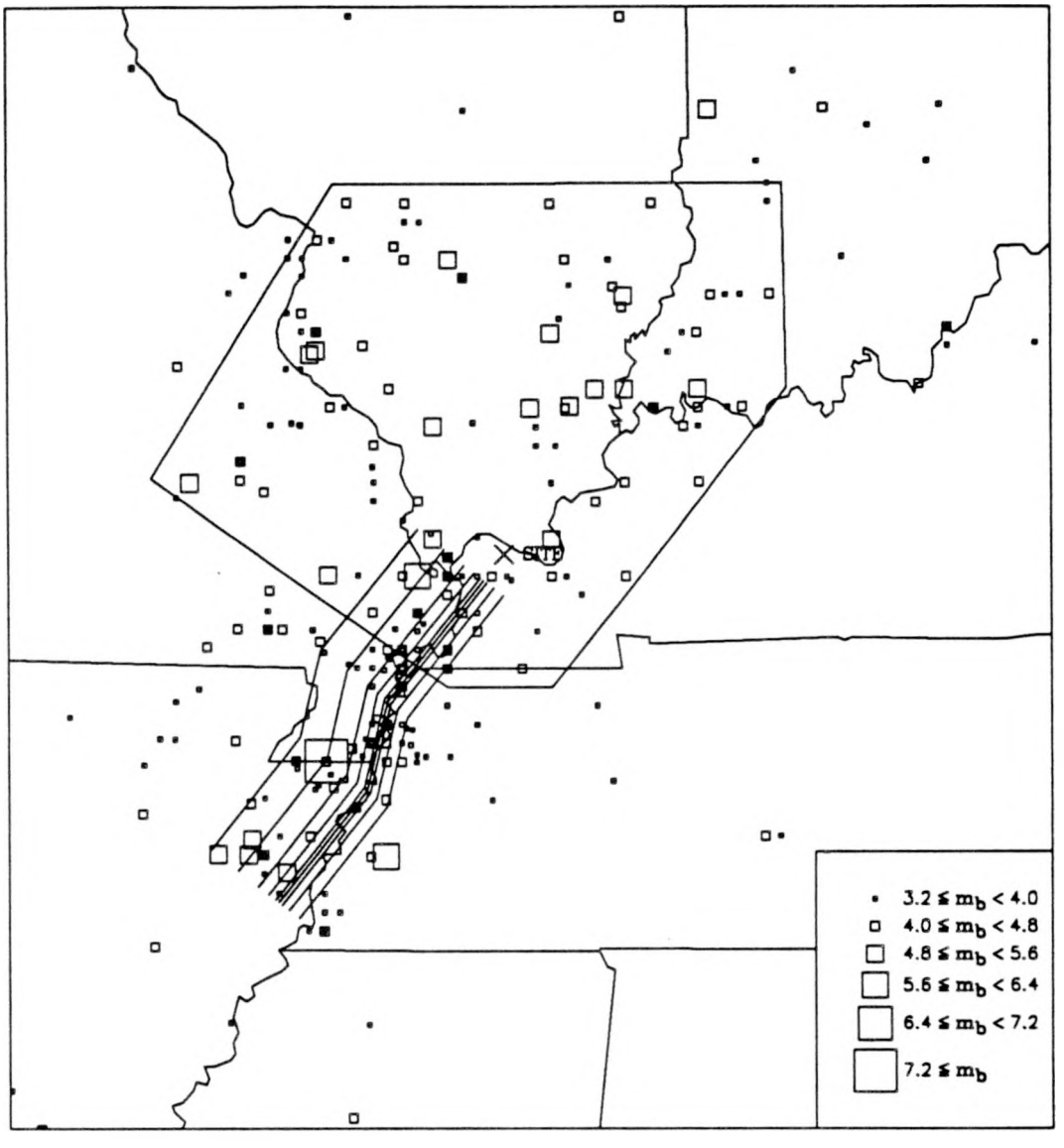

Figure 5-3. Type C faults in New Madrid region. Also shown is the southern Illinois seismic source. The historical seismicity is based on the EPRI catalog.

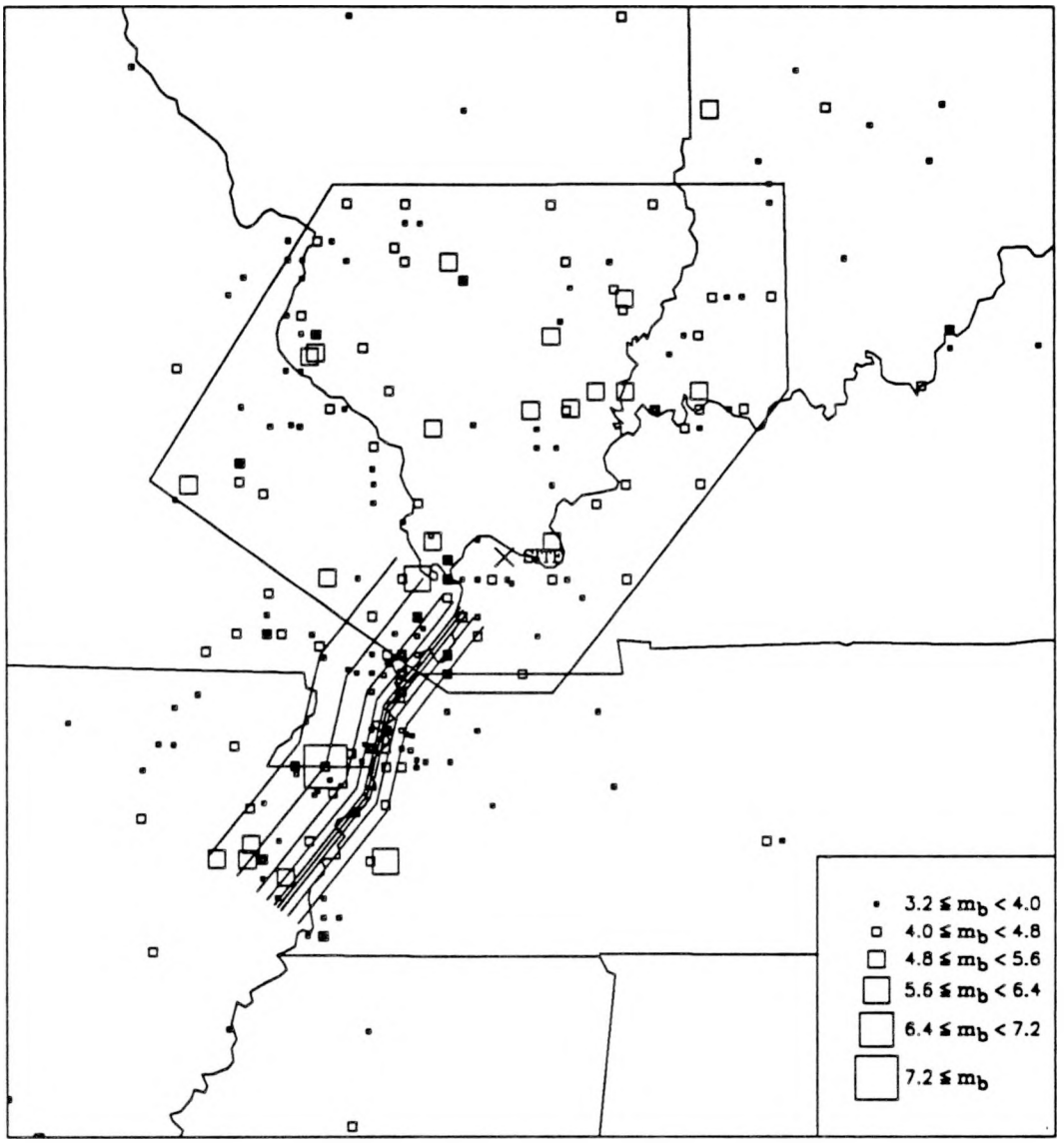

Figure 5-4. Type D faults in New Madrid region. Also shown is the southern Illinois seismic source. The historical seismicity is based on the EPRI catalog.

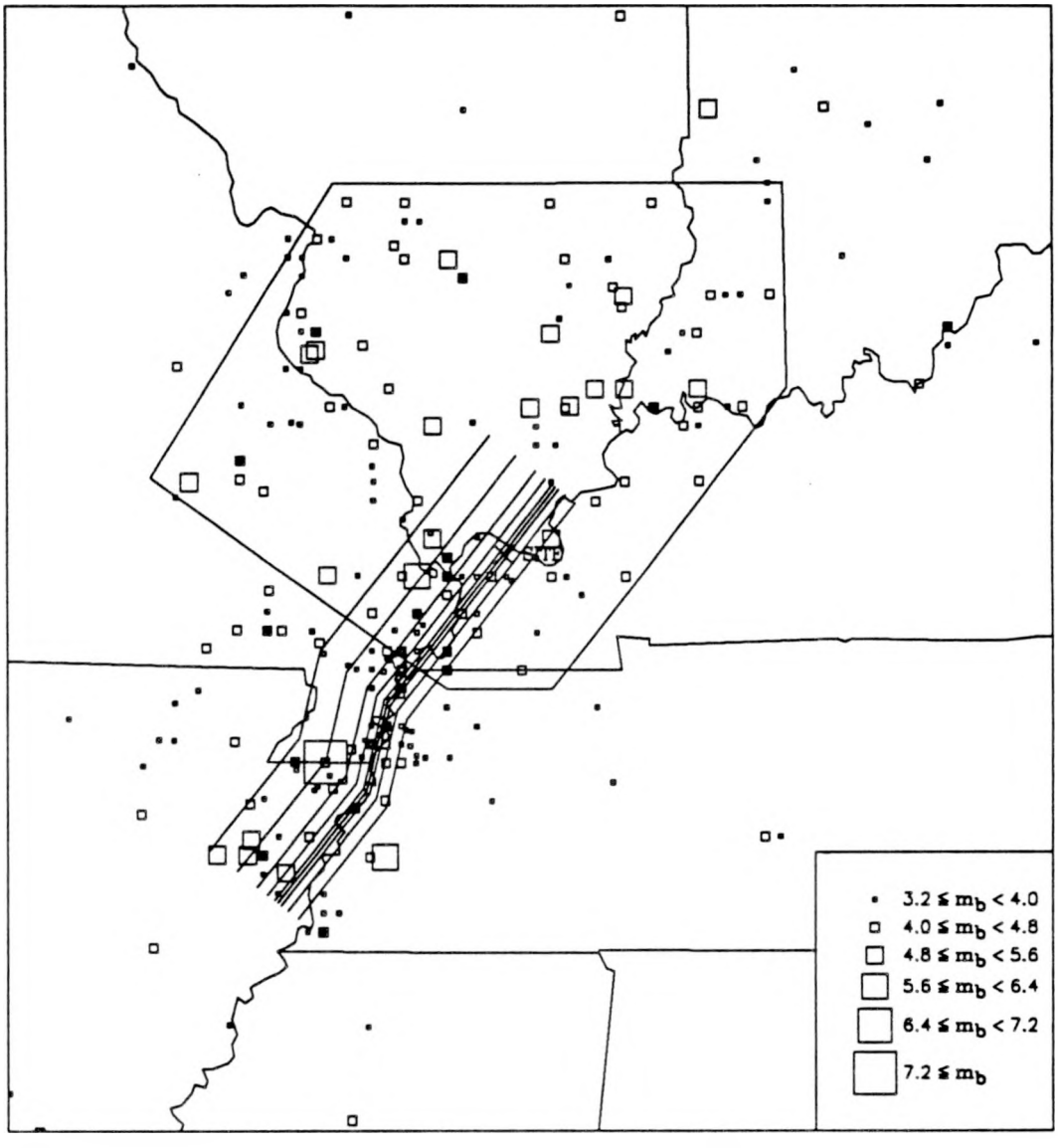

Figure 5-5. Type E faults in New Madrid region. Also shown is the southern Illinois seismic source. The historical seismicity is based on the EPRI catalog.

Also shown in Figures 5–1 through 5–5 is a source encompassing parts of southern Illinois, southwestern Indiana, southeastern Missouri, and western Kentucky. This represents the local seismicity north of the New Madrid region, and corresponds to the "host source" interpretations in Table 5–1. This region was drawn to include most of the historical seismicity north of the Mississippi embayment. Because the seismic hazard at Paducah is dominated by potential large earthquakes in the embayment, the exact representation of the boundaries of this host source is not critical. In particular it is unnecessary to break the region into several sources, each with its own set of parameters.

The historical seismicity shown in Figures 5–1 through 5–5 is taken from the catalog of earthquakes developed during the EPRI study. Main events with magnitudes above $m_b = 3.2$ are shown; in the EPRI catalog only one of the 1811-1812 earthquakes is considered a main event, so only one is shown in the figures. The exact treatment of large earthquakes using the characteristic magnitude model is described below.

5.2.2 Seismicity Parameters

To derive seismicity parameters for the sources shown in Figures 5–1 through 5–5, the EPRI catalog was used with two sets of calculations. First, two sets of regions were designated to represent fault types A, B, C, and E (Figure 5–6) and fault type D (Figure 5–7). The boundary of the New Madrid area follows the embayment, extended slightly to the north in Figure 5–6 to include moderate seismicity in southeastern Missouri and southern Illinois. The alternative northern boundary in Figure 5–7 was drawn to the south to exclude these events, so they would be included in the area source.

With the geometries of the sources selected, two analyses were conducted to estimate seismic activity rates and Richter b-values. The first corresponds to a standard analysis in which one picks periods over which each magnitude level is considered complete, obtains the observed seismicity in those time periods, and calculates the corresponding rate ν and b–value with the maximum likelihood technique. The second analysis applies the EPRI–derived periods of completeness, which includes accounting for periods of partially–complete reporting of events calibrated to observations in the entire eastern US, and derives maximum likelihood estimates of ν and b that incorporate data from a longer time period.

The two sets of estimates are given in Table 5–2; they indicate largely consistent analyses, and the differences represent uncertainty in the rates of occurrence of events in the region based on historical seismicity.

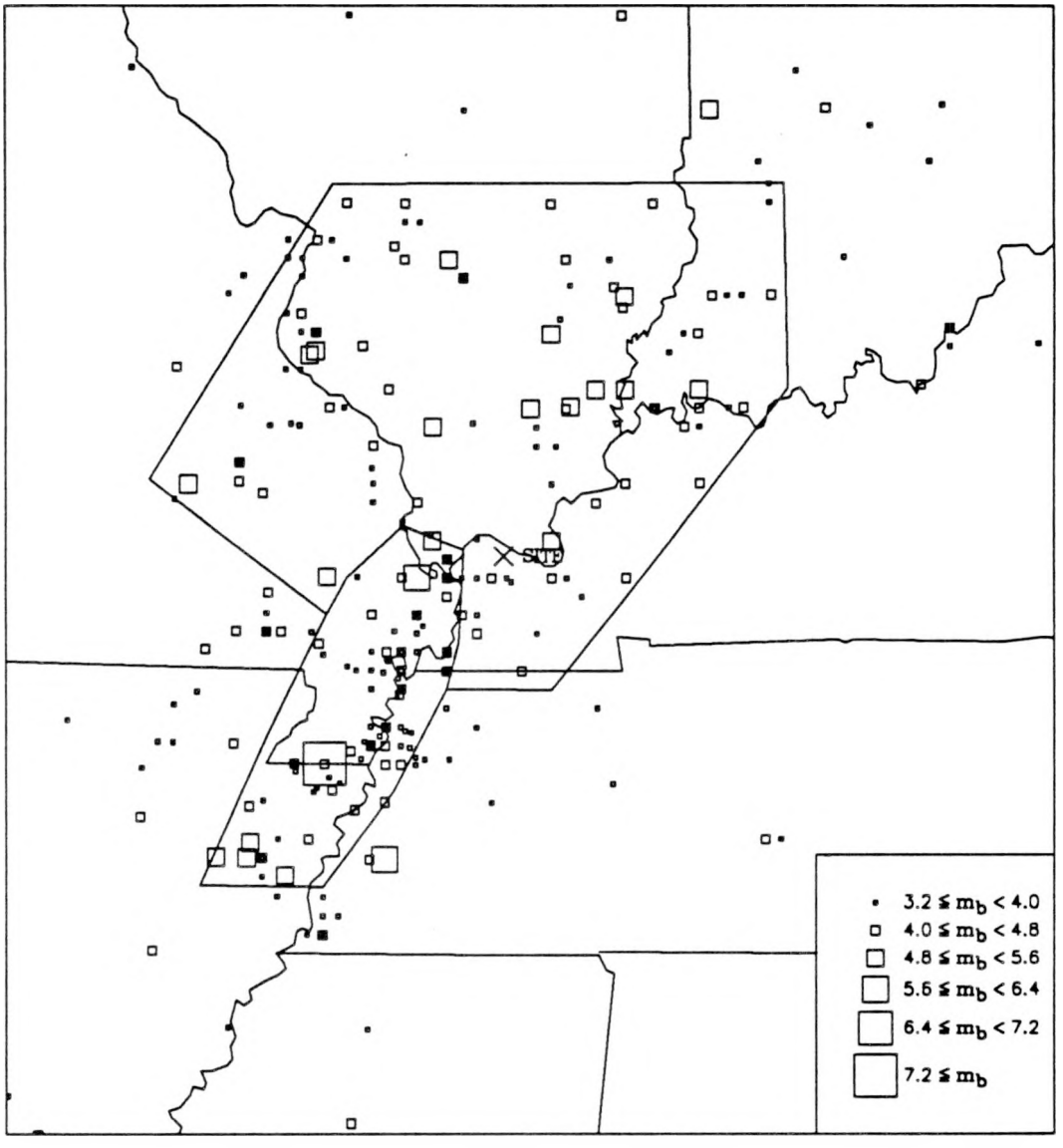

Figure 5-6. Regions used for analysis of seismicity for Type A, B, C, and E faults.

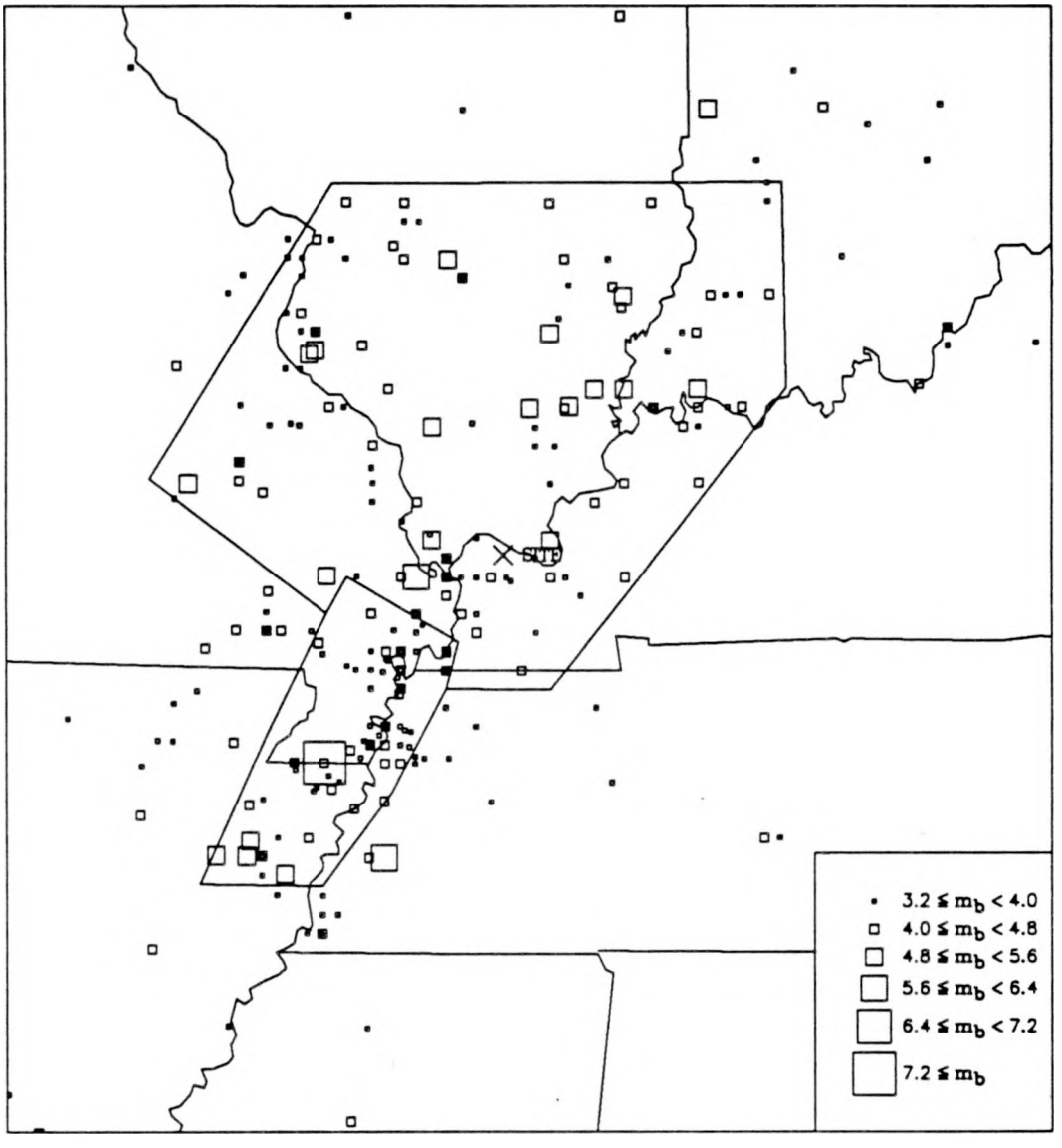

Figure 5-7. Regions used for analysis of seismicity for Type D faults.

Table 5-2

Estimates of Seismicity Parameters

Fault Types	Source	Analysis	Rate of events with $m_b > 5.0$	Richter b–value
A, B, and C	New Madrid	Standard	0.044	0.87
		EPRI	0.058	0.81
A, B, and C	Host source	Standard	0.062	0.68
		EPRI	0.064	0.74
D	New Madrid	Standard	0.030	0.96
		EPRI	0.040	0.85
D	Host source	Standard	0.073	0.70
		EPRI	0.078	0.74

Plots of the New Madrid seismicity data and of analyses for the "Standard" model and for the "EPRI" model are shown in Figure 5–8 (for fault types A, B, C, and E) and in Figure 5–9 (for fault type D). In these two figures, three fits to the data are indicated: an exponential model, a characteristic model that assumes an average rate of occurrence of large events of 1 in 500 years, and a characteristic model that assumes an average rate of occurrence of large events of 1 in 700 years. These rates for the characteristic model were chosen to represent a range of recurrence intervals estimated for large events in the New Madrid region [approximately 600 years, as reported by Russ (2)]. For this analysis a large event is taken to be one with $m_b > 7.0$, and in the figures an observed rate of 1/600 is used for the 1811-1812 earthquakes. The exponential model apparently underestimates the rate of occurrence of the large events; as a result only the characteristic magnitude model (with the two rates for the large events) is used in calculations.

An analysis of seismicity for the southern Illinois area source is shown in Figure 5–10. For this source the exponential magnitude modeled is used, as is conventional for area sources in the CEUS (3). Analyses for two configurations of the source are shown, corresponding to the geometries of this source illustrated in Figures 5–6 and 5–7.

Maximum magnitudes for the sources were selected to represent the range of interpretations specified by the EPRI teams and LLNL experts, as listed in Table 5–1. These are as follows.

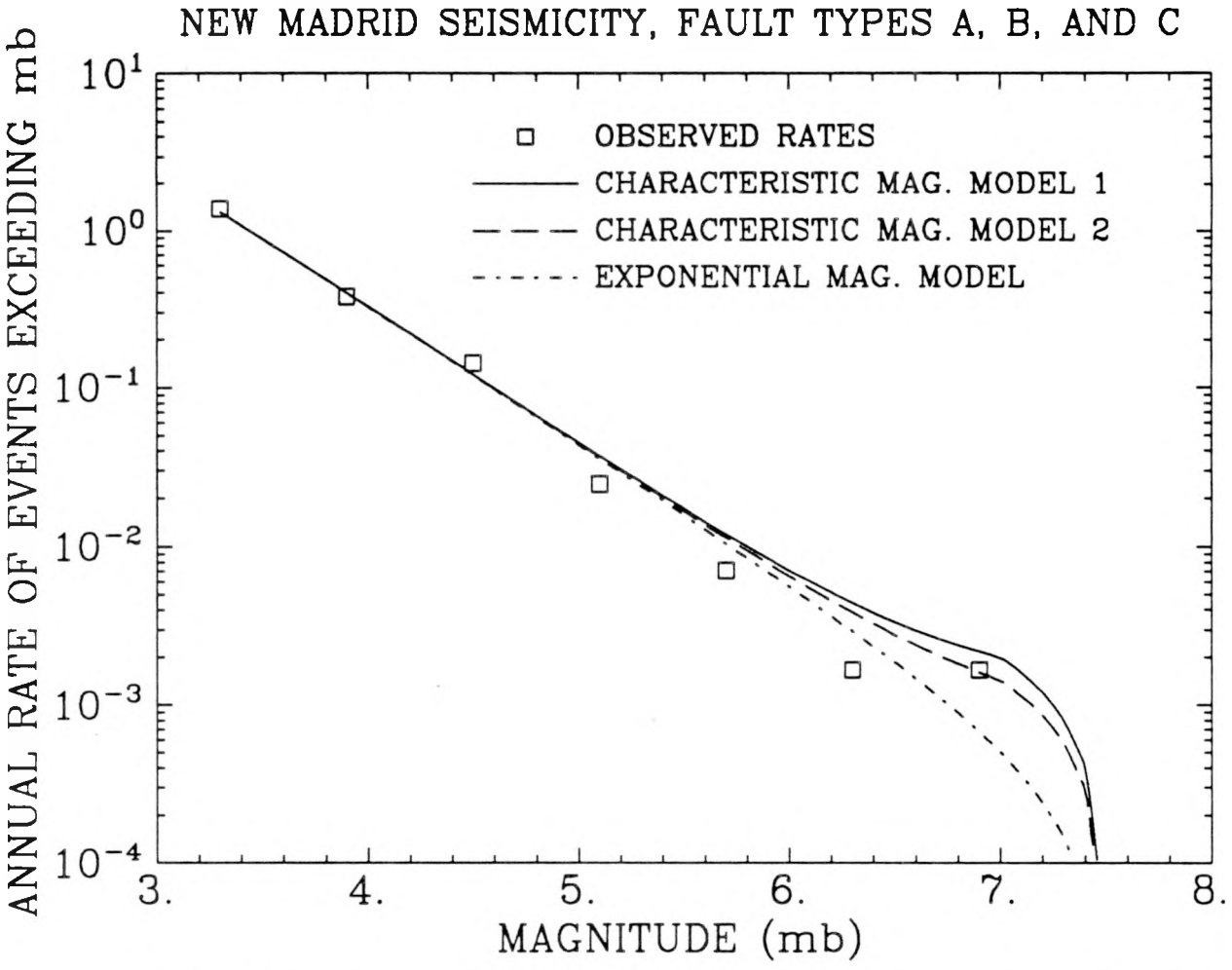

Figure 5-8. Observed and modeled seismicity for New Madrid fault types A, B, C, and E.

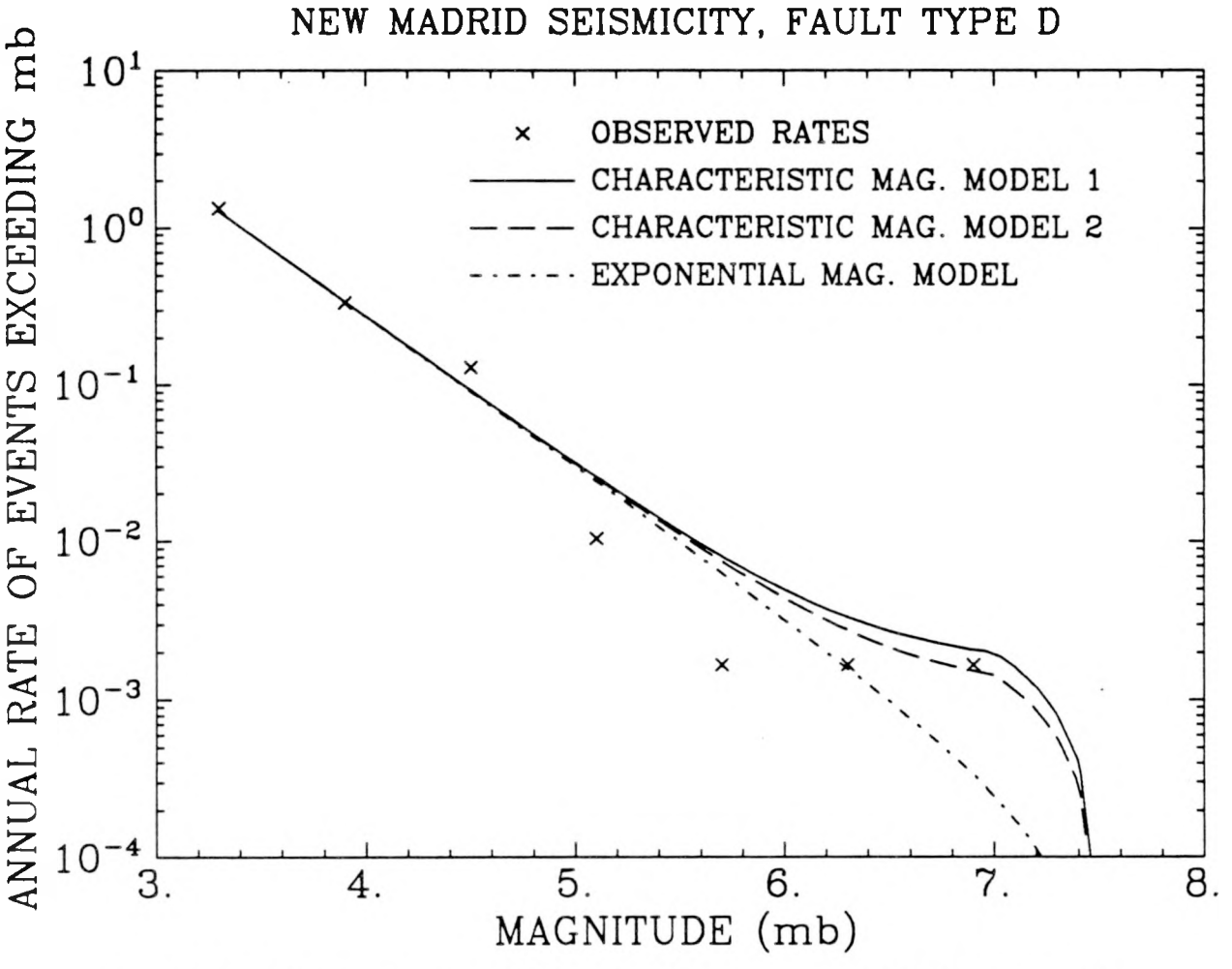

Figure 5-9. Observed and modeled seismicity for New Madrid fault type D.

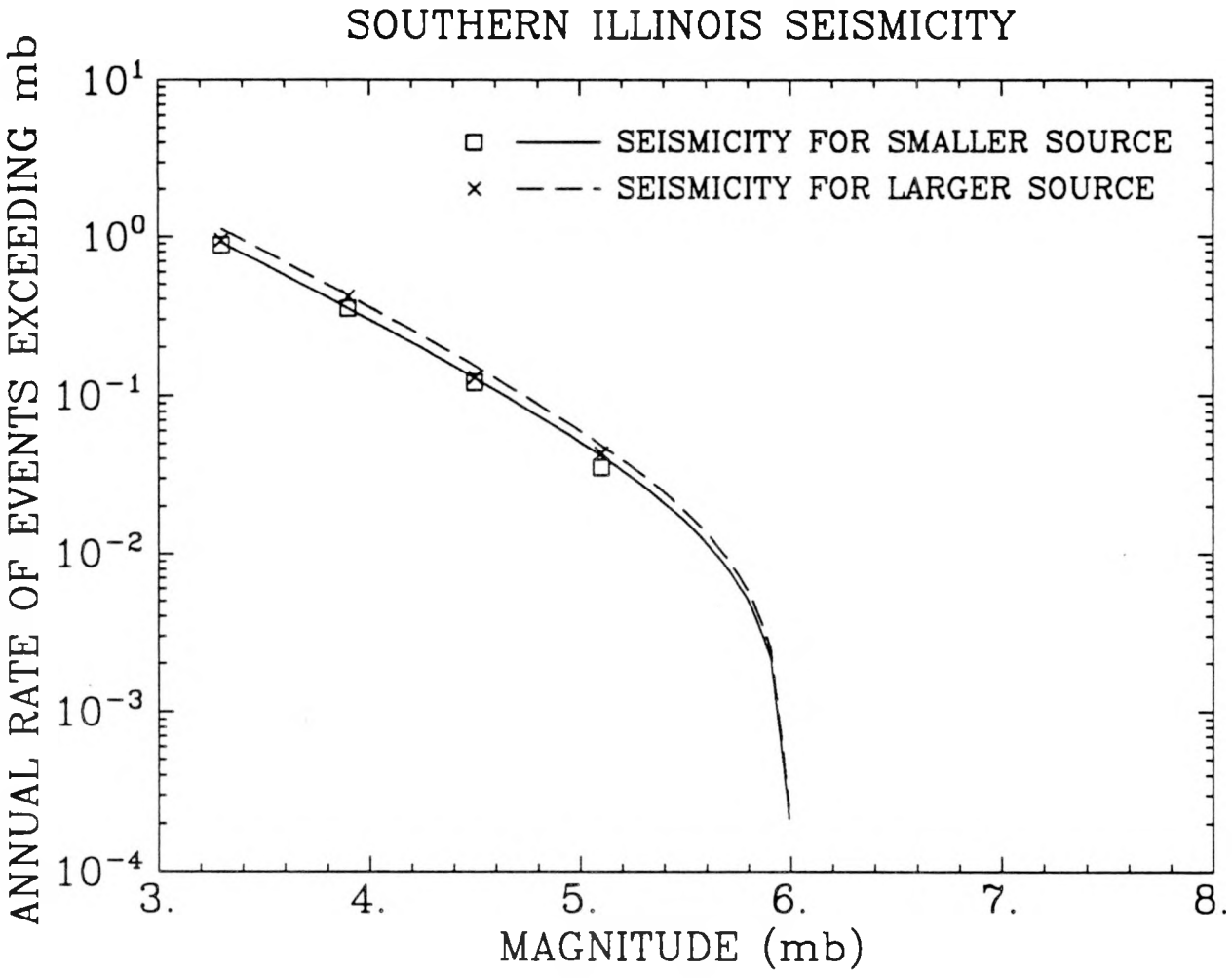

Figure 5-10. Observed and modeled seismicity for Southern Illinois source.

For the New Madrid source, values of maximum magnitude of 7.2, 7.5, and 7.8 were assigned weights of 0.2, 0.6, and 0.2, respectively. For the host source, values of 6.2, 6.5, and 6.8 were assigned weights of 0.2, 0.6, and 0.2, respectively.

5.2.3 Other Parameters

To estimate rupture length RL, the following equation was used:

$$RL = 10^{-2.18+0.51m_b} \qquad (5-1)$$

This equation was fitted to the rupture lengths predicted by Nuttli et al. (4) for magnitudes 6.6 and 7.6. It predicts a rupture length of 8 km for m_b 6, and a rupture length of 44 km for m_b 7.5.

Depths of earthquakes in the New Madrid sources were taken to range between 2 and 20 km, with a uniform distribution. This reflects the possibility that large earthquakes may occur at relatively deep depths in the eastern US (although they may also occur a shallow depths). For the host source a constant depth of 10 km was used; the small contribution of this source to seismic hazard at Paducah makes a more detailed assumption unnecessary.

5.3 ATTENUATION FUNCTIONS FOR EXTENDED RUPTURES

5.3.1 Motivation

As mentioned in Section 2.1, the evaluation of seismic hazard at the Paducah site must consider the effect of rupture size on the amplitude of near-source ground motions and must use an appropriate measure of distance. The ground-motion attenuation functions in the EPRI/SOG and LLNL methodologies do not consider the effect of extended ruptures.

Attenuation functions that predict magnitude saturation at small distances[1] due to extended ruptures have become standard in California. The EPRI/SOG and LLNL attenuation functions do not include saturation effects because no commercial nuclear plants in the CEUS are located near faults capable of generating large earthquakes.

5.3.2 Development

The EPRI/SOG attenuation functions were selected as a starting point for the development of attenuation functions for Paducah. These attenuation functions embody the results of an

[1] Magnitude saturation is the phenomenon whereby the ground-motion amplitude from very large earthquakes is almost independent of magnitude. Quantitatively, saturation implies that $\frac{\partial}{\partial m} \ln Y$ decreases as magnitude increases.

extensive research effort and numerous interactions with other experts in the field. Experience from other sites (5, Appendix A) indicates that the EPRI/SOG attenuation functions are roughly equivalent (in their central predictions and their uncertainty bands) to the LLNL attenuation functions without ground-motion Expert 5.

Comparison of the attenuation functions by Nuttli (8) to predictions that use Nuttli's (4) scaling assumptions but use other methods to predict peak amplitudes (9,10, and Appendix A, for example) indicates that the Nuttli attenuation function predicts much higher ground motions for large earthquakes. The Nuttli attenuation functions are based on scientifically defensible source-scaling assumptions, but Nuttli's process to obtain peak time-domain amplitudes from spectra is very rudimentary in comparison to methods in current use.

As a result, the Nuttli attenuation functions were replaced by attenuation functions developed using the source scaling model of Nuttli et al.[2] (4). The mathematics used to obtain peak time-domain values, and other model parameters, are identical to those used in (9); only the scaling assumptions are changed. The resulting attenuation functions are identified as "Modified Nuttli Scaling."

In order to quantify the effect of extended ruptures on near-fault ground-motion saturation, we generated synthetic high-frequency ground motions from an extended rupture. We used assumptions based on the work of Jost (6) and Nuttli et al. (4). These assumptions were suitably modified in order to generate high-frequency ground motions, which depend less on wave-propagation phenomena. Details of these simulations are contained in Appendix A. Using the simulation results for m_{Lg} 6.6 and 7.6, we obtained a magnitude saturation term of the form

$$\ln[Y] \propto \ln[R + 0.006e^{m_{Lg}}] \qquad (5-2)$$

where Y represents ground-motion amplitude (e.g., PGA) and R represents the closest distance to the rupture.

The magnitude-dependent term in the above equation (i.e., the magnitude-saturation term) is equal to 4.4 km for m_{Lg} 6.6 and 12 km for m_{Lg} 7.6. This model predicts lower saturation than models for California, because the underlying source scaling model assumes smaller ruptures for CEUS earthquakes than for California earthquakes of the same magnitude. For

[2]The scaling model by Nuttli et al. predicts stress drops lower than 100 bars for small and moderate earthquakes, causing some of the ground-motion amplitudes predicted by this model to be lower than the predictions by the McGuire et al. and Boore-Atkinson models. For these lower magnitudes, we use a stress drop of 100 bars.

instance, Campbell's attenuation functions (7), predict a magnitude-saturation term of 21 km for M_S 8.4, which corresponds to to m_{Lg} 7.6.

The three sets of attenuation functions—namely, Boore and Atkinson (11), McGuire et al. (9), and Modified Nuttli Scaling—are modified by introducing the saturation term of Equation 5–2. The resulting attenuation functions are given equal weights in the seismic-hazard calculations. Figures 5–11 through 5–17 show the ground-motion amplitudes predicted by these three models. In some of the figures, the predictions by the Modified Nuttli scaling are not visible. This is because these predictions coincide with those by McGuire et al. (9) because the stress drop for the former model was set to 100 bars.

The term R in Equation 5–2 represents distance to the rupture—as opposed to hypocentral distance. As a result, the attenuation functions used in the extended-source hazard analysis predict that the isoseismals associated with a large earthquake are elongated.

The same three sets of attenuation functions, without the magnitude-saturation term, are used in computing the hazard from the southern Illinois source zone. We do not include the magnitude-saturation term for earthquakes in southern Illinois because these earthquakes are modeled as point sources.

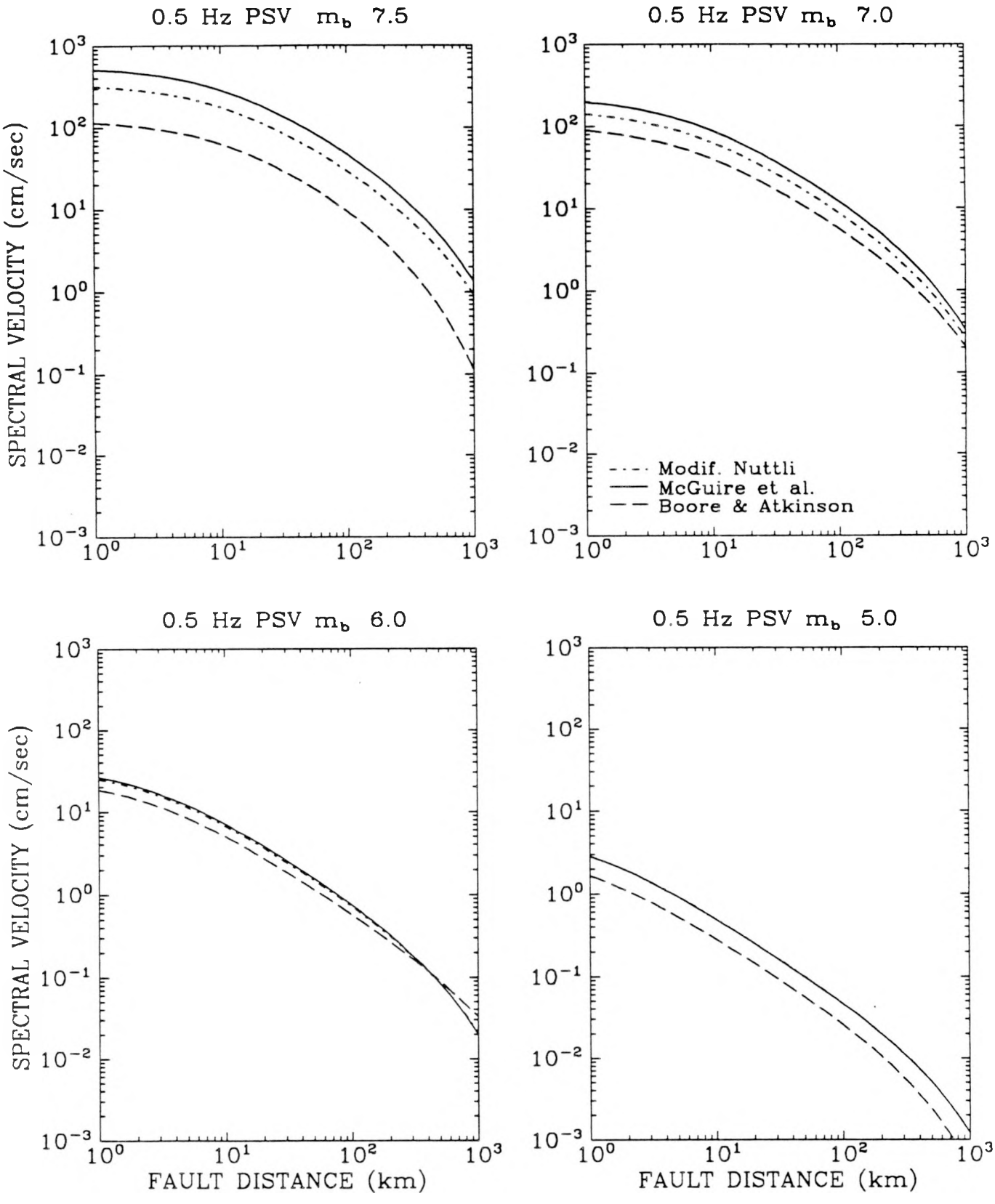

Figure 5-11. Ground motions models used for the New Madrid source in the extended-source seismic-hazard calculations: predictions for 0.5-Hz spectral velocity. Note: the predictions by the Modified Nuttli Scaling model may not be visible in some figures because they coincide with those by McGuire et al. (9).

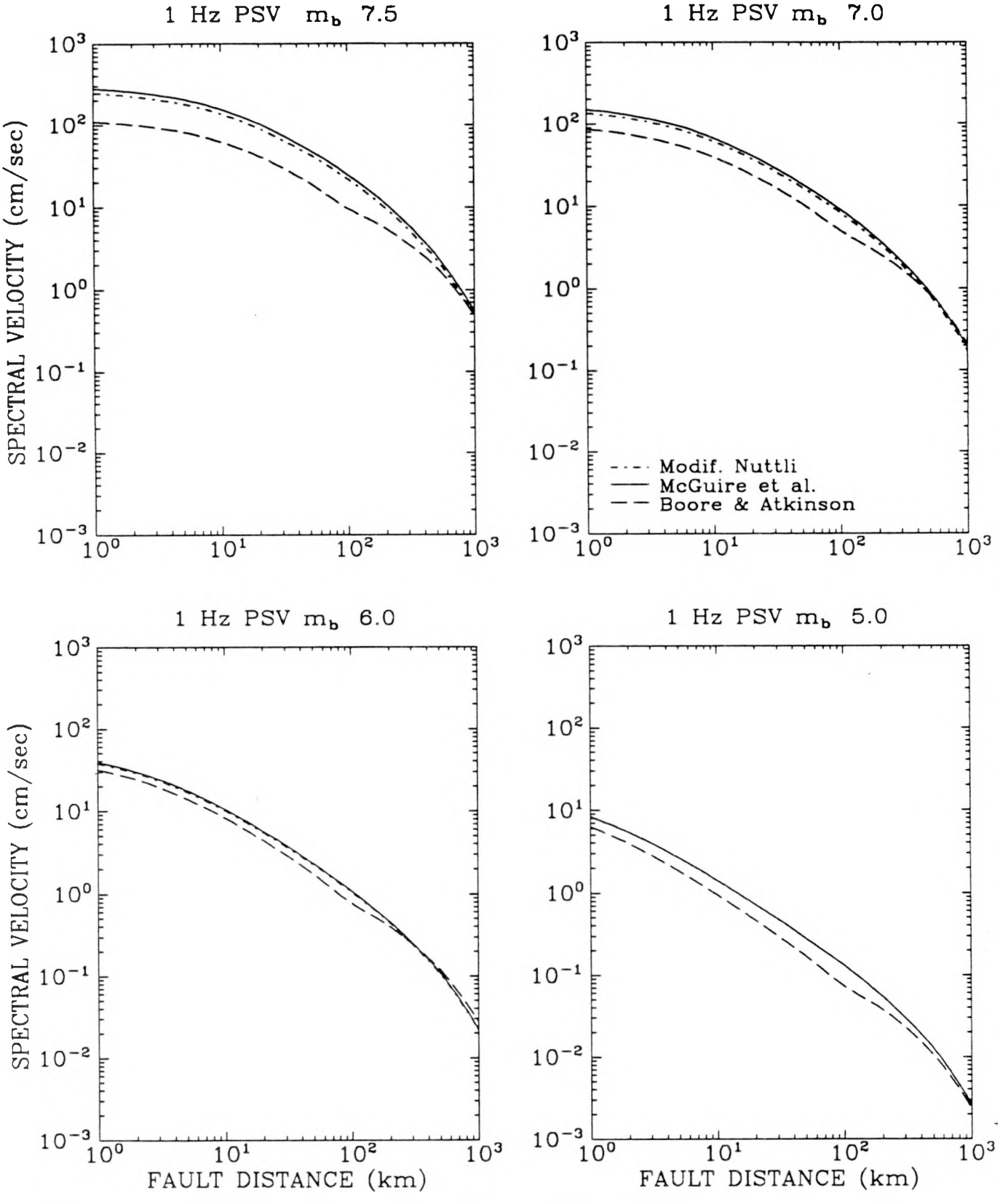

Figure 5-12. Ground motions models used for the New Madrid source in the extended-source seismic-hazard calculations: predictions for 1-Hz spectral velocity. Note: the predictions by the Modified Nuttli Scaling model may not be visible in some figures because they coincide with those by McGuire et al. (9).

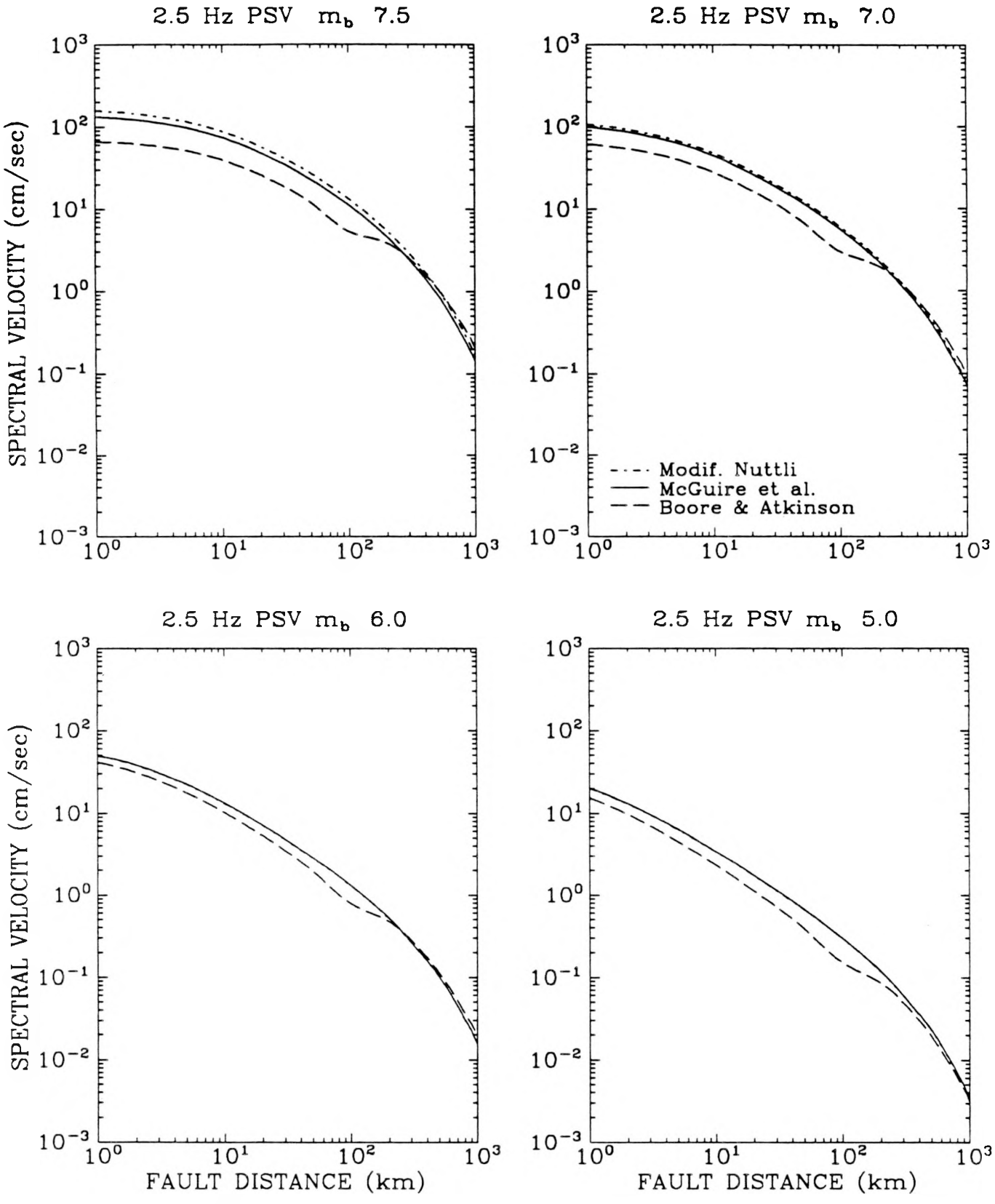

Figure 5-13. Ground motions models used for the New Madrid source in the extended-source seismic-hazard calculations: predictions for 2.5-Hz spectral velocity. Note: the predictions by the Modified Nuttli Scaling model may not be visible in some figures because they coincide with those by McGuire et al. (9).

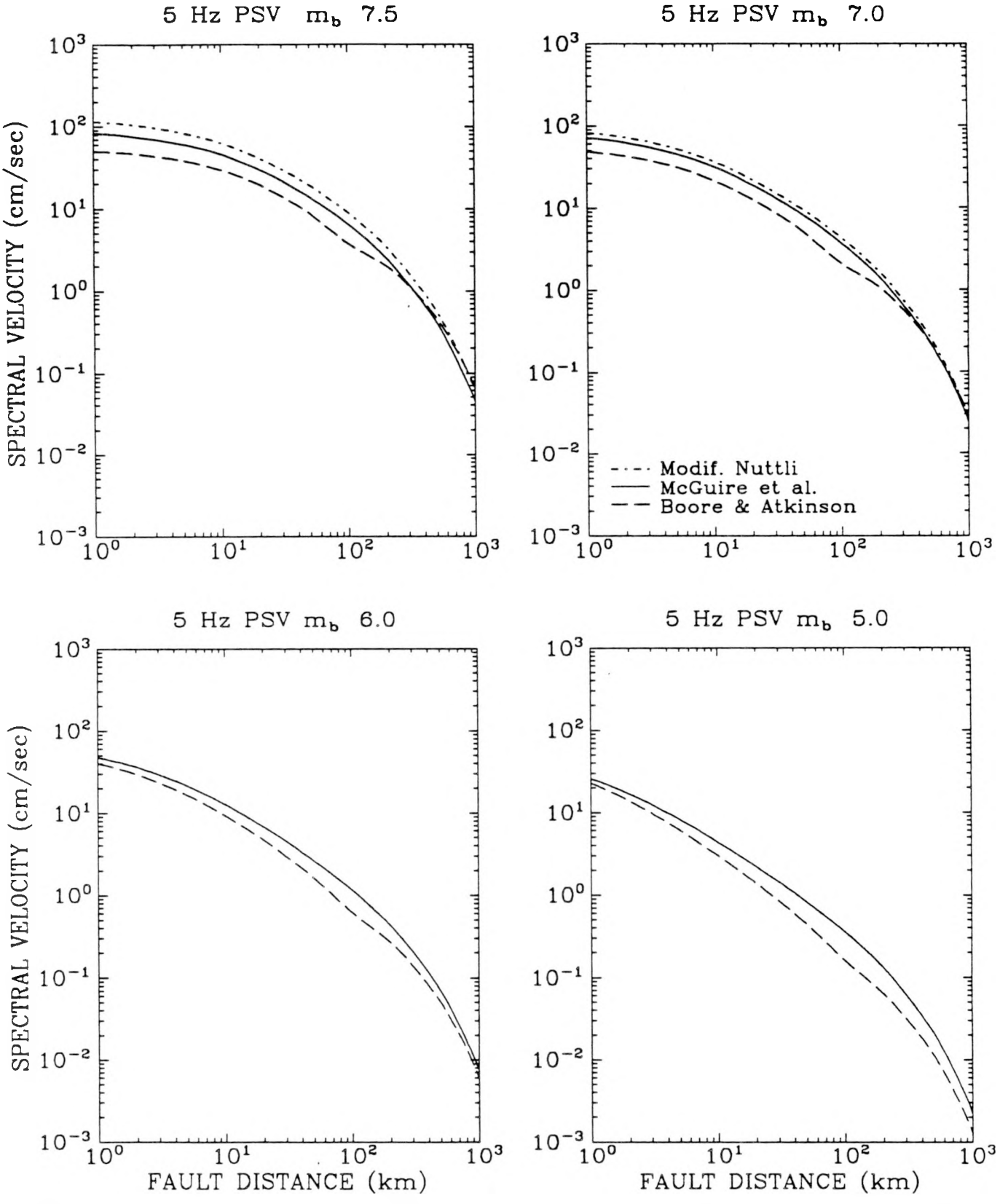

Figure 5-14. Ground motions models used for the New Madrid source in the extended-source seismic-hazard calculations: predictions for 5-Hz spectral velocity. Note: the predictions by the Modified Nuttli Scaling model may not be visible in some figures because they coincide with those by McGuire et al. (9).

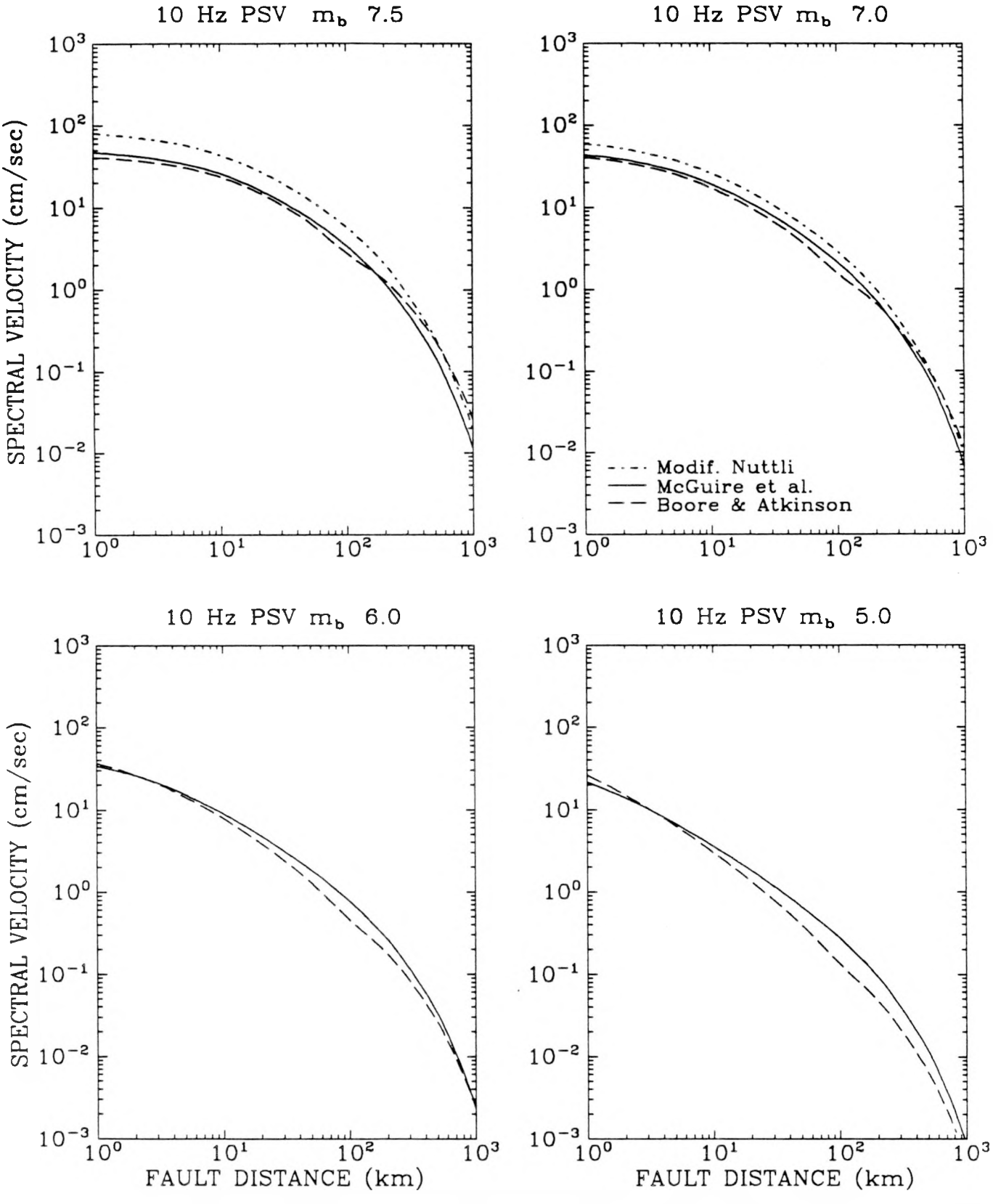

Figure 5-15. Ground motions models used for the New Madrid source in the extended-source seismic-hazard calculations: predictions for 10-Hz spectral velocity. Note: the predictions by the Modified Nuttli Scaling model may not be visible in some figures because they coincide with those by McGuire et al. (9).

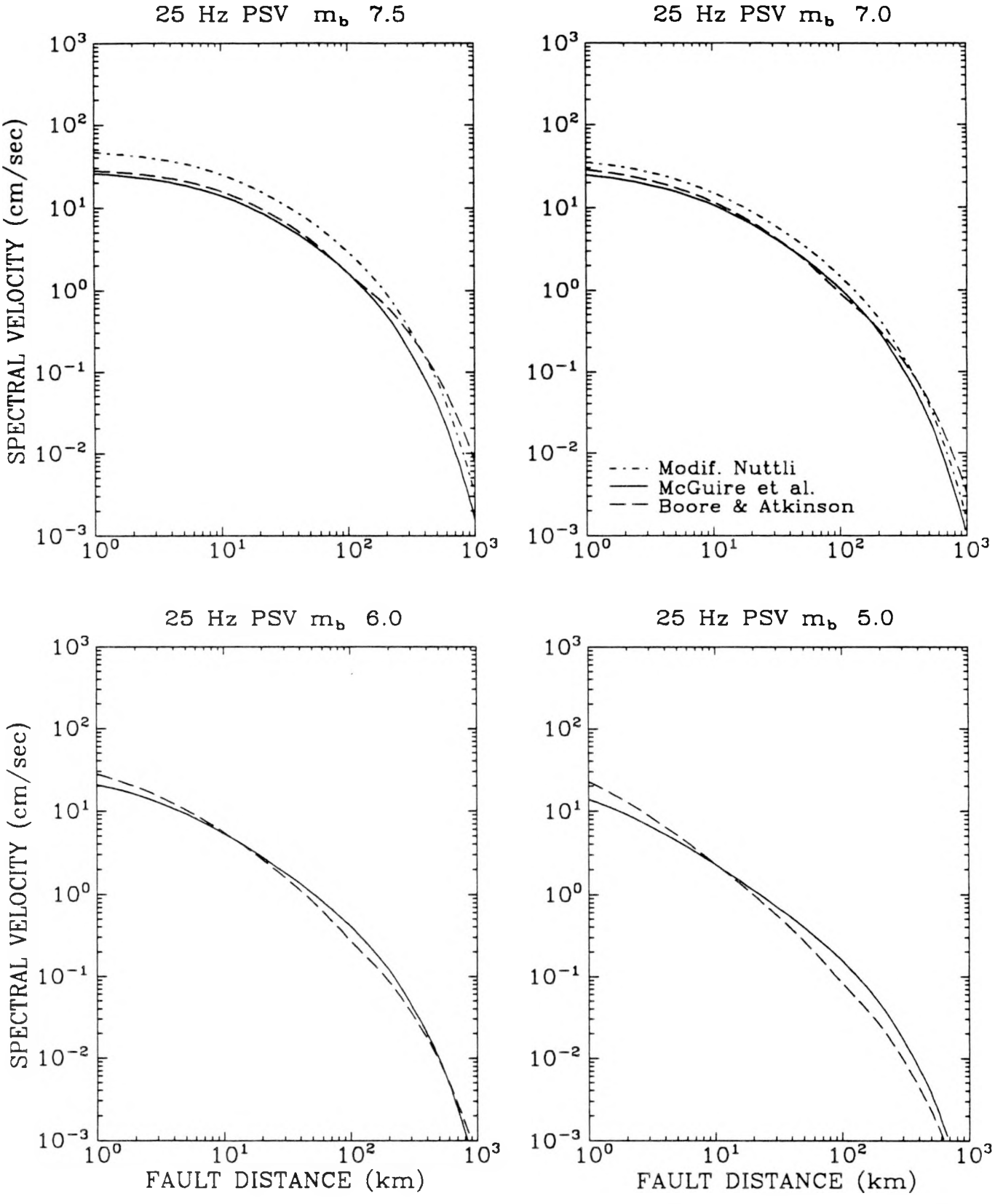

Figure 5-16. Ground motions models used for the New Madrid source in the extended-source seismic-hazard calculations: predictions for 25-Hz spectral velocity. Note: the predictions by the Modified Nuttli Scaling model may not be visible in some figures because they coincide with those by McGuire et al. (9).

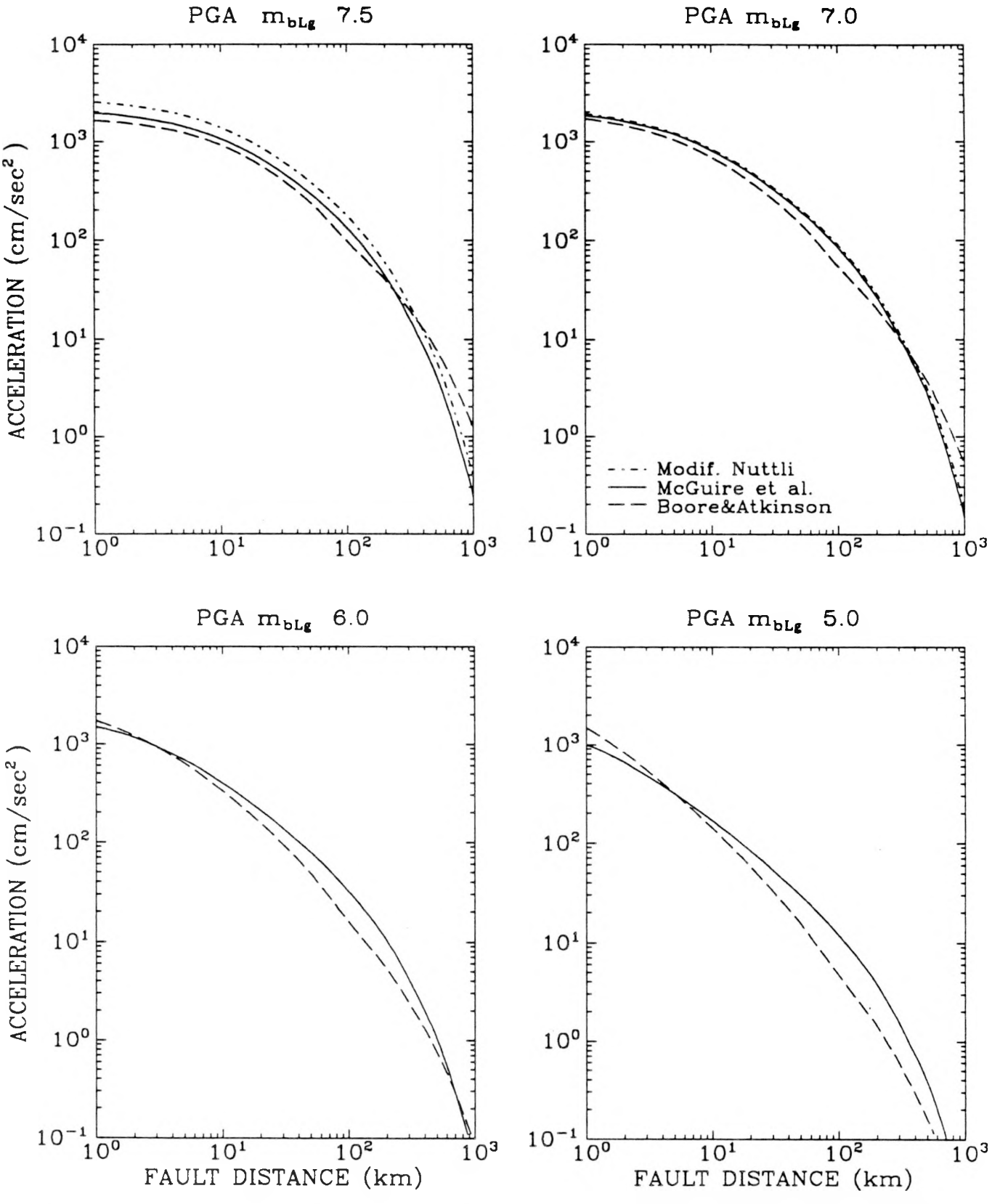

Figure 5-17. Ground motions models used for the New Madrid source in the extended-source seismic-hazard calculations: predictions for peak ground acceleration. Note: the predictions by the Modified Nuttli Scaling model may not be visible in some figures because they coincide with those by McGuire et al. (9).

5.4 RESULTS

Results of the seismic hazard analysis are presented as seismic hazard curves in figures in this section. These curves are for peak ground acceleration PGA and for spectral velocities (PSV) in the frequency range 0.5 to 25 Hz. All PSV values have been calculated using 5% of critical damping. Results presented in this section are for rock site conditions; they are appropriate for input into site–specific analyses of dynamic soil response.

Figures 5–18 through 5–24 present the seismic hazard at the Paducah site, for PGA and for spectral velocities at frequencies between 0.5 and 25 Hz. Curves are shown for the 0.15, 0.50, and 0.85 fractiles and for the mean of the distribution (other fractiles are tabulated in Appendix B). The uncertainty in these curves (i.e., the spread among fractile curves) represents the combined effects of uncertainty in fault geometry (specifically the closest distance between New Madrid faults and the site), seismicity parameters (ν and b), maximum magnitude, and attenuation equation. Figure 5–25 presents median uniform hazard spectra for 5% damping based on the PSV results.

5.4.1 Uniform Hazard Spectra for Additional Damping Ratios

We calculate approximate uniform hazard spectra for damping ratios of 2, 7, 10, 12, and 15 % from the 5% results presented in Figure 5–25. We use the expression:

$$\frac{\mathrm{PSV}(f,\zeta)}{\mathrm{PSV}(f,0.05)} \simeq \left[\frac{1+4.9\zeta fT}{1+4.9\times 0.05 fT}\right]^{-0.41} \qquad (5-3)$$

in which f is frequency (Hz), ζ is damping ratio (as a fraction of critical damping, not as a percentage), and T is the duration of the strongest phase of the ground motion. Equation 5-3 is based on a semi-empirical expression by Rosenblueth (11, Equation 1.11). The PSV ratios predicted by Equation 5-3 agree with results from random-vibration theory for large values of fT, and with real and artificial records for all interesting values of fT. Comparisons with records also show that the ratio $\mathrm{PSV}(f,\zeta)/\mathrm{PSV}(f,0.05)$ has a low variability from record to record.

We use the strong-motion durations obtained in Section 6. These durations are listed in Table 5–3, for various exceedance probabilities. Figures 5–26 through 5–31 present the uniform hazard spectra calculated for the additional damping ratios.

Table 5-3

Strong-Motion Durations used with Equation 5–3

Probability of Exceedance	T (sec)
2×10^{-3}	5.5
1×10^{-3}	8
2×10^{-4}	8
1×10^{-4}	8

5.5 REFERENCES

1. T. Hildenbrand, M. Kane, and J. Hendricks. "Magnetic Basement in the Upper Mississippi Embayment Region – A Preliminary Report". In F. McKeown and L. Pakiser, editors, *Investigations of the New Madrid, Missouri Earthquake Region*, pp. 39–53, USGS, 1982. U.S. Geological Survey Professional Paper 1236.

2. D. Russ. "Style and Significance of Surface Deformation of the Paleozoic Bedrock Surface in the New Madrid Seismic Zone". In F. McKeown and L. Pakiser, editors, *Investigations of the New Madrid, Missouri Earthquake Region*, pp. 39–53, USGS, 1982. U.S. Geological Survey Professional Paper 1236.

3. S. T. Algermissen, D. M. Perkins, P. C. Thenhaus, S. L. Hanson, and B. L. Bender. *Probabilistic Estimates of Maximum Acceleration and Velocity in Rock in the Contiguous United States.* Technical Report 82-1033, U. S. Geological Survey, 1982.

4. O. W. Nuttli, M. L. Jost, R. B. Herrmann, and G. A. Bollinger. *Numerical models of the rupture mechanics and far-field ground motion of the 1886 South Carolina earthquake.* Bulletin 1586, U. S. Geological Survey, 1989.

5. R. K. McGuire, G. R. Toro, J. P. Jacobson, T. F. O'Hara, and W. J. Silva. *Probabilistic Seismic Hazard Evaluations in the Central and Eastern United States: Resolution of the Charleston Earthquake Issue.* Special Report NP-6395-D, Electric Power Research Institute, April 1989.

6. M. L. Jost. *Long-Period Strong Ground Motions and Response Spectra of Large Historical Earthquakes in the Central and Eastern United States from Kinematic Source Models.* PhD thesis, Saint Louis University, 1989.

7. K. W. Campbell. "Near Source Attenuation of Peak Horizontal Acceleration". *Bulletin of the Seismological Society of America*, 71:2039–2070, December 1981.

8. O. W. Nuttli. Letter dated September 19, 1986 to J. B. Savy. Reproduced in: D. Bernreuter, J. Savy, R. Mensing, J. Chen, and B. Davis. *Seismic Hazard Characterization of 69 Nuclear Plant Sites East of the Rocky Muntains: Questionnaires.* U. S. Nuclear Regulatory Commission, Technical Report NUREG/CR-5250, UCID-21517, Volume 7, 1989. Prepared by the Lawrence Livermore National Laboratory.

9. R. K. McGuire, G. R. Toro, and W. J. Silva. *Engineering Model of Earthquake Ground Motion for Eastern North America.* Technical Report NP-6074, Electric Power Research Institute, 1988.

10. R. B. Herrmann. *Numerical Simulation of Ground Motions at Paducah Kentucky for a Large New Madrid Earthquake.* Report to Martin Marietta Energy Systems, September 1990.

11. D. M. Boore and G. M. Atkinson. "Stochastic Prediction of Ground Motion and Spectral Response Parameters at Hard-Rock Sites in Eastern North America". *Bulletin of the Seismological Society of America*, 77(2):440–467, 1987.

12. E. Rosenblueth. "Characteristics of Earthquakes". In E. Rosenblueth, editor, *Design of Earthquake Resistant Structures*, chapter 1, Wiley, 1980.

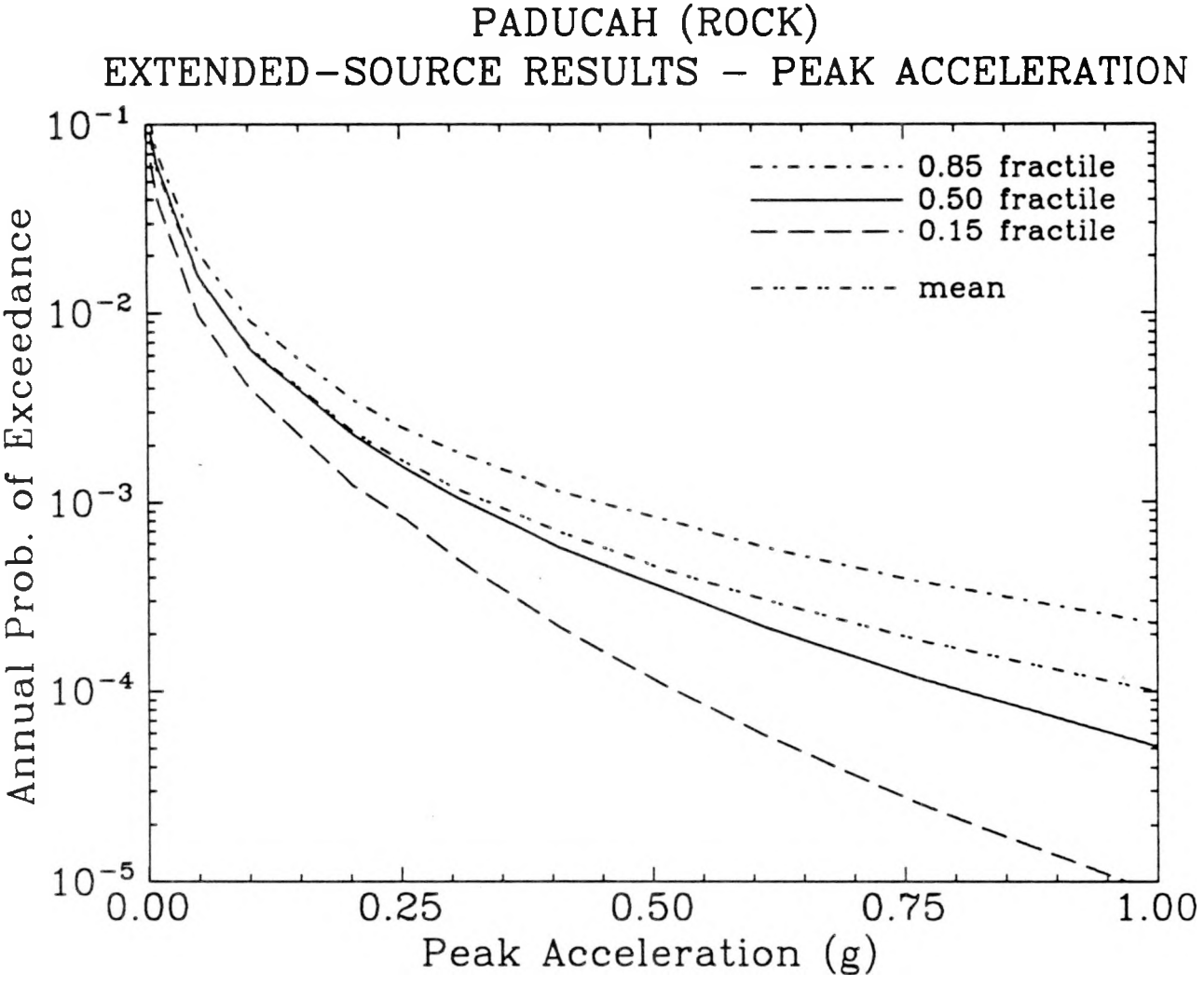

Figure 5-18. Peak ground acceleration hazard curves for Paducah (for rock site conditions) computed from the extended-source hazard analysis.

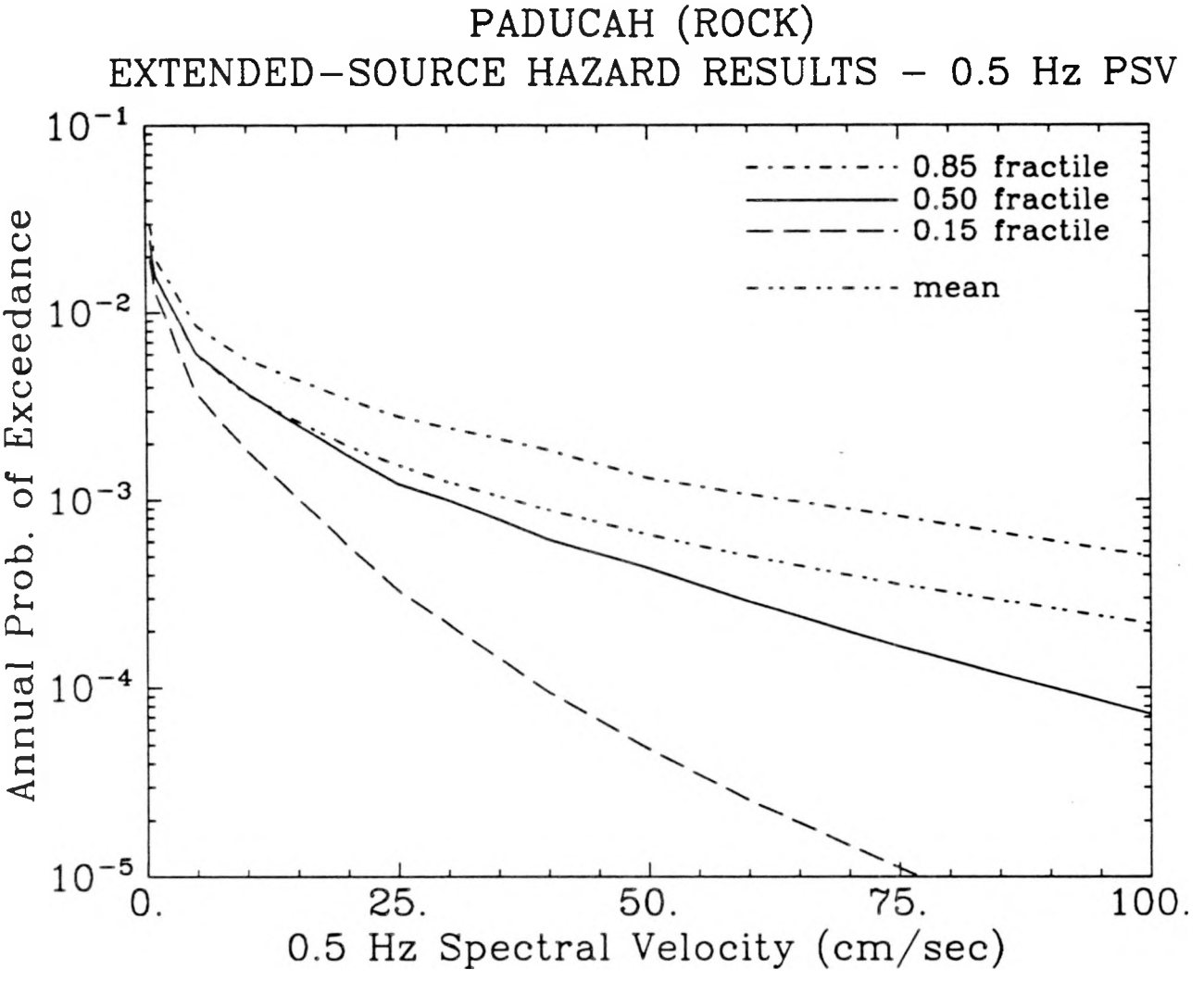

Figure 5-19. 0.5-Hz spectral velocity hazard curves for Paducah (for rock site conditions) computed from the extended-source hazard analysis.

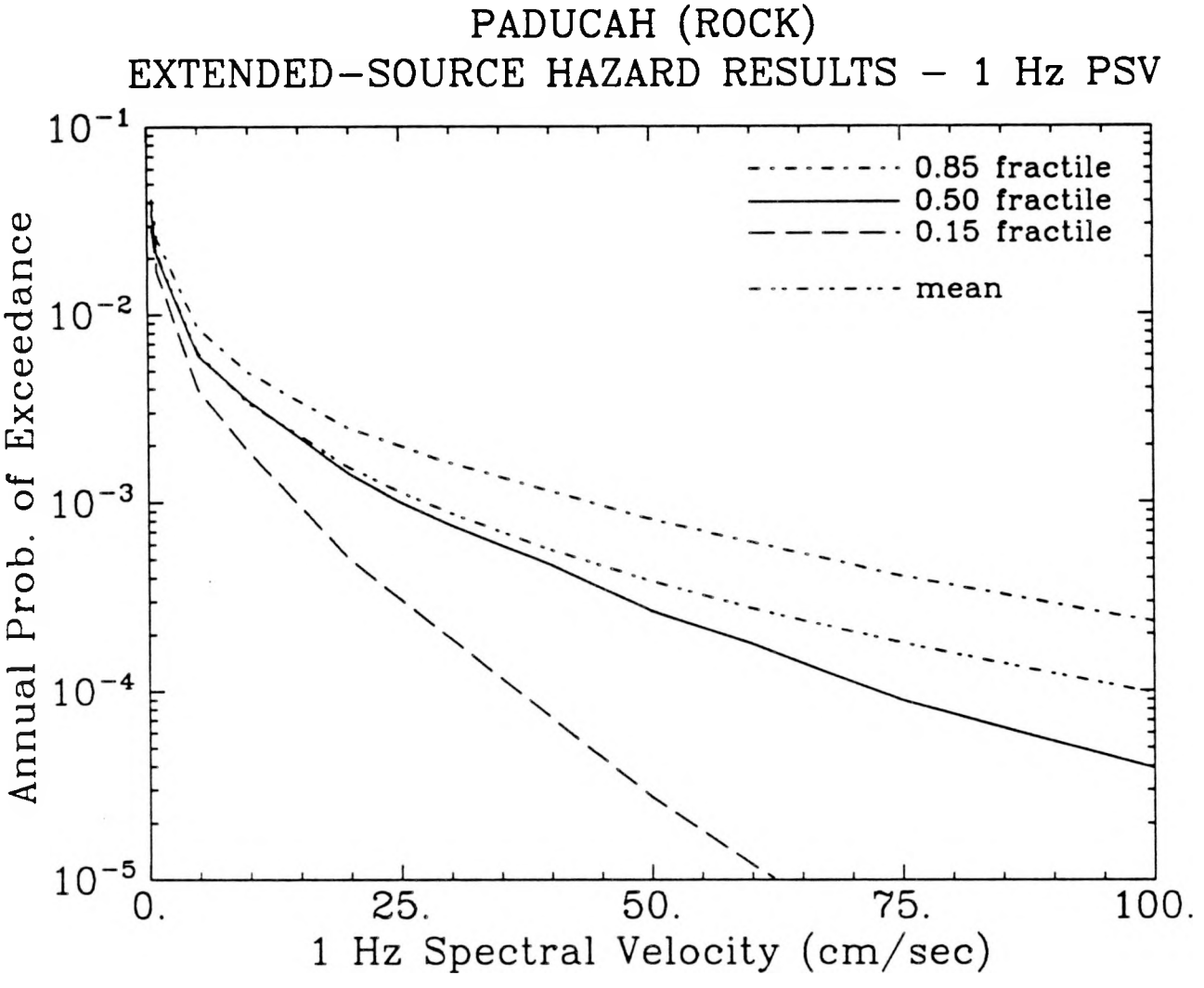

Figure 5-20. 1-Hz spectral velocity hazard curves for Paducah (for rock site conditions) computed from the extended-source hazard analysis.

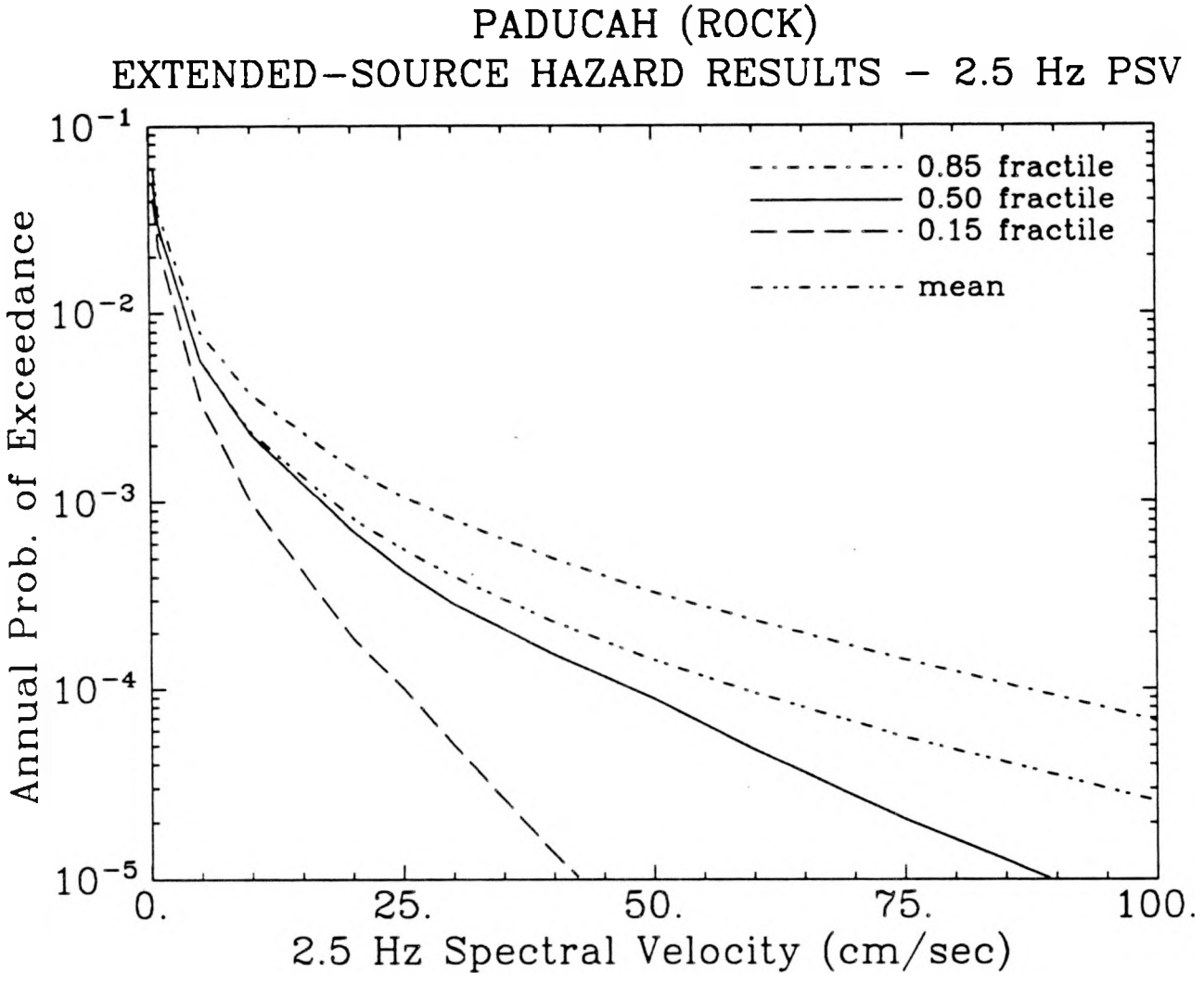

Figure 5-21. 2.5-Hz spectral velocity hazard curves for Paducah (for rock site conditions) computed from the extended-source hazard analysis.

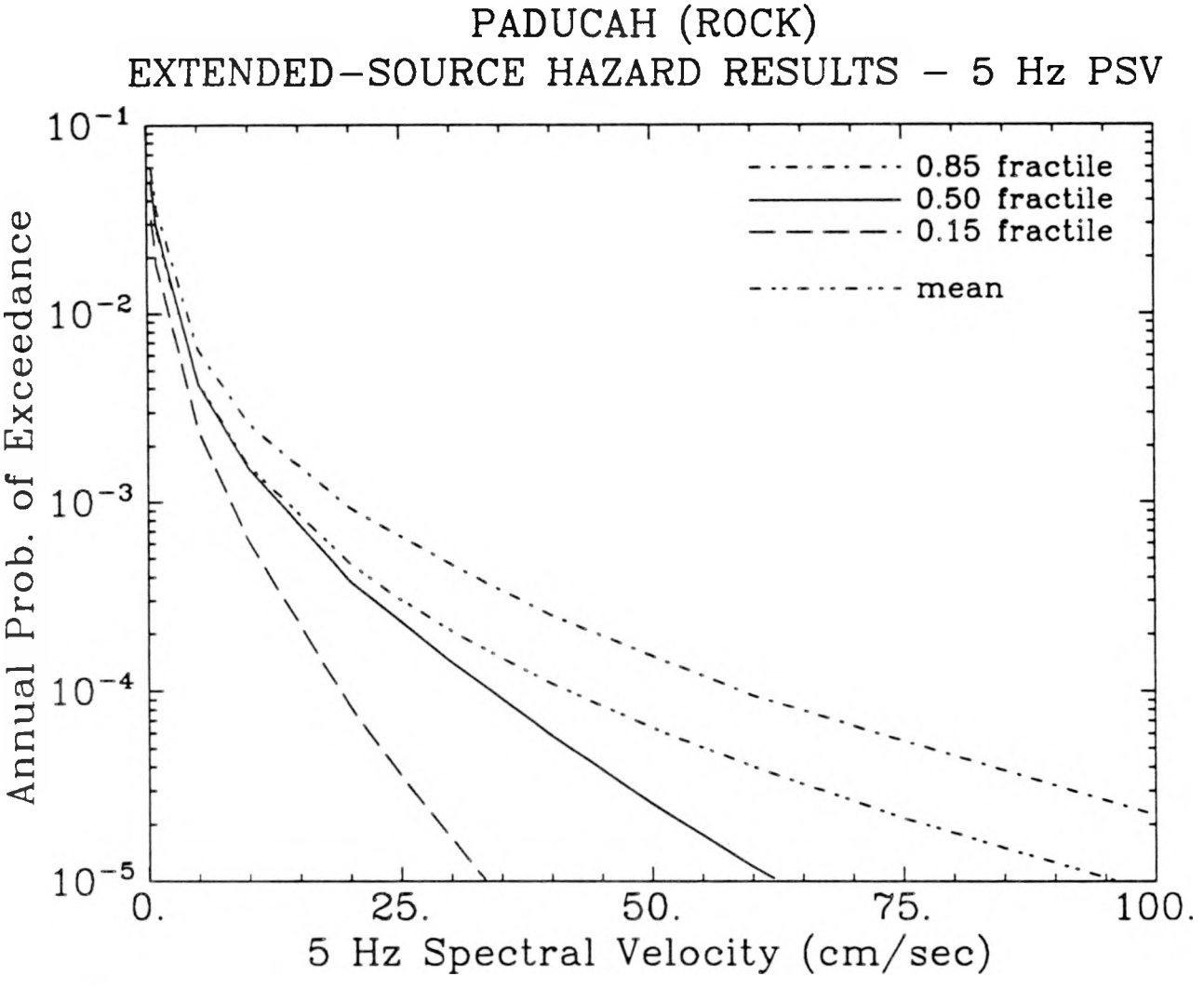

Figure 5-22. 5-Hz spectral velocity hazard curves for Paducah (for rock site conditions) computed from the extended-source hazard analysis.

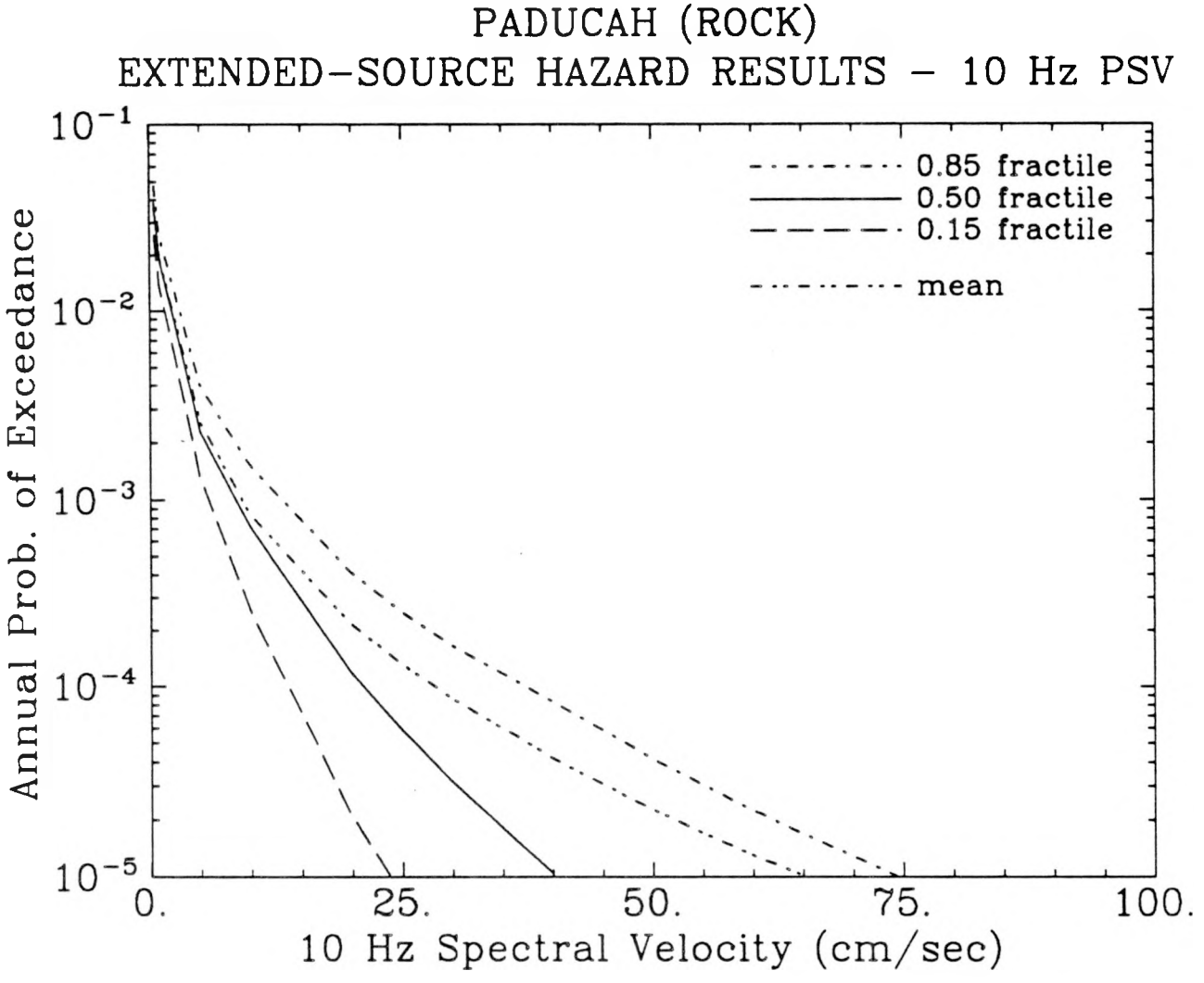

Figure 5-23. 10-Hz spectral velocity hazard curves for Paducah (for rock site conditions) computed from the extended-source hazard analysis.

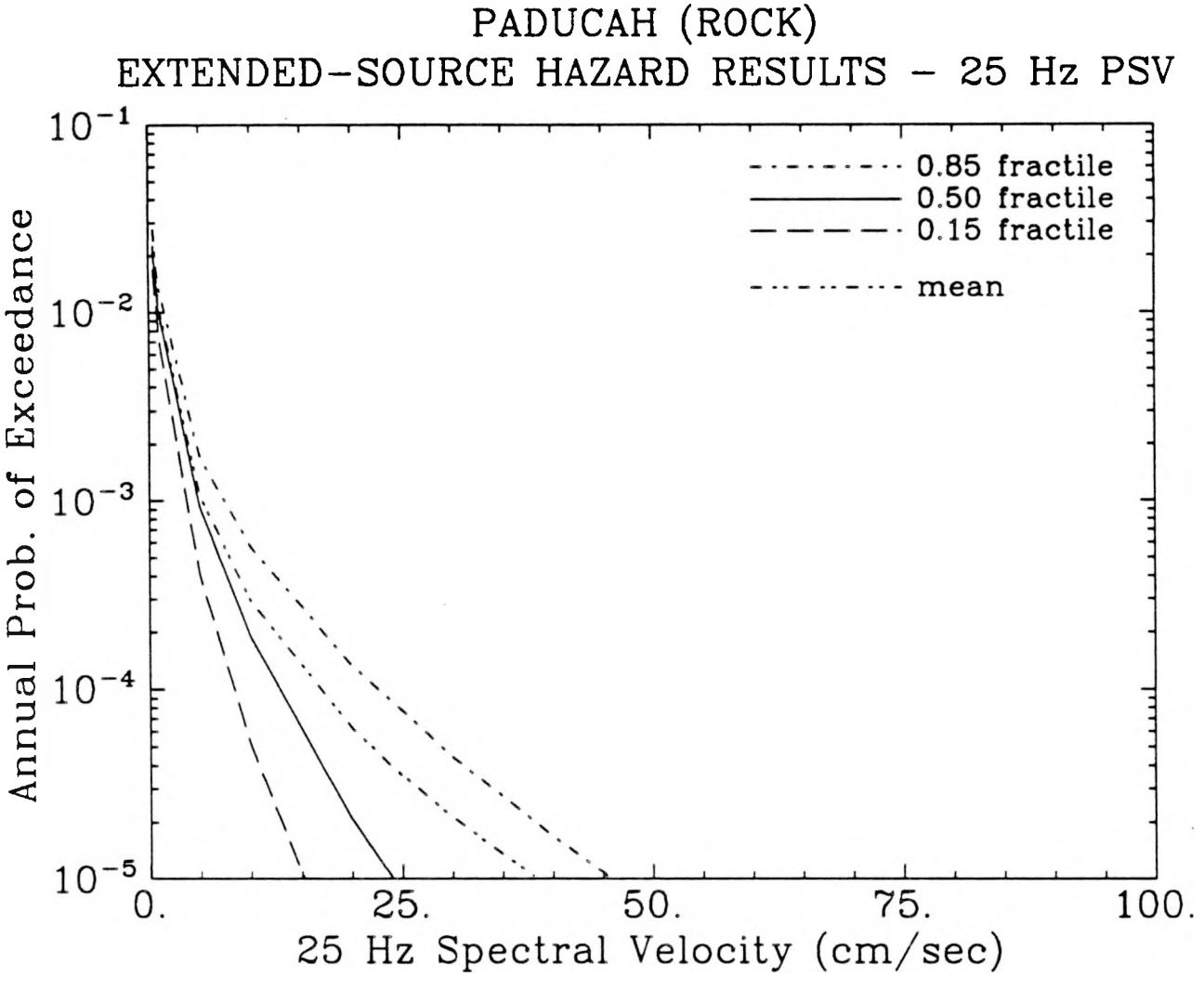

Figure 5-24. 25-Hz spectral velocity hazard curves for Paducah (for rock site conditions) computed from the extended-source hazard analysis.

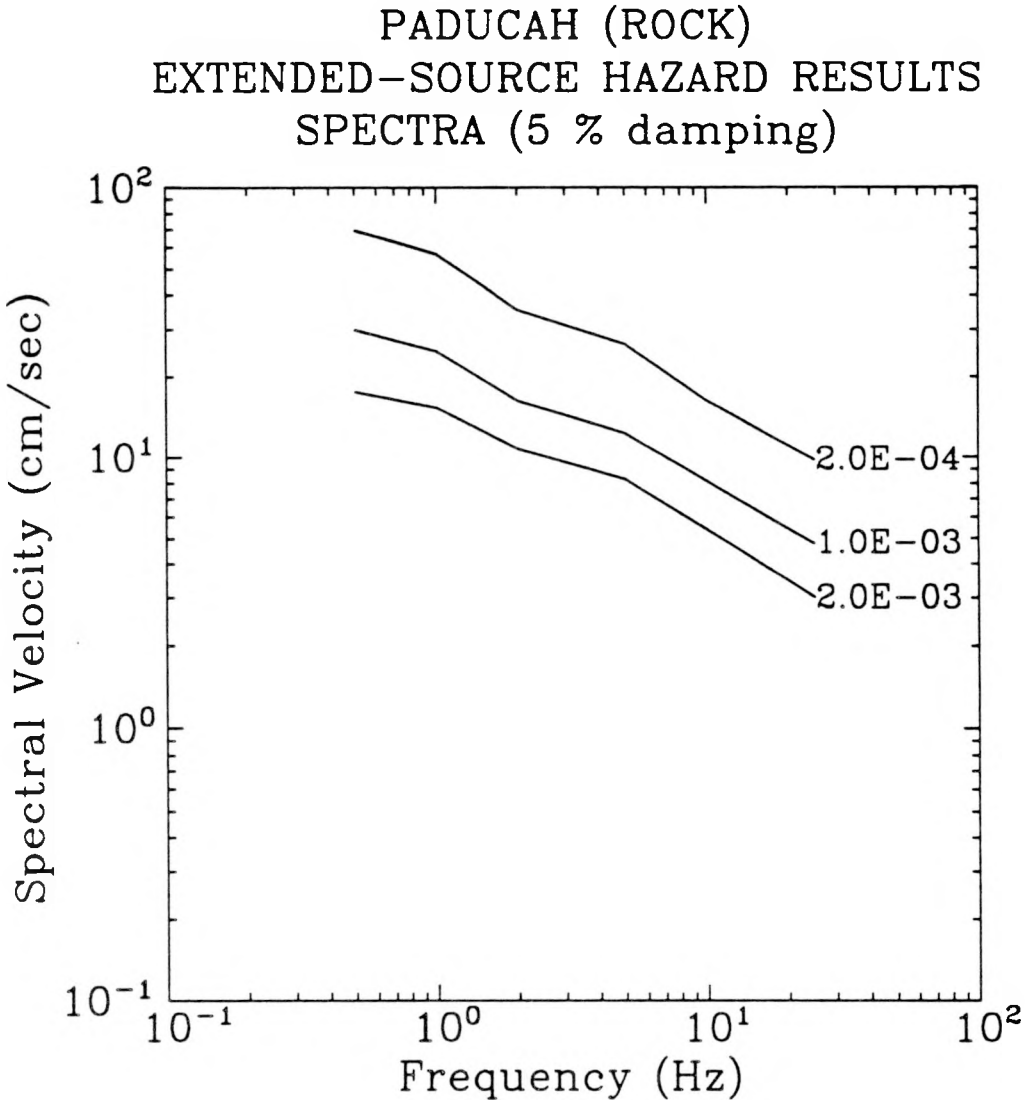

Figure 5-25. Seismic hazard at Paducah (5 % damping; rock site conditions) computed from the extended-source hazard analysis. Results shown as uniform hazard spectra for three values of the annual probability of exceedance.

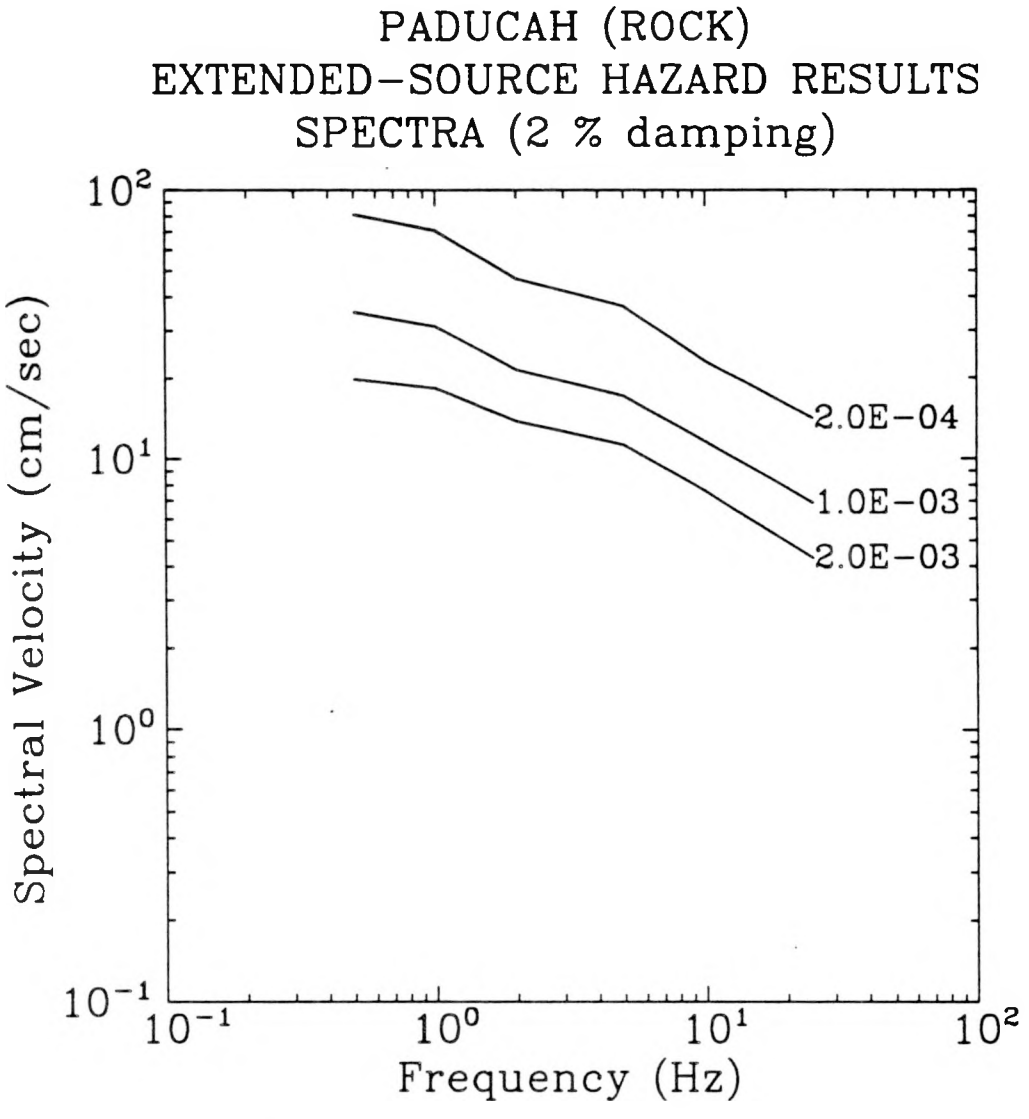

Figure 5-26. Seismic hazard at Paducah (2 % damping; rock site conditions) computed from the extended-source hazard analysis. Results shown as uniform hazard spectra for three values of the annual probability of exceedance.

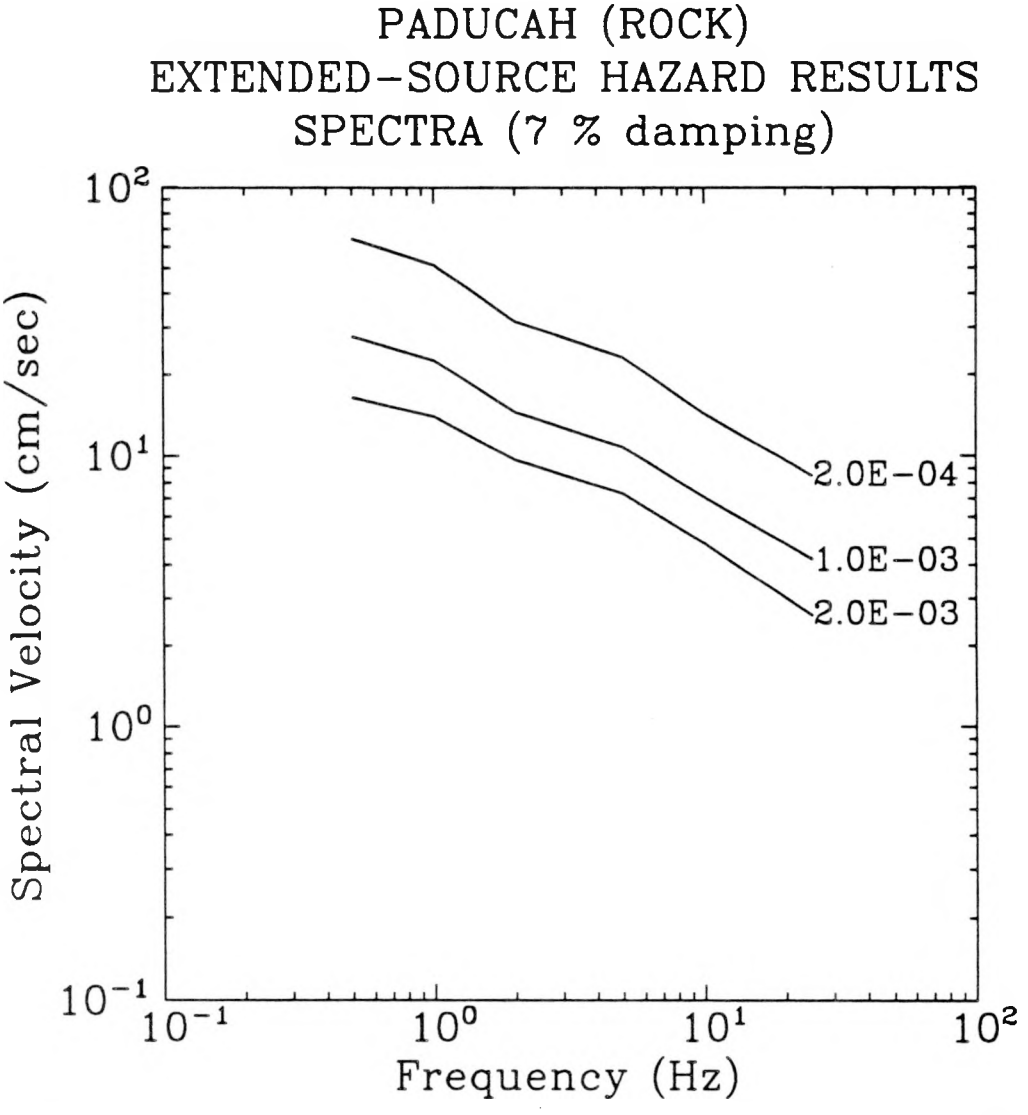

Figure 5-27. Seismic hazard at Paducah (7 % damping; rock site conditions) computed from the extended-source hazard analysis. Results shown as uniform hazard spectra for three values of the annual probability of exceedance.

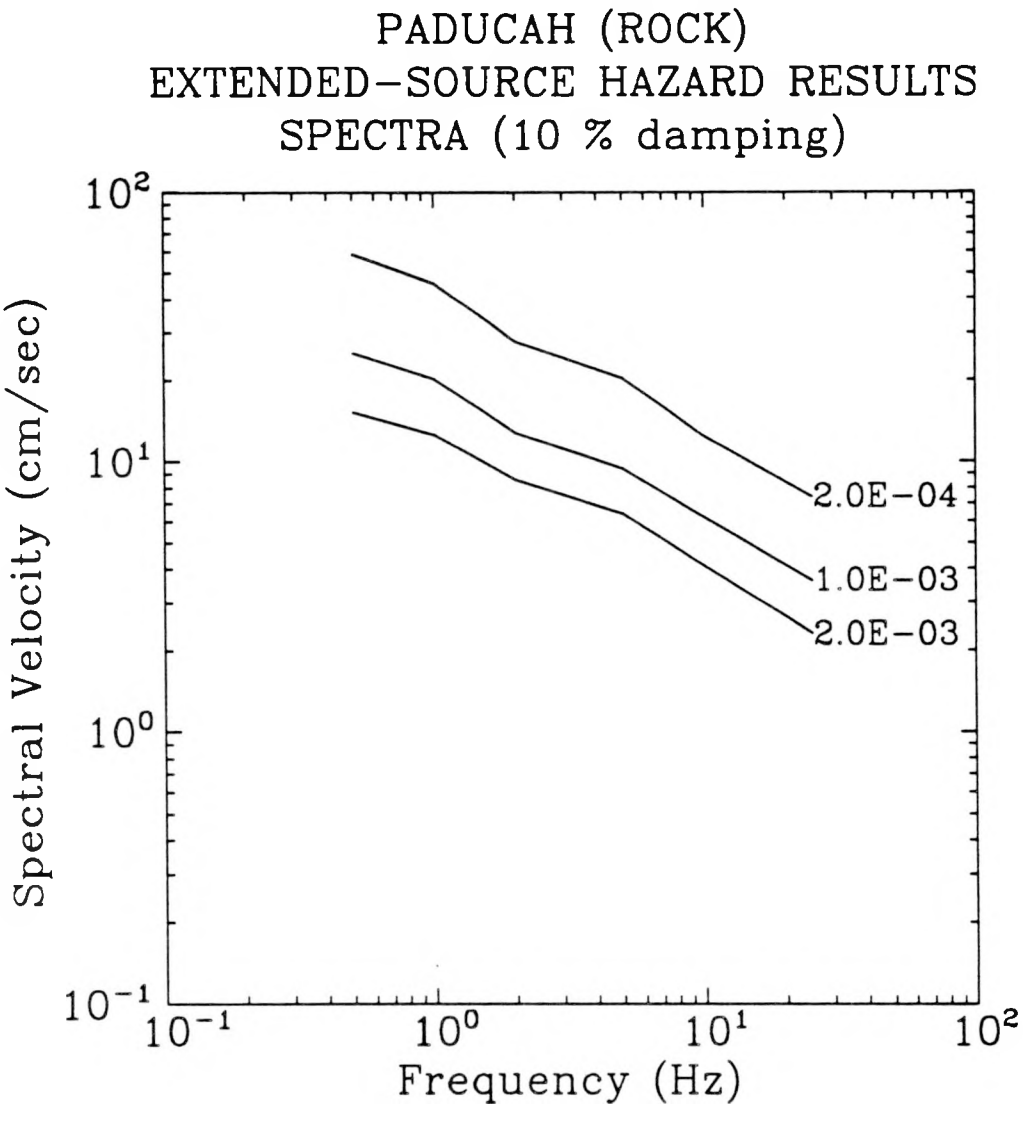

Figure 5-28. Seismic hazard at Paducah (10 % damping; rock site conditions) computed from the extended-source hazard analysis. Results shown as uniform hazard spectra for three values of the annual probability of exceedance.

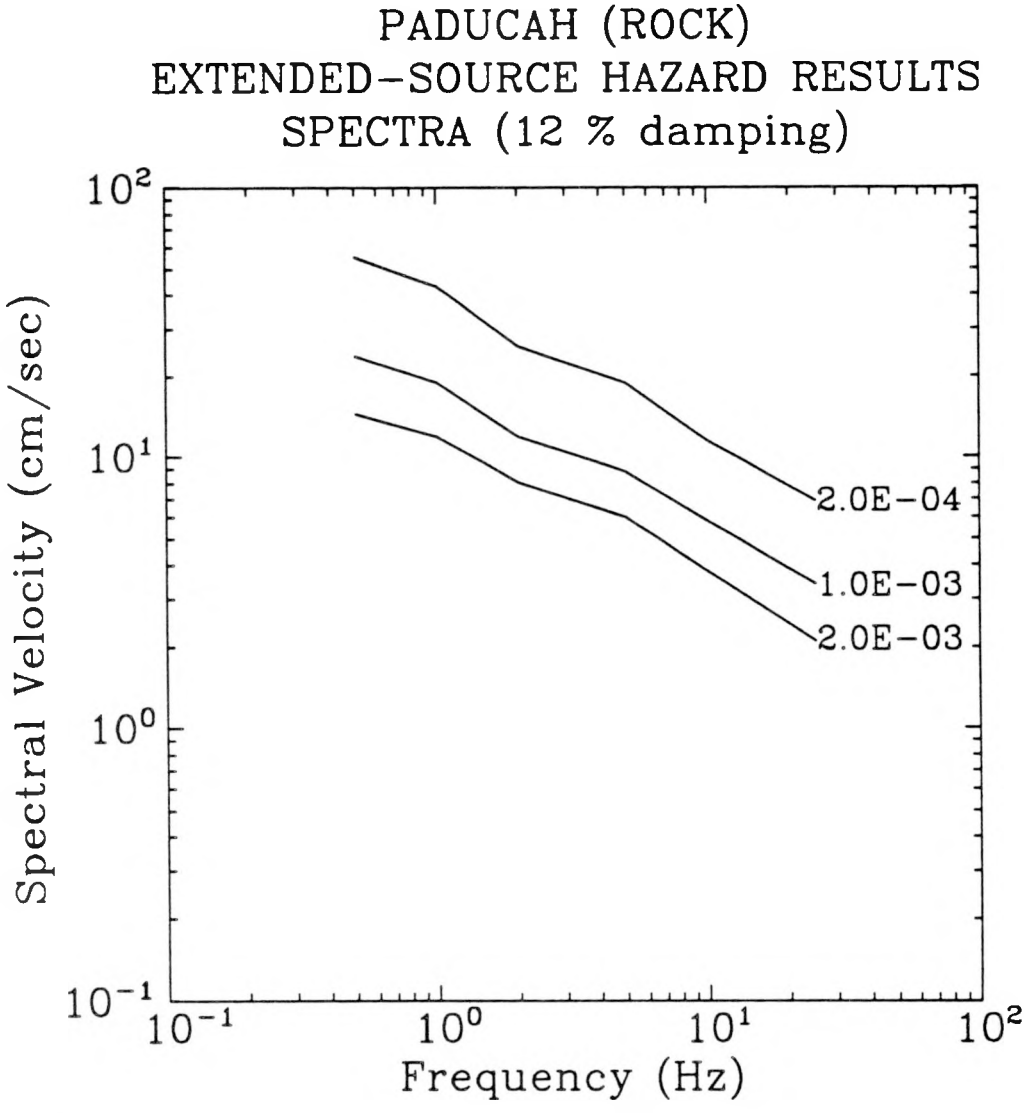

Figure 5-29. Seismic hazard at Paducah (12 % damping; rock site conditions) computed from the extended-source hazard analysis. Results shown as uniform hazard spectra for three values of the annual probability of exceedance.

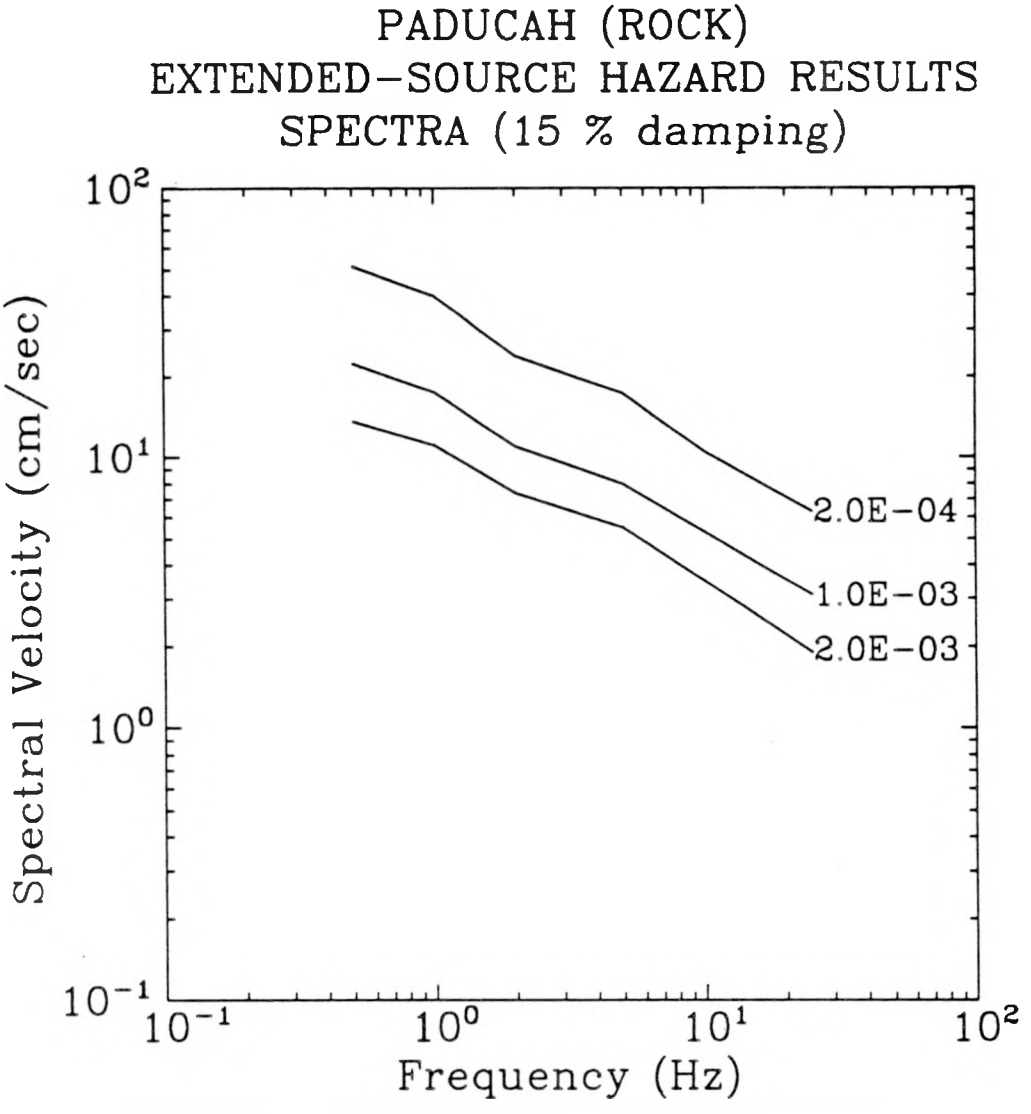

Figure 5-30. Seismic hazard at Paducah (15 % damping; rock site conditions) computed from the extended-source hazard analysis. Results shown as uniform hazard spectra for three values of the annual probability of exceedance.

Section 6

CHARACTERISTICS OF CONTROLLING GROUND MOTIONS

6.1 INTRODUCTION

In this section, we define the characteristics of the earthquake ground motions that dominate the calculated hazard of the Paducah site. For this purpose, we use the seismicity models and attenuation functions developed in Section 5.

In Section 6.2 we calculate the expected magnitude and distance for a given exceedance probability. We then use these magnitude and distance and the spectra obtained in Section 5 to generate artificial ground motions (Section 6.3). Finally, we investigate these characteristic ground motions in terms of the durations of their build-up, strong-motion and decay phases (Section 6.4).

6.2 EXPECTED MAGNITUDE AND DISTANCE

The expected magnitude and distance for a given exceedance probability provide information about the types of earthquakes that dominate the hazard at the site. These two quantities are evaluated as follows:

$$\overline{M}_p = \frac{\sum_k w_k \left[\sum_i \nu_i \iint m P[Y > y_p | m,r] \; f_{M(i)}(m) \; f_{R(i)|M(i)}(r;m) \; dm \; dr \right]_k}{\sum_k w_k \left[\sum_i \nu_i \iint P[Y > y_p | m,r] \; f_{M(i)}(m) \; f_{R(i)|M(i)}(r;m) \; dm \; dr \right]_k} \qquad (6-1)$$

$$\overline{R}_p = \frac{\sum_k w_k \left[\sum_i \nu_i \iint r P[Y > y_p | m,r] \; f_{M(i)}(m) \; f_{R(i)|M(i)}(r;m) \; dm \; dr \right]_k}{\sum_k w_k \left[\sum_i \nu_i \iint P[Y > y_p | m,r] \; f_{M(i)}(m) \; f_{R(i)|M(i)}(r;m) \; dm \; dr \right]_k} \qquad (6-2)$$

where $\sum_k$ indicates summation over all branches of the logic tree of uncertain parameters and assumptions and w_k is the weight associated with branch k. y_p is the ground-motion amplitude associated with a median exceedance probability p. $\sum_i$ indicates summation over all seismic sources. $P[y_p > y|m,r]$ represents the attenuation function, and $f_{M(i)}(m)$ and

$f_{R(i)|M(i)}(r;m)$ represent the distributions of earthquake magnitude and distance[1] in source i. The attenuation function, the activity rate ν_i, and the distributions of magnitude and distance are different for the different branches of the logic tree.

Equations 6–1 and 6–2 indicate that the expected magnitude and distance $\overline{M}_p$ and $\overline{R}_p$ depend on the selected exceedance probability p (through the amplitude y_p) and on the ground-motion measure (through the attenuation function $P[Y > y_p|m,r]$).

We calculate the expected magnitudes and distances using the seismicity models and attenuation functions developed in Section 5 and considering 1-Hz spectral velocity and PGA. Results are presented in Figures 6–1 through 6–8, as functions of ground-motion amplitude and of exceedance probability. Because the frequencies of greatest engineering interest for structures at the Paducah site are 0.5–3.0 Hz (J. Hunt, personal communication, 1990), we use 1-Hz PSV to define the dominant magnitude and distance. Values of dominant magnitude and distance for selected exceedance probabilities are shown in Table 6–1. These results clearly indicate that the New Madrid seismic source dominates the hazard at ground-motion amplitudes of engineering interest.

Table 6-1

Expected Magnitudes and Distances

Median Exceedance Probability (p)	Dominant Magnitude ($\overline{M}_p$)	Dominant Distance ($\overline{R}_p$)
2×10^{-3}	7.1	65
1×10^{-3}	7.3	52
2×10^{-4}	7.3	38

6.3 ARTIFICIAL GROUND MOTIONS

We use the extended-source ground-motion model of Appendix A to generate artificial ground motions that represent the dominant event (as characterized by the expected magnitude and distance), and envelope the corresponding uniform-hazard spectra. We consider a rupture-site geometry where the northern end of the rupture is closest to the site and the line from the site to the northern end makes a 135° angle with the rupture. This is the most likely

[1] We use a conditional probability distribution of distance given magnitude (i.e., $f_{R(i)|M(i)}(r;m)$), because the distribution of distance is affected by rupture length.

geometry because most configurations of the New Madrid source zone do not extend to the site (see Section 5). We also assume that the epicenter is located in the middle of the rupture.

In order to obtain spectra with shapes close to the target spectra, we make small modifications to the parameters used in Appendix A. Then, we scale the records in order to meet the enveloping requirements in the NRC Standard Review Plan (1), for damping ratios of 2, 5, 7, 10, and 12%.

Ground motions are generated for two horizontal components and for the vertical component. These three ground motions are independent of each other. The target spectra for the vertical component are taken as 2/3 the horizontal spectra. This is standard practice and is permitted by the NRC Standard Review Plan (1). A recent study on the amplitude of vertical ground motions (2) finds that the ratio of 2/3 is adequate, except for distances shorter than 20 km and very large magnitudes ($M \simeq 8$). Because the dominant ground motions at Paducah are associated with distances larger than 20 km, the vertical/horizontal ratio of 2/3 is appropriate.

We generated artificial ground motions for median exceedance probabilities of 2×10^{-3} (500 years), 10^{-3} (1000 years), and 2×10^{-4} (5000 years. The resulting artificial ground motions and their response spectra are shown in Figures 6–9 through 6–26.

6.4 DURATION CHARACTERISTICS

We determine the duration characteristics of the dominant ground motions at Paducah by examining the artificial ground motions generated in Section 6.3. These duration characteristics are related to the ground-motion model of Appendix A and depend on magnitude, distance, and orientation of the rupture relative to the site. Due to the large magnitude and short distance of the dominant earthquake, duration characteristics are controlled by rupture-site orientation, location of the hypocenter, and duration of the rupture process during the earthquake.

We obtain the rise time, strong-motion duration, and decay time by examining the records and the normalized cumulative energy plots[2] shown in Figures 6–27 through 6–29. The tran-

[2]The normalized cumulative energy is defined as

$$\frac{\int_0^t a^2(\tau)d\tau}{\int_0^\infty a^2(\tau)d\tau}$$

where t represents time and $a(t)$ represents the acceleration time history. The plot of normalized cumulative energy as a function of time is sometimes called the Husid plot.

sitions between the build-up, strong motion, and decay phases are associated with changes in slope on the cumulative energy plot. We have doubled the decay time calculated from the records because the ground-motion simulation procedure in Appendix A does not include the effects of scatter and surface waves. These two phenomena contribute substantially to the duration of the decay phase. We also compute the number of strong-motion cycles by counting the number of zero up-crossings during the strong-motion phase. Results are presented in Table 6–2.

Table 6-2

Duration of Characteristic Ground Motions

Return Period (years)	Rise Time (sec)	Strong Motion Duration (sec)	Decay Time (sec)	Total Duration (sec)	No. of Strong-Motion Cycles
500	1	5.5	4	10.5	99
1000	1	8	6	15	144
5000	1	8	6	15	135

The durations in Table 6–2 are somewhat shorter than those of California records of similar magnitudes, because we have used higher stress drop (hence, shorter ruptures) to generate the artificial ground motions.

6.5 REFERENCES

1. *Standard Review Plan, Revision 1.* NUREG-0800, Nuclear Regulatory Commission, Office of Nuclear Reactor Regulation, July 1981.

2. N. A. Abrahamson and J. J. Litehiser. "Attenuation of Vertical Peak Ground Acceleration". *Bulletin of the Seismological Society of America*, 79(3):549–580, 1989.

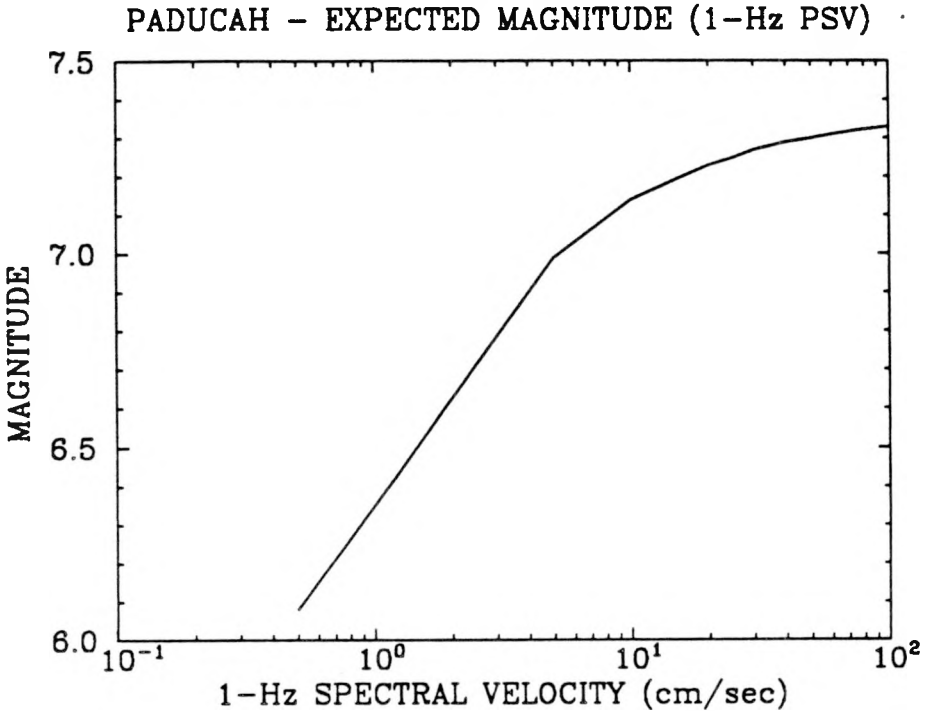

Figure 6-1. Magnitude of earthquakes that dominate the hazard for 1-Hz spectral velocity. Results shown as a function of amplitude.

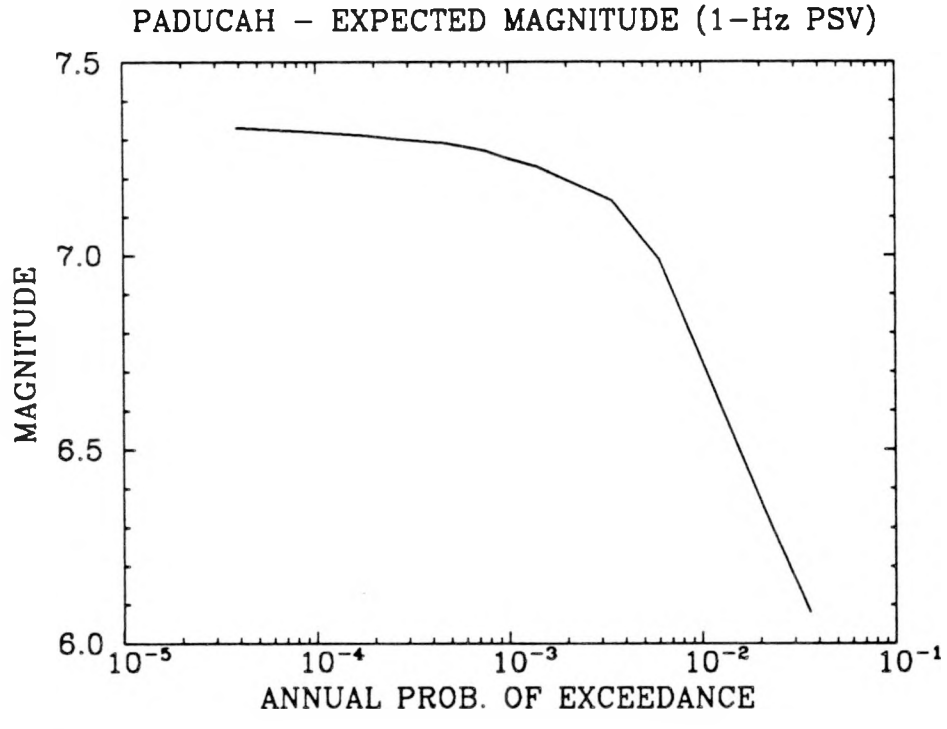

Figure 6-2. Magnitude of earthquakes that dominate the hazard for 1-Hz spectral velocity. Results shown as a function of hazard.

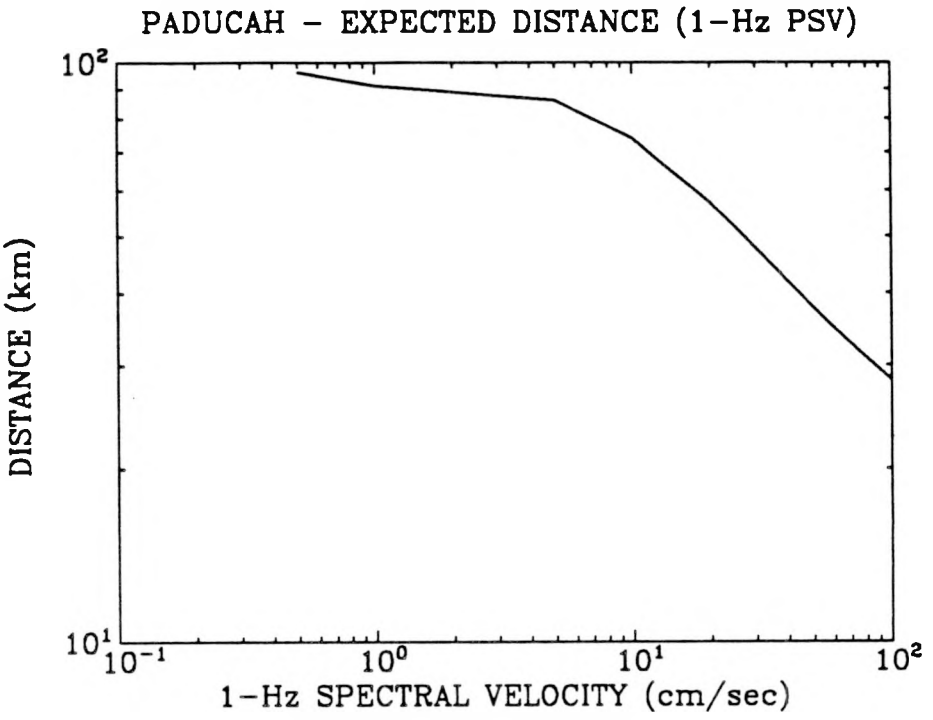

Figure 6-3. Distance of earthquakes that dominate the hazard for 1-Hz spectral velocity. Results shown as a function of amplitude.

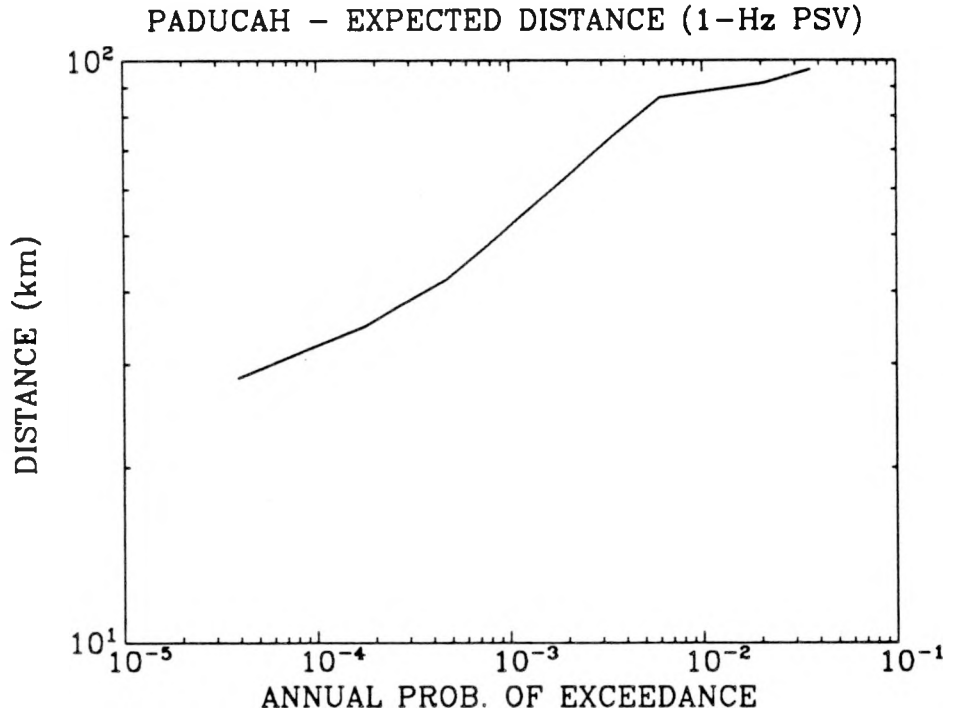

Figure 6-4. Distance of earthquakes that dominate the hazard for 1-Hz spectral velocity. Results shown as a function of hazard.

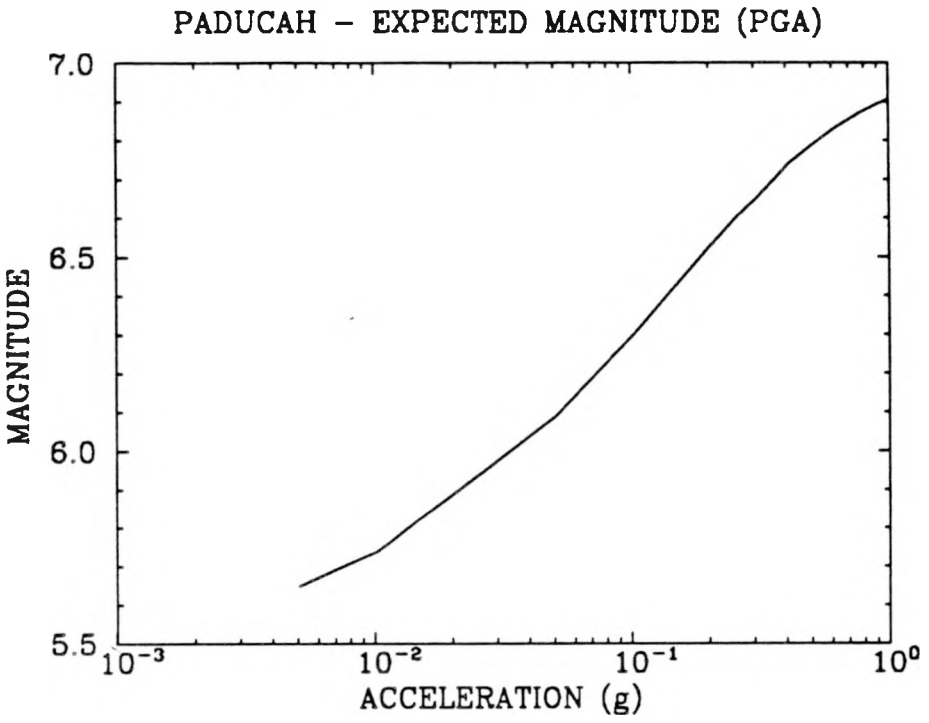

Figure 6-5. Magnitude of earthquakes that dominate the hazard for peak acceleration. Results shown as a function of amplitude.

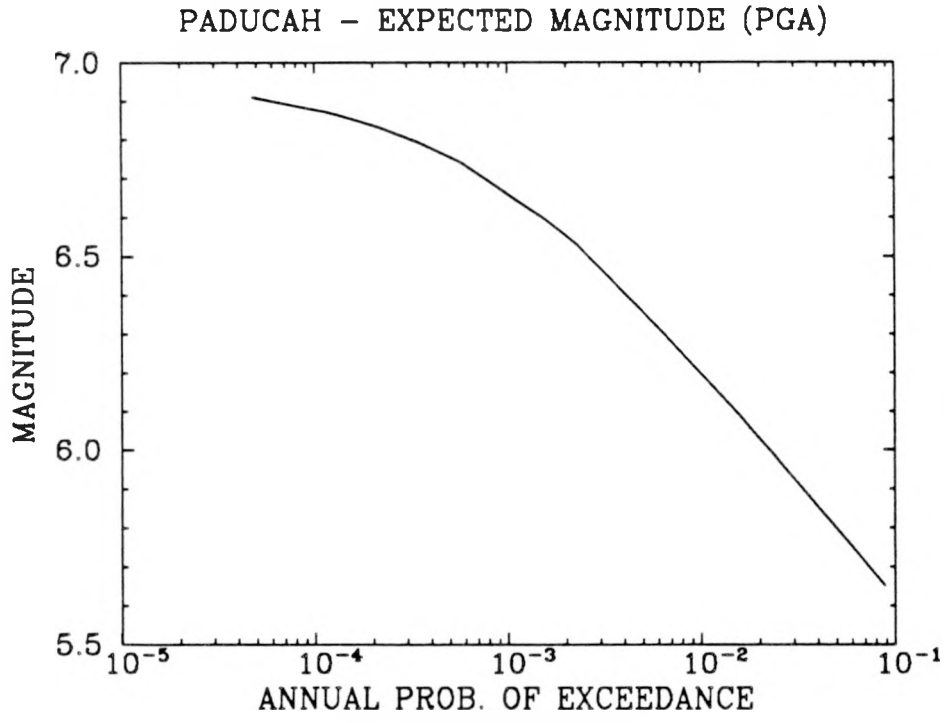

Figure 6-6. Magnitude of earthquakes that dominate the hazard for peak acceleration. Results shown as a function of hazard.

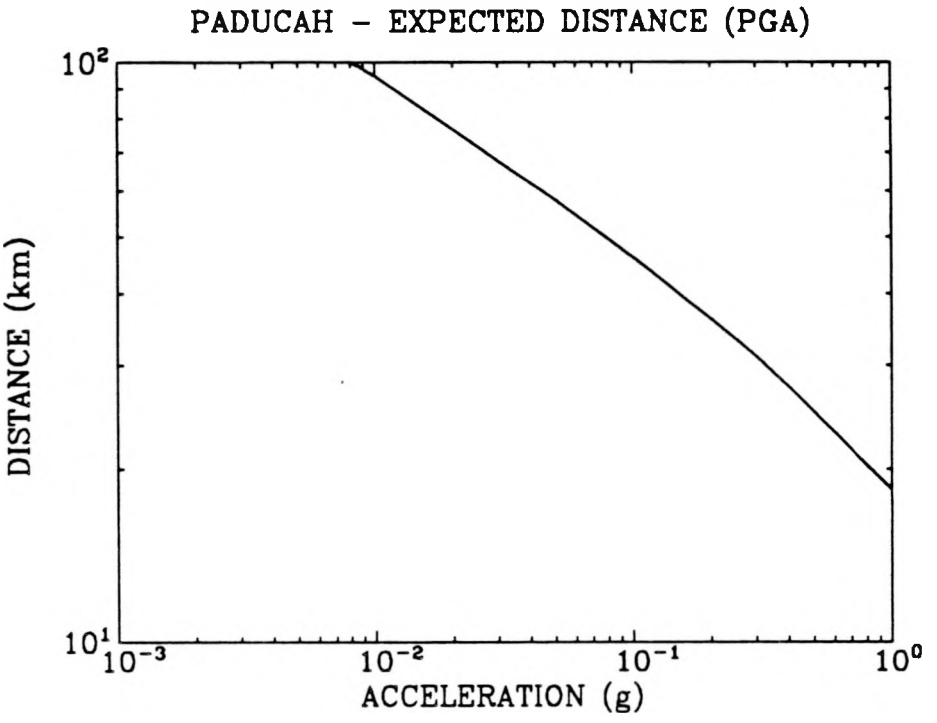

Figure 6-7. Distance of earthquakes that dominate the hazard for peak acceleration. Results shown as a function of amplitude.

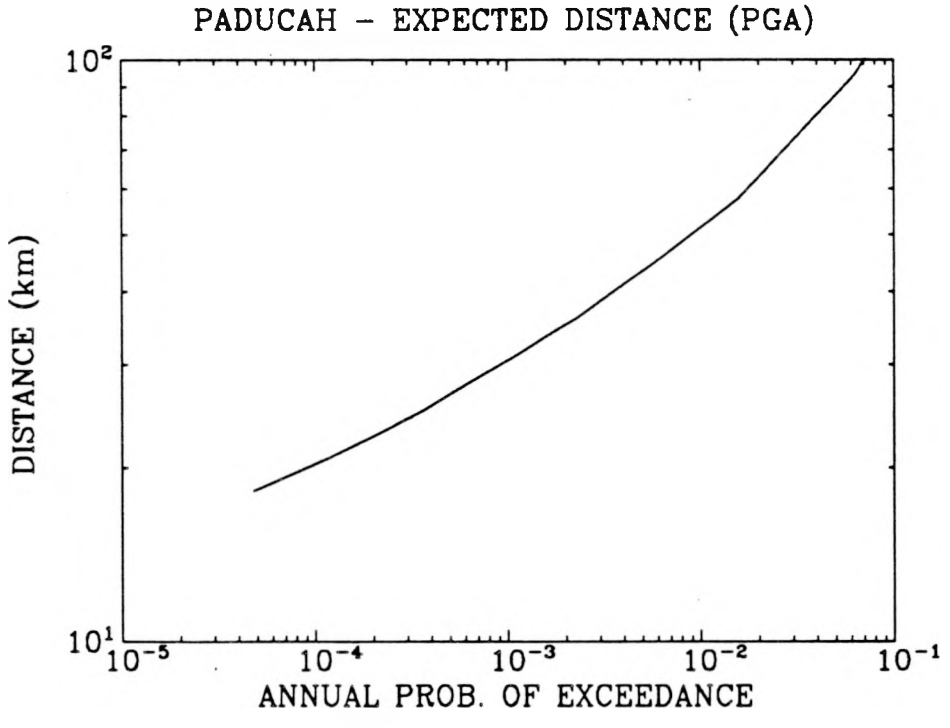

Figure 6-8. Distance of earthquakes that dominate the hazard for peak acceleration. Results shown as a function of hazard.

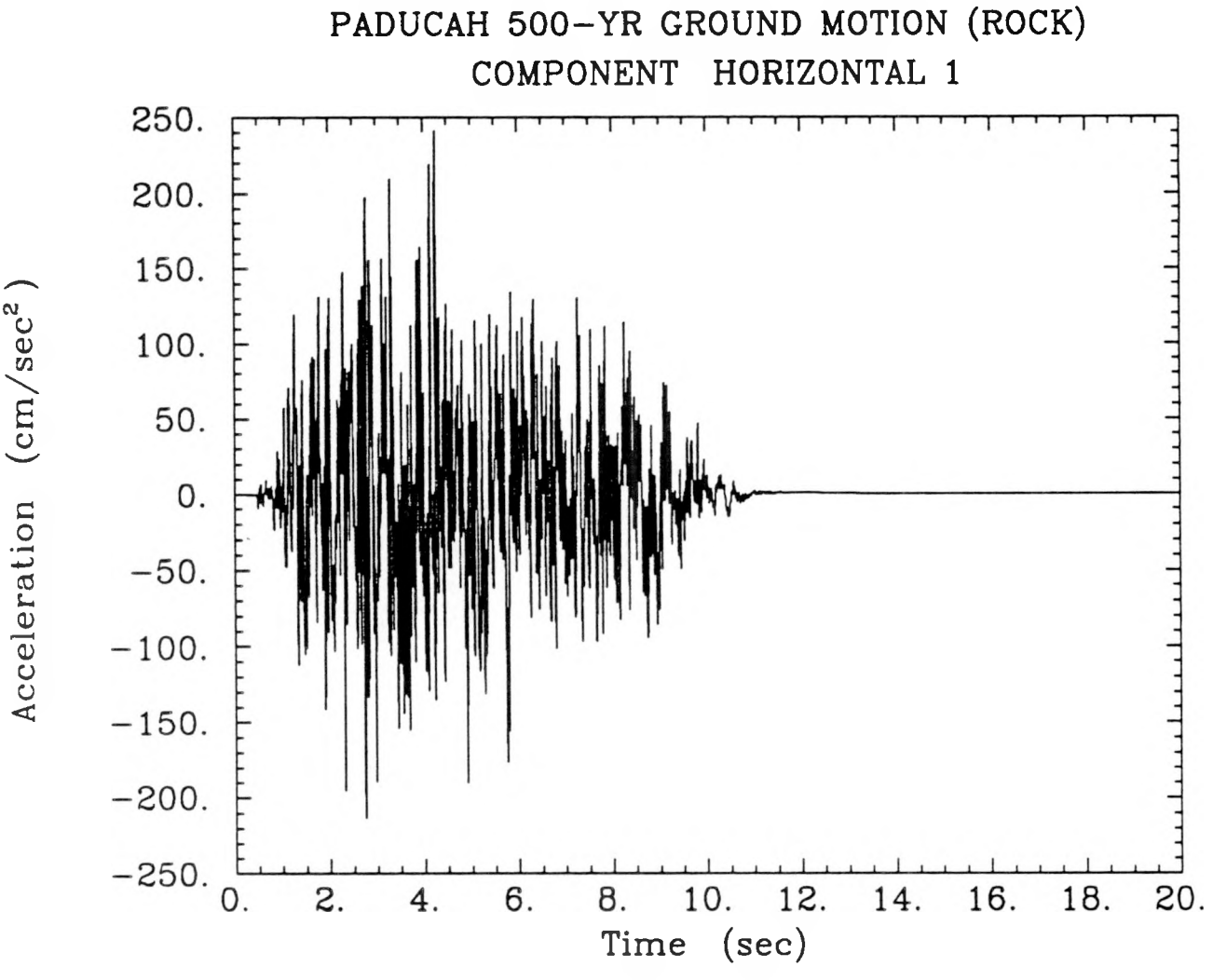

Figure 6-9. Artificial time history for a return period of 500 years; first horizontal component.

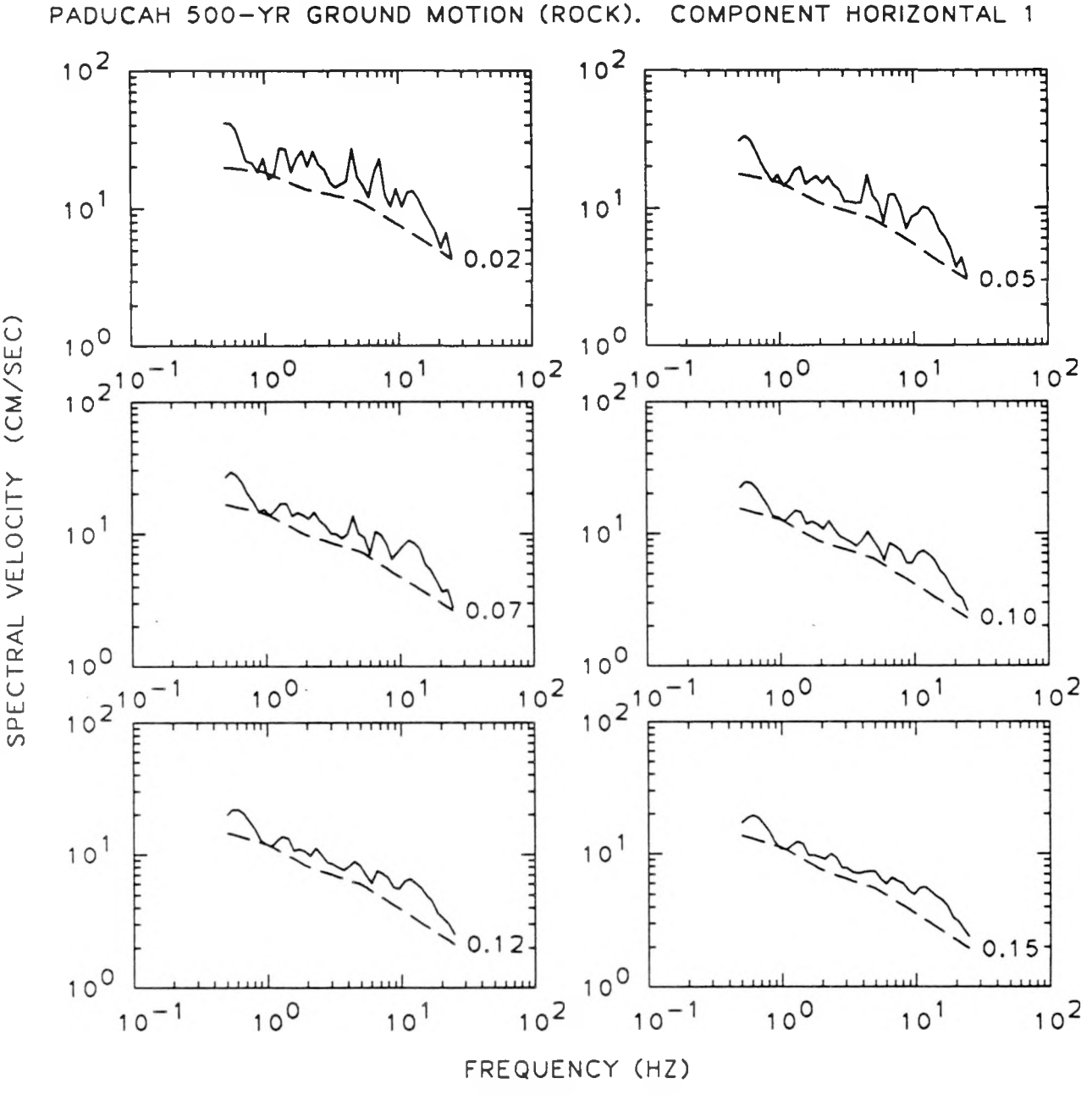

Figure 6-10. Response spectra from artificial time history for a return period of 500 years; first horizontal component. Spectra are shown for six values of damping ratio. Solid lines: response spectra; dashed lines: uniform-hazard spectra.

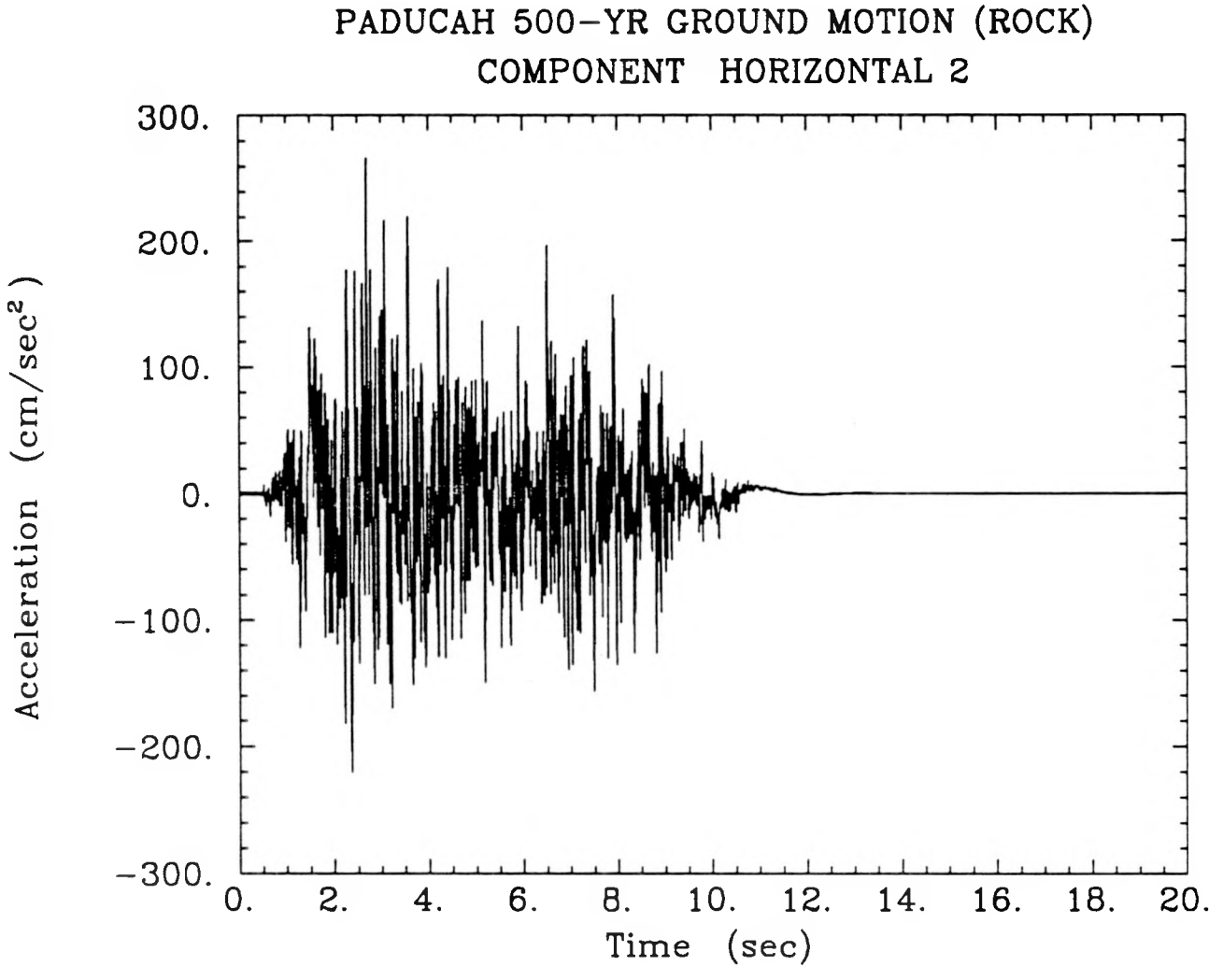

Figure 6-11. Artificial time history for a return period of 500 years; second horizontal component.

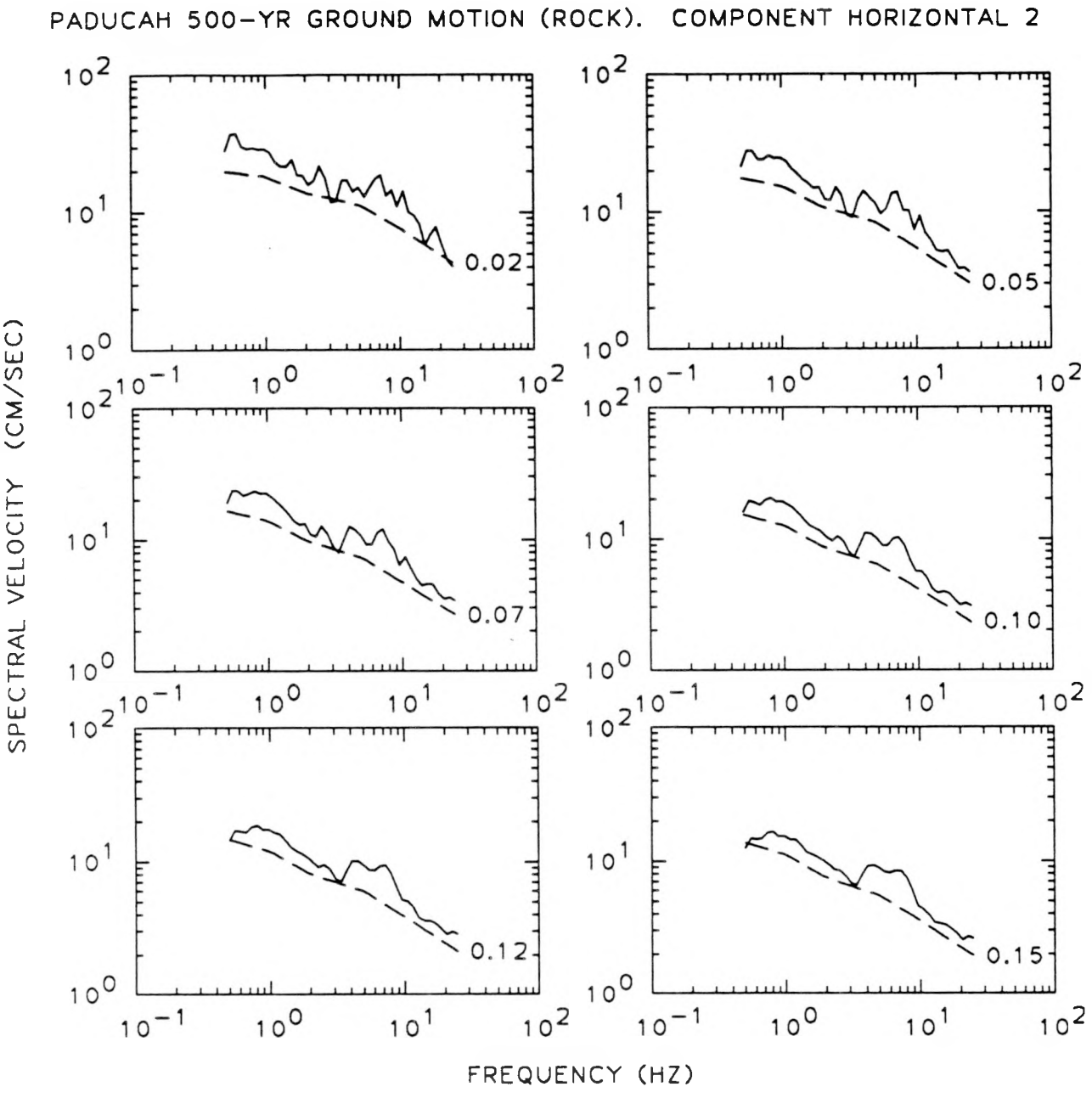

Figure 6-12. Response spectra from artificial time history for a return period of 500 years; second horizontal component. Spectra are shown for six values of damping ratio. Solid lines: response spectra; dashed lines: uniform-hazard spectra.

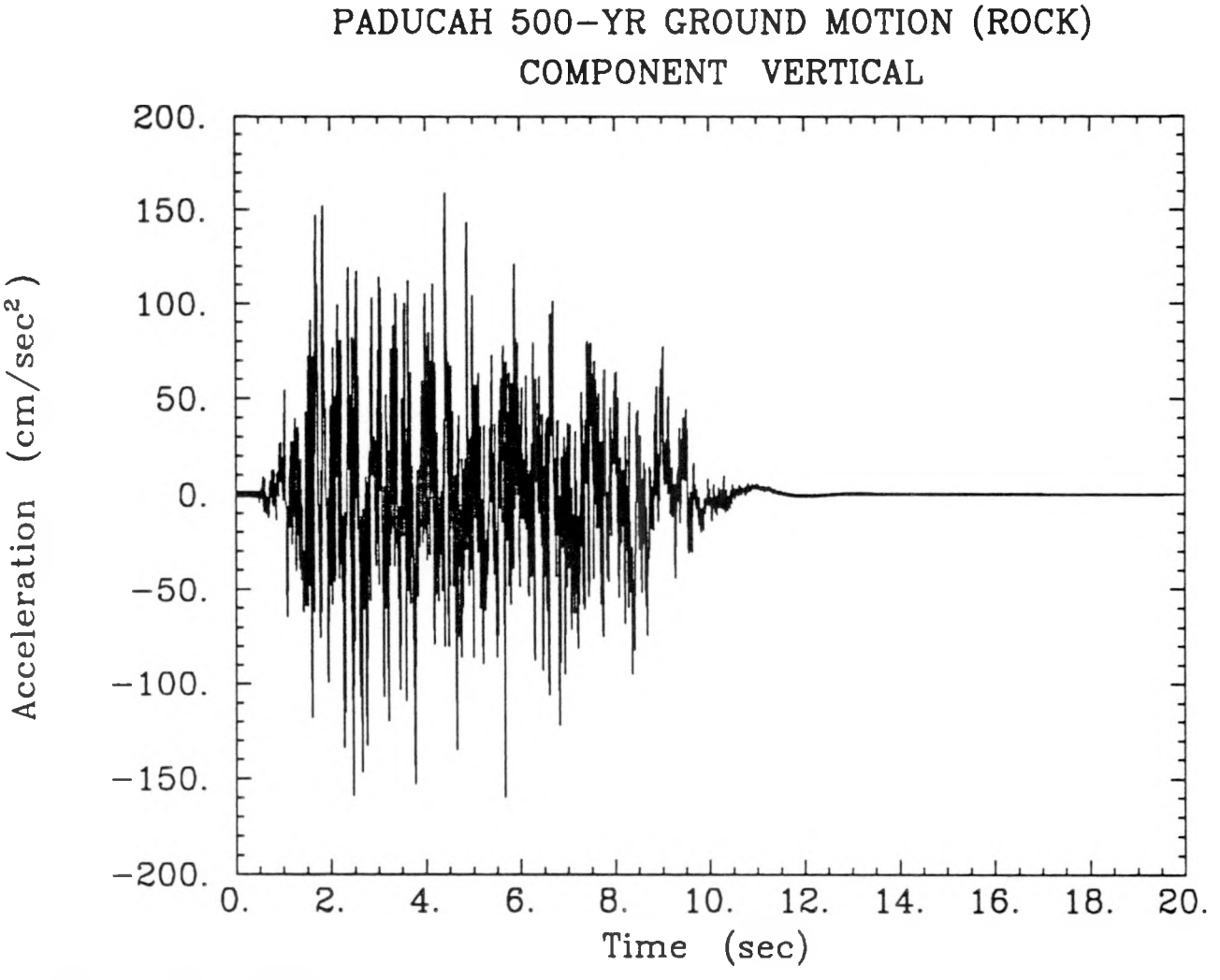

Figure 6-13. Artificial time history for a return period of 500 years; vertical component.

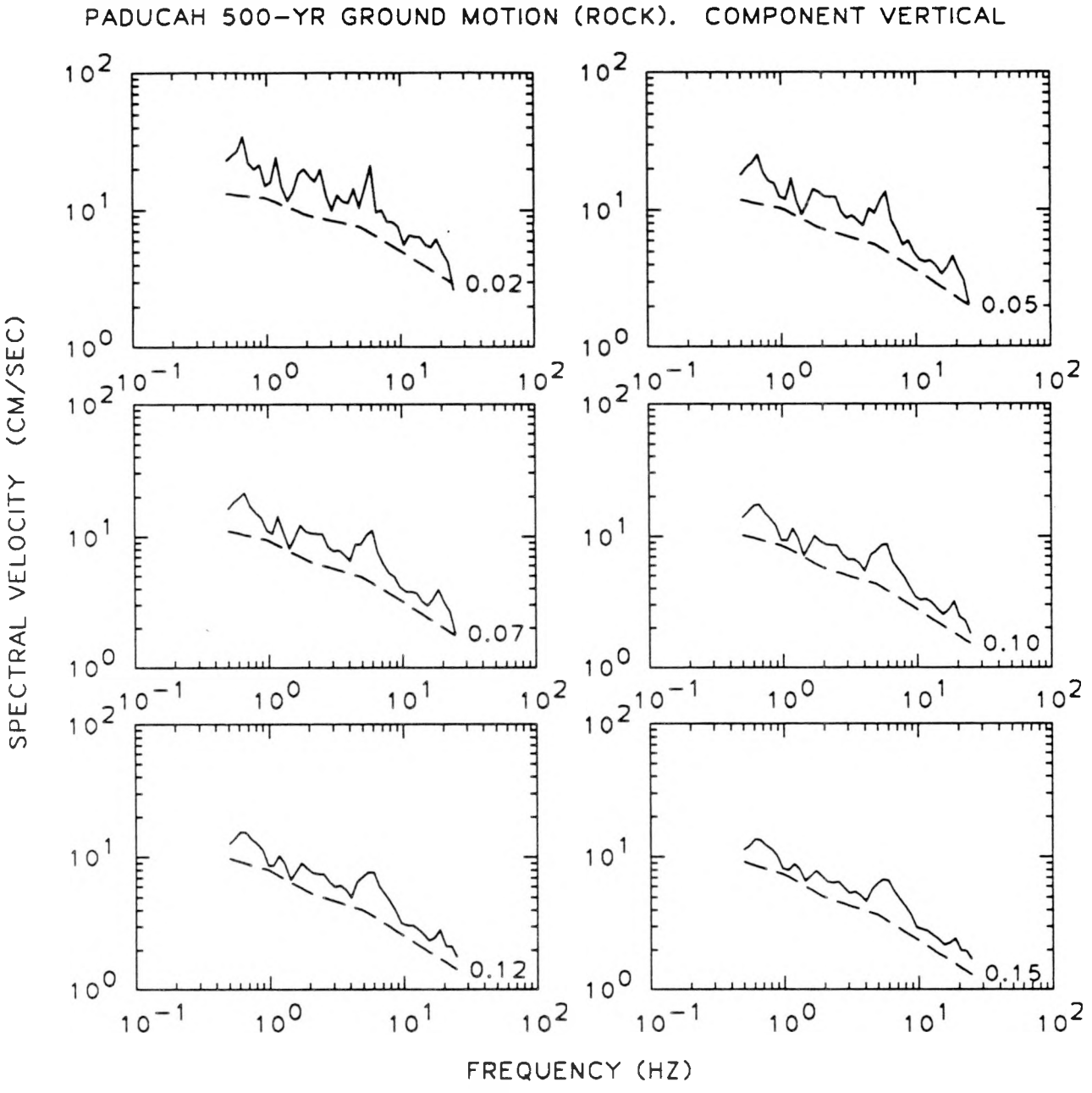

Figure 6-14. Response spectra from artificial time history for a return period of 500 years; vertical component. Spectra are shown for six values of damping ratio. Solid lines: response spectra; dashed lines: uniform-hazard spectra.

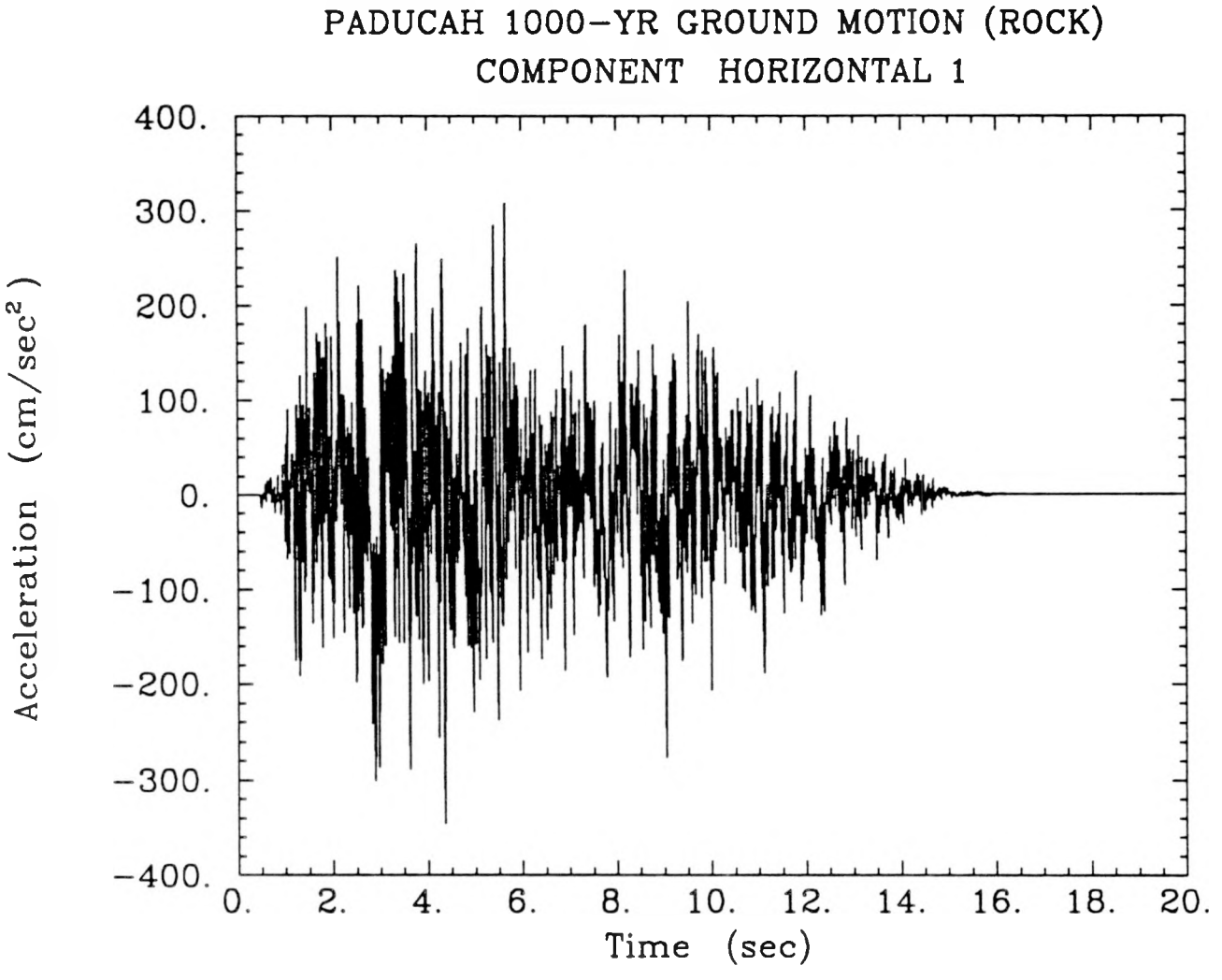

Figure 6-15. Artificial time history for a return period of 1000 years; first horizontal component.

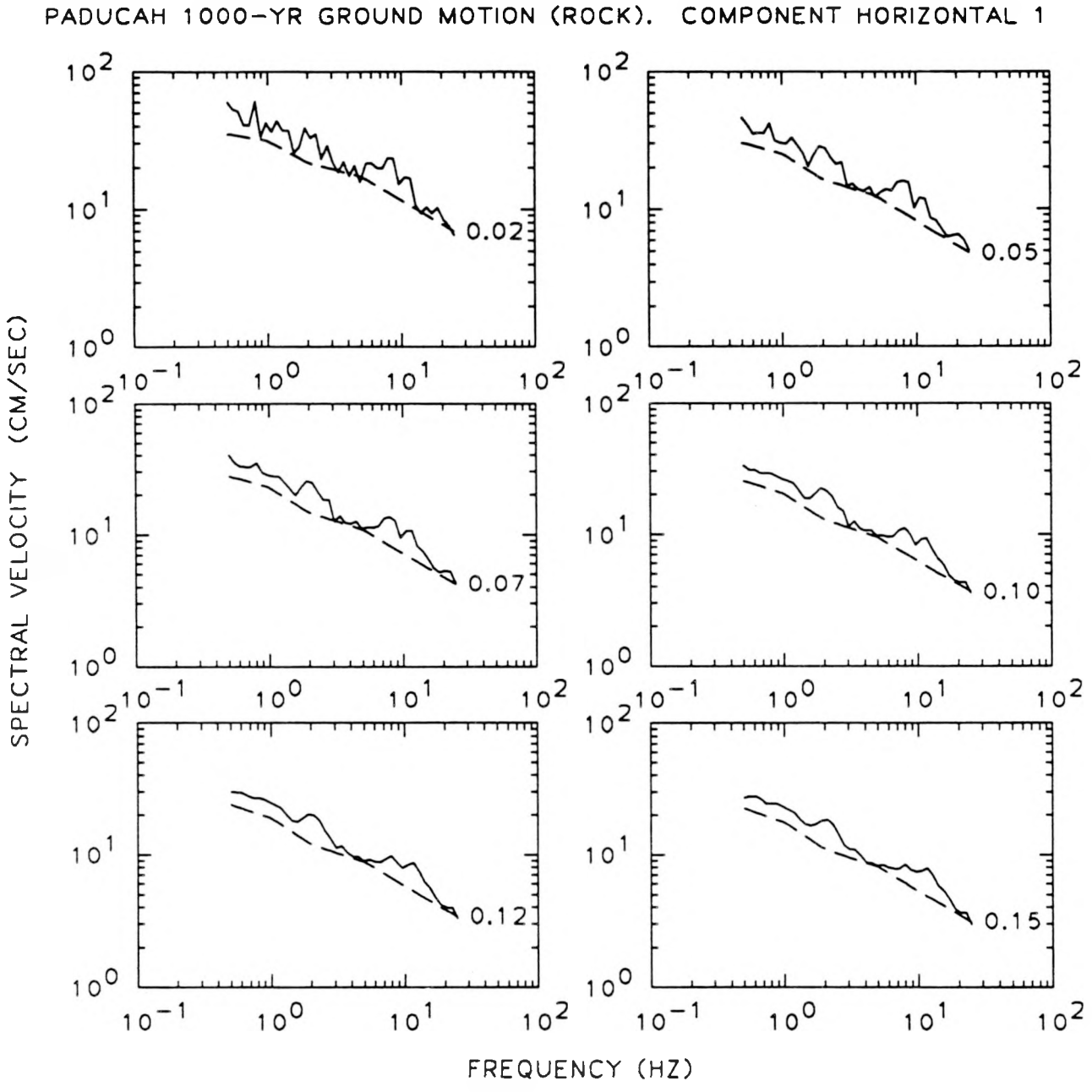

Figure 6-16. Response spectra from artificial time history for a return period of 1000 years; first horizontal component. Spectra are shown for six values of damping ratio. Solid lines: response spectra; dashed lines: uniform-hazard spectra.

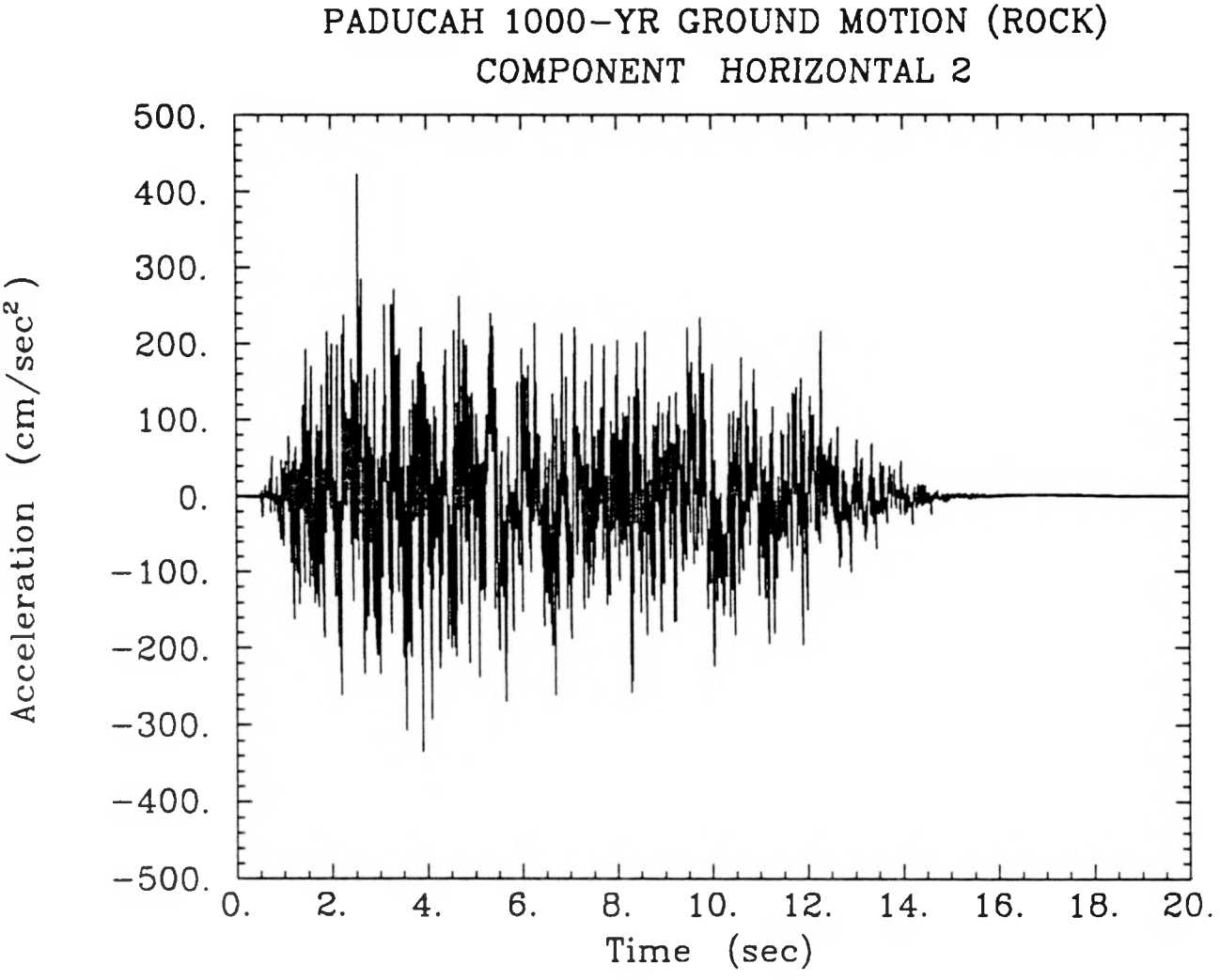

Figure 6-17. Artificial time history for a return period of 1000 years; second horizontal component.

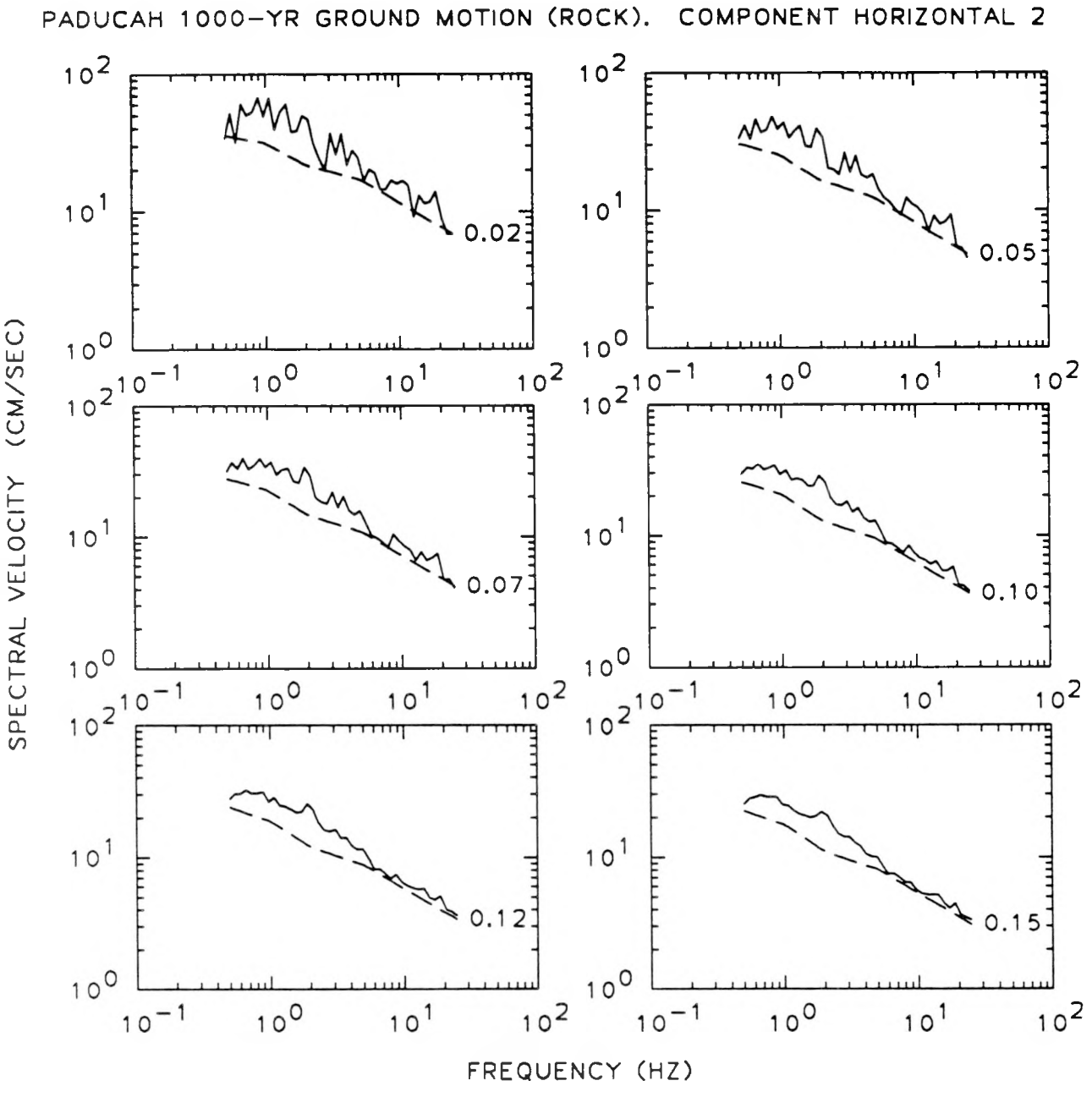

Figure 6-18. Response spectra from artificial time history for a return period of 1000 years: second horizontal component. Spectra are shown for six values of damping ratio. Solid lines: response spectra; dashed lines: uniform-hazard spectra.

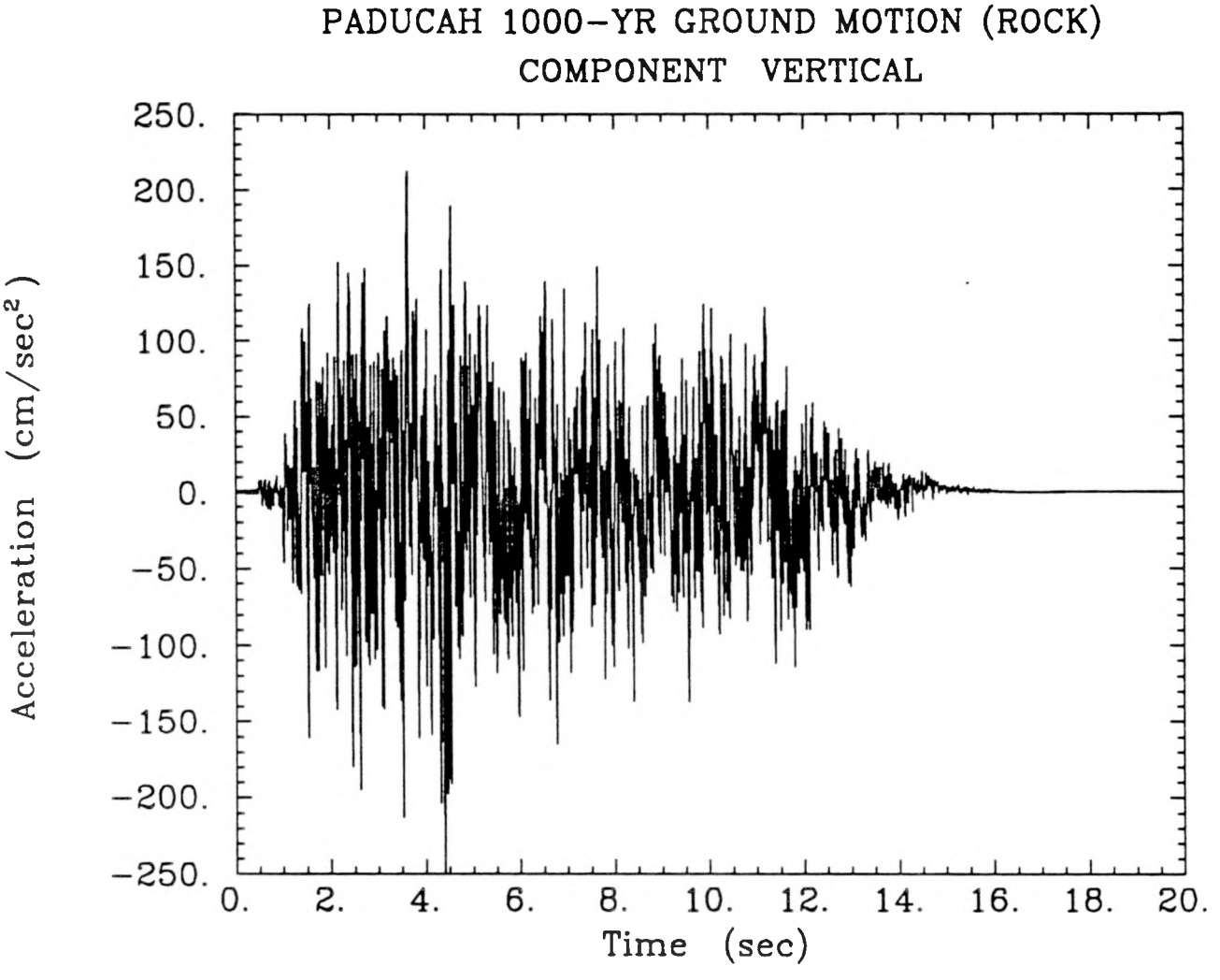

Figure 6-19. Artificial time history for a return period of 1000 years; vertical component.

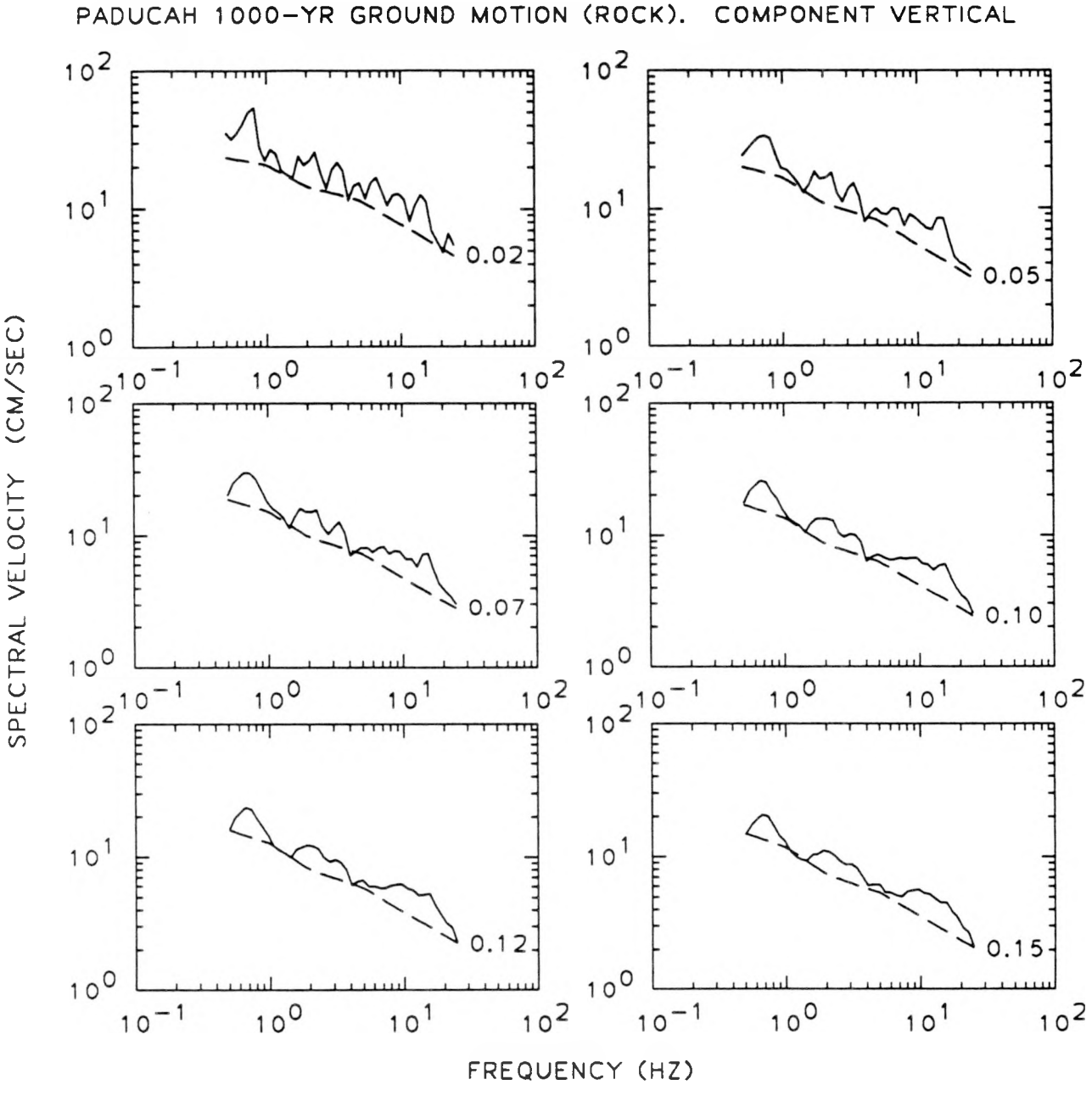

Figure 6-20. Response spectra from artificial time history for a return period of 1000 years; vertical component. Spectra are shown for six values of damping ratio. Solid lines: response spectra; dashed lines: uniform-hazard spectra.

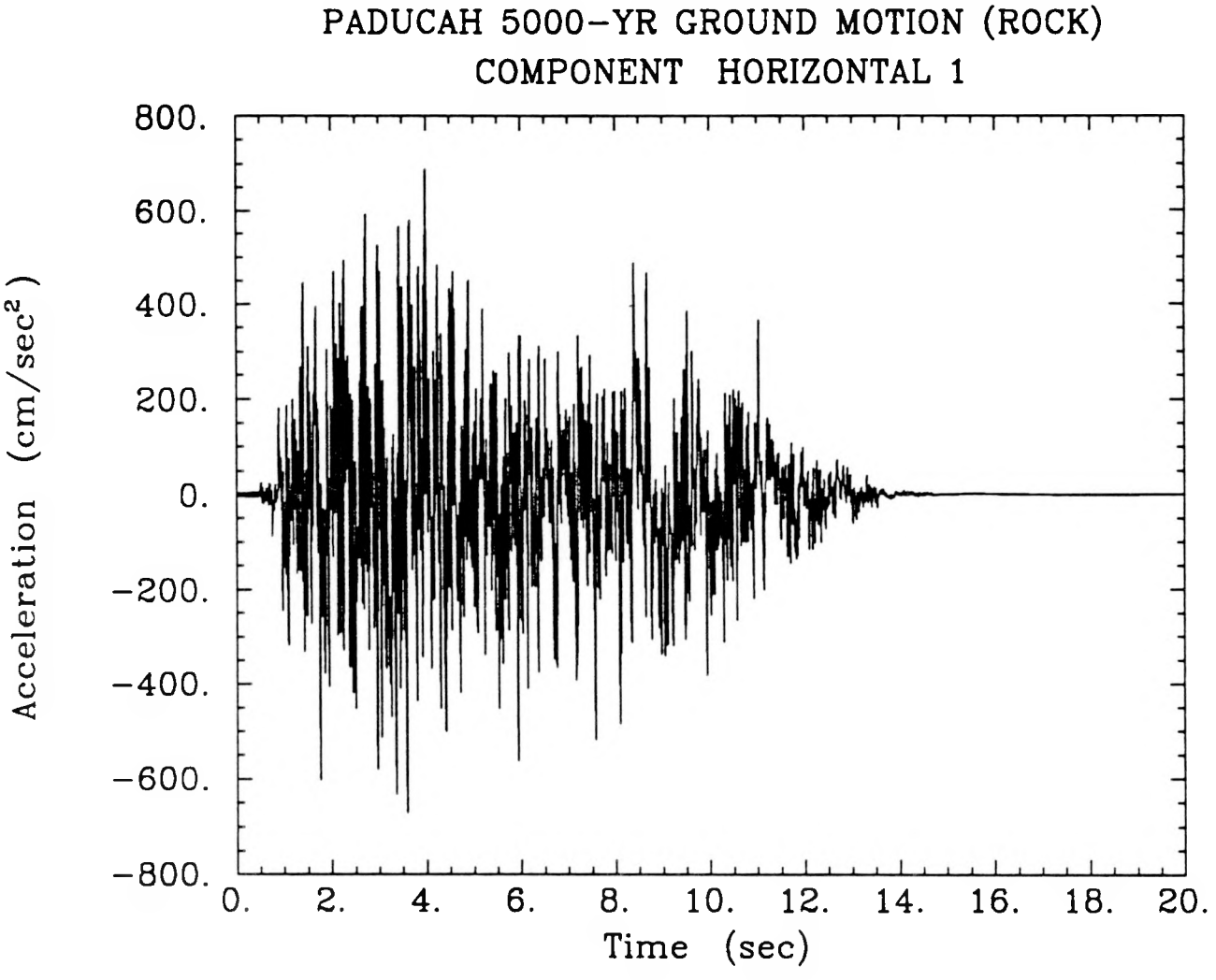

Figure 6-21. Artificial time history for a return period of 5000 years; first horizontal component.

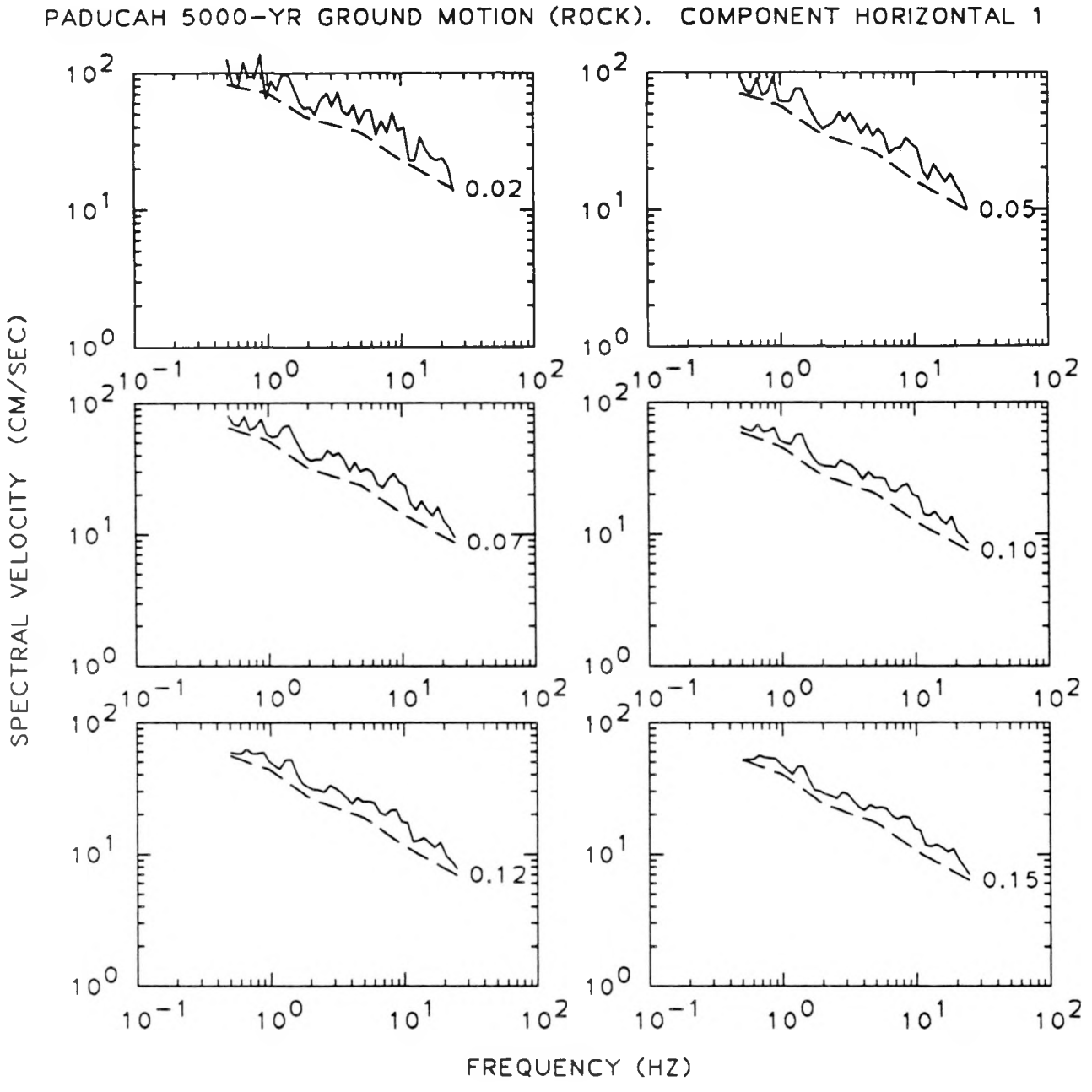

Figure 6-22. Response spectra from artificial time history for a return period of 5000 years; first horizontal component. Spectra are shown for six values of damping ratio. Solid lines: response spectra; dashed lines: uniform-hazard spectra.

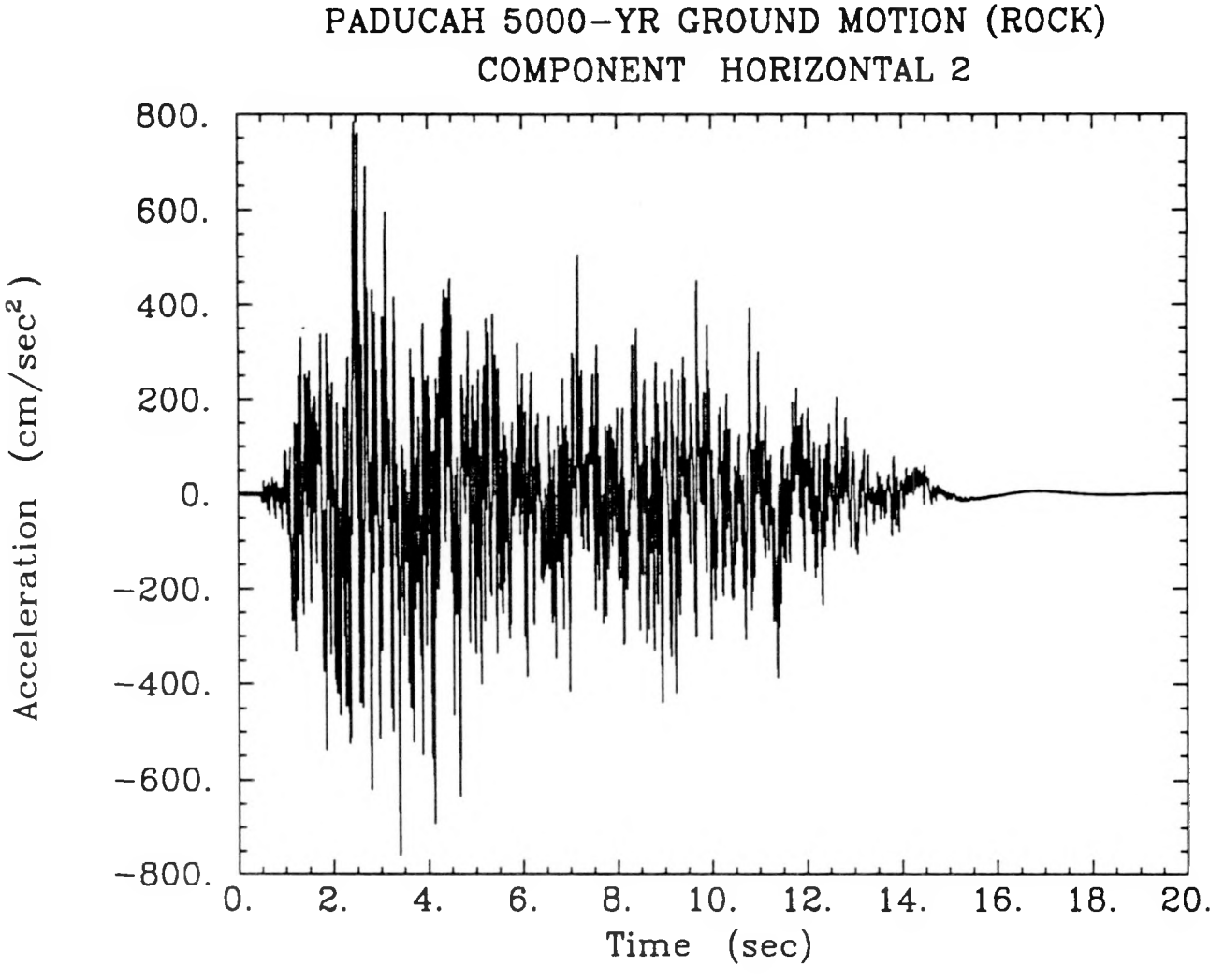

Figure 6-23. Artificial time history for a return period of 5000 years; second horizontal component.

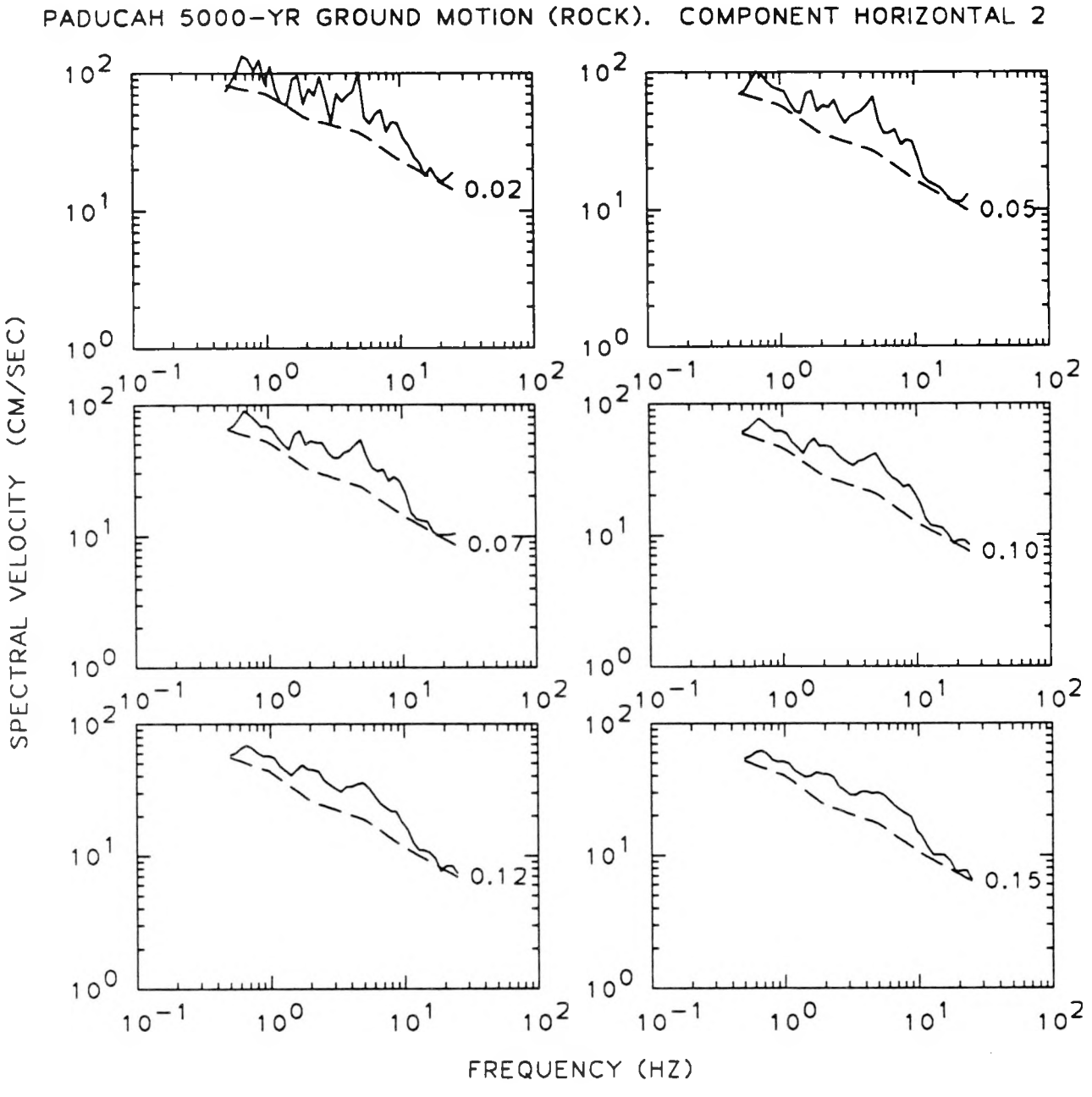

Figure 6-24. Response spectra from artificial time history for a return period of 5000 years; second horizontal component. Spectra are shown for six values of damping ratio. Solid lines: response spectra; dashed lines: uniform-hazard spectra.

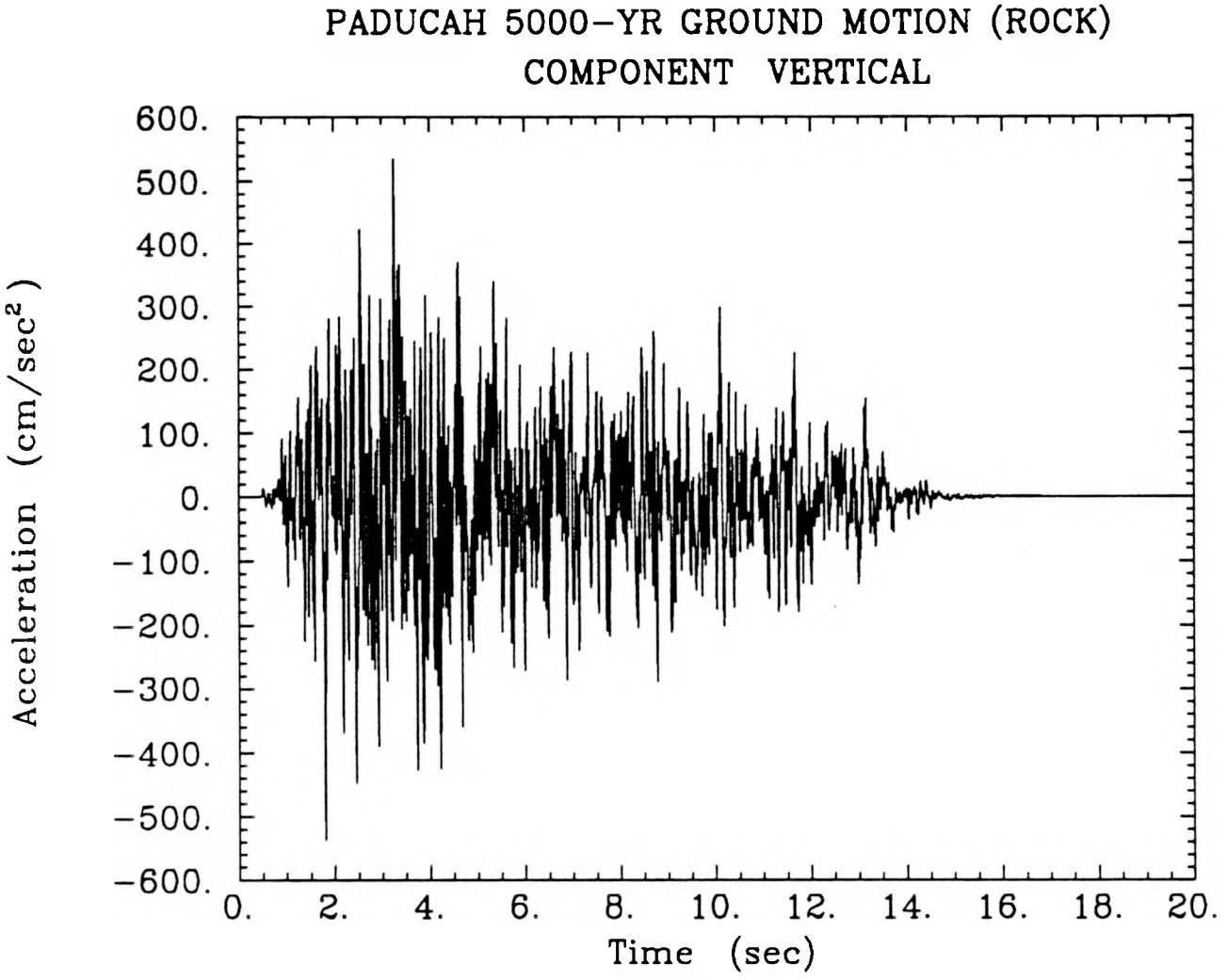

Figure 6-25. Artificial time history for a return period of 5000 years; vertical component.

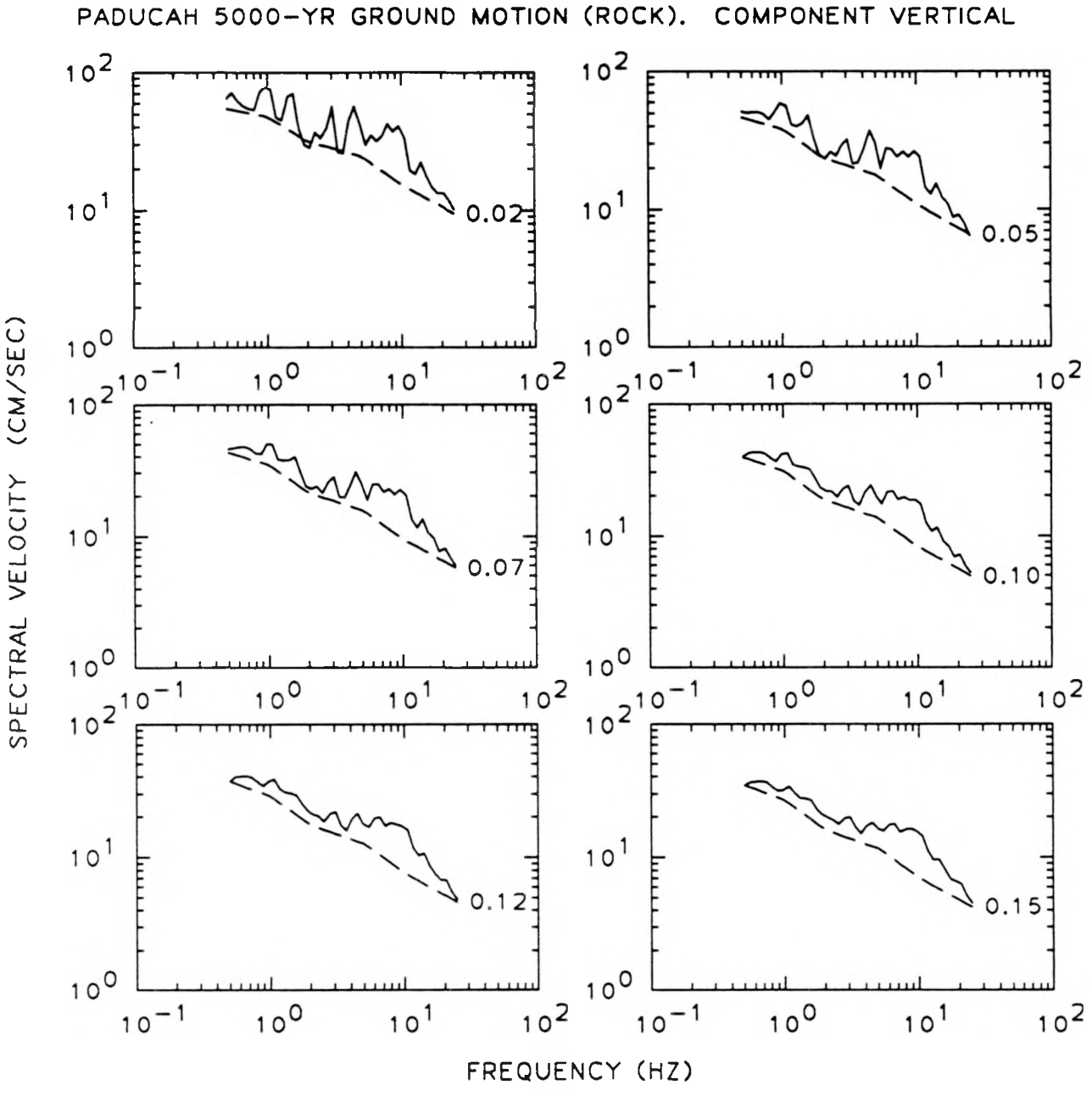

Figure 6-26. Response spectra from artificial time history for a return period of 5000 years; vertical component. Spectra are shown for six values of damping ratio. Solid lines: response spectra; dashed lines: uniform-hazard spectra.

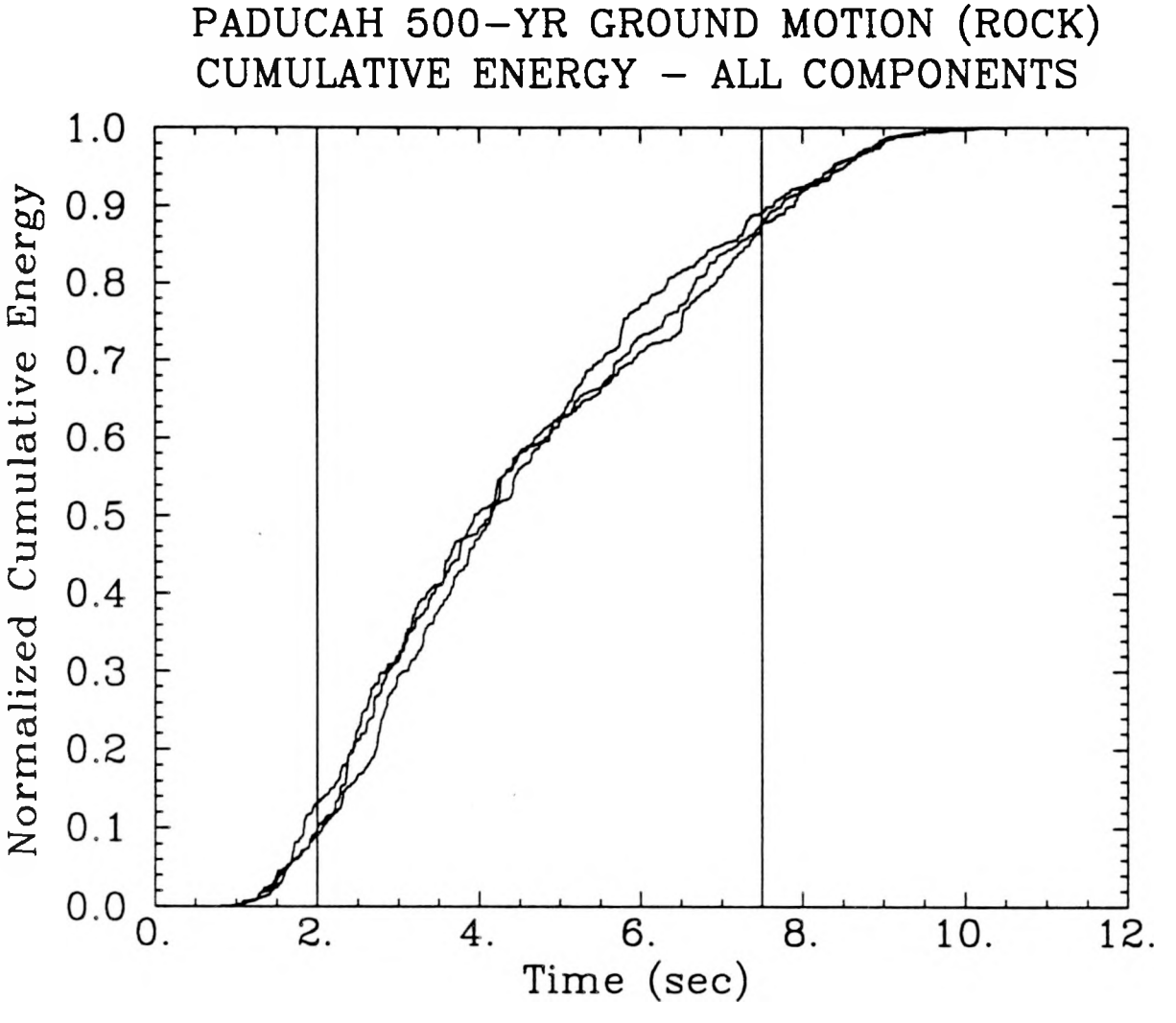

Figure 6-27. Cumulative energy plot for the 500-year artificial ground motions (all components). The vertical bars indicate the beginning and end of the strong-motion phase

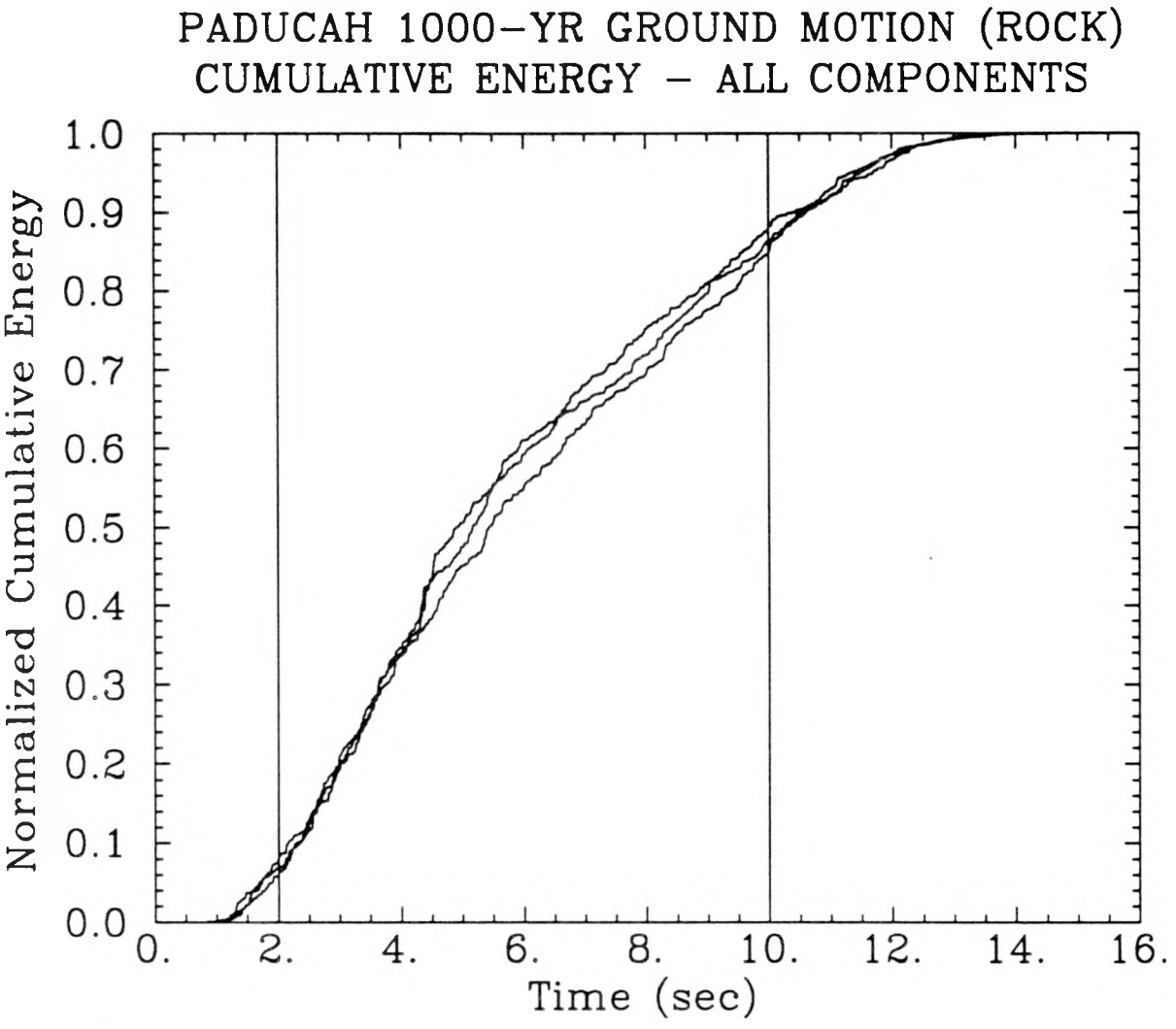

Figure 6-28. Cumulative energy plot for the 1000-year artificial ground motions (all components). The vertical bars indicate the beginning and end of the strong-motion phase

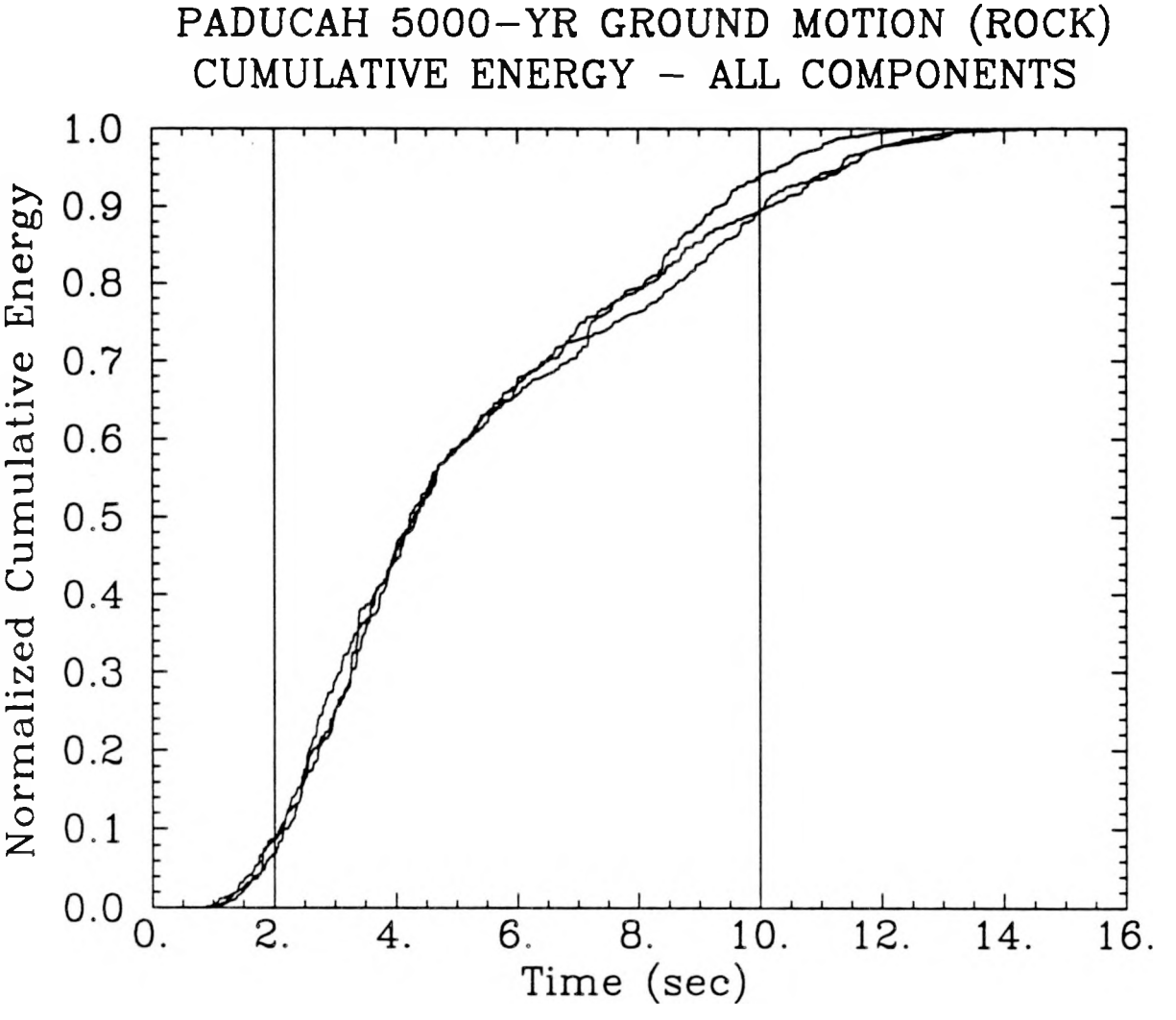

Figure 6-29. Cumulative energy plot for the 5000-year artificial ground motions (all components). The vertical bars indicate the beginning and end of the strong-motion phase

Section 7
CONCLUSIONS

This study presents seismic hazard results that represent the annual frequency of exceedance of various ground motion levels at the Paducah facility, and the uncertainty in the annual frequency of exceedance. These results are represented as a family of fractile seismic hazard curves, and as uniform-hazard spectra corresponding to annual probabilities of 2×10^{-3}, 1×10^{-3}, and 2×10^{-4}. The uncertainties in hazard derive from uncertainties on input assumptions regarding seismic sources, seismicity parameters, and ground motion attenuation equations. In this sense the analysis presented here is state-of-the-art, because it incorporates and presents uncertainties in the major factors affecting seismic hazard in the central and eastern Unites States.

The results from the extended-source hazard analysis include estimates of the effects of finite fault rupture lengths for earthquakes in the Mississippi embayment, a characteristic magnitude distribution, the possible depths of large earthquakes in the eastern US, and saturation of average ground motion amplitudes with distance at sites near to the causative rupture of an earthquake. The geometry of faults in the Mississippi embayment is based on the range of interpretations documented in the EPRI/SOG and LLNL studies; other assumptions are made accounting for relevant interpretations that have been made regarding earthquakes in the central US.

The results from the extended-source analysis were calculated for rock site conditions only. These hazard results are appropriate to input into a site-specific model of dynamic soil effects for the Paducah facility, in order to account for the effects that local soils will have on ground motions.

For the sake of comparison, Table 7–1 presents the median results for peak ground acceleration and 1-Hz spectral velocity, as obtained from all seismic hazard analyses reported here.

It should be noted that the finite-rupture analysis used here—like the EPRI and LLNL studies—was undertaken with low and moderate levels of ground motion in mind (e.g. PGA

Table 7-1

Ground-Motion Amplitudes for Selected Values of the Median Annual Exceedance Probability

Ground Motion Measure	Annual Exceedance Probability	EPRI	LLNL (4 GX†)	LLNL (5 GX†)	Combined EPRI+LLNL (4 GX†)	Combined EPRI+LLNL (5 GX†)	Extended Source
Peak Ground	2×10^{-3} (500 yr)	0.15	0.18	0.23	0.16	0.16	0.22
Acceleration	1×10^{-3} (1000 yr)	0.21	0.25	0.31	0.22	0.22	0.31
on rock (g)	2×10^{-4} (5000 yr)	0.40	0.47	0.57	0.42	0.43	0.62
Peak Ground	2×10^{-3} (500 yr)	0.20	0.18	0.21	0.20	0.20	—
Acceleration	1×10^{-3} (1000 yr)	0.25	0.25	0.29	0.25	0.26	—
on soil (g)	2×10^{-4} (5000 yr)	0.37	0.48	0.56	0.41	0.41	—
1-Hz Spectral	2×10^{-3} (500 yr)	4.1	9.2	14.0	5.2	5.6	15.0
Velocity on	1×10^{-3} (1000 yr)	6.6	14.0	21.0	8.3	8.5	25.0
rock (cm/sec)	2×10^{-4} (5000 yr)	18.0	32.0	47.0	20.0	23.0	57.0
1-Hz Spectral	2×10^{-3} (500 yr)	6.2	18.0	24.0	13.0	13.0	—
Velocity on	1×10^{-3} (1000 yr)	10.0	27.0	36.0	21.0	21.0	—
soil (cm/sec)	2×10^{-4} (5000 yr)	28.0	61.0	83.0	52.0	60.0	—

† 4GX and 5GX denote results obtained considering 4 and 5 LLNL ground-motion experts

levels up to $0.5g$). At those ground motion levels certain effects such as truncation of the ground motion distribution and decrease of the scatter in ground motion with increasing earthquake magnitude can and were ignored, because they have a minor effect. If results presented here are relied upon for higher ground motions (e.g. $1g$ and above), and those results are critical for seismic safety decisions, the effects of limits on ground motion may be quite important. In this sense the results presented here are conservative, in that they generally ignore factors that might reduce the frequency of occurrence of these large amplitude ground motions. In this case studies should be undertaken to refine the hazard curves at these high amplitudes to account for truncation and other effects that would reduce the frequencies compared to current results.

Appendix A

SIMULATION OF GROUND MOTIONS FROM EXTENDED RUPTURES

A.1 INTRODUCTION

We generate artificial ground motions from extended ruptures in order to quantify the effect of extended ruptures on near-fault ground-motion saturation. We use assumptions based on the work of Jost (1) and Nuttli et al. (2), who generate ground motions from postulated New Madrid earthquakes by summing the radiation from multiple sub-events. These assumptions are simplified and modified in order to generate high-frequency ground motions based on a random-process representation of the ground motions radiated by each sub-event. Because high-frequency ground motions at the distances of interest depend little on wave-propagation effects, we use a model similar to that of Hanks and McGuire (3) and Boore (4).

The emphasis here is on the quantification of saturation effects (by comparing predictions for short distances to the predictions for 100 km), rather than on the prediction of absolute amplitudes for a given magnitude and distance. We fit the observed distance dependence with a closed-form expression and then use this expression to modify existing attenuation functions.

A.2 MODEL FORMULATION

A.2.1 Scaling of Whole Event and Sub-Events

We use the source scaling assumptions of Jost (1) and Nuttli et al. (2) for the fault dimensions, seismic moment, and corner frequency of the whole event (see Section 3.3 of Jost). To calculate the characteristics of the sub-events, we obtain the sub-event seismic moment by dividing the whole-event seismic moment by the number of sub-events and apply these same equations.

The assumed spatial distribution of seismic moments is not uniform. It has a cosine taper at both ends of the rupture and a moderate tapering at the top and bottom. Random variation is also introduced by multiplying each sub-event moment by a uniformly distributed random factor between -33% and +33% (which corresponds to a coefficient of variation of 20%). The resulting sub-event seismic moments are then normalized so that the whole-event seismic moment is maintained.

A.2.2 Generation of Ground Motions

The rupture front propagates from a pre-specified hypocenter with rupture velocity that is random. Following Jost (1), the rupture velocity in each sub-fault is uniformly distributed between 0.8 and 0.9 times the average shear-wave velocity. Each sub-fault breaks and starts emitting seismic waves when the rupture front reaches the center of the sub-fault.

The spectrum of ground displacement at the site (in an arbitrary horizontal direction), due to sub-event i is assumed to be of the form

$$\tilde{u}_i(\omega) = \frac{0.85 M_{0,i}}{4\pi\rho\beta^3 R_i} \frac{\omega_{c,sub}^2}{\omega_{c,sub}^2 + 2i\omega_{c,sub}\omega - \omega^2} H_Q(\omega) H_m(\omega) \qquad (A-1)$$

where $M_{0,i}$ is the sub-event seismic moment; R_i is the distance of sub-fault i to the site, $\omega = 2\pi f$ is frequency (rad/sec), $H_Q(\omega) = \exp(-\frac{\omega R}{2Q\beta})$ represents crustal anelastic attenuation, $H_m(\omega) = \exp(-\frac{\kappa\omega}{2})$ represents near-site anelastic attenuation, ρ and β are the average density and shear-wave velocity in the crust (2.7 g/cm^3 and 3.5 km/sec), and $\omega_{c,sub}$ is the sub-event corner frequency.

The above expression is analogous to that used by Hanks and McGuire (3) and Boore (4); the only difference being that the above spectrum contains the proper phasing information (this is required in order to generate a causal displacement pulse).

Time-domain realizations of displacement $u_i(t)$ are obtained using a procedure modified from Boore (4). The procedure consists of the following steps:

1. Generate discrete-time, gaussian, white noise in the time domain, with mean 0, duration equal to the sub-event duration and unit energy (the latter condition implies that the standard deviation of the gaussian noise is $\sqrt{2\pi/(dtT_{sub})}$).
2. Transform the noise to the frequency domain.
3. Multiply the noise Fourier transform by eq. A–1.
4. Transform back to the time domain.
5. Invert the sign of the displacement pulse if its average value (which is related to the seismic moment) is negative. This operation ensures that the displacements add coherently.

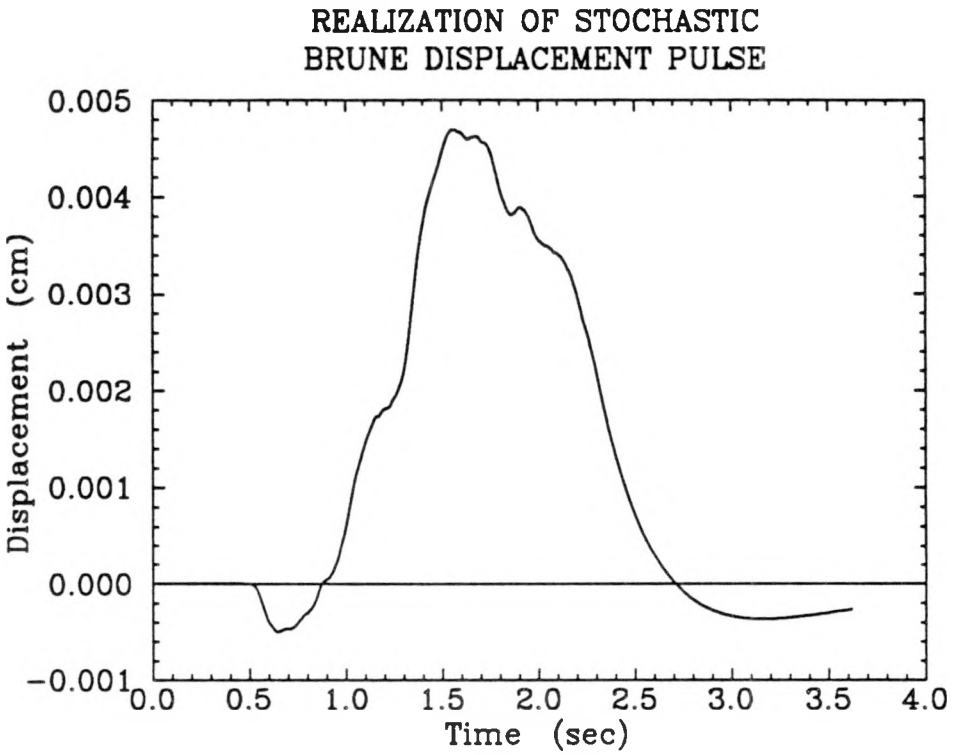

Figure A-1. Typical stochastic Brune displacement pulse

Figure A–1 shows a typical displacement pulse from one sub-event obtained in this manner (we call this a stochastic Brune displament pulse). We generate a different displacement pulse for each sub-event.

The displacements from all sub-events are lagged and added, obtaining the displacement time history at the site. The lag time for sub-event i is the sum of the time from the start of the earthquake to the rupture of sub-fault i, plus the propagation time R_i/β. The displacement time series is then differentiated to obtain velocity and acceleration. Figure A–2 shows a typical acceleration time history generated by this model.

A.3 APPLICATION

We use the ground-motion simulation model described above in order to generate artificial ground motions. We consider magnitudes m_{Lg} of 7.6 and 6.6. Table A–1 presents the characteristics of the whole events and sub-events for these magnitudes.

We consider multiple events for each magnitude, where each event has a specified seismic moment distribution (characterized by the amount of tapering at the ends) and an epicentral location. For each event, we consider multiple site azimuths and vary the distance to the

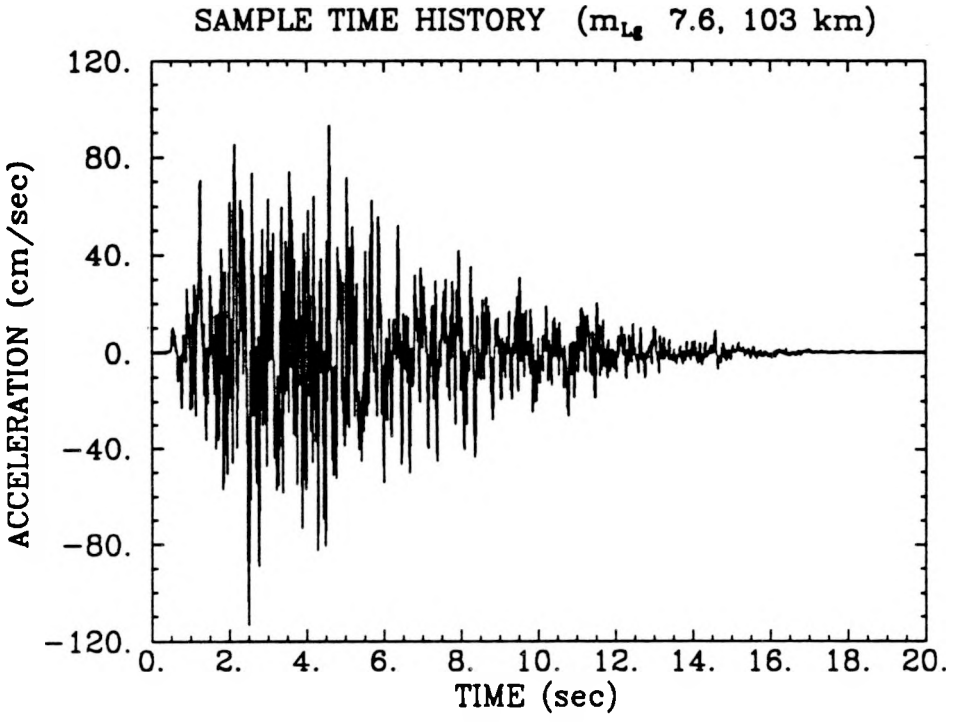

Figure A-2. Typical acceleration time history generated with the ground-motion simulation model

Table A-1

Characteristics of Whole Events and Sub-Events

	Whole Event		Sub-Events			
	Seism. Moment	Size		Seism. Moment	Corner Freq.	Duration
m_{Lg}	(dyne-cm)	(km)	Number	(dyne-cm)	(Hz)	(sec)
6.6	1×10^{26}	16×8.1	8×6	2.1×10^{24}	0.55	1.6
7.6	2×10^{27}	52×14	20×10	1.0×10^{25}	0.35	2.2

fault from 5 to 100 km. For each event-azimuth-distance combination, we generate multiple realizations and calculate average results.

Results for peak acceleration are shown in Figures A–3 and A–4, in the form of PGA vs. distance curves for each combination of event and azimuth. Table A–2 presents the codes used to label the curves. Figures A–3 and A–4 show that sites perpendicular to the mid-point of the rupture experience less saturation than sites along the fault or oblique sites. This indicates that the purely geometric effect (i.e., how much of the energy is released near the site) is more important than the effect of directivity[1]

Based on the results for up-rupture, down-rupture, and oblique azimuths (which are the most like, given the site location and the geometries of the New Madrid source used in Section 5), we fit a functional relationship of the form used by Campbell (5). Using the results for 5 and 100 km for m_{Lg} 6.6 and 7.6, we obtain

$$\ln[PGA] \propto \ln[R + 0.006e^{m_{Lg}}] \qquad (A-2)$$

where R is distance to the rupture.

The magnitude-dependent term in the above equation (i.e., the magnitude-saturation term) is equal to 4.4 km for m_{Lg} 6.6 and 11 km for m_{Lg} 7.6. This model predicts lower saturation than models for California (5, for example), because the underlying source scaling model assumes smaller ruptures for CEUS earthquakes than for California earthquakes of the same magnitude. Figure A–4 shows the predictions by Campbell (5) Joyner and Boore (6) for California earthquakes with magnitudes comparable to m_{Lg} 7.6. As mentioned earlier, the Campbell model predicts stronger saturation. The Joyner and Boore model—which does not predict magnitude saturation but shows a curvature because it contains a magnitude-independent depth term—predicts a weaker curvature, leading to a higher value of PGA(5 km)/PGA(100 km).

Results for 1-Hz spectral velocity show similar saturation effects. As a result, we use Equation A–2 for all spectral velocities.

[1]Directivity is the phenomenon whereby down-fault sites experience shorter but more intense ground motions than up-fault sites; it is a result of propagation of the rupture towards the down-fault sites. The simulation model used here predicts moderate directivity for the frequencies of interest, as can be seen by comparing curves BU and BD in Figure A–3.

Table A-2

Event-Azimuth Codes used in Figures A–3 and A–4

Event Code (first letter)	Tapering	Epicentral Location
A	50%	Mid point
B	50%	Quarter point
C	25%	Mid point
E	5%	Mid point

Azimuth Code (second letter)	Description	Line type
U	Up-rupture	——
D	Down-rupture	——
P	Perpendicular	· · · ·
O	Oblique (45°)	- - - -

A.4 REFERENCES

1. M. L. Jost. *Long-Period Strong Ground Motions and Response Spectra of Large Historical Earthquakes in the Central and Eastern United States from Kinematic Source Models.* PhD thesis, Saint Louis University, 1989.

2. O. W. Nuttli, M. L. Jost, R. B. Herrmann, and G. A. Bollinger. *Numerical models of the rupture mechanics and far-field ground motion of the 1886 South Carolina earthquake.* Bulletin 1586, U. S. Geological Survey, 1989.

3. T. C. Hanks and R. K. McGuire. "The Character of High-Frequency Strong Ground Motion". *Bulletin of the Seismological Society of America*, 71–6:2071–2095, December 1981.

4. D. M. Boore. "Stochastic Simulation of High-Frequency Ground Motions Based on Seismological Models of the Radiated Spectra". *Bulletin of the Seismological Society of America*, 73:1865–1984, 1983.

5. K. W. Campbell. "Near Source Attenuation of Peak Horizontal Acceleration". *Bulletin of the Seismological Society of America*, 71:2039–2070, December 1981.

6. W. B. Joyner and D. M. Boore. "Peak Horizontal Acceleration and Velocity from Strong Motion Records Including Records from the 1979 Imperial Valley, California Earthquake". *Bulletin of the Seismological Society of America*, 71:2011–2038, December 1981.

7. R. K. McGuire, G. R. Toro, and W. J. Silva. *Engineering Model of Earthquake Ground Motion for Eastern North America.* Technical Report NP-6074, Electric Power Research Institute, 1988.

8. O. W. Nuttli. Letter dated September 19, 1986 to J. B. Savy. Reproduced in: D. Bernreuter, J. Savy, R. Mensing, J. Chen, and B. Davis. *Seismic Hazard Characterization of 69 Nuclear Plant Sites East of the Rocky Muntains: Questionnaires.* U. S. Nuclear Regulatory Commission, Technical Report NUREG/CR-5250, UCID-21517, Volume 7, 1989. Prepared by the Lawrence Livermore National Laboratory.

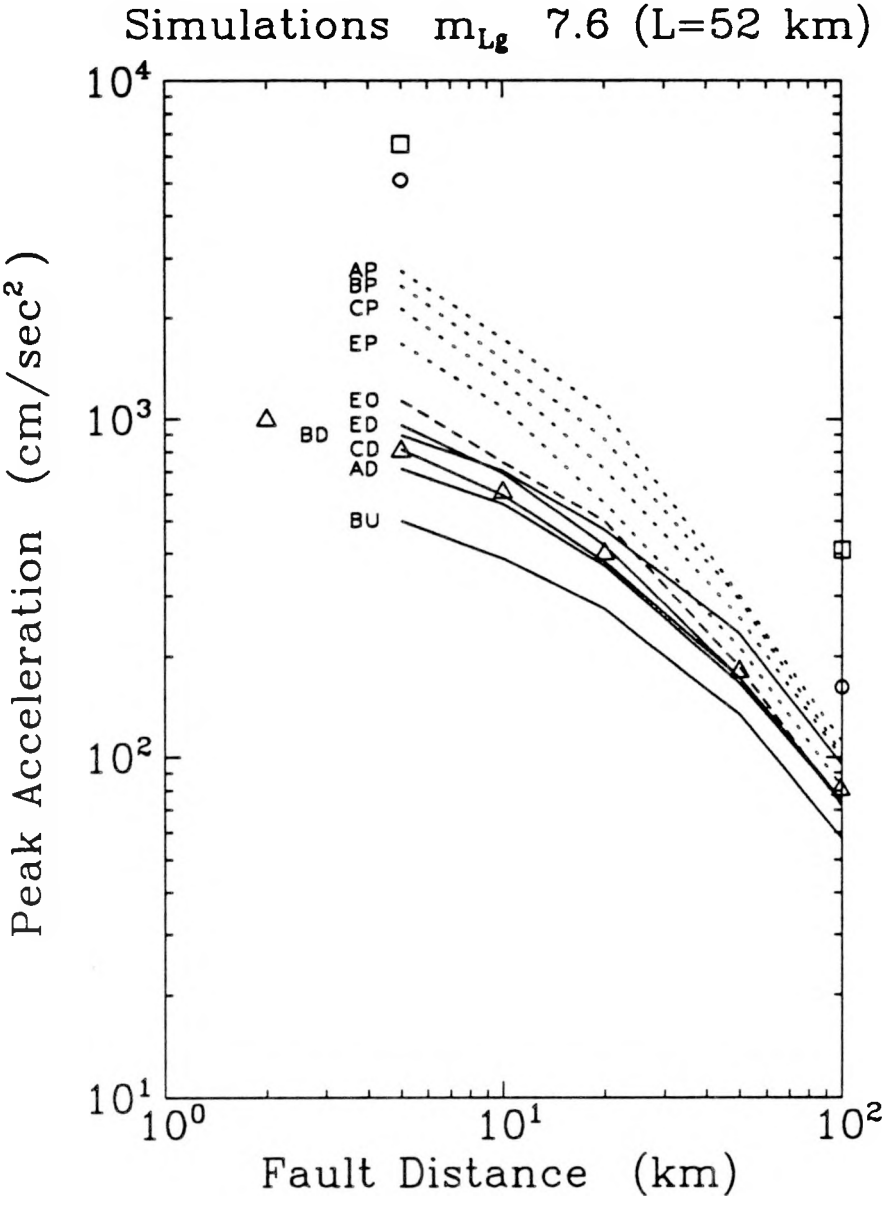

Figure A-3. Attenuation of peak acceleration with distance for m_{Lg} 7.6 and multiple combinations of event characteristics and azimuths. See Table A–2 for description of codes and line types. Key to symbols: o, McGuire et al (7); □, Nuttli (8); △, proposed saturation model.

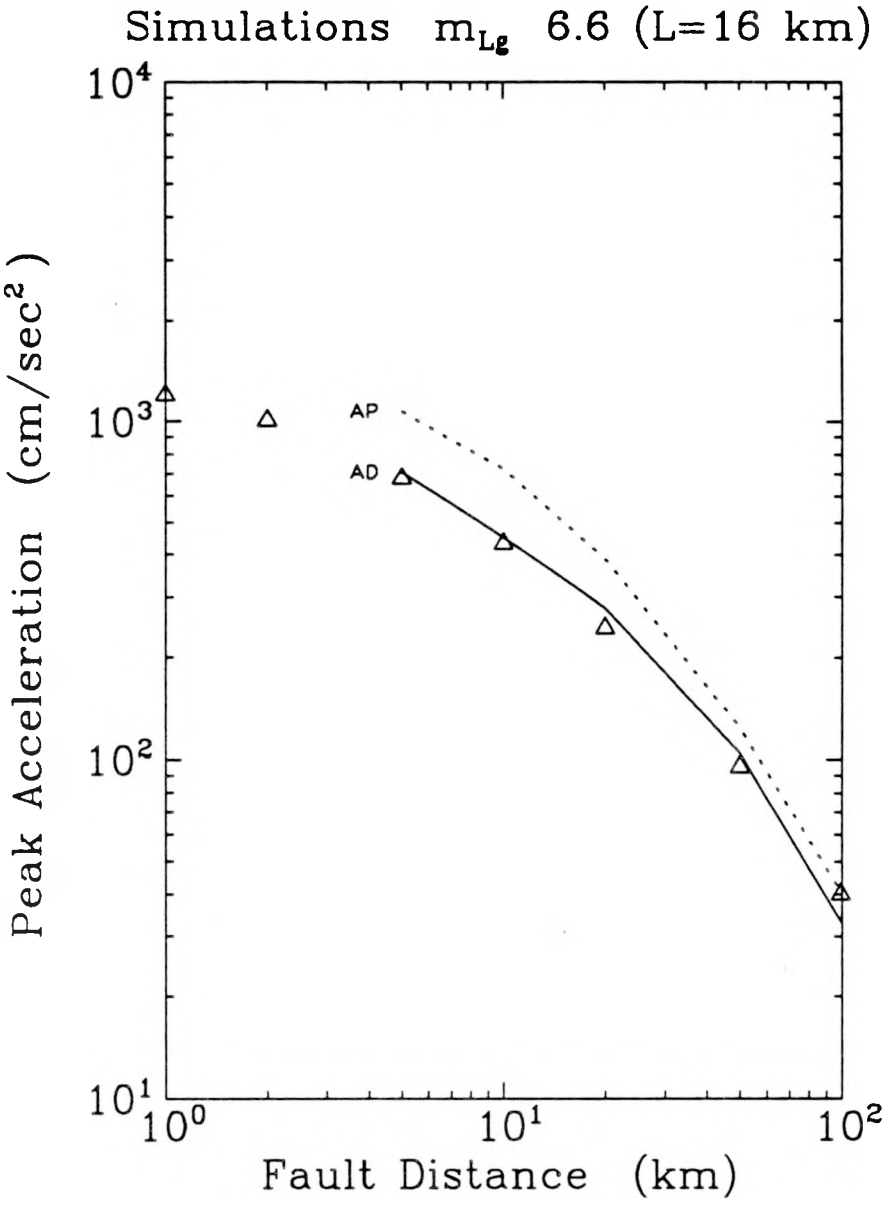

Figure A-4. Attenuation of peak acceleration with distance for m_{Lg} 6.6 and multiple combinations of event characteristics and azimuths. See Table A-2 for description of codes and line types. Key to symbols: △, proposed saturation model.

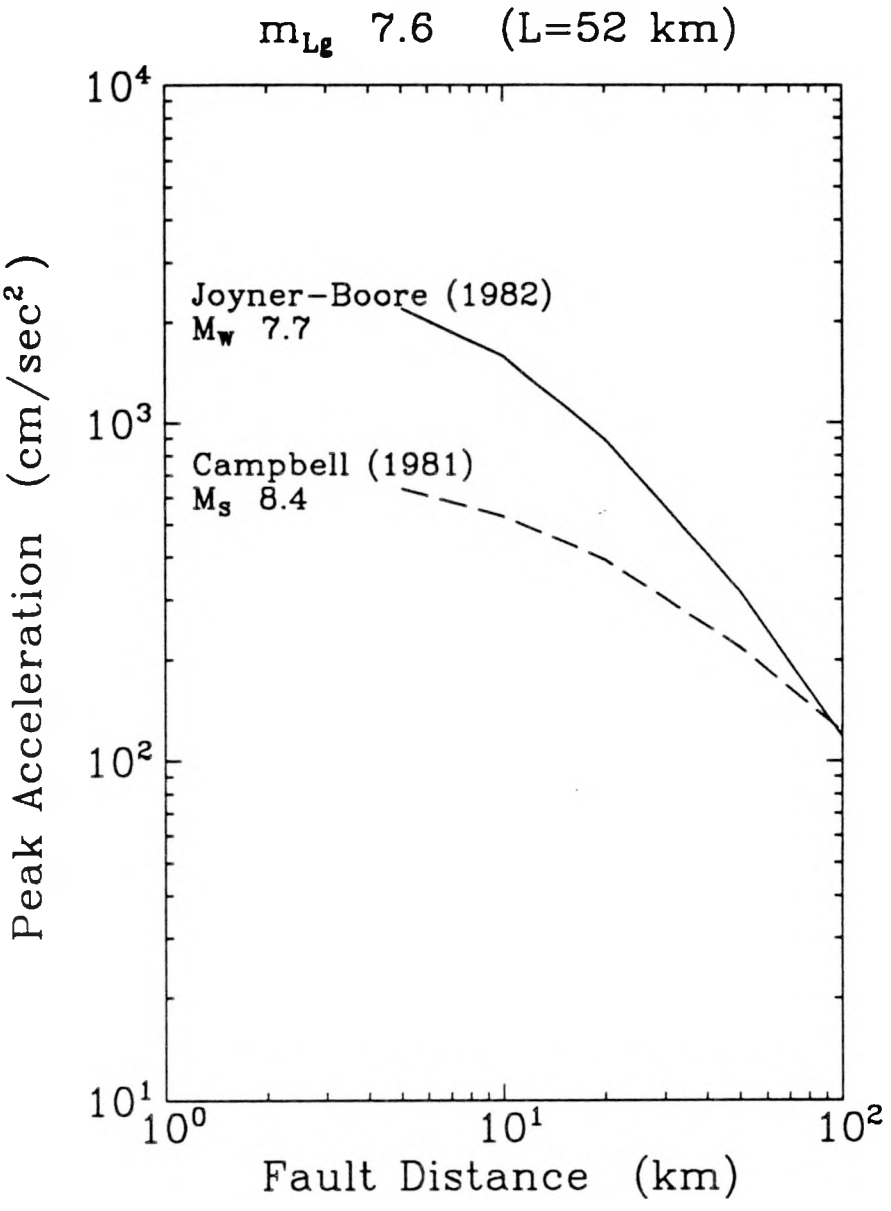

Figure A-5. Attenuation of peak acceleration with distance for California earthquakes with magnitudes comparable to m_{Lg} 7.6, according to the attenuation functions by Campbell and by Joyner and Boore.

Appendix B

TABULATED RESULTS

This appendix presents the results from Sections 2, 4, and 5 in tabular form. Results are organized by sections.

B.1 RESULTS FROM THE EPRI/SOG ANALYSIS

Table B-1

Peak ground acceleration hazard curves (rock site conditions)

AMPLITUDE	MEAN	FRACTILES						
(cm/sec2)		0.100	0.150	0.300	0.500	0.700	0.850	0.900
20.01	3.13E-02	1.32E-02	1.50E-02	1.98E-02	2.61E-02	3.67E-02	4.54E-02	5.78E-02
50.00	1.17E-02	5.07E-03	5.38E-03	6.33E-03	1.05E-02	1.27E-02	1.85E-02	2.24E-02
69.97	7.50E-03	2.91E-03	3.23E-03	4.08E-03	6.86E-03	7.91E-03	1.22E-02	1.41E-02
99.98	4.39E-03	1.48E-03	1.74E-03	2.49E-03	4.14E-03	4.58E-03	7.54E-03	8.49E-03
149.90	2.18E-03	6.43E-04	7.78E-04	1.25E-03	1.91E-03	2.41E-03	4.00E-03	4.38E-03
199.94	1.25E-03	3.40E-04	4.14E-04	6.80E-04	1.05E-03	1.42E-03	2.42E-03	2.59E-03
300.07	5.19E-04	1.24E-04	1.53E-04	2.75E-04	4.11E-04	5.90E-04	1.02E-03	1.09E-03
500.20	1.46E-04	2.67E-05	3.27E-05	7.33E-05	1.01E-04	1.70E-04	2.96E-04	3.28E-04
699.94	5.76E-05	7.93E-06	1.04E-05	2.43E-05	3.78E-05	6.74E-05	1.14E-04	1.40E-04
1000.24	1.95E-05	2.01E-06	2.49E-06	6.71E-06	1.12E-05	1.94E-05	3.63E-05	4.93E-05

Table B-2

0.5-Hz spectral velocity hazard curves (rock site conditions)

AMPLITUDE	MEAN	FRACTILES						
(cm/sec)		0.100	0.150	0.300	0.500	0.700	0.850	0.900
0.05	7.35E-02	4.16E-02	4.51E-02	5.24E-02	6.97E-02	8.81E-02	1.02E-01	1.18E-01
0.10	5.77E-02	2.83E-02	3.02E-02	3.62E-02	4.74E-02	6.16E-02	8.91E-02	1.11E-01
0.20	4.36E-02	1.71E-02	1.83E-02	2.26E-02	2.97E-02	3.92E-02	8.26E-02	1.04E-01
0.50	2.66E-02	7.88E-03	8.39E-03	1.06E-02	1.41E-02	1.89E-02	5.76E-02	7.46E-02
1.00	1.57E-02	4.02E-03	4.35E-03	5.49E-03	7.28E-03	1.02E-02	3.58E-02	4.67E-02
2.00	8.34E-03	1.91E-03	2.09E-03	2.65E-03	3.48E-03	5.17E-03	1.98E-02	2.52E-02
5.00	3.12E-03	6.18E-04	6.64E-04	8.90E-04	1.18E-03	1.93E-03	7.75E-03	9.19E-03
10.00	1.35E-03	2.02E-04	2.27E-04	3.43E-04	5.13E-04	8.42E-04	3.25E-03	3.94E-03
20.01	5.39E-04	5.38E-05	6.18E-05	1.23E-04	2.12E-04	3.23E-04	1.38E-03	1.69E-03
50.00	1.37E-04	3.96E-06	6.45E-06	2.14E-05	4.38E-05	7.57E-05	3.47E-04	4.09E-04
99.98	4.07E-05	1.66E-07	5.66E-07	2.88E-06	7.84E-06	2.34E-05	1.01E-04	1.32E-04

Table B-3

1-Hz spectral velocity hazard curves (rock site conditions)

AMPLITUDE (cm/sec)	MEAN	FRACTILES 0.100	0.150	0.300	0.500	0.700	0.850	0.900
0.05	9.30E-02	5.92E-02	6.24E-02	6.97E-02	8.98E-02	1.11E-01	1.22E-01	1.30E-01
0.10	7.77E-02	4.63E-02	4.92E-02	5.69E-02	7.22E-02	9.13E-02	1.06E-01	1.20E-01
0.20	5.82E-02	3.04E-02	3.24E-02	3.85E-02	5.08E-02	6.44E-02	8.50E-02	1.04E-01
0.50	3.34E-02	1.39E-02	1.49E-02	1.88E-02	2.34E-02	3.17E-02	5.76E-02	7.46E-02
1.00	1.88E-02	6.64E-03	7.11E-03	9.45E-03	1.15E-02	1.60E-02	3.58E-02	4.67E-02
2.00	9.46E-03	2.83E-03	3.12E-03	4.18E-03	5.15E-03	7.28E-03	1.98E-02	2.52E-02
5.00	3.30E-03	7.45E-04	8.52E-04	1.12E-03	1.53E-03	2.17E-03	7.75E-03	9.19E-03
10.00	1.35E-03	2.17E-04	2.69E-04	3.48E-04	5.40E-04	7.87E-04	3.25E-03	3.94E-03
20.01	5.17E-04	4.78E-05	6.74E-05	9.48E-05	1.72E-04	2.57E-04	1.38E-03	1.69E-03
50.00	1.25E-04	2.79E-06	4.08E-06	1.06E-05	2.41E-05	4.93E-05	3.45E-04	4.06E-04
99.98	3.56E-05	1.06E-07	2.19E-07	1.08E-06	3.82E-06	1.38E-05	9.22E-05	1.32E-04

Table B-4

2.5-Hz spectral velocity hazard curves (rock site conditions)

AMPLITUDE (cm/sec)	MEAN	FRACTILES 0.100	0.150	0.300	0.500	0.700	0.850	0.900
0.05	9.99E-02	6.41E-02	6.70E-02	7.28E-02	9.34E-02	1.25E-01	1.29E-01	1.35E-01
0.10	9.19E-02	5.90E-02	6.19E-02	6.91E-02	8.88E-02	1.09E-01	1.21E-01	1.29E-01
0.20	7.39E-02	4.52E-02	4.76E-02	5.45E-02	6.89E-02	8.60E-02	9.96E-02	1.13E-01
0.50	4.25E-02	2.24E-02	2.38E-02	2.91E-02	3.61E-02	4.80E-02	6.02E-02	7.48E-02
1.00	2.32E-02	1.04E-02	1.12E-02	1.49E-02	1.78E-02	2.45E-02	3.60E-02	4.67E-02
2.00	1.10E-02	4.02E-03	4.45E-03	5.74E-03	7.88E-03	1.03E-02	1.98E-02	2.51E-02
5.00	3.45E-03	8.13E-04	9.34E-04	1.23E-03	2.06E-03	2.50E-03	7.66E-03	9.09E-03
10.00	1.27E-03	1.79E-04	2.05E-04	2.95E-04	5.62E-04	7.66E-04	3.15E-03	3.77E-03
20.01	4.23E-04	2.55E-05	3.42E-05	5.62E-05	1.20E-04	1.97E-04	1.18E-03	1.45E-03
50.00	7.77E-05	7.65E-07	1.25E-06	3.26E-06	1.07E-05	2.43E-05	2.55E-04	2.80E-04
99.98	1.69E-05	1.29E-08	2.77E-08	1.83E-07	9.67E-07	3.21E-06	5.30E-05	6.51E-05

Table B-5

5-Hz spectral velocity hazard curves (rock site conditions)

AMPLITUDE (cm/sec)	MEAN	FRACTILES 0.100	0.150	0.300	0.500	0.700	0.850	0.900
0.05	9.83E-02	6.34E-02	6.54E-02	7.22E-02	9.31E-02	1.18E-01	1.29E-01	1.32E-01
0.10	8.91E-02	5.54E-02	5.92E-02	6.67E-02	8.40E-02	1.05E-01	1.18E-01	1.29E-01
0.20	7.13E-02	3.88E-02	4.44E-02	5.36E-02	6.29E-02	8.53E-02	9.88E-02	1.13E-01
0.50	4.14E-02	1.84E-02	2.20E-02	2.70E-02	3.41E-02	4.88E-02	6.04E-02	7.48E-02
1.00	2.25E-02	9.09E-03	9.99E-03	1.26E-02	1.76E-02	2.46E-02	3.57E-02	4.61E-02
2.00	1.04E-02	3.65E-03	3.94E-03	4.69E-03	7.91E-03	1.02E-02	1.89E-02	2.37E-02
5.00	2.90E-03	6.38E-04	7.02E-04	1.03E-03	1.85E-03	2.32E-03	6.36E-03	7.57E-03
10.00	8.95E-04	1.20E-04	1.35E-04	2.08E-04	4.24E-04	6.26E-04	2.39E-03	2.69E-03
20.01	2.30E-04	1.31E-05	1.75E-05	3.25E-05	7.27E-05	1.29E-04	7.02E-04	8.06E-04
50.00	2.61E-05	2.63E-07	4.52E-07	1.14E-06	4.16E-06	1.05E-05	7.66E-05	9.87E-05
99.98	3.23E-06	3.73E-09	6.98E-09	3.47E-08	2.19E-07	6.30E-07	8.22E-06	1.28E-05

Table B-6

10-Hz spectral velocity hazard curves (rock site conditions)

AMPLITUDE (cm/sec)	MEAN	FRACTILES 0.100	0.150	0.300	0.500	0.700	0.850	0.900
0.05	9.41E-02	6.04E-02	6.31E-02	7.05E-02	8.95E-02	1.10E-01	1.24E-01	1.30E-01
0.10	8.08E-02	4.88E-02	5.26E-02	6.14E-02	7.37E-02	9.46E-02	1.09E-01	1.24E-01
0.20	6.10E-02	3.13E-02	3.60E-02	4.38E-02	5.36E-02	7.31E-02	8.53E-02	1.02E-01
0.50	3.24E-02	1.45E-02	1.60E-02	2.01E-02	2.50E-02	3.52E-02	4.96E-02	6.44E-02
1.00	1.61E-02	6.64E-03	7.13E-03	8.70E-03	1.23E-02	1.64E-02	2.70E-02	3.43E-02
2.00	6.46E-03	2.01E-03	2.55E-03	3.41E-03	5.03E-03	6.19E-03	1.22E-02	1.42E-02
5.00	1.35E-03	2.80E-04	3.83E-04	6.46E-04	9.34E-04	1.23E-03	3.10E-03	3.44E-03
10.00	2.98E-04	4.13E-05	5.09E-05	1.23E-04	1.71E-04	2.63E-04	7.60E-04	8.42E-04
20.01	4.92E-05	3.69E-06	5.01E-06	1.38E-05	2.44E-05	3.92E-05	1.15E-04	1.49E-04
50.00	2.56E-06	4.81E-08	6.66E-08	2.53E-07	6.69E-07	1.24E-06	5.23E-06	8.48E-06
99.98	1.45E-07	3.22E-10	6.60E-10	2.98E-09	1.15E-08	4.77E-08	1.96E-07	4.68E-07

Table B-7

25-Hz spectral velocity hazard curves (rock site conditions)

AMPLITUDE (cm/sec)	MEAN	FRACTILES 0.100	0.150	0.300	0.500	0.700	0.850	0.900
0.05	7.85E-02	4.98E-02	5.26E-02	5.97E-02	7.28E-02	9.20E-02	1.03E-01	1.16E-01
0.10	5.69E-02	3.46E-02	3.76E-02	4.45E-02	5.20E-02	6.65E-02	7.57E-02	8.56E-02
0.20	3.40E-02	2.08E-02	2.25E-02	2.72E-02	3.04E-02	4.00E-02	4.60E-02	5.12E-02
0.50	1.31E-02	7.78E-03	8.53E-03	1.10E-02	1.29E-02	1.52E-02	1.74E-02	1.79E-02
1.00	5.18E-03	2.40E-03	2.70E-03	4.54E-03	5.34E-03	6.14E-03	6.59E-03	6.88E-03
2.00	1.62E-03	5.78E-04	6.67E-04	1.29E-03	1.68E-03	1.94E-03	2.27E-03	2.43E-03
5.00	2.16E-04	5.92E-05	6.77E-05	1.27E-04	1.97E-04	2.85E-04	3.38E-04	3.81E-04
10.00	3.06E-05	5.17E-06	6.69E-06	1.37E-05	2.47E-05	4.00E-05	5.82E-05	6.01E-05
20.01	2.74E-06	1.94E-07	3.72E-07	8.48E-07	1.70E-06	3.36E-06	4.97E-06	6.53E-06
50.00	3.98E-08	5.10E-10	9.97E-10	4.15E-09	1.32E-08	3.60E-08	6.82E-08	1.20E-07
99.98	5.20E-10	5.78E-13	1.54E-12	1.42E-11	1.00E-10	2.75E-10	7.58E-10	1.28E-09

Table B-8

Median uniform-hazard spectra (rock site conditions)

PSV (cm/sec)

FREQ (Hz)	ANNUAL EXCEEDANCE PROBABILITY 2E-3	1E-3	2E-4	1E-4
0.50	3.19	5.74	20.8	31.0
1.00	4.08	6.63	18.3	25.8
2.50	5.08	7.34	15.9	21.5
5.00	4.76	6.67	13.4	17.7
10.00	3.30	4.82	9.36	12.1
25.00	1.80	2.49	4.97	6.27

Table B-9

Peak ground acceleration hazard curves (soil site conditions)

AMPLITUDE (cm/sec2)	MEAN	0.150	0.500	0.850
3.201E+01	3.224E-02	1.380E-02	2.570E-02	5.495E-02
8.000E+01	1.168E-02	4.898E-03	9.772E-03	2.089E-02
1.119E+02	7.590E-03	3.020E-03	5.623E-03	1.288E-02
1.600E+02	4.411E-03	1.318E-03	3.236E-03	7.943E-03
2.219E+02	2.348E-03	4.677E-04	1.622E-03	4.898E-03
2.699E+02	1.463E-03	1.778E-04	8.128E-04	3.020E-03
3.301E+02	8.112E-04	8.318E-05	3.548E-04	1.413E-03
4.252E+02	3.306E-04	2.089E-05	1.023E-04	6.607E-04
5.600E+02	9.986E-05	7.943E-06	3.631E-05	1.778E-04
8.002E+02	2.625E-05	1.995E-06	1.122E-05	5.129E-05
1.280E+03	5.397E-06	2.692E-07	1.862E-06	1.047E-05

Table B-10

0.5-Hz spectral velocity hazard curves (soil site conditions)

AMPLITUDE (cm/sec)	MEAN	0.150	0.500	0.850
7.498E-02	7.436E-02	4.169E-02	6.761E-02	1.175E-01
1.499E-01	5.715E-02	2.754E-02	4.786E-02	1.096E-01
3.001E-01	4.287E-02	1.698E-02	2.754E-02	9.550E-02
7.501E-01	2.555E-02	7.943E-03	1.288E-02	6.761E-02
1.500E+00	1.511E-02	3.981E-03	6.918E-03	3.890E-02
3.000E+00	7.975E-03	1.995E-03	3.236E-03	2.089E-02
7.597E+00	2.890E-03	6.607E-04	1.148E-03	7.413E-03
1.581E+01	1.228E-03	2.188E-04	4.677E-04	3.020E-03
3.301E+01	5.139E-04	5.888E-05	1.905E-04	1.318E-03
8.750E+01	1.219E-04	5.248E-06	3.890E-05	2.884E-04
1.750E+02	3.861E-05	2.188E-07	9.120E-06	8.913E-05

Table B-11

1-Hz spectral velocity hazard curves (soil site conditions)

AMPLITUDE (cm/sec)	MEAN	0.150	0.500	0.850
7.498E-02	9.196E-02	5.888E-02	8.913E-02	1.259E-01
1.499E-01	7.746E-02	4.786E-02	7.244E-02	1.175E-01
3.001E-01	5.812E-02	3.162E-02	4.786E-02	9.550E-02
7.501E-01	3.301E-02	1.380E-02	2.239E-02	6.761E-02
1.500E+00	1.859E-02	6.918E-03	1.202E-02	3.890E-02
3.000E+00	9.330E-03	3.020E-03	5.623E-03	2.089E-02
7.597E+00	3.113E-03	8.128E-04	1.514E-03	7.413E-03
1.581E+01	1.237E-03	2.344E-04	5.012E-04	3.020E-03
3.301E+01	4.885E-04	5.129E-05	1.549E-04	1.318E-03
8.750E+01	1.089E-04	3.236E-06	2.239E-05	2.884E-04
1.750E+02	3.575E-05	1.445E-07	4.571E-06	8.318E-05

Table B-12

2.5-Hz spectral velocity hazard curves (soil site conditions)

AMPLITUDE (cm/sec)	MEAN	0.150	0.500	0.850
1.050E-01	9.786E-02	6.761E-02	9.550E-02	1.349E-01
2.099E-01	9.089E-02	5.888E-02	8.913E-02	1.259E-01
4.202E-01	7.392E-02	4.467E-02	6.761E-02	1.096E-01
1.050E+00	4.276E-02	2.239E-02	3.388E-02	6.761E-02
2.100E+00	2.364E-02	1.047E-02	1.950E-02	3.890E-02
4.199E+00	1.125E-02	3.981E-03	7.413E-03	1.950E-02
9.996E+00	3.431E-03	8.128E-04	1.862E-03	6.918E-03
1.751E+01	1.249E-03	1.778E-04	5.012E-04	2.818E-03
3.001E+01	4.338E-04	2.754E-05	1.096E-04	1.000E-03
6.250E+01	7.805E-05	8.710E-07	8.511E-06	1.778E-04
1.250E+02	1.793E-05	1.820E-08	7.079E-07	3.890E-05

Table B-13

5-Hz spectral velocity hazard curves (soil site conditions)

AMPLITUDE (cm/sec)	MEAN	0.150	0.500	0.850
1.050E-01	9.557E-02	6.761E-02	8.913E-02	1.349E-01
2.099E-01	8.795E-02	5.495E-02	8.318E-02	1.259E-01
4.202E-01	7.108E-02	3.890E-02	6.310E-02	1.023E-01
1.050E+00	4.129E-02	1.820E-02	3.388E-02	6.761E-02
2.100E+00	2.279E-02	9.120E-03	1.698E-02	4.169E-02
4.199E+00	1.071E-02	3.467E-03	7.413E-03	1.950E-02
9.996E+00	3.010E-03	6.607E-04	1.622E-03	5.623E-03
1.751E+01	9.999E-04	1.096E-04	3.548E-04	1.995E-03
3.001E+01	2.861E-04	1.380E-05	6.761E-05	5.370E-04
6.250E+01	3.286E-05	3.090E-07	3.236E-06	5.495E-05
1.250E+02	4.466E-06	4.266E-09	1.549E-07	6.026E-06

Table B-14

10-Hz spectral velocity hazard curves (soil site conditions)

AMPLITUDE (cm/sec)	MEAN	0.150	0.500	0.850
8.498E-02	9.202E-02	6.310E-02	8.913E-02	1.259E-01
1.699E-01	8.052E-02	4.786E-02	7.244E-02	1.175E-01
3.401E-01	6.134E-02	3.162E-02	5.495E-02	9.550E-02
8.501E-01	3.258E-02	1.479E-02	2.399E-02	5.495E-02
1.700E+00	1.644E-02	6.457E-03	1.122E-02	2.951E-02
3.399E+00	6.820E-03	2.138E-03	4.571E-03	1.288E-02
7.547E+00	1.604E-03	2.884E-04	7.586E-04	3.020E-03
1.251E+01	5.162E-04	3.631E-05	1.549E-04	1.072E-03
1.740E+01	9.001E-05	2.818E-06	1.950E-05	1.905E-04
4.000E+01	3.877E-06	5.888E-08	5.012E-07	6.457E-06
7.999E+01	2.523E-07	4.074E-10	1.288E-08	3.311E-07
1.599E+02	6.842E-09	5.370E-13	6.310E-11	8.511E-09

Table B-15

25-Hz spectral velocity hazard curves (soil site conditions)

AMPLITUDE (cm/sec)	MEAN	0.150	0.500	0.850
5.998E-02	7.854E-02	5.129E-02	7.244E-02	1.096E-01
1.199E-01	5.724E-02	3.631E-02	5.129E-02	8.318E-02
2.401E-01	3.490E-02	2.089E-02	3.162E-02	4.786E-02
6.001E-01	1.360E-02	7.943E-03	1.202E-02	1.950E-02
1.200E+00	5.587E-03	2.630E-03	4.898E-03	9.772E-03
2.100E+00	2.045E-03	5.012E-04	1.413E-03	3.981E-03
3.998E+00	2.923E-04	5.129E-05	1.549E-04	5.754E-04
8.003E+00	4.197E-05	5.248E-06	1.950E-05	7.762E-05
1.600E+01	4.830E-06	2.042E-07	1.230E-06	7.943E-06
4.000E+01	1.005E-07	6.166E-10	1.047E-08	1.660E-07
7.999E+01	2.012E-09	7.586E-13	4.786E-11	1.995E-09
1.599E+02	8.696E-12	2.188E-19	4.786E-14	8.511E-12

Table B-16

Median uniform-hazard spectra (soil site conditions)

PSV (cm/sec)

FREQ (Hz)	ANNUAL EXCEEDANCE PROBABILITY 2E-3	1E-3	2E-4	1E-4
0.50	4.62	8.50	31.7	49.0
1.00	6.24	10.0	28.1	41.2
2.50	9.56	13.0	24.2	30.8
5.00	8.87	11.9	21.1	26.4
10.00	4.91	6.68	11.5	13.4
25.00	1.80	2.32	3.71	4.63

B.2 COMBINED RESULTS FROM EPRI/SOG AND LLNL ANALYSES

Table B-17

Peak ground acceleration hazard curves (rock, all LLNL G-experts)

AMPLITUDE (cm/sec2)	MEAN	0.050	0.150	0.250	0.350	0.450	0.500	0.550	0.650	0.750	0.850	0.930
2.001E+01	1.237E-01	7.413E-03	1.820E-02	2.239E-02	2.754E-02	3.631E-02	3.631E-02	4.169E-02	5.888E-02	1.023E-01	1.549E-01	3.548E-01
5.000E+01	4.440E-02	1.738E-03	5.248E-03	8.511E-03	9.772E-03	1.202E-02	1.288E-02	1.380E-02	2.089E-02	3.162E-02	4.786E-02	1.349E-01
6.997E+01	3.027E-02	1.000E-03	3.236E-03	5.248E-03	6.918E-03	7.413E-03	7.413E-03	8.511E-03	1.288E-02	1.950E-02	3.162E-02	8.913E-02
9.998E+01	1.906E-02	5.012E-04	1.738E-03	2.818E-03	3.981E-03	4.266E-03	4.571E-03	4.571E-03	7.413E-03	1.122E-02	1.820E-02	5.495E-02
1.499E+02	1.041E-02	2.188E-04	7.586E-04	1.318E-03	1.862E-03	2.138E-03	2.291E-03	2.455E-03	3.467E-03	5.623E-03	9.120E-03	3.162E-02
1.999E+02	6.416E-03	1.175E-04	4.074E-04	7.079E-04	1.000E-03	1.230E-03	1.230E-03	1.514E-03	1.995E-03	3.236E-03	5.623E-03	1.950E-02
3.001E+02	3.083E-03	4.467E-05	1.445E-04	2.692E-04	3.802E-04	4.677E-04	5.012E-04	6.607E-04	8.128E-04	1.318E-03	2.455E-03	9.772E-03
5.002E+02	1.122E-03	9.120E-06	3.388E-05	6.310E-05	9.550E-05	1.175E-04	1.349E-04	1.905E-04	2.188E-04	4.074E-04	7.586E-04	3.715E-03
6.999E+02	5.424E-04	2.291E-06	9.772E-06	2.089E-05	3.388E-05	4.169E-05	5.129E-05	7.244E-05	8.318E-05	1.660E-04	3.311E-04	1.862E-03
1.000E+03	2.285E-04	3.548E-07	2.455E-06	5.248E-06	9.120E-06	1.202E-05	1.585E-05	1.950E-05	2.754E-05	5.495E-05	1.259E-04	8.128E-04

Table B-18

Median uniform-hazard spectra (rock, all LLNL G-experts)

PSV (cm/sec)

FREQ (Hz)	ANNUAL EXCEEDANCE PROBABILITY 2E-3	1E-3	2E-4	1E-4
0.50	4.41	7.35	25.6	38.5
1.00	5.64	8.49	22.5	32.0
2.50	5.64	8.49	19.5	25.2
5.00	5.37	7.75	16.3	21.4
10.00	3.73	5.49	10.9	13.5
25.00	1.92	2.66	5.41	6.88

Table B-19

Peak ground acceleration hazard curves (rock, 4 LLNL G-experts)

AMPLITUDE (cm/sec2)	MEAN	0.050	0.150	0.250	0.350	0.450	0.500	0.550	0.650	0.750	0.850	0.950
2.001E+01	9.651E-02	6.457E-03	1.585E-02	2.239E-02	2.570E-02	3.631E-02	3.631E-02	4.169E-02	5.495E-02	7.762E-02	1.549E-01	2.884E-01
5.000E+01	3.374E-02	1.413E-03	5.248E-03	6.457E-03	9.772E-03	1.122E-02	1.202E-02	1.288E-02	1.585E-02	2.570E-02	4.467E-02	8.318E-02
6.997E+01	2.275E-02	8.128E-04	3.236E-03	3.981E-03	6.026E-03	7.413E-03	7.413E-03	7.413E-03	1.047E-02	1.698E-02	2.951E-02	5.495E-02
9.998E+01	1.352E-02	4.074E-04	1.738E-03	2.291E-03	3.467E-03	4.266E-03	4.266E-03	4.571E-03	6.457E-03	9.772E-03	1.698E-02	3.162E-02
1.499E+02	6.955E-03	1.905E-04	7.586E-04	1.148E-03	1.622E-03	2.138E-03	2.138E-03	2.455E-03	3.236E-03	4.571E-03	8.511E-03	1.698E-02
1.999E+02	4.168E-03	9.550E-05	4.074E-04	6.607E-04	8.710E-04	1.230E-03	1.230E-03	1.318E-03	1.738E-03	2.630E-03	5.248E-03	9.772E-03
3.001E+02	1.854E-03	3.631E-05	1.445E-04	2.188E-04	3.548E-04	4.365E-04	5.012E-04	5.012E-04	7.079E-04	1.072E-03	2.291E-03	4.571E-03
5.002E+02	5.864E-04	6.918E-06	3.388E-05	5.495E-05	8.318E-05	1.096E-04	1.259E-04	1.349E-04	2.042E-04	3.311E-04	6.607E-04	1.514E-03
6.999E+02	2.560E-04	1.862E-06	9.772E-06	2.089E-05	2.754E-05	4.169E-05	4.467E-05	5.129E-05	7.762E-05	1.445E-04	2.692E-04	6.607E-04
1.000E+03	9.928E-05	2.512E-07	2.455E-06	5.248E-06	7.413E-06	1.380E-05	1.380E-05	1.585E-05	2.399E-05	4.786E-05	1.023E-04	2.512E-04

Table B-20

Median uniform-hazard spectra (rock, 4 LLNL G-experts)

PSV (cm/sec)

FREQ (Hz)	ANNUAL EXCEEDANCE PROBABILITY 2E-3	1E-3	2E-4	1E-4
0.50	4.09	7.19	22.9	35.1
1.00	5.23	8.31	20.2	29.2
2.50	5.64	8.49	18.4	24.2
5.00	5.16	7.19	14.7	19.6
10.00	3.49	5.15	10.3	12.9
25.00	1.84	2.53	5.03	6.35

Table B-21

Peak ground acceleration hazard curves (soil, all LLNL G-experts)

AMPLITUDE (cm/sec2)	MEAN	0.050	0.150	0.250	0.350	0.450	0.500	0.550	0.650	0.750	0.850	0.950
3.201E+01	6.438E-02	7.943E-03	1.202E-02	1.585E-02	2.089E-02	2.570E-02	3.162E-02	3.388E-02	4.786E-02	6.310E-02	8.913E-02	1.660E-01
8.000E+01	2.222E-02	1.738E-03	3.467E-03	5.623E-03	6.457E-03	9.120E-03	9.772E-03	1.122E-02	1.380E-02	1.950E-02	3.162E-02	5.495E-02
1.119E+02	1.440E-02	8.710E-04	1.862E-03	3.236E-03	3.981E-03	5.248E-03	5.623E-03	7.413E-03	8.511E-03	1.202E-02	1.950E-02	3.388E-02
1.600E+02	8.311E-03	4.074E-04	8.710E-04	1.622E-03	2.138E-03	3.020E-03	3.236E-03	3.981E-03	4.898E-03	6.457E-03	1.047E-02	1.950E-02
2.219E+02	4.744E-03	8.913E-05	3.311E-04	6.607E-04	1.000E-03	1.413E-03	1.622E-03	1.995E-03	2.818E-03	3.715E-03	6.026E-03	1.122E-02
2.699E+02	3.287E-03	2.754E-05	1.175E-04	2.692E-04	5.370E-04	8.128E-04	9.333E-04	1.230E-03	1.738E-03	2.455E-03	3.981E-03	7.943E-03
3.301E+02	2.199E-03	1.122E-05	6.761E-05	1.660E-04	2.188E-04	3.548E-04	5.370E-04	5.754E-04	9.333E-04	1.622E-03	2.630E-03	5.248E-03
4.252E+02	1.290E-03	4.266E-06	3.162E-05	4.786E-05	8.318E-05	1.660E-04	1.778E-04	2.692E-04	4.365E-04	8.710E-04	1.514E-03	3.236E-03
5.600E+02	6.922E-04	1.318E-06	1.047E-05	1.820E-05	3.388E-05	5.495E-05	7.762E-05	7.762E-05	1.445E-04	2.692E-04	7.586E-04	1.738E-03
8.002E+02	3.110E-04	2.512E-07	2.630E-06	4.571E-06	9.120E-06	1.380E-05	2.239E-05	2.399E-05	4.786E-05	9.550E-05	1.905E-04	8.128E-04
1.280E+03	1.009E-04	1.585E-08	2.188E-07	6.166E-07	1.230E-06	2.291E-06	3.715E-06	4.571E-06	9.120E-06	1.950E-05	4.467E-05	2.512E-04

Table B-22

Median uniform-hazard spectra (soil, all LLNL G-experts)

PSV (cm/sec)

FREQ	ANNUAL EXCEEDANCE PROBABILITY			
(Hz)	2E-3	1E-3	2E-4	1E-4
0.50	9.47	17.9	68.4	108.8
1.00	12.8	21.2	60.5	90.7
2.50	13.6	18.8	48.3	62.6
5.00	9.98	13.4	24.1	30.2
10.00	4.64	6.57	10.7	12.7
25.00	1.66	2.20	3.68	4.59

Table B-23

Peak ground acceleration hazard curves (soil, 4 LLNL G-experts)

AMPLITUDE (cm/sec2)	MEAN	0.050	0.150	0.250	0.350	0.450	0.500	0.550	0.650	0.750	0.850	0.950
3.201E+01	5.508E-02	6.457E-03	1.122E-02	1.585E-02	2.089E-02	2.570E-02	2.570E-02	3.162E-02	3.631E-02	5.495E-02	8.318E-02	1.549E-01
8.000E+01	2.039E-02	1.413E-03	2.630E-03	4.571E-03	6.457E-03	7.943E-03	9.772E-03	1.047E-02	1.288E-02	1.698E-02	2.754E-02	4.786E-02
1.119E+02	1.294E-02	7.079E-04	1.413E-03	2.630E-03	3.981E-03	5.248E-03	5.623E-03	6.457E-03	8.511E-03	1.047E-02	1.698E-02	2.951E-02
1.600E+02	7.400E-03	3.090E-04	6.607E-04	1.230E-03	1.995E-03	3.020E-03	3.236E-03	3.467E-03	4.898E-03	6.457E-03	9.120E-03	1.698E-02
2.219E+02	4.207E-03	8.913E-05	3.090E-04	6.166E-04	1.000E-03	1.318E-03	1.622E-03	1.862E-03	2.818E-03	3.715E-03	4.898E-03	9.772E-03
2.699E+02	2.882E-03	2.754E-05	1.175E-04	2.692E-04	4.074E-04	6.607E-04	8.128E-04	1.072E-03	1.738E-03	2.138E-03	3.467E-03	7.413E-03
3.301E+02	1.882E-03	1.122E-05	5.129E-05	1.096E-04	2.188E-04	3.548E-04	4.074E-04	5.370E-04	7.586E-04	1.413E-03	2.138E-03	4.898E-03
4.252E+02	1.069E-03	3.981E-06	1.950E-05	4.786E-05	8.318E-05	1.175E-04	1.778E-04	2.042E-04	3.802E-04	6.607E-04	1.230E-03	2.630E-03
5.600E+02	5.512E-04	1.318E-06	7.943E-06	1.820E-05	2.951E-05	4.786E-05	5.495E-05	7.762E-05	1.349E-04	2.692E-04	6.166E-04	1.413E-03
8.002E+02	2.382E-04	2.512E-07	1.738E-06	4.571E-06	8.511E-06	1.380E-05	1.380E-05	2.399E-05	3.890E-05	5.888E-05	1.905E-04	6.166E-04
1.280E+03	6.978E-05	1.585E-08	1.549E-07	6.166E-07	1.148E-06	1.862E-06	2.291E-06	4.266E-06	7.413E-06	1.288E-05	4.467E-05	1.660E-04

Table B-24

Median uniform-hazard spectra (soil, 4 LLNL G-experts)

PSV (cm/sec)

FREQ	ANNUAL EXCEEDANCE PROBABILITY			
(Hz)	2E-3	1E-3	2E-4	1E-4
0.50	9.47	18.02	59.3	87.4
1.00	12.8	21.2	52.5	72.8
2.50	11.2	16.2	31.7	40.6
5.00	8.87	11.9	21.3	26.9
10.00	4.21	5.73	9.60	11.4
25.00	1.66	2.19	3.55	4.36

B.3 RESULTS FROM THE EXTENDED-SOURCE ANALYSIS

Table B-25

Peak ground acceleration hazard curves

AMPLITUDE (cm/sec2)	MEAN	0.150	0.500	0.850
5.000E+00	8.442E-02	6.310E-02	8.913E-02	1.023E-01
1.000E+01	5.987E-02	4.169E-02	6.310E-02	7.244E-02
5.000E+01	1.548E-02	9.772E-03	1.585E-02	2.089E-02
1.000E+02	6.596E-03	3.981E-03	6.457E-03	9.120E-03
2.000E+02	2.372E-03	1.230E-03	2.291E-03	3.467E-03
2.500E+02	1.636E-03	8.128E-04	1.514E-03	2.455E-03
3.000E+02	1.188E-03	5.012E-04	1.072E-03	1.862E-03
4.000E+02	6.942E-04	2.188E-04	5.754E-04	1.148E-03
5.000E+02	4.453E-04	1.096E-04	3.548E-04	8.128E-04
6.000E+02	3.043E-04	5.888E-05	2.188E-04	5.754E-04
7.500E+02	1.865E-04	2.570E-05	1.175E-04	3.802E-04
1.000E+03	9.507E-05	7.943E-06	4.786E-05	2.188E-04

Table B-26

0.5-Hz spectral velocity hazard curves

AMPLITUDE (cm/sec)	MEAN	0.150	0.500	0.850
5.000E-01	2.419E-02	1.950E-02	2.399E-02	2.951E-02
1.000E+00	1.565E-02	1.288E-02	1.585E-02	1.950E-02
5.000E+00	5.995E-03	3.715E-03	6.026E-03	8.511E-03
1.000E+01	3.651E-03	1.862E-03	3.715E-03	5.623E-03
2.000E+01	1.957E-03	5.754E-04	1.738E-03	3.467E-03
2.500E+01	1.546E-03	3.311E-04	1.230E-03	2.818E-03
3.000E+01	1.257E-03	2.188E-04	1.000E-03	2.455E-03
4.000E+01	8.818E-04	9.550E-05	6.166E-04	1.862E-03
5.000E+01	6.531E-04	4.786E-05	4.365E-04	1.318E-03
6.000E+01	5.019E-04	2.570E-05	2.884E-04	1.072E-03
7.500E+01	3.554E-04	1.122E-05	1.660E-04	8.128E-04
1.000E+02	2.185E-04	2.818E-06	7.244E-05	5.012E-04

Table B-27

1-Hz spectral velocity hazard curves

AMPLITUDE (cm/sec)	MEAN	0.150	0.500	0.850
5.000E-01	3.594E-02	2.951E-02	3.631E-02	4.169E-02
1.000E+00	2.135E-02	1.698E-02	2.089E-02	2.570E-02
5.000E+00	6.266E-03	3.981E-03	6.026E-03	8.511E-03
1.000E+01	3.359E-03	1.862E-03	3.467E-03	4.898E-03
2.000E+01	1.531E-03	5.012E-04	1.413E-03	2.455E-03
2.500E+01	1.138E-03	3.090E-04	1.000E-03	1.995E-03
3.000E+01	8.776E-04	1.905E-04	7.586E-04	1.622E-03
4.000E+01	5.616E-04	7.244E-05	4.677E-04	1.148E-03
5.000E+01	3.849E-04	2.754E-05	2.692E-04	8.128E-04
6.000E+01	2.765E-04	1.202E-05	1.778E-04	6.166E-04
7.500E+01	1.792E-04	3.981E-06	8.913E-05	4.074E-04
1.000E+02	9.724E-05	7.586E-07	3.890E-05	2.344E-04

Table B-28

2.5-Hz spectral velocity hazard curves

AMPLITUDE (cm/sec)	MEAN	0.150	0.500	0.850
5.000E-01	5.048E-02	4.169E-02	5.129E-02	5.888E-02
1.000E+00	2.873E-02	2.239E-02	2.951E-02	3.388E-02
5.000E+00	5.654E-03	3.467E-03	5.623E-03	7.943E-03
1.000E+01	2.348E-03	1.000E-03	2.291E-03	3.715E-03
2.000E+01	8.266E-04	1.905E-04	7.079E-04	1.514E-03
2.500E+01	5.645E-04	1.023E-04	4.365E-04	1.072E-03
3.000E+01	4.054E-04	5.129E-05	2.884E-04	8.128E-04
4.000E+01	2.311E-04	1.380E-05	1.549E-04	5.012E-04
5.000E+01	1.441E-04	4.266E-06	8.913E-05	3.311E-04
6.000E+01	9.545E-05	1.514E-06	4.786E-05	2.344E-04
7.500E+01	5.557E-05	4.365E-07	2.089E-05	1.445E-04
1.000E+02	2.577E-05	7.762E-08	6.026E-06	6.761E-05

Table B-29

5-Hz spectral velocity hazard curves

AMPLITUDE (cm/sec)	MEAN	0.150	0.500	0.850
5.000E-01	4.864E-02	3.162E-02	5.129E-02	5.888E-02
1.000E+00	2.743E-02	1.820E-02	2.951E-02	3.631E-02
5.000E+00	4.381E-03	2.455E-03	4.266E-03	6.457E-03
1.000E+01	1.578E-03	6.166E-04	1.514E-03	2.630E-03
2.000E+01	4.728E-04	8.318E-05	3.802E-04	9.333E-04
2.500E+01	3.052E-04	3.631E-05	2.344E-04	6.607E-04
3.000E+01	2.091E-04	1.698E-05	1.445E-04	4.677E-04
4.000E+01	1.103E-04	3.715E-06	5.888E-05	2.512E-04
5.000E+01	6.443E-05	1.072E-06	2.570E-05	1.549E-04
6.000E+01	4.025E-05	3.802E-07	1.202E-05	9.550E-05
7.500E+01	2.157E-05	1.023E-07	4.266E-06	5.495E-05
1.000E+02	8.784E-06	1.380E-08	9.333E-07	2.239E-05

Table B-30

10-Hz spectral velocity hazard curves

AMPLITUDE (cm/sec)	MEAN	0.150	0.500	0.850
5.000E-01	3.747E-02	2.570E-02	3.890E-02	4.786E-02
1.000E+00	1.987E-02	1.380E-02	1.950E-02	2.570E-02
5.000E+00	2.595E-03	1.318E-03	2.291E-03	3.981E-03
1.000E+01	8.297E-04	2.512E-04	7.079E-04	1.514E-03
2.000E+01	2.153E-04	2.089E-05	1.175E-04	4.074E-04
2.500E+01	1.321E-04	7.943E-06	5.888E-05	2.512E-04
3.000E+01	8.640E-05	3.236E-06	3.162E-05	1.660E-04
4.000E+01	4.194E-05	7.079E-07	1.047E-05	8.318E-05
5.000E+01	2.260E-05	1.778E-07	3.981E-06	4.169E-05
6.000E+01	1.304E-05	5.495E-08	1.514E-06	2.239E-05
7.500E+01	6.237E-06	1.047E-08	4.074E-07	9.772E-06
1.000E+02	2.128E-06	1.072E-09	5.888E-08	2.630E-06

Table B-31

25-Hz spectral velocity hazard curves

AMPLITUDE (cm/sec)	MEAN	0.150	0.500	0.850
5.000E-01	2.264E-02	1.698E-02	2.239E-02	2.754E-02
1.000E+00	1.082E-02	7.413E-03	1.047E-02	1.380E-02
5.000E+00	1.082E-03	4.074E-04	9.333E-04	1.738E-03
1.000E+01	2.960E-04	5.129E-05	1.905E-04	5.754E-04
2.000E+01	6.318E-05	2.291E-06	2.089E-05	1.349E-04
2.500E+01	3.557E-05	5.754E-07	8.511E-06	7.762E-05
3.000E+01	2.138E-05	1.660E-07	3.715E-06	4.467E-05
4.000E+01	8.742E-06	2.399E-08	8.710E-07	1.698E-05
5.000E+01	3.988E-06	4.571E-09	2.344E-07	6.918E-06
6.000E+01	1.960E-06	8.710E-10	6.761E-08	3.020E-06
7.500E+01	7.475E-07	1.023E-10	1.380E-08	9.333E-07
1.000E+02	1.818E-07	6.026E-12	1.413E-09	1.660E-07

Table B-32

Median uniform-hazard spectra (5% damping)

PSV (cm/sec)

FREQ (Hz)	ANNUAL EXCEEDANCE PROBABILITY 2E-3	1E-3	2E-4	1E-4
0.50	17.6	30.0	69.6	89.4
1.00	15.3	25.0	57.0	72.3
2.00	10.8	16.3	35.5	47.7
5.00	8.30	12.3	26.5	33.8
10.00	5.42	8.16	16.3	21.1
25.00	3.01	4.78	9.79	12.2

Table B-33

Median uniform-hazard spectra (other damping ratios)

		PSV (cm/sec)			
DAMPING	FREQ.	ANNUAL EXCEEDANCE PROBABILITY			
RATIO (%)	(Hz)	2.E-3	1.E-3	2.E-4	1.E-4
2	0.5	19.8	35.0	81.3	104.4
	1.0	18.3	31.1	70.9	89.9
	2.0	13.8	21.5	46.8	62.8
	5.0	11.3	17.1	36.8	46.9
	10.0	7.6	11.6	23.1	29.9
	25.0	4.3	6.9	14.1	17.6
7	0.5	16.5	27.7	64.4	82.7
	1.0	14.0	22.6	51.6	65.4
	2.0	9.7	14.5	31.6	42.5
	5.0	7.3	10.8	23.3	29.7
	10.0	4.8	7.1	14.3	18.5
	25.0	2.6	4.2	8.5	10.7
10	0.5	15.2	25.2	58.6	75.2
	1.0	12.6	20.2	46.0	58.3
	2.0	8.6	12.8	27.8	37.4
	5.0	6.4	9.4	20.3	25.9
	10.0	4.1	6.2	12.4	16.0
	25.0	2.3	3.6	7.4	9.2
12	0.5	14.5	23.9	55.5	71.3
	1.0	11.9	19.0	43.2	54.8
	2.0	8.1	11.9	26.0	34.9
	5.0	6.0	8.8	18.9	24.1
	10.0	3.8	5.8	11.5	14.9
	25.0	2.1	3.4	6.9	8.6
15	0.5	13.7	22.4	51.9	66.6
	1.0	11.1	17.5	40.0	50.7
	2.0	7.4	11.0	23.9	32.1
	5.0	5.5	8.0	17.3	22.1
	10.0	3.5	5.3	10.5	13.6
	25.0	1.9	3.1	6.3	7.8

DISTRIBUTION

Martin Marietta Energy Systems, Inc.
Angelelli, T. A.
Beavers, J. E.
Brock, W. R.
Burnett, W. A. - PGDP
Crowley, W. K.
Flanagan, G. F.
Gamm, C. E. - PORTS
Gourieux, P. A. - PGDP
Hickey, F. H.
Hortell, J. M. - PORTS
Hunt, R. J.
Miller, R. R.
O'Kain, D. U.
Rogers, M. D. - PGDP
Rushton, J. E.
Shaffer, K. E. (3)
Staub, W. P.
GDP SAR Document
Management Center (2) - RC

Department of Energy
Caves, C. A. - DOE-HQ
Hampton, W. A. - DOE-OR
Hill, J. R. - DOE-HQ
Hughlett, J. D. - DOE-OR
Hultgren, R. O. - DOE-OR
Jackson, J. D. - DOE-OR
Kimball, J. K. - DOE-HQ
Littman, A. P. - DOE-HQ

U. S. Army Engineer
Waterways Experiment Station
Sykora, D. W.

U. S. Geological Survey
Algermissen, S. T.

University of Kentucky
Street, R. L.

University of Tennessee
Hatcher, R. D.

Lawrence Livermore National Laboratory
Harri, J. G.
Savy, J. B.

St. Louis University
Herrmann, R. B.